

Technical Report Documentation Page

| | | | | | |
|---|--|-----------------------------|---|----------------------------|--|
| 1. Report No. FHWA/TX-14/0-6717-1 | | 2. Government Accession No. | | 3. Recipient's Catalog No. | |
| 4. Title and Subtitle Evaluating the Performance of Alternative Supplementary Cementing Material in Concrete | | | 5. Report Date October 2014; Published January 2014 | | |
| | | | 6. Performing Organization Code | | |
| 7. Author(s) Saamiya Seraj, Rachel Cano, Shukui Liu, David Whitney, David Fowler, Raissa Ferron, Jinying Zhu, Maria Juenger | | | 8. Performing Organization Report No. 0-6717-1 | | |
| 9. Performing Organization Name and Address Center for Transportation Research The University of Texas at Austin 1616 Guadalupe Street, Suite 4.202 Austin, TX 78701 | | | 10. Work Unit No. (TRAIS) | | |
| | | | 11. Contract or Grant No. 0-6717 | | |
| 12. Sponsoring Agency Name and Address Texas Department of Transportation Research and Technology Implementation Office P.O. Box 5080 Austin, TX 78763-5080 | | | 13. Type of Report and Period Covered Technical Report, 8/1/2012–8/31/2014 | | |
| | | | 14. Sponsoring Agency Code | | |
| 15. Supplementary Notes Project performed in cooperation with the Texas Department of Transportation and the Federal Highway Administration. | | | | | |
| 16. Abstract Uncertainty in the supply of Class F fly ash due to impending environmental restrictions has made it imperative to find and test alternate sources of supplementary cementitious materials (SCMs) that can provide similar strength and durability benefits to concrete as Class F fly ash. This project summarizes the key findings of research that was conducted to characterize and evaluate the performance of eight natural pozzolans, commercially available in Texas, to assess their potential as Class F fly ash replacements in concrete. Of the eight pozzolans tested, six were found to be viable alternatives for Class F fly ash. Methods to further enhance the performance of these SCMs were explored and guidelines are provided on the optimum SCM replacement levels for different applications. Finally, recommendations are presented on how to improve current testing practices for SCMs. | | | | | |
| 17. Key Words Alternative SCMs, Class F fly ash, Pozzolans, ASTM C 618, Strength, Durability, Reactivity, Rheology, Workability | | | 18. Distribution Statement No restrictions. This document is available to the public through the National Technical Information Service, Springfield, Virginia 22161; www.ntis.gov . | | |
| 19. Security Classif. (of report) Unclassified | 20. Security Classif. (of this page) Unclassified | 21. No. of pages 144 | | 22. Price | |



**THE UNIVERSITY OF TEXAS AT AUSTIN
CENTER FOR TRANSPORTATION RESEARCH**

Evaluating the Performance of Alternative Supplementary Cementing Material in Concrete

Saamiya Seraj
Rachel Cano
Shukui Liu
David Whitney
David Fowler
Raissa Ferron
Jinying Zhu
Maria Juenger

| | |
|-----------------------|---|
| CTR Technical Report: | 0-6717-1 |
| Report Date: | October 2014; Published January 2014 |
| Project: | 0-6717 |
| Project Title: | Investigation of Alternative Supplementary Cementing Materials (SCMs) |
| Sponsoring Agency: | Texas Department of Transportation |
| Performing Agency: | Center for Transportation Research at The University of Texas at Austin |

Project performed in cooperation with the Texas Department of Transportation and the Federal Highway Administration.

Center for Transportation Research
The University of Texas at Austin
1616 Guadalupe, Suite 4.202
Austin, TX 78701

<http://ctr.utexas.edu/>

Disclaimers

Author's Disclaimer: The contents of this report reflect the views of the authors, who are responsible for the facts and the accuracy of the data presented herein. The contents do not necessarily reflect the official view or policies of the Federal Highway Administration or the Texas Department of Transportation (TxDOT). This report does not constitute a standard, specification, or regulation.

Patent Disclaimer: There was no invention or discovery conceived or first actually reduced to practice in the course of or under this contract, including any art, method, process, machine manufacture, design or composition of matter, or any new useful improvement thereof, or any variety of plant, which is or may be patentable under the patent laws of the United States of America or any foreign country.

Notice: The United States Government and the State of Texas do not endorse products or manufacturers. If trade or manufacturers' names appear herein, it is solely because they are considered essential to the object of this report.

Engineering Disclaimer

NOT INTENDED FOR CONSTRUCTION, BIDDING, OR PERMIT PURPOSES.

Project Engineer: Dr. David W. Fowler
Professional Engineer License State and Number: Texas No. 27859
P. E. Designation: Researcher

Acknowledgments

The authors express appreciation to Darrin Jensen, TxDOT Project Manager, and to the 0-6717 Project Management Committee: Darlene Goehl, Courtney Holle, Andy Naranjo, Robert Owens, Terry Paholek, and Kevin Pruski. The authors also thank Cliff Coward (TxDOT) for helping with some of the data collection for this project. The authors also wish to acknowledge the undergraduate research assistants, Juan Pablo Gevaudan and Victoria Valdez, for their assistance with the project.

Table of Contents

| | |
|--|-----------|
| Chapter 1. Introduction and Identification of Materials | 1 |
| 1.1 Motivation..... | 1 |
| 1.2 Literature Review | 2 |
| 1.2.1 TxDOT Requirement for SCMs..... | 2 |
| 1.2.2 Introduction to Natural Pozzolans | 3 |
| 1.2.3 Perlite..... | 3 |
| 1.2.4 Pumice..... | 6 |
| 1.2.5 Volcanic Ash..... | 10 |
| 1.2.6 Zeolites..... | 13 |
| 1.2.7 Clay..... | 17 |
| 1.2.8 Shale..... | 22 |
| 1.2.9 Diatomite (Diatomaceous Earth) | 25 |
| 1.2.10 Conclusion of Literature Review | 29 |
| 1.3 Identification of Materials | 29 |
| Chapter 2. Material Characterization | 33 |
| 2.1 ASTM C 618 Characterization Tests..... | 33 |
| 2.1.1 ASTM C 618 Requirements and Procedures..... | 33 |
| 2.1.2 ASTM C 618 Results..... | 35 |
| 2.2 Advanced Characterization Tests | 38 |
| 2.2.1 Advanced Characterization Procedures..... | 38 |
| 2.2.2 Advanced Characterization Results..... | 39 |
| 2.3 Conclusions from Characterization Tests..... | 42 |
| Chapter 3. Paste and Mortar Studies..... | 43 |
| 3.1 Procedures..... | 43 |
| 3.1.1 Compressive Strength | 43 |
| 3.1.2 Rheological Properties | 44 |
| 3.1.3 Heat of Hydration | 45 |
| 3.1.4 Calcium Hydroxide Content | 45 |
| 3.1.5 Drying Shrinkage..... | 46 |
| 3.1.6 Resistance to Alkali-Silica Reaction..... | 46 |
| 3.1.7 Resistance to Sulfate Attack | 47 |
| 3.2 Results..... | 48 |
| 3.2.1 Compressive Strength | 48 |
| 3.2.2 Rheological Properties | 49 |
| 3.2.3 Heat of Hydration | 50 |
| 3.2.4 Calcium Hydroxide Content | 50 |
| 3.2.5 Drying Shrinkage..... | 51 |
| 3.2.6 Resistance to Alkali-Silica Reaction..... | 51 |
| 3.2.7 Resistance to Sulfate Attack | 52 |
| 3.3 Conclusions from Mortar and Paste Studies..... | 65 |
| Chapter 4. Concrete Studies | 67 |
| 4.1 Procedures..... | 68 |
| 4.1.1 Mixture Design | 68 |

| | |
|---|------------|
| 4.1.2 Mixing, Casting, Consolidation, and Curing | 69 |
| 4.1.3 Compressive Strength | 70 |
| 4.1.4 Fresh State Properties | 70 |
| 4.1.5 Drying Shrinkage | 70 |
| 4.1.6 Resistance from Alkali-Silica Reaction | 71 |
| 4.1.7 Resistance to Chloride Ion Penetration | 71 |
| 4.1.8 Coefficient of Thermal Expansion | 72 |
| 4.2 Results | 72 |
| 4.2.1 Compressive Strength | 72 |
| 4.2.2 Fresh State Properties | 73 |
| 4.2.3 Drying Shrinkage | 73 |
| 4.2.4 Resistance to Alkali-Silica Reaction | 74 |
| 4.2.5 Resistance to Chloride Ion Penetration | 74 |
| 4.2.6 Coefficient of Thermal Expansion | 74 |
| 4.2.7 Ultrasonic Tests for Setting Time Monitoring | 74 |
| 4.3 Conclusions from Concrete Studies | 84 |
| Chapter 5. Treatments and Modification of SCMs | 85 |
| 5.1 Modification Methods | 85 |
| 5.1.1 Calcination | 85 |
| 5.1.2 Crushing and Calcination | 86 |
| 5.1.3 Pre-soaking in Hydrated Lime and Polyethylene Glycol | 86 |
| 5.2 Results | 86 |
| 5.2.1 Zeolite-A | 86 |
| 5.2.2 Zeolite-T | 87 |
| 5.2.3 Zeolite-Z | 87 |
| 5.3 Conclusions from Material Treatment and Modification | 90 |
| Chapter 6. Conclusions and Recommendations | 91 |
| 6.1 Optimum SCM Replacement Dosage | 91 |
| 6.1.1 Specific Recommendations | 92 |
| 6.2 Evaluation of Current Testing Practices for SCMs | 93 |
| 6.2.1 Specific Recommendations | 93 |
| Appendix A. X-ray Diffractograms & TGA/DSC Plots of Pozzolans | 95 |
| Appendix B. Admixture Dosages | 105 |
| Appendix C. Ultrasonic Tests for Concrete Setting Time Measurement | 107 |
| C.1 Introduction | 107 |
| C.2 Materials and Experimental Setup | 107 |
| C.2.1 Materials | 107 |
| C.2.2 Ultrasonic Test Setups | 108 |
| C.3 Results and Discussion | 109 |
| C.3.1 Mortar Mixtures | 109 |
| C.3.2 Mortar Sieved from Concrete Mixtures | 112 |
| C.3.3 Concrete Mixtures | 113 |
| C.4 Conclusions | 114 |
| References | 117 |

List of Figures

| | |
|---|----|
| Figure 1.1: Uses of perlite in the US..... | 6 |
| Figure 1.2: Uses of pumice in the US..... | 10 |
| Figure 1.3: Common applications of DE in US..... | 29 |
| Figure 2.1: Particle size distribution of pozzolans..... | 41 |
| Figure 2.2: Amount of methylene blue absorbed per gram of SCM..... | 42 |
| Figure 3.1: Compressive strength of mortar mixtures with a w/cm of 0.50..... | 53 |
| Figure 3.2: Compressive strength of mortar mixtures with a w/cm of 0.55..... | 54 |
| Figure 3.3: Representative rheology flow curves for control and SCM paste mixtures..... | 55 |
| Figure 3.4: Rate of heat evolved during hydration per gram of cement and SCM..... | 56 |
| Figure 3.5: Calcium hydroxide content of pastes with 20% SCM..... | 57 |
| Figure 3.6: Percentage shrinkage of mortar mixtures in 50% RH..... | 58 |
| Figure 3.7: Shrinkage vs. weight loss of mortar mixtures in 50% RH..... | 59 |
| Figure 3.8: ASR expansion of mortar bars, with a 20% SCM replacement dosage..... | 60 |
| Figure 3.9: Minimum amount of SCM needed to pass ASTM C 1567ASR Testing..... | 61 |
| Figure 3.10: Expansions of ASTM C 1012 mortars bars, with 15% SCM replacement..... | 62 |
| Figure 3.11: Expansion of ASTM C 1012 mortar bars with 25 or 35% SCM replacement..... | 63 |
| Figure 3.12: Expansion of ASTM C 1012 mortar bars made with a fixed w/cm..... | 64 |
| Figure 4.1: Compressive strength of concrete mixtures with 15% SCM..... | 75 |
| Figure 4.2: Compressive strength of concrete mixtures with 25% or 35% SCM..... | 76 |
| Figure 4.3: Percent shrinkage of concrete mixtures with 15% SCM..... | 78 |
| Figure 4.4: Percent shrinkage of concrete mixtures with 25% or 35% SCM..... | 78 |
| Figure 4.5: Drying shrinkage vs. weight loss of concrete mixtures with 15% SCM..... | 79 |
| Figure 4.6: Drying shrinkage vs. weight loss of concrete mixtures with 25% or 35% SCM..... | 79 |
| Figure 4.7: Average ASR expansion of concrete mixtures with 15% SCM..... | 81 |
| Figure 4.8: Average ASR expansion of concrete mixtures with 25% or 35% SCM..... | 81 |
| Figure 4.9: ASTM C 1202 rapid chloride testing results at 32 weeks..... | 83 |
| Figure 4.10: Correlation between shear wave velocity and penetration resistance on mortar sieved from concrete mixtures in (a) linear scale and (b) logarithm scale..... | 84 |
| Figure 5.1: Effect of modification on the rheological properties of Zeolite-A mixtures..... | 88 |
| Figure 5.2: Effect of modification on the rheological properties of Zeolite-T Mixtures..... | 89 |
| Figure 5.3: Effect of modification on the rheological properties of Zeolite-Z mixtures..... | 90 |
| Figure 6.1: Finding the optimum replacement dosage..... | 91 |
| | |
| Figure A1: XRD plot of amorphous Pumice-D..... | 95 |
| Figure A2: XRD plot of amorphous Perlite-I..... | 96 |
| Figure A3: XRD plot of Vitric Ash-S with its crystalline impurities..... | 96 |

| | |
|---|-----|
| Figure A4: XRD plot of Metakaolin-D with its crystalline impurities..... | 97 |
| Figure A5: XRD plot of Shale-T with its crystalline impurities..... | 97 |
| Figure A6: XRD plot of crystalline Zeolite-Z | 98 |
| Figure A7: XRD plot of crystalline Zeolite-T | 98 |
| Figure A8: XRD plot of crystalline Zeolite-A..... | 99 |
| Figure A10: TGA/DSC plot of Pumice-D | 99 |
| Figure A11: TGA/DSC plot of Perlite-I | 100 |
| Figure A12: TGA/DSC plot of Vitric Ash-S | 100 |
| Figure A13: TGA/DSC plot of Metakaolin-D | 101 |
| Figure A14: TGA/DSC plot of Shale-T..... | 101 |
| Figure A15: TGA/DSC plot of Zeolite-Z | 102 |
| Figure A16: TGA/DSC plot of Zeolite-T | 102 |
| Figure A17: TGA/DSC plot of Zeolite-A..... | 103 |
| Figure C1: Ultrasonic test setups: (a) setup using bender elements, (b) picture of bender element, (c) setup using shear wave transducers, and (d) setup using P wave transducers | 109 |
| Figure C2: Ultrasonic P wave and shear wave velocities measured in mortar mixtures..... | 110 |
| Figure C3: Penetration resistance of mortar mixtures with different w/c..... | 110 |
| Figure C4: Correlation between P and shear wave velocities and penetration resistance on mortar mixtures with different w/c in (a) linear scale and (b) logarithm scale (shear wave velocity only)..... | 111 |
| Figure C5: Ultrasonic P and shear wave velocities in sieved concrete mixtures..... | 112 |
| Figure C6: Correlation between shear wave velocity and penetration resistance on mortar sieved from concrete mixtures in (a) linear scale and (b) logarithm scale | 113 |
| Figure C7: Correlation between P and shear wave velocities and penetration resistance of different concrete mixtures | 114 |

List of Tables

| | |
|--|-----|
| Table 1.1: Production and Uses of Different Clay in the US..... | 22 |
| Table 1.2: Price, Origin, and Availability of the Eight SCMs Chosen for TxDOT 0-6717 | 31 |
| Table 1.3: Price, Origin, and Availability of Materials that Were Cut from Testing Matrix | 31 |
| Table 2.1: Material Characterization Tests Performed on the SCMs | 33 |
| Table 2.2: Summary of ASTM C 618 Results..... | 37 |
| Table 2.3: Oxide Composition Results from XRF Analysis..... | 37 |
| Table 2.4: Average Density from Pycnometer | 37 |
| Table 2.5: XRD and TGA Results | 41 |
| Table 3.1: Experiments Performed in the Paste and Mortar Studies | 43 |
| Table 3.2: Yield Stress and Viscosity of Mixtures from Bingham Model | 55 |
| Table 3.3: Weight Loss and Shrinkage of SCM Mortar Bars Compared to Control..... | 59 |
| Table 3.4: Expansion of ASTM C 1567 Mortar Bars with 20% SCM..... | 60 |
| Table 3.5: Expansion of Mortar Bars with Adequate SCMs to Meet ASTM C 1567 Limit | 61 |
| Table 3.6: Summary of Sulfate Exposure Qualification and Mortar Bar Expansion | 65 |
| Table 4.1: Tests Performed on Concrete Mixtures | 67 |
| Table 4.2: SCM Replacement Dosages (by Weight of Cement) in Concrete Mixtures | 68 |
| Table 4.3: Mixture Design for All Concrete Experiments, except ASTM C 1293 | 69 |
| Table 4.4: Mixture Design for ASTM C 1293 ASR Testing..... | 69 |
| Table 4.5: Fresh State Properties of Concrete Mixtures | 77 |
| Table 4.6: Weight Loss and Drying Shrinkage of SCM Mixtures at 64 Weeks..... | 80 |
| Table 4.7: Average ASR Expansion of Concrete Mixtures at 24 Months..... | 82 |
| Table 4.8: CoTE Results of Concrete Cylinders..... | 83 |
| Table 5.1: Modification Techniques Used on Zeolite SCMs | 85 |
| Table 5.2: Yield Stress and Viscosity of Zeolite-A Mixtures..... | 88 |
| Table 5.3: Yield Stress and Viscosity of Zeolite-T Mixtures | 89 |
| Table 5.4: Yield Stress and Viscosity of Zeolite-Z mixtures..... | 90 |
| Table 6.1: Summary of SCM Performance at Different Replacement Dosages..... | 92 |
| Table 6.2: Summary of Evaluations and Modifications Needed in Current Concrete Tests..... | 94 |
| | |
| Table B1: Admixture Dosage for ASTM C 1567 Mortar Mixtures | 105 |
| Table B2: Admixture Dosage for Concrete Used to Measure Fresh State Properties | 105 |
| Table C1: Concrete and Mortar Mixture Designs, Setting Times, and Ultrasonic Test Setups..... | 108 |
| Table C2: Ultrasonic Wave Velocities Measured at Initial and Final Setting Times..... | 114 |

Glossary

| | |
|--------------------------------|---------------------------------------|
| ACI | American Concrete Institute |
| Al ₂ O ₃ | aluminum oxide |
| ASR | alkali-silica reaction |
| CaO | calcium oxide |
| C-S-H | calcium silicate hydrate |
| CoTE | coefficient of thermal expansion |
| DE | diatomaceous earth |
| DSC | differential scanning calorimetry |
| Fe ₂ O ₃ | iron oxide |
| HL | hydrated lime |
| HRM | high-reactivity metakaolin |
| LOI | loss on ignition |
| MgO | magnesium oxide |
| OPC | ordinary portland cement |
| PEG | polyethylene glycol |
| RH | relative humidity |
| SAI | strength activity index |
| SCM | supplementary cementitious material |
| SiO ₂ | silica oxide |
| TGA | thermal gravimetric analysis |
| USGS | US Geological Survey |
| w/c | water-to-cement ratio |
| w/cm | water-to-cementitious-materials ratio |
| WRA | water-reducing admixture |
| XRD | X-ray diffraction |
| XRF | X-ray florescence |

Chapter 1. Introduction and Identification of Materials

1.1 Motivation

Supplementary cementitious materials (SCMs) provide many benefits to concrete mixtures, especially in terms of long-term strength and durability. Since the production of cement is responsible for 5% of the global anthropogenic carbon dioxide emissions [1], SCMs can reduce the environmental footprint of concrete, as SCMs are used to partially replace cement. In Texas, Class F fly ash is extensively used as an SCM [2], because of its ability to control thermal cracking in mass concrete and to mitigate deleterious expansions in concrete from alkali-silica reaction (ASR) and sulfate attack [2–6]. Replacing cement with Class F fly ash is also beneficial from a cost perspective since fly ash is cheaper than cement (about \$40 per ton) [7].

As a by-product of coal-burning power plants, fly ash is widely available with at least 50 million short tons of fly ash being produced each year in the US since 1994 [8]. In recent years, however, the future availability of fly ash in the US has become a source of concern because of impending environmental regulations from the US Environmental Protection Agency (EPA). The failure of a fly ash retaining pond in Kingston, Tennessee, in 2008 spurred the EPA to examine new regulations for the disposal of coal combustion residuals (CCRs), which include fly ash. The first proposal, known as a Subtitle C classification of the Resource Conservation and Recovery Act (RCRA), would regulate CCRs as hazardous wastes, with the federal government controlling and enforcing the associated rules [2, 9, 10]. The second proposal, known as a Subtitle D classification of RCRA, would consider CCRs as non-hazardous, but would enforce a higher minimum standard for CCR disposal. Unlike Subtitle C, the enforcement of rules under Subtitle D would be left up to the states [2, 9, 10]. Regardless of which rule is finally adopted, the EPA has maintained that fly ash can still be used in concrete due to the “beneficial use” exemption, which permits the use of fly ash when it is completely encapsulated [2]. However, the rising cost of fly ash associated with these environmental rulings will most likely make the use of fly ash in concrete prohibitive.

Additionally, environmental regulations, like the Clean Air Interstate Rule and Cross State Air Pollution Rule [11, 12], that aim to reduce air pollution have forced coal-burning power plants to adopt emission reduction techniques that have consequently led to a lower quality of fly ash. For example, in order to reduce nitrogen oxide (NO_x) emissions, power plants have switched to low NO_x burners that do not fully combust the coal. This results in coarser ashes with higher carbon contents, making the fly ashes unsuitable for use in concrete mixtures with air-entraining agents [13]. In order to decrease sulfur dioxide emissions, power plants are combusting low sulfur coals, like the Powder River Basin coal from Wyoming. However, low sulfur coals tend to produce the high calcium Class C ash, instead of the low calcium Class F ash [14], which is more beneficial for concrete durability problems like ASR and sulfate attack [3–5]. An additional problem with the use of low sulfur coals is that ammonium has to be added to the fly ashes they produce, since these ashes do not retain sufficient charge to be attracted towards the electrostatic precipitators that are used for dust control. This results in ammoniated fly ash, which can cause odor problems when used with alkaline cement [15]. As these changes in the coal power generation industry are causing considerable uncertainty for the future availability and quality of fly ash, it becomes imperative to identify and test other SCMs that can provide similar strength and durability benefits to concrete as Class F fly ash.

The Texas Department of Transportation (TxDOT) project 0-6717 was undertaken with the purpose of finding new SCMs that could replace Class F fly ash in concrete. The researchers characterized and evaluated the performance of eight natural pozzolans in cementitious mixtures, the details of which are outlined in this report. The remainder of Chapter 1 contains a literature review on natural pozzolans and descriptions of the materials tested in this project. Chapter 2 contains details of the characterization of these materials, while Chapters 3 through 5 contain the performance results of the pozzolans in paste, mortar, and concrete. Finally, Chapter 6 provides guidelines for the implementation of these pozzolans in concrete applications.

1.2 Literature Review

An extensive literature review on natural pozzolans was conducted to serve as an initial screening of materials that could be used by TxDOT as alternatives to Class F fly ash in concrete. Since the natural pozzolans were appraised in a manner that resembles the TxDOT evaluation criteria, the first section of the literature review (Section 1.2.1) contains a summary of the TxDOT specifications on the usage of SCMs in concrete. The rest of the sections in the literature review contain detailed reviews of different natural pozzolans, like perlite, pumice, volcanic ash, zeolites, clay, shale, and diatomaceous earth. Please note that not all of the SCMs that were reviewed were chosen to be included in the final list of materials for this project.

1.2.1 TxDOT Requirement for SCMs

As per Section 421.2.B, in the 2004 TxDOT Standard Specifications for Construction and Maintenance of Highways, Streets, and Bridges [16], Class C and F fly ashes, ground-granulated blast furnace slag (GGBFS), silica fume, and metakaolin (calcined kaolin clay) are acceptable SCMs for use in hydraulic cement concrete, provided each material meets the requirements of its respective Departmental Materials Specification (DMS). Fly ash, GGBFS, silica fume, and metakaolin are controlled by DMS 4610, 4620, 4630, and 4635 respectively.

Presently, metakaolin is the only natural pozzolan mentioned in the most current TxDOT Specifications from 2004 [16]. However, other natural pozzolans may be used in hydraulic cement concrete mixture designs provided they meet the requirements of Section 421.4.A.6 [16], a section that provides eight options for acceptable mixture designs. Options 1, 2, 3, and 5, listed in Section 421.4.A.6 [16], utilize at least one of the SCMs classified in 421.2.B [16] for use in hydraulic cement concrete. In order to use other SCMs that are not explicitly mentioned in 421.2.B [16], Option 8 must be used, which requires only that a mixture design utilizing the natural pozzolan or SCM is sufficient to limit expansion to 0.10% when testing for ASR using the procedures described in ASTM C 1260 (i.e., the accelerated mortar bar test for ASR).

Other than improving the durability of concrete in terms of ASR resistance, TxDOT also recognizes the benefits of SCMs in lowering the heat of hydration of concrete mixtures. TxDOT requires concrete mixtures to have their core temperature and temperature gradient be minimized to 160 °F and 35 °F respectively. The two permissible methods for achieving this are to either cool the concrete using ice, liquid nitrogen, or other techniques described in 420.4.G.14 [16], or to reduce the heat of hydration by using different materials in the mixture. The heat of hydration of a concrete mixture can be lowered by using certain aggregates and cement types, as well as through the use of SCMs.

TxDOT also has specifications that directly and indirectly limit the use of SCMs in concrete. Specifications such as those in Section 421.4.A.1 [16] directly prohibit the use of SCMs when white hydraulic cement is specified in the concrete design. Other specifications,

such as the ones listed in Section 420.4.J [16], indirectly limit the use of SCMs by calling for additional curing time when SCMs are used, which makes some contractors unwilling to use SCMs. Specifications such as those in Section 421.4.A.2 [16] that prohibit the use of high-range water-reducing admixtures (WRA) and accelerating admixtures in bridge deck concrete also indirectly limit the use of SCMs that require admixtures in order to achieve the required slump or the targeted strength. The use of natural pozzolans with a high water demand can also be limited in other applications, as the slump recommendations and requirements, found in section 421.4.A.5 [16], might necessitate the use of expensive WRAs when pozzolans are incorporated into the mix design, to meet the required slump. As such, the natural pozzolans that are presented in this literature review have been evaluated, not only in terms of their improvement to concrete strength and durability, but also in terms of their enhancements to the fresh state properties of concrete.

1.2.2 Introduction to Natural Pozzolans

A pozzolan, as defined in ASTM C 125 [17], is “a siliceous or siliceous and aluminous material that in itself possesses little or no cementitious value but will, in finely divided form and in the presence of water, chemically react with calcium hydroxide at ordinary temperatures to form compounds possessing cementitious properties.” ASTM C 618 [18] is the standard specification for natural pozzolans, and classifies them as “Class N” SCMs on the basis of several composition and performance indices, such as oxide composition, fineness, strength, and water requirement. ASTM C 618 [18] gives some examples of natural pozzolans or “Class N” SCMs such as pumice, volcanic ash, clay, shale, and diatomaceous earth. Each of these materials is discussed in detail in the upcoming sections.

1.2.3 Perlite

1.2.3.1 Background

Perlite is a hydrated volcanic glass, which is often characterized as displaying a “pearly, vitreous luster” [19] and “concentric onion-skin-like fractures” [20]. More specifically, perlite is defined as a hydrated natural rhyolite, which is glass formed from highly siliceous (felsic) volcanic lava [20]. As a result of its origin, perlite contains a high percentage of silica (SiO_2). Based on the studies reviewed [19–23], typical compositions of perlite range from 70–76% SiO_2 , 10–14% aluminum oxide (Al_2O_3), and 1–2% iron oxide (Fe_2O_3). Typical X-ray diffraction (XRD) analysis results show that perlite is mainly amorphous with a few crystalline impurities like quartz, biotite, and alkali feldspars [20, 21].

A high water content of 2–5% differentiates perlite from other hydrated volcanic glasses like obsidian or pumice [19]. It is generally hypothesized that perlite has a high internal water content because its hydration occurs in two steps. The primary hydration takes place during the formation of the volcanic glass, and the secondary hydration occurs late in the cooling history of the glass. Water for the primary hydration mostly comes from magma. Water for the second hydration is generally attributed to external sources, such as ground water or surface water [20, 24].

When heated rapidly, natural perlite expands to form a white, porous, lightweight aggregate known as expanded perlite [19, 20]. The high water content of natural perlite is crucial in the formation of expanded perlite. As perlite is heated, it starts to soften, like most glasses. At temperatures between 870–1100 °C, the glass becomes soft enough for the internal water to boil

[20]. The resultant steam forms bubbles within the glass, which allows the perlite to expand up to 20 times its original volume and form expanded perlite [19, 20].

1.2.3.2 Pozzolanic Nature of Perlite

The highly siliceous and amorphous nature of perlite makes it an ideal material to be considered for use as a pozzolan in concrete. However, only a few studies have examined perlite as an SCM. Erdem et al. [21] found that perlite samples from Turkey conformed to the standards set in ASTM C 618. A similar study by Ray et al. [22] reports the use of perlite fines (that were stockpiled as waste in Australian perlite mines) as an SCM. Using differential thermal analysis and XRD, Ray et al. [22] showed that mortar mixtures with these perlite fines had similar characteristics to mortars prepared with more traditional SCMs, such as fly ash and silica fume, at the same replacement dosage

1.2.3.3 Effect on Strength

Erdem et al. [21] found that using perlite as a cement replacement generally led to a decreased compressive strength in mortars. At 91 days, the compressive strength of mortars incorporating perlite was generally lower than the compressive strength of the control mortars without SCMs. When 20% of the cement by weight was replaced by perlite, the compressive strength of the perlite mortars were 4–6% lower than those of the control mortars. When the replacement amount was increased to 30%, the perlite-containing mortars had compressive strengths 13–20% lower than the control mortars. However, increasing the fineness of the perlite helped to reduce the difference in strength between the control and perlite mortars. When the fineness of the perlite was increased from 320 m²/kg to 370 m²/kg, the difference in compressive strength between the 20% perlite mortars and the control mortars was 1–2%, while the difference between the 30% perlite mortars and the control was 6–11%.

In a similar study, Yu et al. [23] tested the effect of varying perlite replacement dosages in concrete. Contrary to the results of Erdem et al., Yu et al. [23] found that at 28 days, concrete specimens with perlite replacement dosages between 10 and 30% had compressive strengths that were either equal to or higher than those of the control concrete specimen. The strength of concrete with a perlite replacement dosage of 40% was only slightly less than that of the control at 28 days. By 91 days, the compressive strengths of all the concrete specimens had exceeded that of the control, by at least 7%. Considering that perlite is a natural pozzolan whose properties can vary depending upon its sourcing, these differences in reported results are not unusual.

Uzal et al. [25] found that concrete in which 50% of cement by weight was replaced by perlite reached a compressive strength of 2530 psi by 7 days and 4230 psi by 28 days when a water-to-cement ratio (w/c) of 0.45 was used. Concrete made with fly ash, at the same replacement dosage and w/c, had a compressive strength that was similar to the perlite concrete at 28 days.

1.2.3.4 Effect on Fresh State Properties

Following the ASTM C 187 method of determining normal consistency, Erdem et al. [21] found that a higher w/c was needed to achieve normal consistency for pastes containing a blend of perlite and cement than what was needed for the control with only cement. Increasing the replacement dosages of perlite resulted in requiring an even higher w/c to achieve normal consistency. The same trend was observed for mortars, where a higher w/c was needed for the

perlite mortars to achieve the same flow as the control mortar. Uzal et al. [25] reported that in order to achieve the same slump, concrete mixtures with a 50% cement replacement dosage of perlite needed a slightly higher dosage of high-range WRA (about 1 lb. more per yd³) than a concrete mixture with 50% Class F fly ash.

Erdem et al. [21] also reported that the initial and final setting times of cementitious pastes, where 20 to 30% perlite was used as a cement replacement, were greater than those of the control. However, the differences in setting times were within the limits stated in ASTM C 595 and ASTM C 1157, which are standard performance specifications for hydraulic cement [21]. Using ASTM C 403, which finds the time of set of concrete mixtures using a penetrometer, Uzal et al. [25] found that the initial and final setting times of the concrete mixture with 50% perlite replacement were 4.67 hours and 7.08 hours, respectively. Comparatively, the initial and final setting times of the concrete mixture, with 50% Class F fly ash replacement, were significantly higher at 8.67 hours and 12.75 hours, respectively.

1.2.3.5 Impact on Durability

Using ASTM 1260, which is the accelerated mortar bar test method to determine ASR, Bektas et al. [19] found that both natural perlite and expanded perlite were successful in mitigating the adverse effects of ASR when used as SCMs in mortar. Bektas et al. [19] found that a 16% replacement of expanded perlite for cement could keep expansion well below the ASTM 1260 limit of 0.1% (after 14 days of immersion in NaOH solution at 80 °C), when using a highly reactive river aggregate containing 2% opal. When used with a marginally reactive monzo-diorite aggregate, even a 4% replacement dosage of expanded perlite was sufficient to keep expansions below 0.1% at 14 days. However, for natural perlite, a higher dosage of replacement was needed to mitigate the expansions from ASR. To keep the mortar expansions below 0.10% at 14 days, 16% natural perlite replacement of cement by weight was needed when using the marginally reactive monzo-diorite [19]. Contrary to the study by Bektas et al., Gokce et al. [26] found that a 35% replacement dosage of perlite was needed to mitigate the expansions of ASR, when tested according to ASTM C 1260, with a highly reactive aggregate from Turkey.

Using ASTM C 1202, which measures the ability of concrete specimens to resist chloride ion penetration, Uzal et al. [25] found that the total charge passing through concrete specimens, where 50% of the cement by weight was replaced with perlite, was only 684 coulombs at 91 days. According to the rating system suggested in ASTM C 1202, the perlite concrete falls under a “Very Low Penetrability to Chloride Ions” category, since the total charge passing through it was less than 1000 coulombs. The concrete specimen with a 50% replacement dosage of Class F fly ash performed slightly better in this test, with a charge of only 545 coulombs passing through it.

1.2.3.6 Sources of Perlite in the US and Common Uses

According to the US Geological Survey (USGS), in 2011, the US had a perlite reserve of 50,000,000 metric tons [27]. Domestic production of processed crude perlite was 420,000 metric tons, which was valued at \$23.6 million. The major perlite ore producing states in the US are Arizona, California, Idaho, Nevada, New Mexico, and Oregon, with the mines in Arizona, New Mexico, and Oregon accounting for most of the tonnage mined in 2011. Major ore producers in the US are Harborlite Corp. in Arizona and New Mexico, American Perlite Co. in California, Idaho Minerals LLC in Idaho, EP Minerals LLC in Nevada, Wilkins Mining and Trucking Inc. in

Nevada, Dicapert Minerals Corp. in New Mexico, and Cornerstone Industrial Minerals Corp. in Oregon [28].

In industry, perlite is mainly used in its expanded form. The thermal, acoustic, lightweight and fire-resistant properties of expanded perlite make it invaluable in the building and construction industry, where it is generally used as a lightweight aggregate in concrete or as an insulation material in hollow bricks. Expanded perlite is also used extensively in horticulture for its ability to retain water in its cellular structure. Furthermore, its high porosity enables it to be used as a filtration aid and oil absorbent [27]. Figure 1.1 shows the percentage of perlite used in various industries in the US, as reported by the USGS in 2011 [27].

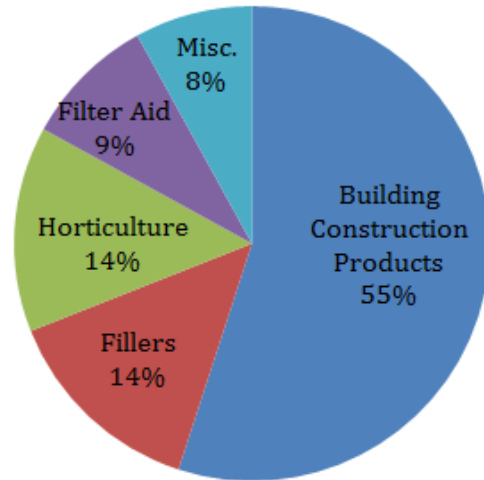


Figure 1.1: Uses of perlite in the US

1.2.4 Pumice

1.2.4.1 Background

Pumice is a porous volcanic rock formed by extruded lava containing dissolved gases. As the lava rapidly cools down and hardens, the dissolved gases form pores or vesicles that result in a low density rock. The walls of the vesicles have a glassy structure due to the rapid cooling rate of the lava. The volume, shape, and size of the vesicles, however, depend on the chemical composition of the magma. Felsic magma, which is characterized by its high silica content, results in a viscous lava flow that tends to hold more of the dissolved gases, while basaltic lava flows, with a lower silica content, tend to de-gas quickly without creating a stable vesicular structure [29]. Pumice made from the highly siliceous felsic lava is often referred to as being rhyolitic pumice, while pumice made from the basaltic lava is called basaltic pumice. Pumice that is mined commercially usually comes from air-fall deposits [29]. These deposits are created from explosive eruptions that are often associated with highly silicic felsic magma [29, 30]. The particle size and the depth of the deposits typically decrease as the distance from the volcanic source increases [29].

1.2.4.2 Physical and Chemical Characteristics

Pumice is generally light in color (white to light gray) with vesicles that have micrometer to centimeter size ranges and walls that are “visibly glassy” [29]. Pumices with isolated and/or interconnected vesicles both result in a low density rock. However, pumices with interconnected vesicles have the potential for high absorption capacity and high permeability [29]. Most pumice can be cut or broken with steel tools, while some can even be crushed by hand. These strength characteristics of pumice are usually attributed to its porous structure, as the specific gravity and hardness of the volcanic glass itself is similar to solid feldspars [29].

Rhyolitic pumices have high silica contents, typically in the 60–70% range. Basaltic pumices tend to have lower silica contents than do the rhyolitic pumices, usually containing less

than 52% SiO₂ by weight [30]. Regardless of the total silica content, the majority of the silica is glassy, which can be confirmed by XRD [30]. Researchers at the University of Utah, conducting a study for Hess Pumice Products, found that pumice from Idaho had an amorphous structure and “no well-defined crystalline minerals” [31]. According to Snellings et al. [30], pumice generally has a substantial amount of Al₂O₃ (about 15–20%) and minor quantities of Fe₂O₃ and magnesium oxide (MgO) (about 3–7% and 0–5% respectively). Alkali content can vary significantly and is primarily linked to the volcanic region of origin [30]. Phenocrysts—large chunks of minerals surrounded by a homogenous matrix of a different mineral or rock—can significantly alter the mineral and chemical composition of pumice. For example, if a pumice sample contains large phenocrysts of alkali-feldspars, it may have a higher alkali content than a pumice sample with phenocrysts of pure quartz.

1.2.4.3 Pozzolanic Nature of Pumice

Pumice has been used as a natural pozzolan throughout history, dating back to the ancient Greek and Roman civilizations. Pumice, created from eruptions in Santorin, Greece, between 1600 and 1500 BC, and from the eruption of Mt. Vesuvius in 79 AD, was used extensively as a pozzolan in the Mediterranean region [32]. In the US, the use of pumice as an SCM dates back to the early 1900s. The Los Angeles aqueduct, constructed in 1910–1912, used a blend of portland cement and rhyolitic pumice in equal parts, as reported by an American Concrete Institute (ACI) study titled “The Use of Raw or Processed Natural Pozzolan” [32]. Several dams were also built using pumice, with some examples being the Friant Dam in 1942, the Altus Dam in 1945 and the Glen Canyon Dam in 1964 [33]. In a paper on the effects of pozzolans in mass concrete, Meissner [34] reported that the addition of pumice to the Friant Dam concrete contributed very effectively to compressive strength, especially in lean mixtures. He found that a concrete mixture with 266 lbs. of cement per cubic yard and 40 lbs. of pumice had the same compressive strength as a mixture with 304 lbs. of cement per cubic yard concrete mixture with no pumice added [34].

Studies on pumice samples have shown that they meet all chemical requirements of ASTM C 618 along with most physical requirements as long as the natural pumice was ground before testing [31, 35, 36]. According to a study from Papua New Guinea, when 15% of cement by mass was replaced with pumice, the resulting blended cement met the Australian standard (AS 3972:1997) for type C cements [35]. Hossain [37] reported that calcium hydroxide contents of concrete containing pumice were lower than the calcium hydroxide content of a control concrete with only cement, as tested by XRD on ground samples. In a separate study, Hossain et al. [38] used differential scanning calorimetry (DSC) and found that concrete where 20% of the cement had been replaced by pumice had 63.2% less calcium hydroxide than the control concrete without any pumice replacement after 12 weeks of hydration.

1.2.4.4 Effect on Strength

A majority of the studies reviewed agree that replacing cement with finely ground pumice generally decreases compressive strengths. Hossain [35] found that mortars containing 10% pumice by weight of cement had their compressive strength reduced by 12% and 9% at 1 and 28 days, respectively. When the pumice content was increased to 20%, the reduction in strength increased to 21% and 20% at 1 and 28 days, respectively [35]. This trend was seen in concrete specimens as well. Hossain et al. [38] found that concrete where 20% of the cement by

weight had been replaced by pumice had a 20% reduction in compressive strength and 21.6% reduction in tensile strength, when compared to the control concrete after 28 days of hydration.

A study by Mielenz et al. [39], where 25% of the cement by weight was replaced with pumice, had more promising results in terms of mortar strength. At 28 days, 1 of the 10 pumice mortars tested had a strength higher than the control. At 90 days, 2 of the 10 pumices had greater compressive strengths than the control. Mielenz et al. [39] also showed that the use of calcined pumices in mortar generally yielded higher compressive strength when compared to mortar samples with uncalcined pumice.

Ramasamy and Tikalsky [31] showed that the difference in compressive strength between pumice and control concrete samples decreased with decreasing pumice particle size. The strength of the concrete mixture where 20% of the cement had been replaced by the pumice with the smallest particle size was only 4% lower than the control at 28 days. On the other hand, the strength of the concrete mixture containing 20% pumice with a larger particle size was 22% lower than the strength of the control.

1.2.4.5 Effect on Fresh State Properties

The use of pumice as an SCM can increase the water demand in concrete because the interconnected vesicles in the pumice particles can absorb and hold water. In addition, the finely ground pumice particles also have jagged edges that require more fluid to coat the surface of the particle. However, Hossain and Lachemi [40] and Hossain et al. [38] showed that the slumps of concretes using blended cement containing 20% pumice by weight did not significantly differ from the control, at a w/c of 0.45. The same studies found that concretes containing pumice as an SCM did not significantly alter the air content as measured by the pressure method described in ASTM C 231 [38, 40].

Using isothermal calorimetry, Ramasamy and Tikalsky [31] found that paste samples containing 20% and 30% pumice reduced the heat of hydration during the first 75 hours of measurement, when compared to a control paste with 100% cement [31]. They also observed that the amount of reduction in the heat of hydration depended upon the particle size of the pumice, with the largest reduction in heat observed in the paste with the coarsest pumice SCM.

Using Vicat needle penetration, Ramasamy and Tikalsky [31] also found that the setting time of pastes with 20% pumice were longer than that of the control. Although the pumice pastes had increased initial and final set, the setting times were within the limits for blended hydraulic cement as per ASTM C 595 [31]. In a separate study using Australian Standards, Hossain [35] found that pumice from Papua New Guinea did not significantly change the setting time in pastes containing 10 and 20% pumice by weight of cement.

1.2.4.6 Impact on Durability

Researchers [26, 31, 36] have shown that using pumice as an SCM in mortars increased the resistance to ASR. Hossain [36] found that 30% pumice by weight of cement was necessary to control ASR expansion, following the requirements in ASTM C 311, which provides instructions on standard test methods for fly ash and natural pozzolans. Using ASTM C 1260, Ramasamy and Tikalsky [31] and Gokce et al. [26] both established that a 20% replacement dosage of pumice kept expansions from ASR below the 0.1% limit prescribed in the standard.

Hossain et al. [38] found that concrete made with 20% pumice by weight of cement experienced slightly less drying shrinkage than the control concrete. However, the difference in

drying shrinkage was not significant according to ASTM C 157 [41], which describes the standard test method for measuring length change of mortar and concrete.

Ramasamy and Tikalsky [31] used ASTM C 1012, which describes the standard test method for measuring length change of mortar bars under sulfate solution, to evaluate the sulfate resistance of mortars containing three different size pumice powders at replacement dosages of 20% by weight of cement. An increase in sulfate resistance was observed for all mortar specimens containing pumice as an SCM. The control specimen with 100% ordinary portland cement (OPC) had a 26-week expansion of 0.07%, whereas the mortar made with finest pumice (mean particle size 4.0 μm) had a 26-week expansion of approximately 0.035% [31]. Mortars made with the two coarser pumices had expansions just under 0.05% over the same time period [31]. Hossain and Lachemi [40] tested the sulfate resistance of concretes containing 20% pumice by weight of cement at two different w/c. However, unlike the study of Ramasamy and Tikalsky, Hossain and Lachemi [40] reported that the concrete specimens incorporating pumice had increased deterioration compared to control concrete samples made with Type I and Type V cement.

Litvan [42] found that using pumice from Iceland as a cement replacement significantly increased the freeze-thaw durability of concrete specimens without air-entrainment when tested according to ASTM C 666-80, the standard test method for testing resistance of concrete to rapid freezing and thawing. In his study, the 100% cement reference concrete, with no air-entrainment, failed after 60 freeze-thaw cycles while concrete specimens containing 12.9% and 25.9% pumice by weight of cement lasted for 400 cycles, without any air entrainment [42]. According to the most recent ASTM C 666 standard, the test is completed once a specimen reaches an expansion of 0.1% or the specimen has been subjected to 300 cycles [43].

In a study by Hossain et al. [38], researchers found that concrete samples containing 20% ground pumice by weight of cement had a total pore volume that was 34.5% lower than concrete made with 100% portland cement, as measured by mercury intrusion porosimetry. In another study, Hossain and Lachemi [40] found that the blended cements containing 20% pumice decreased chloride penetration by over 18% when compared to a control specimen with 100% Type I cement, as measured by ASTM C 1202.

1.2.4.7 Sources of Pumice in the US and Common Uses

According to the 2012 USGS Mineral Commodity Summaries [44], there are about 25 million tons of pumice in known reserves in the western US. The USGS estimates that there are 250 million to 1 billion tons of pumice (both known and yet undiscovered deposits) in the western and Great Plains states. In 2011, 11 US companies produced 539,000 tons of pumice, mostly through open pit methods, valued at just over \$11 million [45]. The primary pumice producing states are Oregon, Nevada, Idaho, Arizona, California, New Mexico, and Kansas, with Nevada and Oregon carrying 46% of the annual production [44].

Although most of the pumice produced in the US is used as building or decorative blocks, pumice has a variety of uses that take advantage of its lightweight and porous structure, its chemical composition, and its hardness. Pumice is frequently used as an aggregate in lightweight concrete and as an SCM in blended cements, when locally available. Pumice makes a good abrasive because the glassy vesicle walls create sharp edges when broken and continue to break during use to create “fresh cutting edges” [29]. Pumice is used in block form in the restaurant industry to clean grills and for commercial use for cosmetic skin removal [29]. Figure 1.2 shows the breakdown of pumice use in the US in 2011, as reported by the USGS [45]. The “Other” category in Figure 1.2 refers to pumice used in laundries (stone washing), in pottery, and as absorbents, diluents, fill, and filter aids [45].

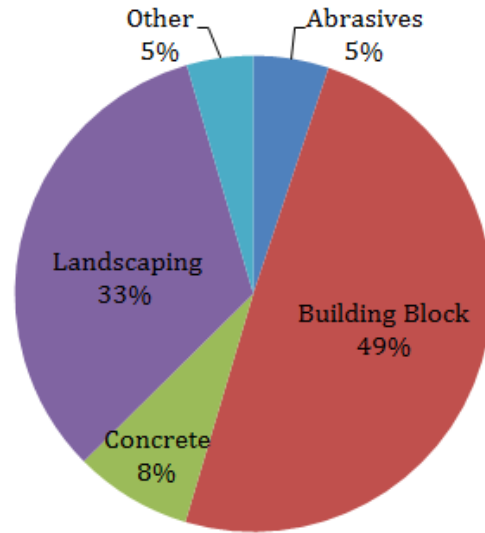


Figure 1.2: Uses of pumice in the US

1.2.5 Volcanic Ash

1.2.5.1 Background

Volcanic ash is formed when gases that are dissolved in molten rock expand rapidly from exposure to atmospheric temperature and pressure. As a result of this expansion, a violent explosion occurs that can break the molten rock apart. These fragments then cool down quickly and form glass. Fragments that are less than 2 mm (0.079 in.) in diameter are considered volcanic ash and can be composed of rock, minerals, and/or volcanic glass [32].

Chemically, volcanic ash is very similar to the other volcanic materials discussed in this literature review. Explosive eruptions, which form large plumes of volcanic ash and hot gases, are predominantly indicative of highly siliceous magmas, making volcanic ash similar in chemical composition to pumice or perlite [29]. However, volcanic ash is more likely to contain significant amounts of mineral impurities that may increase the crystallinity of the ash.

1.2.5.2 Pozzolan Nature of Volcanic Ash

Volcanic ash has been used as a natural pozzolan throughout history dating back to the ancient Greek and Roman civilizations [32]. However, because availability is dependent on volcanic activity and, more specifically, pyroclastic eruptions (eruptions that are accompanied with fast moving currents of hot gas and rock), the use of volcanic ash in concrete is less prevalent in the US than in countries with frequent volcanic eruptions. However, studies conducted on ash from the 1980 Mount Saint Helens eruption and more recent ash deposits in Papua New Guinea show that volcanic ash meets most requirements of ASTM C 618 for natural pozzolans and contributes to the pozzolan reaction in cementitious systems. In a study from 1982, Campbell et al. [46] found that while volcanic ash collected from the 1980 Mount Saint

Helens eruption met chemical requirements for ASTM C 618, the ash did not meet ASTM C 618-78 standards for pozzolanic lime activity. However, the researchers found that grinding the raw ash samples increased its reactivity by increasing the surface area of the particles. Mortar with a 20% replacement dosage of raw volcanic ash yielded a compressive strength that was 75% of the control mortar mix, when tested in accordance with ASTM C 109, the standard test method for measuring compressive strength of 2-inch mortar cubes. However, when 20% of the cement was replaced with volcanic ash that was ground down, the mortar cubes had a compressive strength that was 90% of the control mix [46]. Hossain [47] found that volcanic ash from Mount Tavorvur in Papua New Guinea met most ASTM C 618 requirements, including chemical composition, autoclave expansion, and strength activity index. Several other studies [40, 48–50] have been conducted wherein researchers have shown (using DSC) that using volcanic ash as a cement replacement in mortar reduced the calcium hydroxide content of the mixture.

1.2.5.3 Effect on Strength

Studies have shown that using volcanic ash as a cement additive (i.e., as a sand replacement) increased compressive strength of mortars. However, using it as a cement replacement decreased the compressive strength of mortars and concrete. Campbell et al. [46] found that using 20% volcanic ash as a cement additive in mortars increased compressive strength by 25% at 28 days. The same study found that replacing 20% cement with volcanic ash decreased the compressive strength of mortars by as much as 43% at 28 days [46]. Reactivity of the ashes was not only dependent upon particle size, but also upon the location where the ash was collected relative to the volcanic source. Ashes that were collected a greater distance from the source performed better than the ashes collected near the volcanic source [46].

The same behavior was observed for concrete mixtures in numerous studies reported by Hossain and Lachemi [40, 48, 49]. For example, in one study, they found that replacing 20% cement with volcanic ash reduced the 28-day compressive strength of concrete by 16% compared to the control [40]. In another study, Hossain and Lachemi [48] found that the trend of decreasing compressive strength continued as the replacement dosages of volcanic ashes were increased. After curing for 91 days, concrete specimens containing 10%, 20%, and 30% volcanic ash by weight of cement had strengths that were 8%, 16%, and 31% lower than that of the control concrete mixture containing 100% OPC [48]. A later study by Hossain and Lachemi [49] had similar results, wherein the strength of concrete samples, with a 20% replacement dosage of volcanic ash, was 22.5% lower than that of the control concrete.

1.2.5.4 Effect on Fresh State Properties

Some studies [40, 48] have shown that, like fly ash, volcanic ash also increases the slump of cementitious mixtures. Using ASTM C 143, the standard test method for measuring concrete slump, Hossain and Lachemi [40, 48] found that concrete with 20% cement replaced by volcanic ash had a slump almost 40% higher than the control, when the total aggregate-to-binder ratio (TA/B) was greater than 4.0. Concrete with a TA/B of 3.5 had an even larger increase in slump, nearly 80% higher than the control [48]. Contradictory to these studies, Hossain and Ahmed [50] found that concrete where 20% of the cement was replaced by volcanic ash did not have a significantly different slump than the control concrete, with the difference in slump values being less than 3 mm (0.118 inches).

Hossain and Lachemi [40, 48, 49] found that concrete mixtures containing volcanic ash as a cement replacement had little effect on air content. They found that replacing 20% of the cement with volcanic ash increased the air content a total of 0.3% [40, 48, 49]. Hossain and Ahmed [50] reported similar results. In their study, concrete mixtures containing 20% volcanic ash by weight of cement had air content increases of only 0.2% when TA/B ratio was 3.7. A higher TA/B ratio of 4.5 yielded an even lower air content increase of 0.1% [50].

Escalante-Garcia and Sharp [51] studied the effects of temperature on the hydration of blended cement incorporating volcanic ash from Mexico. They used an isothermal conduction calorimeter to measure the heat produced by hydration over a 72 hour period at 20 °C, 30 °C, and 60 °C [51]. Their research showed that at the two lower temperatures, 20 °C and 30 °C, the pastes containing 22% volcanic ash by weight of cement had a higher heat release per gram of cement compared to the control paste. However, at 60 °C the volcanic ash-OPC paste produced less heat per gram of cement than the control paste [51].

Hossain [35] found that using volcanic ash as a cement replacement did not significantly alter the initial and final setting time as measured by Australian standard AS 2350.4:1999. He found that mixtures, which had 10% cement replaced with volcanic ash, had an initial and final setting time very similar to that of the control sample. The mixture where 20% cement was replaced with volcanic ash, had an initial and final set that was 30 minutes longer than the control [35]. However, all setting times were within the standard deviation for a single operator as stated in ASTM C 191 [52], the standard test method for measuring setting time using a Vicat needle.

1.2.5.5 Impact on Durability

Tests on mortars containing volcanic ash as a cement replacement have shown that it is effective in reducing the expansion due to ASR. Campbell et al. [46] found that mortars, which had 20% cement by weight replaced with volcanic ashes, had their ASR expansion reduced by approximately 60% after 5 months as measured by ASTM C 441, the standard test method for measuring the effectiveness of pozzolans in preventing expansions of concrete from ASR. Hossain [47] found that replacing 10% cement with volcanic ash from Mount Tavorvur was sufficient to control expansion due to ASR, following the procedures listed in ASTM C 311.

Hossain and Lachemi [48] observed that the use of volcanic ash as a cement replacement did not have a significant effect on the drying shrinkage of concrete. They found that concrete specimens, where 20% of the cement by weight was replaced by volcanic ash, had a drying shrinkage value of 540 microstrain, whereas the value for the control specimens was 493 microstrain. These values are within the accepted standard deviation for ASTM C 157 [41].

Hossain and Lachemi [40] tested the sulfate resistance of concrete incorporating 20% volcanic ash as a cement replacement. They found that regardless of the type of cement that was used (Type I vs. Type V) the concrete specimens with volcanic ash actually had increased deterioration compared to the control.

Several studies [40, 48–50] have shown that using volcanic ash as a cement replacement decreases the total pore volume of concrete specimens when compared to a control concrete containing 100% OPC. Results showed that depending on the mix design and w/c, the total pore volume in concrete, containing 20% volcanic ash by weight of cement, decreased anywhere from 9% to over 30% when compared to the control specimens [40, 48–50]. In general, the decrease in total pore volume was greater for concrete specimens with a higher paste content and a lower w/c.

Using ASTM C 1202, Hossain and Lachemi [40, 48, 49] conducted a series of rapid chloride ion penetrability tests on 2 inch concrete specimens. With a w/c of 0.45 and TA/B of approximately 4.5, the concrete specimens containing 20% volcanic ash by weight of cement decreased the total charge passed by approximately 20% when compared to the control [40, 48]. Using the same test, the reduction in total charge increased to 60% when concrete specimens with a lower w/c (0.30) and higher paste content (TA/B = 3.55) were used [49].

1.2.5.6 Sources of Volcanic Ash in the US and Common Uses

The 2011 USGS Minerals Yearbook chapter for pumice and pumicite states “pumicite and volcanic ash are descriptive terms that are often interchangeably used” [45]. For this reason, the materials commodity data for pumice and pumicite published by the USGS includes volcanic ash reserves without any distinction between the two. Thus, for volcanic ash availability in the US, please see Section 1.2.4.7.

In investigating the possible uses of volcanic ash from the 1980 Mount St. Helens eruption, the Washington Department of Natural Resources [53] stated that volcanic ash can be used as fillers and abrasives, and in construction and ceramics. While its lightweight and pozzolanic properties make volcanic ash suitable for use in concrete, its angular shape and hardness makes it an ideal abrasive or texturing compound for paints.

1.2.6 Zeolites

1.2.6.1 Background

Zeolites are hydrated crystalline aluminosilicate minerals. The crystalline framework consists of silicate and aluminate tetrahedra that are arranged in rings [30]. These rings connect to form pores or channels of a consistent diameter throughout the crystal structure [30, 32]. As a result of the framework, zeolites are highly porous, with their pore volume often taking up as much as 50% of the total volume [54]. The pores contain exchangeable cations, which help to balance the net negative charge of the zeolite framework that is caused by the substitution of Al^{3+} for Si^{4+} in the tetrahedra. Water molecules are also held in these pores due to charge-dipole interactions [30].

Zeolites are typically formed by diagenetic alteration (physical or chemical change in deposited sediment, generally under low temperature and pressure) of volcanic glasses by alkaline fluids [30]. Consequently, the chemical composition of the zeolitized materials often coincides broadly with that of their unaltered counterparts [30]. Along with zeolites, the diagenetic alteration can also form other products like quartz, cristobalite, aragonite, thenardite, smectite, halite, calcite, feldspar, montmorillonite, unaltered volcanic glass, non-crystalline aluminosilicate gels, and hydrated iron oxides [54–56]. As a result, zeolite tuffs (rocks) usually contain other mineral impurities [54].

There are many different types of natural zeolites, with clinoptilolite being the most frequently identified zeolite mineral in natural zeolite-rich pozzolans [30]. Sprynskyy et al. [56] reported that some zeolite tuffs contain as much as 70% clinoptilolite. Clinoptilolite is a member of the heulandite family of zeolites, and is differentiated from heulandite by the ratio of silicon and aluminum in the crystal matrix. An Si/Al ratio greater than 4 indicates the presence of clinoptilolite, while a Si/Al ratio less than 4 is representative of heulandite [57]. In other words, clinoptilolite is a silica-rich polymorph of heulandite [30]. Clinoptilolite has a compositional flexibility which promotes its formation [30], and has a greater thermal stability than heulandite

[56]. Examples of clinoptilolite chemical compositions from around the world, as reported in previous literature [57–66], show that the silica content of clinoptilolite can vary widely from 58 to 70%, while the alumina content ranges from 9 to 21%. The average void volume of clinoptilolite zeolite is 34% [56]. In addition to clinoptilolite, some other common siliceous zeolites are mordenite and erionite. Common aluminous zeolites include phillipsite, chabazite, analcime, and heulandite [30].

1.2.6.2 Pozzolanic Nature of Zeolites

In ancient Rome, concrete for hydraulic projects (such as dams and aqueducts) was prepared by mixing lime, water, powdered clay brick, and pieces of zeolitic tuff. The durable properties of such concrete have been attributed to the presence of zeolitic tuffs and their capability to act as a pozzolanic material [55]. Currently, zeolites are being used as a cement additive in many countries, such as Bulgaria, China, Cuba, Germany, Jordan, Russia, Turkey, and the US [55]. In a study titled the “Use of Zeolitic Tuff in the Building Industry,” Colella et al. [55] reported that zeolitic tuff from California was one of the main constituents of the pozzolanic cement that used to be manufactured by the Monolith Portland Cement Company in the US.

Published research has shown encouraging evidence of zeolites being good pozzolans in cementitious mixtures [62, 65]. Lilkov et al. [62] found that cement pastes with 5–10% zeolites had lower calcium hydroxide contents than the control paste, as early as 28 days. Perraki et al. [65] also found that pastes where 10–20% cement by weight was replaced with zeolites contained less calcium hydroxide than the control paste at all ages tested.

1.2.6.3 Effect on Strength

The effect of using zeolites as a cement replacement on the strength of cementitious mixtures is disputed in the literature. Ahmadi et al. [58] tested zeolites at cement replacement dosages of 5–20% by weight and saw that the compressive strengths of the concrete specimens containing zeolites were higher than that of the control at all the ages tested and for all replacement levels. The optimum replacement dosage, based on strengths at 90 days, was found to be 15% [58]. Other researchers saw a reduction in compressive strength development with increasing dosages of cement replacement with zeolite [61, 65, 67]. All zeolite-cement mortars studied by Lilkov et al. [61] had reduced compressive and flexural strengths at 28 days. Similarly, Perraki et al. [65] found that pastes where 20% cement by weight was replaced with zeolite had lower compressive strengths at all ages when compared to the control. In another study, particle size has been shown to have a marked effect on compressive strength, with decreasing zeolite particle size leading to increasing compressive strengths in mortars [68].

1.2.6.4 Effect on Fresh State Properties

Cementitious mixtures with zeolites have a high water demand because of the zeolites’ high surface area and porous crystal structure. Several studies have demonstrated that the water demand increase is proportional to the dosage of zeolite used in the mixture [58, 59, 61, 65]. Ahmadi et al. [58] reported that as the replacement dosage increased, a greater amount of superplasticizers was needed to maintain the slump.

Perraki et al. [65] found that the initial and final setting time of pastes with up to 20% zeolites did not vary significantly from that of the control. These results contrast sharply with the

findings of Bilim [59], who found that the incorporation of zeolites at a 20% replacement dosage of cement increased the initial and final setting time of pastes by about an hour.

Some researchers have shown that replacement of cement with zeolite results in the cementitious mixture having a lower heat of hydration [61, 69]. However, some zeolites have been shown to advance the onset of the acceleration period of cement hydration [70]. Lilkov et al. [62] found that although the zeolite-cement paste mixtures initially generated less heat, in the long run their cumulative heat was greater than that of the control. This suggested that there was a slower but more prolonged reaction occurring between the zeolites and the cement hydration products.

1.2.6.5 Impact on Durability

Although studies have shown that natural zeolites can mitigate deleterious expansions of ASR in mortars [58, 71], the results vary on the minimum percentage needed to mitigate expansions. Using ASTM C 1260, Ahmadi et al. [58] found that a 20% replacement dosage of zeolites was needed to keep expansions below the prescribed limit of 0.1%, whereas the research by Gokce et al. [26] and Karakurt et al. [71] showed that higher replacement dosages (of 25% and 30%, respectively) were needed to mitigate the expansions from ASR.

Janotka et al. [72] found that blended cements containing 35% zeolites had a resistance to sulfate attack that was similar to Type V cements (high sulfate resistant cements). Similarly, Karakurt et al. [71] found that mortars containing zeolites at a cement replacement level of 30% had an expansion of 0.017% when submerged in 10% sodium sulfate solution for 26 weeks, which is under the ASTM C 1157 [73] expansion limit of 0.05% for high sulfate resistant cement (when tested in 5% sodium sulfate solution). SEM images of the zeolite mortars did not show any evidence of extensive ettringite formation, unlike the images of the control mortars [71].

Bilim [59] looked at the performance of mortars with zeolites, when subjected to freezing and thawing. He found that up to a replacement dosage of 5%, the zeolite mortars performed better than control specimens in freeze-thaw conditions. However, higher replacement levels of zeolites led to mortars with a lower freeze-thaw resistance than the control [59].

Bilim [59] saw reduced carbonation depths in mortars where 5–30% cement by weight was replaced by zeolites, after 28 days of hydration. At 28 and 56 days, the minimum depth of carbonation was seen in mortars with a 30% replacement dosage. However, at 90 days the minimum depth of carbonation was observed in the mortar with a 20% zeolite replacement.

Bilim [59] found that the water sorption and oxygen permeability of mortars, where 5–30% cement by weight had been replaced by zeolite, were lower than that of control. The lowest water sorption and oxygen permeability was seen for mortars with a 20% replacement dosage. Similarly, Ahmadi et al. [58] showed that concrete specimens where 5–20% cement by weight was replaced with zeolites had a lower water absorption than that of the control. However, he found that the oxygen permeability of the concrete specimens became higher than the control, when the replacement dosage exceeded 10%. However, at a lower dosage of 5–10%, the oxygen permeability of the zeolite concrete was lower than both the control and the silica fume concrete (made with the same replacement percentages).

Ahmadi et al. [58] investigated the chloride resistance of concrete specimens with zeolite using ASTM C 1152, which is the standard test method for determining the amount of acid soluble chloride in mortar and concrete. He also measured the electrical resistivity of the zeolite concrete specimens using AC Impedance Spectrometry. The results from the study show that

replacing 10–20% cement by weight with zeolites decreased chloride diffusion and increased electrical resistivity of the concrete specimens.

Lilkov [61] found that after 28 days of hydration, mortars containing 10–20% zeolites as a cement replacement had a lower specific pore volume, when compared with the control mortar.

1.2.6.6 Pretreatments to Increase Zeolite Reactivity

Several studies have suggested that calcination could increase the reactivity of zeolites for use in concrete, as heating past 300 °C causes destabilization of the zeolite crystal latticework and increases the ability of the zeolites to participate in pozzolanic reactions [57, 74–76]. However, the results of previous investigations on the effect of calcination on zeolite performance are inconsistent. Some research has suggested that heating zeolites can increase strength or pozzolanic reactivity considerably [75, 76], while others saw only marginal gains [57, 74]. Similarly, the optimum calcination temperature is debated. One study reported that calcining zeolites to temperatures equal to or above 500 °C provided the most benefit [75], while others have suggested that lower calcination temperatures of 350–400 °C produced zeolites with a higher reactivity [57, 74, 76].

The basic structure of zeolites is a three-dimensional framework of silicate tetrahedra. As mentioned earlier, the substitutions of aluminate within the crystal structure of the zeolite result in a net negative charge throughout the structure, which is balanced by cations such as Na^+ , K^+ , and Ca^{2+} [30, 54]. The cations sit within the pores formed by the aluminosilicate tetrahedra, and are only loosely bound to the structure [54]. Pabalan and Bertetti [54] reports that the ease with which cations exchange from the zeolite system depends on a number of factors, including the dimensions of the pores and channels, the “polarizability” of the ion, the charge density of the zeolite framework, the ionic charge, and finally the concentration in the surrounding electrolyte medium [54]. Temperature could also play a role in the exchange of cations from zeolites [77]. As a result of these contributing factors, it is not possible to predict ion-exchange selectivity as a function of the zeolite composition only [78].

Although it has been suggested that exchangeable cation content influences pore solution chemistry and short-term pozzolanic reactivity [70], very little research has been done in this area. Mertens et al. [63] combined cation-exchanged zeolites, lime, and water and tracked the calcium hydroxide content of the pastes over 180 days using thermal gravimetric analysis (TGA) and DSC. They found that the clinoptilolite exchanged with K^+ or Na^+ ions reacted with a greater quantity of lime than did clinoptilolite exchanged with Ca^{2+} ions [63]. Similar results were found by Snellings et al. [79], indicating that K^+ and Na^+ rich zeolites will have a greater pozzolanic reactivity than Ca^{2+} rich zeolites.

1.2.6.7 Sources of Zeolites in the US and Common Uses

According to the USGS, in 2011 the US had a zeolite production of 65,400 metric tons. Six US companies currently mine zeolites, with reserves in Arizona, California, Idaho, Nevada, New Mexico, Oregon, and Texas [80]. The major US ore producers are St. Cloud Mining, Inc. in Arizona, California, and New Mexico; UOP LLC in Arizona; KMI Zeolite Inc. in California; Bear River Zeolite Co., Inc., Steelhead Specialty Minerals, Inc., and Teague Mineral Products Co. in Idaho; and Zeotech Corp. in Texas [80]. Possible resources in the US may be as much as 10 trillion tons for zeolite-rich deposits [81].

Zeolites are used in many industries as molecular sieves. However, the zeolites used in industrial applications are often synthesized to decrease impurities and control the pore opening

sizes. According to the USGS, in 2011, the uses for natural zeolites in the US, in decreasing order by tonnage, were “animal feed, pet litter, cement, odor control, water purification, wastewater treatment, fungicide or pesticide carrier, gas absorbent (and air filtration), fertilizer carrier, oil absorbent, desiccant, catalyst, and aquaculture” [80].

1.2.7 Clay

1.2.7.1 Background

Clays are fine-grained soils containing phyllosilicate particles, which can incorporate a considerable amount of water [30]. The level of fineness of the particle size at which soil is considered to be clay varies depending on the profession or the standards being used. The US Department of Agriculture defines the particle size of clays to be less than 2 μm [82]. The Unified Soil Classification System (ASTM D 2487) identifies a fine-grained soil (a soil with 50% of its particles passing the No. 200 sieve) to be a clay based on its liquid limit and its plasticity index [83]. The definitions of “liquid limit” and “plasticity index” and the methods to determine these limits are presented in ASTM D 4318 [84].

1.2.7.2 Clay Minerals: Types and Crystal Structure

The phyllosilicate particles in clay are commonly called “clay minerals.” Diagenetic alteration of volcanic rocks in low temperatures or by mild alkaline fluids usually leads to the development of clay minerals [30]. These minerals are composed of tetrahedrally (T) coordinated sheets of SiO_4 and AlO_4 , connected to octahedrally (O) coordinated sheets composed of cations, such as Al^{3+} and Mg^{2+} . These sheets then come together in a T-O or a T-O-T formation to create layers [30]. Depending on the charge of the layer, interchangeable interlayer cations (such as K^+ , Na^+ , Mg^{2+} , Ca^{2+}) can be present [30,85]. When in contact with water, these interlayer cations form adsorption complexes with the water molecules, causing the layers to become negatively charged and repulse each other, which ultimately results in the swelling of the clay [85, 86]. The structure of clay and its water absorption capacity has important implications in the use of clay as a pozzolan, as will be discussed in Section 1.2.7.3.

Common clay minerals are kaolinite, smectite (montmorillonite), illite, chlorite, and palygorskite-sepiolite [30]. The layers in kaolinite have two sheets only, forming a T-O structure, with no interlayer cations. This makes it a non-swelling clay. Montmorillonite has a T-O-T structure, with weakly bonded interchangeable interlayer cations that can be easily separated by the adsorption of polar liquids such as water [85]. Illite has a crystal structure similar to montmorillonite, except the resulting charge deficiency in the layers is balanced by strongly bonded K^+ cations that cannot be easily interchanged [85, 86]. Therefore, the swelling capacity of illite is less than that of the montmorillonite.

1.2.7.3 Pozzolan Nature of Clay

In general, clays are highly siliceous and contain an appropriate amount of $\text{SiO}_2 + \text{Al}_2\text{O}_3 + \text{Fe}_2\text{O}_3$ to be classified as Class N pozzolans, as required by ASTM C 618. However, tests of untreated clays as pozzolans have been unsatisfactory both in terms of reactivity and workability [30, 87]. He et al. [87] suggested that the highly stable crystal structure of the unaltered clays makes them unreactive. Furthermore, the high specific surface area of the clay particles decreases the workability of the cementitious mixtures they are incorporated into

[87]. In order to make the clay particles more reactive, it is necessary to break down this stable structure. Several studies have found that calcining clay beyond dehydroxylation activates its pozzolanic properties by turning the clay minerals more amorphous [30, 87, 88]. However, the optimum calcination temperature of a clay is dependent upon the clay mineral it contains, as the behavior of each type of clay mineral is different during heating [85, 89].

1.2.7.4 Effects of Thermal Treatment

Fernandez et al. [85] performed XRD and derivative thermogravimetric analysis at different calcination temperatures to compare the thermal decomposition of kaolinite, montmorillonite, and illite. The results show that during dehydroxylation, kaolinite undergoes a significant loss of crystallinity, while illite and montmorillonite are able to lose their hydroxyl ions without much change to their crystal structure. For kaolinite, all crystalline peaks disappeared from XRD patterns after calcination to about 600 °C. However, for illite, the XRD patterns of the raw sample and the samples calcined at 600 and 800 °C were almost identical. Montmorillonite showed a slightly higher level of decomposition than illite, with one of the major crystalline peaks shifting to indicate a collapse of the basal plane due to interlayer water removal [85]. These results corroborate well with the relative reactivity of these different clay minerals. Generally, the more amorphous the clay minerals are, the higher their reactivity is. Most studies agree that kaolinite, which experiences the highest amount of decomposition during calcination, is the most reactive of all clays minerals, and can significantly enhance the mechanical properties of cementitious mixtures [85, 90]. Illite and montmorillonite clays, which do not have significant decomposition during calcination, react much slower than the kaolinite. Fernandez et al. [85] found that calcined illite behaved almost like an inert filler, while calcined montmorillonite exhibited some late pozzolanic activity (between 28 to 90 days) in terms of compressive strength and calcium hydroxide consumption [85].

Habert et al. [89] argued that the pozzolanic activity of calcined clays depended more on the amount of amorphous clay in the sample, rather than the type of clay mineral. Their study found a direct correlation between the amount of activated clay present in the calcined sample and the compressive strength of the cementitious mixture made with that clay [89]. However, finding the correct calcination temperature to activate the clay is difficult. Overheating the clay samples causes crystallization of inactive high temperature phases, which reduces the amorphous content [30, 89]. Using XRD analysis, Habert et al. showed that the window of temperature between dehydroxylation and recrystallization is much larger for kaolinite than for illite and montmorillonite [89]. This makes it harder to find an optimum calcination temperature for soils containing illite or montmorillonite than for soils containing kaolinite.

Studies have also shown that thermal treatments tend to agglomerate the clay particles and reduce their surface area [85, 87]. Additionally, the workability of the cementitious mixtures incorporating calcined clays was reported to be better than those mixtures with untreated clays. He et al. [87] suggested that the improved water demand was a result of the changes in particle size distribution of the heated clay minerals.

1.2.7.5 Distinction between Metakaolin and High-Reactivity Metakaolin

Since kaolinite is the most reactive clay mineral, a majority of the research that has looked into the benefits and drawbacks of using clay as an SCM has concentrated on calcined kaolinite clays, which are also called metakaolin. An important distinction to note while discussing these research papers is the difference between metakaolin and high-reactivity

metakaolin (HRM). Ramlochan et al. [91] stated that “the term ‘high-reactivity’ is used to distinguish a white, purified, manufactured, thermally activated kaolinite from lesser reactive calcined clay pozzolans, which contain impurities that cannot be activated to a pozzolanic form at the temperatures used to produce metakaolin.” The ACI report “The Use of Raw or Processed Natural Pozzolans in Concrete” [32] provides a similar description and used the AASHTO M321-04 specification to distinguish between metakaolin and HRM.

In this review, care has been taken to highlight the type of metakaolin that was used for each of the papers. However, very few papers explicitly mention the “high-reactivity” term, and instead provide a sample description. This review will mention when the samples were determined (from the sample description) to fall within the “high reactivity” category.

1.2.7.6 Effect on Strength

Zhang and Malhotra [92] found that concretes incorporating HRM (determined by sample description) as a cement replacement had a rapid strength development. The compressive strength of concrete specimens with 10% HRM had caught up to that of the control by the third day and remained higher than the control at all ages. Furthermore, during the first week, the concrete with 10% HRM replacement exhibited higher strengths than the concrete with 10% silica fume replacement. However, the reverse was true after 28 days, when the rate of strength development for the concrete with HRM started to slow down [92]. Similarly, Guneyisi et al. [93] found that concrete with 20% of cement replaced by HRM had significantly higher compressive strengths than the control at 7 days. Badogiannis et al. [94] compared the compressive strengths of concrete incorporating a poor calcined kaolinite and a commercially distributed calcined kaolinite of high purity. After the first three days, both the poor and the commercial calcined kaolinite concretes had higher compressive strengths than that of the control for cement replacement dosages of 10 and 20%.

As discussed in Section 1.2.7.4, it is generally agreed in literature that clays containing montmorillonite or illite react slower than kaolinite clays. However, there is not a consensus on whether the use of these other clays as a cement replacement results in a compressive strength higher than that of the control with 100% OPC. There has been some research looking at the effect of bentonites (which is a clay primarily composed of montmorillonite) on the properties of concrete. Mirza et al. [95] found that the strength gain by concrete incorporating calcined bentonite (heated up to 150°) was faster than the concrete specimens with untreated bentonite. However, the strength of concrete mixtures, with a 20% replacement dosage of calcined bentonite, was only 74% of the control at 28 days. Ahmad et al. [96] found more promising results, where concrete with 20% untreated bentonite had a compressive strength that was 12% lower than that of the control at 28 days. The strength gained by these concrete samples was faster when the bentonite was calcined at 500 °C. By 28 days, the calcined bentonite concrete specimen had reached a compressive strength that was only 6% lower than that of the control. Memon et al. [97], working with bentonite from the same region, found that calcining the clay to 200 °C produced better results than what was observed by Ahmad et al. At 28 days, the concrete specimens where 21% of the cement was replaced by bentonite (calcined at 200 °C) had strengths similar to that of the control.

1.2.7.7 Effect on Fresh State Properties

Zhang and Malhotra [92] reported that concrete mixtures with a 10% HRM (as determined by sample description) had a workability that was similar to concrete mixtures with

10% silica fume. The final setting time of the HRM concrete was about 45 minutes earlier than that of the control. The setting times correlated well with the autogenous temperature rise in a 6 in. x 12 in. (152 mm x 305 mm) cylinders of HRM concrete. The maximum temperature of the HRM concrete was not only higher than that of the control, but also reached the maximum level 5 hours earlier than the control specimen [92]. These results point to an early reactivity for metakaolin.

For bentonite clays, most studies found that for a fixed w/c, the slump decreased as the percentage of bentonite in the concrete increased [95–97]. Ahmad et al. [96] found that, at a w/c of 0.55, a concrete mixture with a 20% replacement dosage of bentonite had a slump value that was about an inch lower than that of the control.

1.2.7.8 Impact on Durability

A study by Ramlochan et al. [91] used the Canadian standard CAN/CSA A23.3-14A (similar to ASTM C 1293, which measures the length change of concrete prisms due to ASR) to investigate the effect of HRM in preventing expansions from ASR. When using a highly reactive aggregate called Spratt, it was found that replacing 15% cement with HRM was sufficient to limit the ASR expansion of the concrete prisms at 2 years to less than the 0.04% limit criterion of CAN/CSA A23.2-14A. When a lesser reactive aggregate known as Sudbury was used, only 10% HRM replacement was needed. Pore solution studies of equivalent cement-HRM pastes showed a significant reduction of alkalinity at replacement levels of 20%. However, the study noted that the reduction in pH was not high enough to depassivate reinforcing steel, ensuring that corrosion is not a problem [91].

Concrete with HRM has been reported to improve drying shrinkage [92, 93]. Guneyisi et al. [93] found that, irrespective of the w/c, a higher replacement of HRM resulted in a lower amount of drying shrinkage. At a w/c of 0.55, the concrete specimens with a 20% metakaolin replacement had 18% lower drying shrinkage than the control.

Al-Akhras [98] tested the sulfate resistance of concrete where HRM was used as a cement replacement by measuring the expansion and the compressive strength reduction of concrete specimens that were exposed to 5% sodium sulfate solution for 18 months. While the control concrete specimens completely disintegrated by 18 months, the concrete specimens with HRM showed only marginal levels of deterioration. At a w/c of 0.5, the control specimens had an expansion of 0.4%, while concrete with 10% HRM replacement had only a 0.1% expansion [98]. These results correspond well with a study by Khatib and Wild [99], where mortar bars were exposed to a 5% sodium sulfate solution for up to 520 days. Mortar bars containing cement with a high C₃A content needed a 20% HRM (determined by sample description) replacement by weight of cement to keep expansions below 0.1% and prevent disintegration at 520 days. The control specimen for the high C₃A cement disintegrated within the first 100 days. The mortar bars containing cement with an intermediate C₃A content needed only 10% replacement of HRM by weight of cement to keep expansions below 0.1%. The control specimen for the intermediate C₃A cement reached expansions greater than 0.5% at 520 days [99].

Ahmad et al. [96] found that, after being soaked in a 5% Na₂SO₄ solution for 90 days, mortar containing untreated bentonite at a replacement dosage of 30% had a much higher compressive strength than the control mortar. This indicates that the use of bentonite as an SCM increases the sulfate resistance of mortars. Although a similar trend was seen for the mortars samples soaked in a 2% MgSO₄ solution, the compressive strength of the 30% bentonite mortar was only marginally higher than that of the control.

Using ASTM C 1202, Zhang and Malhotra [92] evaluated the resistance of concrete with HRM (determined by sample description) to chloride ion penetration. The results showed that concrete with a 10% cement replacement by HRM had a much higher resistance to chloride ion penetration than the control specimen with 100% OPC, but similar resistance to concrete with 10% silica fume replacement [92].

Zhang and Malhotra [92] evaluated the performance of concretes incorporating HRM (determined by sample description) in ASTM C 666 freeze-thaw tests and in ASTM C 672 salt scaling tests. After 300 cycles of freezing and thawing, concrete where HRM was used to replace cement by 10% showed excellent resistance to freeze-thaw damage, with a residual flexural strength of 89% and a durability factor of 100.3%. The residual flexural strength and durability factor values for the control portland cement concrete specimens were 85% and 98.3% respectively. It must be noted here that all the concrete specimens used were air-entrained. For the salt-scaling test, the concrete with 10% HRM underperformed slightly when compared to the control concrete, but had similar results to the concrete with 10% silica fume. Both the concrete specimens with HRM and silica fume had moderate salt scaling with some coarse aggregates visible at the surface. The control concrete specimen also had some slight salt scaling, but no coarse aggregates were visible [92].

1.2.7.9 Sources of Clay in the US and Common Applications

According to the USGS, the amount of clay sold or used by domestic producers in 2011 was 25.9 million metric tons valued at \$1.56 billion. Please refer to Table 1.1 for a breakdown of the production values and uses for different types of clay found in the US [100]. The 10 leading producer states in 2010 (listed in decreasing order of tonnage) were Georgia, Wyoming, Texas, Alabama, Missouri, North Carolina, Ohio, Tennessee, Virginia, and Mississippi. The 10 leading producer companies in 2010 were American Colloid Co. (bentonite), BASF SE (bentonite, fuller's earth, and kaolin), Bentonite Performance Minerals LLC (bentonite), Black Hills Bentonite Co. (bentonite), General Shale Products Corp. (common clay and shale), Imerys SA (ball clay and kaolin), Nestle S.A. (fuller's earth), Oil-Dri Corp. of America (fuller's earth), Texas Industries Inc. (common clay and shale), and Unimin Corp. (ball clay and kaolin) [101].

Table 1.1: Production and Uses of Different Clay in the US

| Types of Clay | Production in US mines (thousand metric tons) | Uses | Percentage |
|-----------------------|---|-----------------------|------------|
| Ball Clay | 940 | Floor and wall tile | 39% |
| | | Sanitary ware | 21% |
| | | Other uses | 40% |
| Bentonite | 4950 | Absorbents | 30% |
| | | Drilling mud | 26% |
| | | Iron ore pelletizing | 13% |
| | | Foundry sand board | 12% |
| | | Other uses | 19% |
| Common Clay and Shale | 12,200 | Brick | 47% |
| | | Lightweight aggregate | 25% |
| | | Cement | 21% |
| | | Other uses | 7% |
| Fire Clay | 240 | Heavy clay products | 50% |
| | | Refractory products | 50% |
| Fuller's Earth | 2100 | Absorbent uses | 72% |
| | | Other uses | 28% |
| Kaolin | 5480 | Paper | 44% |
| | | Other uses | 56% |

1.2.8 Shale

1.2.8.1 Background

Shale is a fine-grained sedimentary rock, which is usually formed from diagenetic alteration of clays. When clays undergo compaction, initially mudrock is formed, which eventually transforms into shale when cleavage or laminations are developed [30, 102]. Shales exhibit similar chemical composition to the clays from which they are derived, although the water content is much lower. Shales can also contain opal, which is an amorphous form of silica, usually found as a low temperature mineral in sedimentary rocks, or in the skeletal material of organisms like diatom [32]. Shales containing a significant amount of opaline silica are called opaline shales.

1.2.8.2 Pozzolanic Nature of Shale

The use of shale as a pozzolan in the US dates back as early as 1932, when calcined opaline shales from the Monterey Formation were used by the Santa Cruz Portland Cement Co. of Davenport, California, to make a portland-pozzolan cement. The California Division of Highways used this portland-pozzolan cement in the construction of the Golden Gate Bridge and San-Francisco Oakland Bay Bridge [34]. Additionally, calcined shales were also used as a pozzolan in the construction of dams such as the Davis Dam of 1950, which used opaline shales,

and the Flaming Gorge Dam of 1963, which used montmorillonite shales [33]. In more recent times, a calcined shale product was commercially available in the mid-Atlantic region of US from 1996 to 2004, and was used in the production of ready mix concrete, concrete pipes, and pre-stressed concrete [32]. A precast plant also utilized calcined shale pozzolan to make self-consolidating concrete with early strength development and improved rheological properties [103].

All the applications listed above used shales that were calcined. Since shale is composed of clay minerals, it needs to be heated in order to activate its pozzolanic potential. In 1950, Mielenz et al. [39] looked at the effects of calcination on 70 different pozzolanic materials using data originally gathered at the Bureau of Reclamation. Eleven shale materials were included in the test matrix. In most cases, calcination up to temperature of 1800 °F (980 °C) increased the compressive strength of mortars where shale was used as a cement replacement [39].

The ACI report “The Use of Raw or Processed Natural Pozzolans in Concrete” [32] states that shale is calcined in rotary kilns with temperatures generally ranging from 1800–2000 °F (980 to 1090 °C) and a residence time of approximately 45 minutes. The resulting clinker is air quenched and ground up to a Blaine fineness of about 600 to 800 m²/kg. ACI also reports that the loss on ignition (LOI) value of calcined shale can be between 1–5%. Unlike fly ash, this high LOI is not due to the presence of carbon, but due to the presence of residual water molecules in the clay mineral and uncalcined calcite (CaCO₃). As such, the high LOI of calcined shale does not have any bearing on the effects of air entrainment in concrete with calcined shale [32].

1.2.8.3 Effect on Strength

Khanna and Puri [104] tested the compressive strength of concrete cylinders with various replacement dosages of calcined shale found near the Bhakra dam in India. They found that, with a 20% replacement, the compressive strength was almost 96% of the control at 28 days. Within a year, the concrete with 20% replacement had no difference in compressive strength relative to the control. However, the compressive strength of the concrete with 25% shale replacement was 7% less than the control at the one year mark.

Mielenz et al. [39] also tested the compressive strength of mortars using different types of shale as a pozzolan. Generally, the compressive strength of mortars with calcined shale was greater than that of mortars with raw (uncalcined) shale. Additionally, mortars with calcined opaline shales gained strength faster than mortars with calcined clay shales. Typically, the compressive strength of mortars having a 30% replacement dosage of opaline shale (calcined at temperatures of 1400–1600 °F) exceeded the compressive strength of the control by 28 days. Mortars with 30% replacement dosage of clay shale (calcined above 1800 °F) had compressive strengths equal to or greater than 86% of the control mixture.

Neal and Ramsburg [103] also found that concrete made with pulverized calcined shale (produced by the Lehigh Cement Company) was capable of achieving early-age strength similar to a standard production mix. Self-consolidating concrete mixtures with a 30% replacement of cement by pulverized calcined shale achieved a compressive strength that was 96% of the control mixture compressive strength by 28 days.

1.2.8.4 Effect on Fresh State Properties

Khanna and Puri [104] found that even at cement replacement dosages of 25%, concrete with calcined shale had slumps that were similar to that of the control concrete mixture, provided that a constant w/c was used. Ramsburg and Neal [103] found that using a 30% replacement of

pulverized calcined shale in their self-consolidating concrete improved the flow and the slump spread of the mixture. Not only that, the portland–pozzolan mixture also had a lower tendency for segregation and was less sensitive to minor changes in the water content or aggregate properties. Ramsburg and Neal [103] proposed that the lower specific gravity (2.63) and the smooth surface texture of the calcined shale led to the improvement of rheological properties in their mixture.

Khanna and Puri [104] found that concrete with a 20% replacement of calcined shale had a lower heat of hydration. At 1 day, the temperature rise of the shale concrete was 12% lower than that of the control. As time passed, the relative heat reduction became even greater, with the temperature rise being lowered by about 25% at 3 days, and 30% at 28 days. Elfert et al. [33] presented similar results, where a 30% cement replacement by diatomaceous (opaline) shale, reduced the temperature rise in concrete by about 10 °F at 30 days.

1.2.8.5 Impact on Durability

Using ASTM C 441, Ramsburg and Neal [103] found that ASR expansion in mortars where 25% cement had been replaced by pulverized calcined shale was 70% lower than that of the high alkali control. Results from the Bureau of Reclamation show that when calcined shale was used to replace 20% of cement in mortars, cast with high alkali cement and Pyrex glass, expansion from ASR was effectively kept around 0.1% at 12 months, whereas the expansion for the control, with no calcined shale, exceeded 0.5% at 12 months [33].

Using test method CRD-C 123, from the US Army Corps of Engineers “Handbook for Concrete and Cement,” Pepper and Mather [105] tested the ASR resistance of opaline shales in mortar. The major difference between the CRD-C 123 and ASTM C 227 (the mortar bar method to determine alkali reactivity of cement-aggregate combinations) is how the reactive Pyrex aggregates used in the test are graded [105]. The authors found that using 30% calcined opaline shale in mortar as a cement replacement reduced expansions from ASR by 87% or more, when compared to the control mortar with only cement [105]. A review by Stanton in 1950 [106], which reported results from studies undertaken by the California Division of Highways, showed that a 15% replacement of cement by opaline shales from the Monterey Formation was sufficient to mitigate ASR from any known California reactive aggregates.

While most of the reported studies show that calcined shales are effective in mitigating ASR, in 1986, Davies and Oberholster [107] found that a 25% replacement of calcined shale was not effective in keeping expansions below 0.1% at 12 days when using the NBRI (National Building Research Institute) Accelerated Test (on which ASTM C 1260 was based). However, when they used ASTM C 227, expansions of mortars with 25% and 30% replacement of calcined shales were around 0.05% at 1 year [107].

Khanna and Puri [104] found that the usage of calcined shale did not adversely affect the drying shrinkage of the concrete. The drying shrinkage was either equal to or better than the control at all replacement dosages.

Using ASTM C 1012, Ramsburg and Neal [103] found that mortars with a 25% replacement dosage of calcined shale had an expansion value of 0.023% at 26 weeks when tested with a low C₃A cement. When tested with a high C₃A cement, the expansion was 0.032%. In both cases, the expansion values correspond to a high sulfate resistance, according to the limits prescribed in ASTM C 1157 [73]. Results from the Bureau of Reclamation, reported by Kalousek et al. [108], also showed that concrete made with shales had a high resistance to sulfate

attack. Out of the eight shales that were tested at a replacement dosage of 35%, six of them had expansions of 0.12% or less, after soaking continuously in a 2.1% Na₂SO₄ for around 20 years.

Khanna and Puri [104] found that the demand for air-entraining agent was slightly increased when using calcined shale as a pozzolan in concrete. Ramsburg and Neal [103] reported that their air-entrained self-consolidated concrete, with calcined shale, had a good resistance to freeze-thaw damage and deicer scaling. Under a modified ASTM C 666 test, the SCC with calcined shale had a durability factor of 96%, which is equal to the freeze-thaw durability of the control [103].

1.2.8.6 Sources of Shale in the US and Common Uses

The USGS reports the production of common clay and shale together. Table 1.1 in Section 1.2.7.9 contains production information in the category of “Common Clay and Shale.” According to the USGS, common clay and shale is mostly used in brick, lightweight aggregate, and cement manufacturing [100, 101]. Shales can also be a source rock for oil and natural gas [109]. Shale containing oil and gas is not the same as “Oil Shale,” which is another fine-grained sedimentary rock containing kerogen [110]. There has been a proliferation of activity into new shale plays in the US [109]. For more information on the sources of shale in the US, please refer to a study by the US Energy Information Administration titled “Review of Emerging Resources: U.S. Shale Gas and Shale Oil Plays” [109].

1.2.9 Diatomite (Diatomaceous Earth)

1.2.9.1 Background

Diatomite is a sedimentary rock created by deposits of siliceous diatom skeletons (frustules) and calcareous (composed of calcium carbonate) biogenic material in both fresh and saltwater environments [30]. Researchers have found that the depositional environment (fresh versus salt water) significantly affects the size and reactivity of the siliceous frustules, with lacustrine environments (lake beds) creating the smallest frustules [111]. Mineralogical studies show that diatomites are primarily composed of opal-A (a reactive form of silica) and calcite, with some quartz and clay minerals and minor to trace amounts of feldspars [111]. Although the term diatomaceous earth (DE) more accurately describes unconsolidated sediment, it is sometimes used interchangeably with the term diatomite, which usually refers to the more lithified (consolidated) deposits [112].

1.2.9.2 Physical and Chemical Characteristics of Diatomite/DE

Diatomite is usually light in color, and has an appearance similar to chalk [112]. It can also be considered a lightweight mineral because of its low density and high porosity [112]. Due to its porous structure and intricate surface, diatomite has a specific surface area approximately 10 times greater than that of portland cement [32]. Using Fourier transform infrared spectroscopy, Yilmaz [113] studied the surface structure of a relatively pure diatomite (SiO₂ content of 89%) and found that diatomite is hydrophilic due to the Si-OH bonds on its surface. This affinity for water, coupled with its high specific surface area, may lead to an increase in water demand when diatomite is used as an SCM.

As mentioned before, the chemical compositions of diatomites can vary significantly based on their depositional environment and geographic location. While pure diatomites can

have silica contents greater than 95%, impure diatomites can have SiO₂ contents ranging anywhere between 25 and 90%. A majority (50–90%) of this silica is considered to be reactive [30, 111, 113–116]. Calcium oxide (CaO) content is typically lower and varies in the range of 0–10%. However, some diatomites can have as much as 50% CaO [30]. Diatomite with a CaO content greater than 10% is generally considered “calcareous,” and the higher CaO contents are attributed to calcite (CaCO₃) deposited by the shells of microfossils such as foraminifera [115]. In this literature review, care has been taken to point out when researchers were using calcareous DE/diatomite instead of a more siliceous one. The Al₂O₃ and Fe₂O₃ content of diatomite are typically in the ranges of 0–15% and 0–10%, respectively. The alkali content (Na₂O + K₂O) is usually less than 2% [30]. Typical XRD patterns show that diatomite is mostly amorphous, with a “hump” in the 20–30° region on the 2θ axis, and some crystalline peaks due to calcite and quartz [113, 114, 117].

1.2.9.3 Pozzolan Nature of Diatomite/DE

The ACI’s report on the use of raw or processed natural pozzolans in concrete states that one of the oldest examples of hydraulic binder from 5000 BC contained a mixture of lime and DE from the Persian Gulf [32]. In more recent history, research conducted in the University of California during the 1930s showed that diatomites are one of the fastest reacting natural pozzolans, due to their high reactive silica content and structure [118]. In the US, DE was used extensively in the construction of dams in the 1950s. For example, the Monticello Dam (1957) and the Twitchell Dam (1958) in California were made with calcined diatomaceous clay [33]. Additionally, a mixture of DE and pumice from a lacustrine (lake) deposit north of Reno, Nevada, was used extensively as a natural pozzolan from 1970 to 1989 in the western US and Canada for constructing structures, bridges, and roadways [32].

The most recent studies focusing on the use of DE and diatomite as a natural pozzolan are from outside the US. Using the standards prevalent in their countries, these studies have found that DE/diatomite meets the requirements of a pozzolan, and that DE/diatomite-portland cement blends fulfill the performance criteria of concrete made with blended cements [111, 115, 119]. Furthermore, Sierra et al. [120] found that the calcium hydroxide content of DE-lime cement paste, as measured by TGA, decreased with increasing hydration time while the amount of calcium silicate hydrate (C-S-H) gel in the paste sample increased.

1.2.9.4 Effect on Strength

Stamatakis et al. [111] found that mortars made with cement blends containing diatomites of a high reactive silica content (45% or higher) had compressive strength—higher than that of the control at 1 day—up to clinker replacement dosages of 20%. Regardless of the diatomite’s reactive silica content, by 28 days, the strength of all the mortars made with diatomite-OPC blend cement was higher than the control [111]. The largest strength increase was observed in the mortar containing diatomite with the highest reactive silica content (about 69%). At 28 days, mortar specimens made with this high silica diatomite blended cement, at clinker replacement dosages of 10 and 15%, had compressive strengths that were 18% and 20% higher than that of the control, respectively [111]. Yilmaz [114] also investigated mortars made with cement blends where 5, 10, and 20% of OPC was replaced with Turkish diatomite. He reported that mortars made with the 10% diatomite blended cement had the highest compressive strength at 360 days. However, the increase in strength when compared to the control mortar was only about 7.5% [114]. Tagnit-Hamou et al. [117] studied the effects of using DE in concretes with a low w/c

(0.40). The researchers found that the strength of concrete mixtures where 15% and 30% of the cement by volume was replaced by DE was higher than the control concrete mixture at nearly all ages.

Kastis et al. [115] studied blended cements made with calcareous diatomite. They found that the compressive strength of mortars made with 10% diatomite-90% OPC blended cement did not vary significantly from that of the control. Increasing the diatomite replacement dosage to 20 and 35%, however, led to mortars with lower compressive strengths than that of the control. Papadakis and Tsimas [116] also studied calcareous DE and found that the compressive strength of concrete where DE was used as a cement replacement was generally lower than that of the control.

1.2.9.5 Effect on Fresh State Properties

Most of the studies reviewed have concluded that the use of diatomite or DE in mortars and concrete increased the amount of water required to maintain a certain consistency, flow, or slump. Stamatakis et al. [111] found that mortars made with blended cement where 20% diatomite was used as a clinker replacement had an increase in water demand from the control; this demand ranged from 10 to 42% depending on the type of diatomite that was used and the particle size. Yilmaz [114] found that the use of a 5% diatomite/95% OPC blended cement in mortar increased water demand by only 6% when compared to the control. However, when the diatomite content in the cement blend was increased to 20%, the water demand of the mortar was almost 30% higher than that of the control. Tagnit-Hamou et al. [117] investigated the use of “sulfonated naphthalene formaldehyde condensate” high-range WRA and air-entraining agent in concrete specimens where 15% and 30% of the cement by volume was replaced with DE. With a fixed w/c of 0.40, the researchers found that concretes containing 15% and 30% DE required more WRA than a concrete mixture with 10% silica fume, or a concrete mixture with 30% Class F fly ash, in order to maintain an adequate slump. Also, despite using the maximum dosage suggested by the air-entraining agent manufacturer, neither the 15% nor the 30% DE concrete reached an air content of 4% [117]. Although the most recent studies all agree that the use of diatomite/DE in cementitious mixtures is difficult because of its high water demand, a study in 1950 by David and Klein [118] found that grinding the diatomite to a very high fineness (so that the diatom skeletal structure is destroyed) helps to reduce the water demand, especially if an air-entraining agent is also used in the mix.

Sanchez de Rojas et al. [121] found that mortars where 30% cement by mass was replaced with DE had a reduced heat of hydration when evaluated using a semi-adiabatic calorimeter. However, the reduction was not as significant as mortars containing fly ash at the same replacement percentage [121].

Stamatakis et al. [111] investigated the setting time of blended cements, where the clinker was replaced with five different European diatomites of variable composition. He found that the setting time of pastes containing diatomites of higher silica content (about 50% or higher) did not vary significantly from the control, even at replacement dosages of 20%. However, pastes containing 20% calcareous diatomite of a lower silica content had their initial and final setting time increased by as much as 80 and 100 minutes, respectively. However, in a later study, using calcareous diatomite from the same source, Kastis et al. [115] found that the setting time of pastes made using blended cement containing 35% diatomite and 65% OPC did not vary from the control by more than 10 minutes.

1.2.9.6 Impact on Durability

Tagnit-Hamou et al. [117] conducted ASR testing, in accordance with Canadian standard CSA A23-2.14A, on concrete specimens where 15% and 30% of cement by volume was replaced with DE. The results showed that while the control specimen had an expansion of approximately 0.08% after 3 years, both the 15% and 30% DE concrete specimens experienced less than 0.03% expansion after 3 years.

Using ASTM C 666, Tagnit-Hamou et al. [117] found that concrete specimens where 30% of the cement by volume had been replaced with DE did not have a good resistance to freeze-thaw, having only a durability factor of 46% after 28 days of curing. However, after 91 days of curing, the 30% DE concrete showed improved freeze-thaw resistance, with a durability factor of 86%. The concrete specimen where 15% of the cement by volume had been replaced with DE performed better, with a durability factor greater than 95 after 28 days of curing. Finally, concrete with 15% and 30% replacement dosages of DE were outperformed in salt scaling tests by concrete samples containing 6 or 10% silica fume and concrete mixtures with 30% fly ash. The researchers reported that neither the 15% DE concrete nor the 30% DE concrete met the ASTM C 672 requirements for being resistant to salt scaling [117].

Tagnit-Hamou et al. [117] conducted rapid chloride ion penetrability testing in accordance with ASTM C 1202 and found that the use of DE in concrete as a cement replacement decreased chloride ion penetrability. Concrete specimens containing DE at replacement dosages of 15% and 30% by volume of cement had a chloride ion penetrability that was, respectively, 56% and 63% lower than that of the control. This reduction in chloride ion penetrability was similar to concrete specimens containing 10% silica fume as a cement replacement [117]. Papadakis and Tsimas [116] found that using calcareous DE as a cement replacement in concrete actually increased the chloride ion penetrability of the sample, at dosages of 10% and 20% by mass. On the other hand, when the calcareous DE was used as an additive, the chloride ion penetrability of the concrete specimens decreased with increasing DE content.

Tagnit-Hamou et al. [117] investigated total capillary pore volume and pore size distribution of concrete specimens in which 15% and 30% of cement by volume was replaced with DE. Their results showed that at 91 days, the total pore volume (measured by mercury intrusion porosimetry) for 30% DE concrete was similar to that of a 10% silica fume concrete. The pore size distribution for the 15% and 30% DE concrete specimens was also similar to the pore size distribution of a 10% silica fume concrete. However, the concrete specimens with DE had a smaller proportion of large pores (0.1–1 μm).

1.2.9.7 Sources of Diatomite/DE in the US and Common Uses

According to the 2012 USGS Mineral Commodity Summaries [112], the US has diatomite reserves totaling 250 million metric tons, which is roughly one-quarter of the estimated world reserves. The USGS also reports that diatomite production in 2011 totaled 813,000 tons from 10 different mining areas [112]. The majority of diatomite produced in the US comes from California, Nevada, Oregon, and Washington, with 79% of the US annual production coming from California and Nevada [112]. The major US diatomite producers for 2011 were Celite Corp (California, Nevada, Washington) and EP Minerals, LLC (Nevada and Oregon) [105]. In the US, diatomite sources are usually at or near the earth's surface and can thus be mined at low costs using open pit mining [112].

Diatomite has a variety of uses in different industries that take advantage of its chemical composition, porous structure, large surface area, and high liquid absorption capacity. Although it is primarily used as a filtration medium, diatomite is also used as a silica additive in cement and as an absorbent and filler material in a variety of products. Additionally, diatomite can also be used as an insulation medium, a mild abrasive, and an agent in the purification and extraction of DNA [112]. Figure 1.3 shows the breakdown of diatomite use as a percent of 2011 US diatomite production, as reported by the USGS [112].

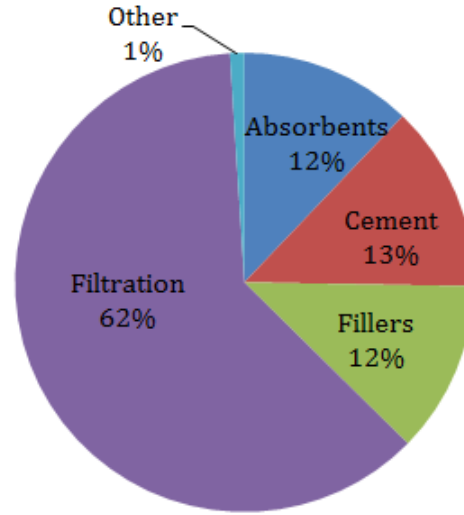


Figure 1.3: Common applications of DE in US

1.2.10 Conclusion of Literature Review

Based on a thorough review of previous literature, the potential of natural pozzolans to replace Class F fly ash in concrete seemed promising. Unaltered volcanic materials like perlite, pumice, and volcanic ash were reported to be amorphous and could be used as pozzolans after grinding. On the other hand, altered volcanic materials, like zeolites, were revealed to have a crystalline structure. Although raw zeolites had pozzolanic properties, numerous studies have reported zeolites to have better performance once they were calcined or pretreated in some way to improve reactivity. Pozzolans like clay and shale, with a sedimentary origin, require calcination to activate their pozzolanic properties.

In general, all of the natural pozzolans were reported to improve the durability properties of concrete, especially in terms of increased resistance to ASR and chloride ion penetrability. The results in terms of compressive strength were varied, but overall natural pozzolans (other than metakaolin and some highly siliceous diatomite) decreased the compressive strength of concrete. Some studies have shown that grinding the natural pozzolans finer helped to increase the compressive strength. In terms of mixture workability, some natural pozzolans like zeolites and DE were found to require a higher water content or admixture dosage to maintain slump. However, other pozzolans like volcanic ash and calcined shale behaved similarly to a Class F fly ash and were reported to increase mixture workability.

1.3 Identification of Materials

The research team's initial task was to identify candidate natural pozzolans tested in the project. Materials were identified through the internet and published literature searches (e.g., trade magazines, journal articles, and conference proceedings), discussions at ACI conventions with members of ACI Committee 232—Fly Ash and Natural Pozzolans in Concrete and 232-0A—Fly Ash-Use of Natural Pozzolans, and phone calls with university researchers and industrial users of SCMs.

While searching for materials, the focus was on pozzolans that were either sourced in Texas or could be shipped from nearby states at a low cost. Preference was also given to materials that were already being marketed and used as SCMs. However, some of the pozzolans

that were used in this project were created in the research lab by grinding down fine aggregate from aggregate producers.

Originally, 15 materials were identified. After initial screening tests, seven of these materials were cut from the testing matrix based on poor performance and cost, leaving eight materials in the final list of SCMs for this project. Table 1.2 shows the price, origin, and availability of these eight SCMs. Table 1.3 lists the materials that were cut from the testing matrix, along with their price, origin, and availability. Please note that the actual product and manufacturer names have not been disclosed in this report.

On the original list of 15 materials were three pumices—Pumice-D, Pumice-N, and Pumice-S—that are commercially available pozzolans from Idaho. Pumice-S was a fine aggregate that was present in our laboratory and was ground down using a Bico Inc. UA V-Belt Drive Pulverizer to activate its pozzolanic properties. Out of the three pumices, only Pumice-D was selected for the final list. Pumice-N, a finely ground pumice better suited to replace silica fume than fly ash, was cut due to its high cost of \$526/ton. The supplier for Pumice-S could not be located, so it was cut from the final selection as well. Other than Pumice-D, two other unaltered volcanic materials were chosen for the final list of SCMs: Perlite-I, a commercially available SCM from Idaho, and Vitric Ash-S, another commercially available SCM from Nevada.

The original list contained six zeolites, which are altered volcanic pozzolans with a crystalline structure. The best overall zeolite performer (Zeolite-Z from Idaho) and the best performers among local sources (Zeolite-T and Zeolite-A from Texas) were chosen.

Among the sedimentary materials, the calcined clay, Metakaolin-D, and the calcined shale, Shale-T, were selected for the final list. It must be noted that although Metakaolin-D is a calcined kaolinite, it is not an HRM, which can be characterized by its pure white color. The powder for Metakaolin-D had a pink hue. Shale-T was originally a fine aggregate that was crushed in our laboratory using the Bico Inc. UA V-Belt Drive Pulverizer and passed through a #200 sieve (with a 75 μm opening). The two other sedimentary materials, Diatomaceous Earth-D and Calcined Montmorillonite-Z, were cut from the final material matrix due to the problems they caused for mixture workability. Due to its large absorption capacity, Diatomaceous Earth-D had to be pre-soaked in water in order to make workable pastes and mortars. Despite this pre-treatment, the mechanical performance remained poor. Additionally, the cost of Diatomaceous Earth-D was very expensive, at \$560/ton.

Table 1.2: Price, Origin, and Availability of the Eight SCMs Chosen for TxDOT 0-6717

| Material Name | Cost (\$/ton) | Source | Availability (tons/year) |
|----------------------|----------------------|------------------|---------------------------------|
| Pumice-D | \$116 | Idaho | 200,000 |
| Perlite-I | \$124 | Idaho | --- |
| Vitric Ash-S | \$100–160 | Nevada | 300,000–1,000,000 |
| Metakaolin-D | \$325 (w/o shipping) | Missouri/Indiana | 30,000 |
| TXI Shale | \$49–51 | Streetman, TX | 4500 |
| Zeolite-Z | \$100 | Idaho | 50,000 |
| Zeolite-T | \$200 (w/o shipping) | Tilden, TX | 10,000 |
| Zeolite-A | \$150 | Marfa, TX | 500,000 |

Table 1.3: Price, Origin, and Availability of Materials that Were Cut from Testing Matrix

| Material Name | Cost (\$/ton) | Source | Availability (tons/year) |
|----------------------------|----------------------|---------------|---------------------------------|
| Pumice-N | \$526 | Idaho | 200,000 |
| Pumice-S | --- | --- | --- |
| Calcined Montmorillonite-Z | \$200 | Tennessee | 50,000 |
| Diatomaceous Earth-D | \$560 | Oregon | 1.2 million |
| Zeolite-B | \$120 | Idaho | 90,000 |
| Zeolite-L | \$200 (w/o shipping) | Tilden, TX | 10,000 |
| Zeolite-C | \$70–200 | Marfa, TX | 1,500,000,000 |

Chapter 2. Material Characterization

Prior to testing the alternative SCM sources in concrete mixtures, the researchers comprehensively characterized the eight materials to examine the variables that could affect their performance in concrete. The characterization information was used to determine cement replacement dosages and to develop effective reactivity enhancement methods. Table 2.1 shows the tests performed, which include standardized ASTM C 618 [18] tests in addition to more advanced characterization techniques like laser particle size analysis, X-ray fluorescence (XRF), XRD, TGA/DSC, and methylene blue testing.

Table 2.1: Material Characterization Tests Performed on the SCMs

| ASTM C 168 Tests | Advanced Characterization Tests |
|---------------------------------|--|
| Oxide composition (XRF) | Particle size distribution (laser diffraction) |
| Moisture content | Phase composition (XRD) |
| LOI | Phase composition (TGA/DSC) |
| Fineness (< 325 sieve) | Swelling clay content (methylene blue value) |
| Density | |
| Soundness (autoclave expansion) | |
| Strength activity index | |
| Water requirement | |

2.1 ASTM C 618 Characterization Tests

ASTM C 618 [18] is the governing specification for coal fly ash (Class C and F) and natural pozzolans (Class N) used in concrete. The criteria set forth in the ASTM specification are divided into three categories: chemical requirements, physical requirements, and supplementary optional requirements. The chemical requirements look at variables like the oxide composition, moisture content, and LOI of SCMs, while the physical requirements examine properties like fineness, density, soundness, strength, and water requirement. A uniformity criteria is also listed under the physical requirements, but was not considered for this study because the materials were collected and used from a single batch. The supplementary optional requirements, which mainly look at the effect of the SCMs on the durability characteristics of concrete, were also not considered during the characterization phase of this study. Instead, the effect of the pozzolans on concrete durability was detailed in the mortar and concrete studies described in Chapters 3 and 4.

2.1.1 ASTM C 618 Requirements and Procedures

While ASTM C 618 [18] lists all the criteria for materials to be classified as Class N pozzolans, the standard refers to ASTM C 311 [123] for the procedures to test the natural pozzolans. The next sub-sections describe each of the tests required by ASTM C 618 [18].

2.1.1.1 Oxide Composition

ASTM C 618 [18] requires a material to have a minimum combined SiO_2 , Al_2O_3 , and Fe_2O_3 composition of 70.0% by mass to be classified as an Class N pozzolan. It also limits the maximum sulfur trioxide (SO_3) composition to 4.0% by mass for Class N pozzolans. The oxide composition of the eight pozzolans were found using XRF. Fused pellets for XRF analysis were prepared in a Claisse M4 Fluxer according to TxDOT test procedure Tex-317-D [124], using 0.5 g of SCM and 6.5 g of lithium borate-lithium bromide. The fused pellets were then analyzed in a Bruker S4 Explorer according to ASTM D 4326 [125], as specified in ASTM C 311 [123].

2.1.1.2 Moisture Content and Loss on Ignition

Moisture content measures the weight lost upon drying at 110 °C, whereas LOI measures the total weight lost when the moisture free sample is heated from 110 °C to 750 °C. High values in these tests provide possible warnings about the effect of the SCM on concrete workability and admixture demand. ASTM C 618 specifies that Class N pozzolans must have moisture contents less than 3.0% and LOI less than 10.0% (by mass). The moisture content and LOI of the eight pozzolans was determined according to the procedures of ASTM C 311 [123]. For the LOI determination, ASTM C 311 [123] uses a modified ASTM C 114 [126] procedure, which calls for the material to be heated in uncovered porcelain, instead of platinum, at 750 °C.

2.1.1.3 Fineness

The fineness test determines the amount of material that is retained on a No. 325 sieve (with a 45 μm opening) after wet sieving the SCM under a water pressure of 10 psi. The fineness test, as the name implies, is useful to get a general idea of how fine the pozzolan particles are, which is related to their reactivity in cementitious systems. ASTM C 618 [18] specifies that Class N pozzolans must have less than 34% by mass retained on the No. 325 sieve after wet-sieving. As specified in ASTM C 311 [123], the fineness test was conducted according to the procedures of wet sieving described in ASTM C 430 [127].

2.1.1.4 Density

Although the uniformity criteria, which uses variations in density to reject materials, was not considered for the study, density measurements of the materials were still conducted. As specified in ASTM C 311 [123], the density of the natural pozzolans was measured using a modified ASTM C 604 [128] procedure. The modification calls for the materials to be tested as received, instead of following the sample preparation steps of ASTM C 604 [128]. A Quantachrome Corporation Ultra Pycnometer 1000 was used for the density measurements.

2.1.1.5 Soundness

The soundness of a cement/SCM combination is tested to identify materials that have the potential to produce delayed expansion due to magnesium and calcium oxides. Soundness of a material is determined by measuring the autoclave expansion using the procedures specified ASTM C 151 [129]. In this method, specimens made of cement paste are exposed to high temperature and pressure for 3 hours, after which they are brought back down to atmospheric pressure and room temperature. The expansion (or contraction) that occurs due to this process is expressed as a percentage of the effective gage length. ASTM C 618 [18] specifies that paste

samples with Class N pozzolans must not have an autoclave expansion (or contraction) of more than 0.8%. Soundness testing was conducted on paste samples containing 20% SCM – 80% cement by weight. The pastes were mixed to normal consistency according to ASTM C 187 [130] and tested according to ASTM C 151 [129], as specified in ASTM C 311 [123].

2.1.1.6 Strength Activity Index

The strength activity index (SAI) gives an indication of the reactivity of SCMs by comparing the compressive strength of mortar cubes made with 80% cement and 20% SCM to the compressive strength of the control mortar cubes made with only cement. The SAI is performed in conjunction with the water requirement test (described in section 2.1.1.7), which requires the mortar mixtures to have a constant flow. ASTM C 618 [18] requires the compressive strength of the SCM mortar to be at least 75% of the control mortar's compressive strength at either 7 or 28 days. The SAI tests were conducted according to the instructions in ASTM C 311 [123], which further refers to ASTM C 109 [131] for the mixing, molding, curing and testing procedure of the mortar cubes. The cement used in the SAI mortar mixtures was an ASTM C 150 [132] Type I portland cement from Buda, Texas. The sand used was a standard graded sand from Ottawa, IL, which meets all the requirements of ASTM C 778 [133].

2.1.1.7 Water Requirement

The mortars with SCM that are made for the SAI test are required to have a flow which is $\pm 5\%$ of the control mortar, made with 100% cement. ASTM C 618 [18] dictates that the amount of water necessary to meet this flow requirement should not exceed 115% of the control mortar. Failing the water requirement test could give an indication of potential workability problems that could arise when the SCM is used in concrete. The water requirement tests were performed using the instructions in ASTM C 311 [123], which further refers to ASTM C 1437 [134] for the flow measurement procedures.

2.1.2 ASTM C 618 Results

Five out of the eight materials passed all the requirements of ASTM C 618 [18] for a Class N pozzolan. The materials that qualified as a Class N pozzolan were Pumice-D, Perlite-I, Vitric Ash-S, Metakaolin-D and Shale-T. The three materials that failed the Class N pozzolan criteria were Zeolite-Z, Zeolite-T and Zeolite-A. Table 2.2 shows a summary of the ASTM C 618 results. The next sub-sections discuss the ASTM C 618 results in detail.

2.1.2.1 Oxide Composition Results

All the eight natural pozzolans met the ASTM C 618 [18] requirement to have a minimum combined SiO_2 , Al_2O_3 , and Fe_2O_3 composition of 70.0% by mass. All the pozzolans were also below the SO_3 limit of 4% by mass. Table 2.3 shows detailed oxide results from the XRF analysis. Other than the sedimentary pozzolans (Metakaolin-D and Shale-T) most of the pozzolans had a similar oxide composition. Surprisingly, Metakaolin-D had a much lower SiO_2 content than the other pozzolans, and a proportionately higher Al_2O_3 content. Shale-T had a slightly higher Fe_2O_3 content than the other materials.

2.1.2.2 Moisture Content and Loss on Ignition Results

Other than the three zeolites, all materials passed the moisture content requirements. Although Zeolite-Z and Zeolite-A failed the moisture content requirement, their values were only about 2% higher than the maximum limit set by ASTM C 618 [18]. However, the moisture content of Zeolite-T was about 8% higher than the limit. The high moisture content value of Zeolite-T indicated that the material had a high absorption capacity and could cause workability problems when making concrete. All materials had LOI values less than the maximum limit prescribed by ASTM C 618 [18].

2.1.2.3 Fineness Results

Other than Zeolite-T and Zeolite-A, all materials passed the fineness requirements for Class N pozzolan. This was not surprising as these two zeolites appeared to be coarse from a visual inspection. The coarseness of these two zeolites could lead to a lower reactivity when used as an SCM in concrete. Although Shale-T passed the test, it had a higher retention percentage compared to the other pozzolans that passed the fineness test. This is most likely due to the fact that Shale-T was crushed in the laboratory, whereas the other materials that passed the fineness test were commercially sold SCMs.

2.1.2.4 Density Results

The average densities of the natural pozzolans are presented in Table 2.4. The density test for Zeolite-Z was not able to be performed correctly due to the airy nature of the powder. As such, the density of Zeolite-Z was assumed to be similar to that of the other two zeolites. Most of the pozzolans were observed to have an approximate density of 2.5 g/cm³.

2.1.2.5 Soundness Results

All materials had autoclave expansions that were well below the ASTM C 618 [18] limit.

2.1.2.6 Strength Activity Index Results

Other than Zeolite-T and Zeolite-A, all materials passed the SAI requirements of having at least 75% of the control compressive strength at 7 or 28 days. It should be noted that Vitric Ash-S, Shale-T and Zeolite-Z had SAI values lower than 75% at 7 days. However, overall they passed the SAI requirements, since by 28 days their SAI values were above 75%. As predicted from the fineness test results, Zeolite-T and Zeolite-A had a lower reactivity than the finer materials. Similarly, it was not surprising that Vitric Ash-S and Shale-T, which had a higher material retention in the fineness test, could not meet the minimum SAI requirement at 7 days. However, the 7-day SAI value of Zeolite-Z was unexpected, considering that all of the material passed the #325 sieve during the fineness test. The low strength was most likely due to the fact that the zeolite mortar cube was made with a much higher w/c than the control to keep a constant flow for the water requirement test.

2.1.2.7 Water Requirement Results

All three zeolites failed the water requirement test, indicating that these materials are likely to cause problems with mixture workability. Zeolite-T had the highest water requirement, which was not surprising when correlated with its high moisture content.

Table 2.2: Summary of ASTM C 618 Results

| Material Name | SiO ₂ + Al ₂ O ₃ + Fe ₂ O ₃ (%) | SO ₃ % | Moisture Content (%) | LOI (%) | Fineness (%) | SAI, 7 day (%) | SAI, 28 day (%) | Water Requirement (%) | Soundness | Passes ASTM C 618? |
|---|---|----------------------|----------------------------|----------------------|--------------------|-------------------------|--------------------------|-----------------------------|-----------------------|--------------------------|
| Pumice-D | 83 | 0.04 | 1.5 | 4.4 | 2 | 82 | 93 | 104 | -0.02 | YES |
| Perlite-I | 84 | 0.05 | 0.6 | 3.4 | 2 | 86 | 94 | 100 | -0.02 | YES |
| Vitric Ash-S | 77 | 0.33 | 2.3 | 5.9 | 15 | 72 | 83 | 102 | -0.01 | YES |
| Metakaolin-D | 89 | 0.06 | 0.9 | 1.0 | 7 | 94 | 108 | 102 | -0.05 | YES |
| Shale-T | 86 | 0.39 | 0.3 | 0.4 | 30 | 72 | 81 | 103 | -0.16 | YES |
| Zeolite-Z | 79 | 0.07 | 5.1 | 2.7 | 0 | 71 | 100 | 116 | -0.01 | NO |
| Zeolite-T | 75 | 0.14 | 11.6 | 4.7 | 59 | 47 | 61 | 132 | 0.00 | NO |
| Zeolite-A | 75 | 0.29 | 4.8 | 4.1 | 61 | 60 | 64 | 118 | 0.00 | NO |
| <i>Passing Criteria in ASTM C 618</i> | <i>70% min</i> | <i>4.0% max</i> | <i>3.0% max</i> | <i>10.0% max</i> | <i>34% max</i> | <i>75% min</i> | <i>75% min</i> | <i>115% max</i> | <i>± 0.8% max</i> | |

Table 2.3: Oxide Composition Results from XRF Analysis

| Material Name | SiO ₂ (%) | Al ₂ O ₃ (%) | Fe ₂ O ₃ (%) | CaO (%) | MgO (%) | SO ₃ (%) | Na ₂ O (%) | K ₂ O (%) |
|---------------|-------------------------|---------------------------------------|---------------------------------------|------------|------------|------------------------|--------------------------|-------------------------|
| Pumice-D | 69.42 | 12.42 | 1.08 | 0.94 | 0.44 | 0.04 | 3.81 | 5.16 |
| Perlite-I | 70.26 | 12.84 | 1.16 | 0.86 | 0.14 | 0.05 | 4.70 | 4.74 |
| Vitric Ash-S | 64.72 | 11.27 | 0.87 | 3.31 | 1.38 | 0.33 | 3.65 | 5.64 |
| Metakaolin-D | 51.66 | 35.23 | 1.98 | 0.57 | 0.45 | 0.06 | 0.10 | 1.42 |
| Shale-T | 65.43 | 14.55 | 5.72 | 2.44 | 2.30 | 0.39 | 1.14 | 2.88 |
| Zeolite-Z | 65.29 | 10.90 | 2.36 | 2.52 | 0.59 | 0.07 | 0.52 | 4.82 |
| Zeolite-T | 62.23 | 11.88 | 1.12 | 2.21 | 0.64 | 0.14 | 1.00 | 1.68 |
| Zeolite-A | 59.50 | 12.93 | 2.17 | 5.07 | 0.82 | 0.29 | 3.07 | 2.58 |

Table 2.4: Average Density from Pycnometer

| Material Name | Average Density (g/cm ³) |
|---------------|---|
| Pumice-D | 2.44 |
| Perlite-I | 2.44 |
| Vitric Ash-S | 2.46 |
| Metakaolin-D | 2.75 |
| Shale-T | 2.58 |
| Zeolite-Z | --- |
| Zeolite-T | 2.29 |
| Zeolite-A | 2.46 |

2.2 Advanced Characterization Tests

Although the ASTM C 618 [18] tests are useful for a basic characterization of pozzolans, more advanced techniques are usually needed for a more comprehensive material characterization. Section 2.2.1 describes the advanced characterization techniques that were used to evaluate the pozzolans for this project, while Section 2.2.2 presents the results of the advanced tests.

2.2.1 Advanced Characterization Procedures

2.2.1.1 Laser Particle Size Analysis

Unlike the fineness test, which only gives a basic indication of material fineness, a laser particle size analysis can be used to determine the entire particle size distribution (PSD) of a pozzolan. Knowing the PSD can be useful in predicting some early age properties, such as acceleration of cement hydration (“filler effect”), increased reactivity of pozzolans, or decreased workability of mixture due to the presence of finer particles. The particle size distributions of the pozzolans were analyzed using a Horiba Partica LA 950-V2 Laser Scattering Particle Size Distribution Analyzer. The pozzolans were tested as received without any sample preparation.

2.2.1.2 X-ray Diffraction

XRD is a compositional characterization test that complements the XRF oxide composition results, as the XRD results can differentiate whether the oxides are present in amorphous or crystalline phases. The XRD tests were carried out using a Siemens D-500 X-ray Diffractometer with Cu-K α radiation. The range of 2θ measured was 5–70°, and a dwell time of 4 seconds was used. To ensure adequate packing, all the pozzolan samples were ground to pass through the No. 325 sieve.

2.2.1.3 Thermal Gravimetric Analysis/Differential Scanning Calorimetry

TGA and DSC can also be used to understand the phases present in a material. TGA and DSC were conducted on the pozzolans using a Mettler Thermogravimetric Analyzer, Model TGA/DSC 1. The pozzolan samples were crushed and sieved through a number #325 sieve (45 μm) prior to being tested. The weight loss of the sample was recorded as it was heated from 40 °C to 1000 °C, at a rate of 20 °C/min. The measured weight loss was used to plot the TGA curve. The heat flow during this interval was recorded as well, and was used to plot the DSC curve. During the test, the chamber gas used was nitrogen and the pozzolan samples were contained in alumina crucibles.

2.2.1.4 Methylene Blue Testing

A methylene blue test for aggregates, developed by W.R. Grace & Co., was used in this project to evaluate the relative absorption capacities of the pozzolans. Additionally, the methylene blue value of a Class F fly ash (from Rockdale, TX) was also measured, to see how the value of fly ash compared with its potential replacement materials. All the pozzolans were crushed to pass the #200 sieve with a 75 μm opening, before being tested.

The procedure of the methylene blue test was detailed in the “Grace Rapid Clay Test Kit: Step-by-Step Procedure,” provided to our laboratory by W.R. Grace and Co. Since the test was

developed for aggregates, it was modified so that instead of using 20 g of standard graded sand, as stipulated in the original method, the modified method for the SCM replaced 5% of the standard graded sand (by mass) with the SCM being tested. The rest of the procedure is the same as the original method. 20 g of standard graded sand containing 5% replacement of SCM was soaked in 30 g of 5% (by mass) methylene blue solution for 5 minutes. The sample was then agitated by hand for 1 minute, followed by 3 minutes of rest and 1 more minute of agitation. After this procedure, approximately 2 mL of the solution was transferred to a 3 mL syringe with a 0.2 μm luer-lok filter. The syringe was then depressed so that 0.5–1.0 mL of the solution was filtered into a new 1 mL vial. Using a micropipette, 130 μL of this filtered solution was transferred to a new container where it was diluted with water to total weight of 45 g. This diluted solution was then mixed and transferred to a clean 16 mm glass tube. The methylene blue concentration in the diluted sample was measured using a Hach DR 850 colorimeter.

The output of the colorimeter is in units of mg methylene blue absorbed per g of sand. A control sample with 100% standard graded sand was also tested to normalize the results. The methylene blue results of the pozzolans were normalized by subtracting 95% of the methylene blue value of the standard graded sand.

2.2.2 Advanced Characterization Results

2.2.2.1 Laser Particle Size Analysis

Figure 2.1 shows the full particle size distributions for the eight pozzolans. The laser particle size analysis showed that Zeolite-Z had the smallest median particle size (d_{50}) at 6.35 μm . Pumice-D, Perlite-I, Metakaolin-D, Vitric Ash-S and Shale-T were in the middle with d_{50} ranging from 13 μm to 23 μm . Zeolite-A and Zeolite-T were the coarsest SCMs, with d_{50} values around 180 μm and 280 μm , respectively.

2.2.2.2 X-ray Diffraction

Table 2.5 contains a summary of the phases found in the eight pozzolans through XRD; X-ray diffractograms are included in Appendix A. XRD results show that Pumice-D and Perlite-I are mainly amorphous. Vitric Ash-S is also amorphous with a few crystalline impurities such as quartz, calcite and albite. For Metakaolin-D the X-ray diffractogram shows an amorphous hump at 2θ angles between 10–14°, which is typical of calcined clays. Furthermore, no kaolinite peaks were found, as is usually the case when kaolinite is calcined to metakaolin. Some muscovite peaks were seen in the XRD images for Metakaolin-D as well as crystalline impurities such as quartz, anatase, and microcline. Shale-T was expected to have some clay, but the XRD plots did not show any peaks from clay minerals. This is not surprising as the clay minerals might have been dehydroxylated when the original shale was calcined. Shale-T also contained crystalline impurities like quartz, albite and microcline. XRD plots of all three zeolites confirmed that they contain clinoptilolite, one of the most common zeolite mineral. Zeolite-Z seemed to be the most purified zeolite out of the three that were tested, as the XRD plots of Zeolite-Z did not show any significant impurities. On the other hand, the XRD plots of Zeolite-T showed some cristobalite and montmorillonite impurities, along with the clinoptilolite peaks. Presence of the montmorillonite could be one of the reasons why Zeolite-T showed such a high water demand during the ASTM C 618 tests. Other than clinoptilolite, the XRD plot for Zeolite-A contained some quartz, calcite, and anorthite peaks.

2.2.2.3 Thermal Gravimetric Analysis/Differential Scanning Calorimetry

Table 2.5 summarizes the TGA mass loss for the SCMs; the measured TGA/DSC plots are provided in Appendix A. The DSC results for Pumice-D and Perlite-I did not really show any phase changes after the initial dehydration between 75 and 200 °C. This corresponds well with the TGA data presented in Table 2.5, which show most of the mass loss occurring at the lower temperatures. Overall, Pumice-D and Perlite-I lost about 3 to 5% of their total mass when heated to 1000 °C. The DSC data for Vitric Ash-S also show dehydration around 75 to 150 °C. Unlike Pumice-D and Perlite-I, the DSC plot has two distinctive endothermic peaks between 650 and 850 °C, which correspond to the decomposition of the impurities detected through XRD analysis. The first endothermic peak most likely corresponds to a phase change of the quartz impurity, while the second endothermic corresponds with the decomposition of calcite. Vitric Ash-S lost about 7% of its mass when heated to 1000 °C. The DSC data of all three zeolites had two major endothermic peaks. According to previous literature [135], the initial endothermic peak corresponds to dehydration, while the later peak at a higher temperature corresponds to the collapse of the zeolitic structure. Overall, the zeolites lost about 10% of their total mass when heated to 1000 °C. The DSC data for Metakaolin-D and Shale-T did not show any significant phase changes after the initial dehydration. This result is expected, since both materials were made by heat treating clays and shale, respectively. The DSC plot for Metakaolin-D has an endothermic peak after 900 °C, which is most likely due to recrystallization of high temperature phases. The recrystallization of phases at high temperatures has been shown for kaolinite in previous literature [89]. Metakaolin-D and Shale-T lost less than 2% of their mass when heated to 1000° C.

2.2.2.4 Methylene Blue Testing

Figure 2.2 presents the amount of methylene blue absorbed per g of SCM. As expected, the zeolites showed the highest values for methylene blue absorption, with values ranging above 1.5 mg of methylene blue absorbed per gram of SCM. Similar to the water requirement test results, the results of the methylene blue test indicated that the use of these zeolites as pozzolans could significantly affect the workability of cementitious mixtures. Although the other materials had lower methylene blue absorptions than the zeolites, their values were higher than that of the Class F fly ash. The methylene blue value of Shale-T was the closest to the value of the fly ash.

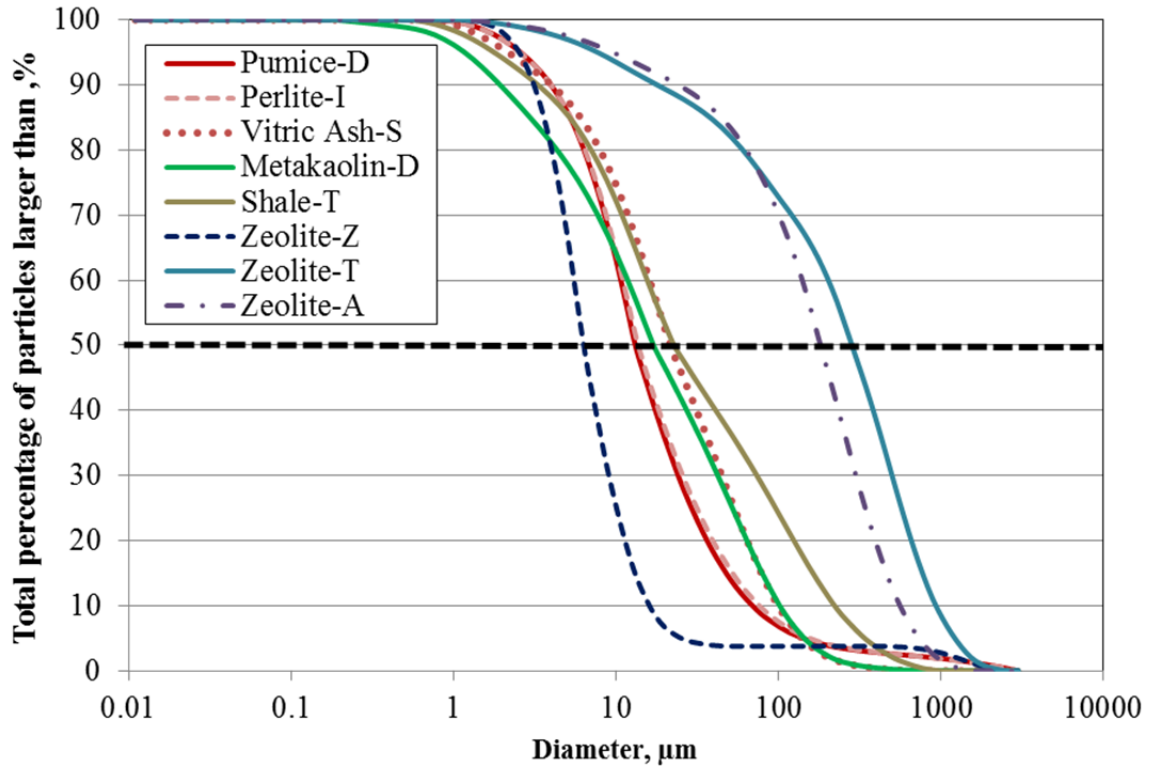


Figure 2.1: Particle size distribution of pozzolans

Table 2.5: XRD and TGA Results

| SCM | Main Phases in XRD | % Total Mass Loss when heated to | | | |
|--------------|---|----------------------------------|--------|--------|---------|
| | | 100° C | 200° C | 500° C | 1000° C |
| Pumice-D | Amorphous | 0.41 | 0.99 | 4.45 | 5.21 |
| Perlite-I | Amorphous | 0.09 | 0.32 | 2.94 | 3.50 |
| Vitric Ash-S | Quartz, Calcite, Albite | 0.67 | 1.40 | 4.17 | 7.11 |
| Metakaolin-D | Quartz, Anatase, Muscovite, Microcline | 0.25 | 0.56 | 1.20 | 1.69 |
| Shale-T | Quartz, Albite, Microcline | 0.08 | 0.16 | 0.27 | 0.69 |
| Zeolite-Z | Clinoptilolite | 2.19 | 5.76 | 8.70 | 9.72 |
| Zeolite-T | Clinoptilolite, Cristobalite, Montmorillonite | 1.82 | 5.68 | 8.47 | 9.99 |
| Zeolite-A | Clinoptilolite, Quartz, Calcite, Anorthite | 1.62 | 4.73 | 6.84 | 9.65 |

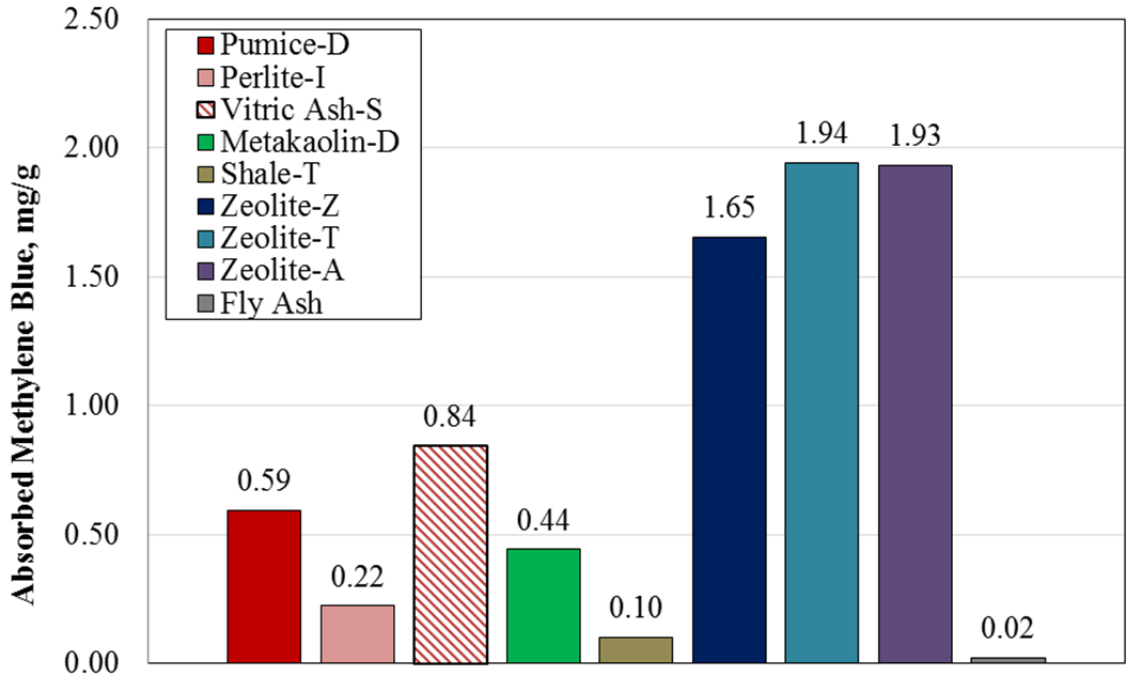


Figure 2.2: Amount of methylene blue absorbed per gram of SCM

2.3 Conclusions from Characterization Tests

The characterization tests showed that other than the 3 zeolites, the rest of the pozzolans, Pumice-D, Perlite-I, Vitric Ash-S, Metakaolin-D and Shale-T, could qualify as Class N pozzolans according to ASTM C 618 [18]. The zeolites failed ASTM C 618 mostly due to problems with water requirement and absorption. Zeolite-T which has some montmorillonite impurities had the highest water demand. In terms of reactivity, Zeolite-Z, the finest and most purified zeolite of the three tested, showed no problems in meeting the minimum strength requirements of ASTM C 618 [18]. However, Zeolite-T and Zeolite-A, which were both found to have a coarser particle size distribution, could not meet the 7- or 28-day compressive strength requirement. Although these three zeolites did not meet the ASTM C 618 [18] Class N criteria, they were not cut from the material matrix. Instead, different techniques were used to try and modify the zeolites to improve their water demand and absorption characteristics. These are discussed further in Chapter 5.

Chapter 3. Paste and Mortar Studies

Before testing the natural pozzolans in concrete mixtures, smaller scale testing was performed on pastes and mortars to identify optimal cement replacement levels for the concrete mixtures. Furthermore, some of the durability testing for concrete can take up to 2 years, so performing accelerated tests on paste and mortars allowed the researchers to rapidly assess how the natural pozzolans could affect important fresh and hardened state properties of cementitious mixtures. Please refer to Table 3.1 for a list of the paste and mortar experiments performed on the natural pozzolans.

Table 3.1: Experiments Performed in the Paste and Mortar Studies

| Paste | Mortar |
|------------------------|--|
| Isothermal calorimetry | Compression testing (ASTM C 109) |
| Rheological testing | Effect on drying shrinkage (ASTM C 596) |
| TGA | Resistance to ASR (ASTM C 1567) |
| --- | Resistance to sulfate attack (ASTM C 1012) |

3.1 Procedures

This sub-section describes the procedures for the paste and mortar experiments in detail. The criteria of success of the tests (if any) are also presented. With respect to the materials used, the cement for all the mixtures was an ASTM C 150 [132] Type I portland cement from Texas Lehigh, in Buda, Texas. Mortar and pastes were also prepared with a Class F fly ash from Rockdale, Texas, in order to compare the performance results of the alternate SCMs with the more commonly known performance results of Class F fly ash. A mixed quartz and chert sand from Texas, which was shown to be reactive in previous literature [136], was used in the ASTM C 1567 [137] mortar mixtures to test resistance to ASR. This reactive fine aggregate was re-graded in the laboratory to meet the requirements of ASTM C 1567 [137]. The sand used in all the other mortar mixes was a standard graded sand from Ottawa, Illinois, that met all the requirements of ASTM C 778 [133].

Since most of the ASTM C 618 tests [18] used a 20% replacement dosage by mass, the initial replacement dosage used for the paste and mortar tests was also 20%. Depending on the performance of the mixture, the replacement dosage was adjusted to meet the criteria of success that was established. For example, for the ASTM C 1567 [137] ASR test, the SCM replacement dosage was reduced if the mortar bars had expansions below the prescribed ASTM C 1567 [137] limit. Similarly if the expansion was greater than the limit, the replacement dosage was increased.

3.1.1 Compressive Strength

Since the SAI test from ASTM C 618 [18] measures compressive strength on the basis of constant flow instead of constant w/c, the results are often unfavorable for mixtures incorporating SCMs with a high water demand, like zeolites. For this reason, compression tests were carried out on mortar cubes made with a constant w/c. Other than the fixed w/c, the cubes

were made according to the instructions in ASTM C 109 [131]. The w/c for the zeolites was fixed at 0.55, due to their high water demand. The w/c of the other materials, Pumice-D, Perlite-I, Vitric Ash-S, Metakaolin-D and Shale-T, were fixed at 0.5. For each w/c, a control mixture (with no SCMs) was also made. The SCM mortar mixtures had 20% of the cement by mass replaced with the SCMs. A mixture containing fly ash, at the same replacement dosage, was also made for each w/c.

The compressive strength of the mortar mixtures was tested at 1, 3, 7, 28, 90, and 365 days. The average compressive strength was calculated using three mortar cube specimens from two separate batches that were made consecutively, on the same day. In certain cases, if the range of the compressive strength data from the three mortar cubes was greater than 8.7% of the average, which is the limit stated in ASTM C 109 [131], the average was calculated from two mortar specimens instead of three. In such cases, the final range of the two samples was checked to see it was less than or equal to 7.6% of the average, as instructed in ASTM C 109 [131]. The results section reports if the 7.6% range was exceeded when the average compressive strength was calculated by two mortar bars.

3.1.2 Rheological Properties

Although the water requirement test of ASTM C 618 [18] provides an empirical assessment of a material's effect on mixture workability, it cannot measure the actual rheological properties of the mixture like yield stress and viscosity. Having a thorough scientific understanding of these properties is crucial when trying to find ways to optimize the fresh state performance of a mixture or modify materials like the zeolites to lower their water demand and absorption capacities.

An MCR 301 Anton Paar rotational rheometer was used to perform the rheological tests. A cup-and-bob measuring system geometry was used, with a 1.0-mm gap between the bottom of the cup and the bob. The control paste mixture was made with 50 g of cement and 22.5 g of water, giving the control paste a w/c of 0.45. For the SCM paste mixtures, 20% of the cement by mass was replaced with the SCM being examined. The water content was kept the same as the control mixture, giving the SCM pastes a water-to-cementitious-materials ratio (w/cm) of 0.45. The pastes were mixed mechanically for 2 minutes using a Caframo Compact Digital BDC 2002 overhead stirrer at 1000 rpm. Approximately 19 mL of the mixed sample was added to the cup for rheological testing. Prior to each test, the pastes were pre-sheared for 4 minutes at a shear rate of 50 s^{-1} . This was done to reduce the effects of shear history on the samples and to ensure a similar starting point across all tests. After pre-shearing, the samples were allowed to rest for 30 s. Then, the shear rate was gradually increased from 10 s^{-1} to 50 s^{-1} and then brought back down to 10 s^{-1} . Both the increase and decrease in shear rate were done in increments of 10 s^{-1} . Furthermore, the shear rate at each step was held constant for 3 minutes to ensure that an equilibrium state had been reached. The total testing time (including the time to pre-shear) was 31.5 minutes. Ten data points were used in each equilibrium range to determine the average resultant shear stress of the paste at each shear rate. The shear stress and the shear rate obtained from the test are then used to graph a rheological flow curve, from which the rheological properties of the mixture, like yield stress and viscosity, can be determined by fitting different models.

In the current study, the Bingham model [138], a popular method to describe the rheological behavior of cementitious mixtures [138, 139], was used to estimate the viscosity and yield stress of the control and SCM pastes. Using a linear trend line to fit the flow curve data, the

Bingham model defines the slope of the linear trend line to be the viscosity, and the y-axis intercept to be the yield stress [140]. It must be noted that the linear trend line was fitted on the region of the flow curve where the shear rate was being gradually decreased from 50 s^{-1} to 10 s^{-1} , as the data are considered to be more stable when the shear rate is being decreased, rather than when it is increased.

3.1.3 Heat of Hydration

A quick and efficient method to assess the effect of SCMs on early age cement hydration is to perform isothermal calorimetry on paste mixtures, which measures the heat from the ongoing hydration reactions for 1–3 days. The data obtained from the test can be used to plot heat of hydration curves, which can give valuable information on whether the addition of the SCMs accelerates or retards the hydration process of cement.

The control paste mixture was made with 50 g of cement and 22.5 g of water, giving the paste a w/c of 0.45. For the SCM paste mixtures, 20% of the cement by mass was replaced with the SCM being tested. The water content was kept the same as the control mixture. Prior to each test, the pastes were mixed by hand for 2 minutes. After mixing, approximately 10 g of paste was added to the calorimetry vials and the heat evolution from hydration was measured at 23°C for 72 hours. A Thermometric TAM Air Isothermal Calorimeter was used for calorimetry tests, which were conducted in accordance with ASTM C 1679 [141] and ASTM C 1702 [142].

3.1.4 Calcium Hydroxide Content

While isothermal calorimetry is a good characterization test to understand the early reaction rate of an SCM, it does not provide any information on pozzolanic reactions that typically occur at a later stage. Since a pozzolanic reaction involves the conversion of calcium hydroxide into C-S-H, an easy way to track the progress of a pozzolanic reaction is to monitor the decrease of calcium hydroxide in a cementitious mixture over time, using TGA.

For the thermal gravimetry tests, the paste designs were identical to those used for isothermal calorimetry. After mixing the pastes by hand for 2 minutes, they were cured at room temperature and 100% relative humidity (RH), until they reached the desired test age, which was 7, 28, or 90 days for the current study. After curing, the samples were weighed and then broken into small chunks using a pestle, which were stored in a vacuum desiccator for 14 ± 1 days. The samples were reweighed after being removed from the desiccator at 14 days, and the change in weight was recorded as the amount of water lost on drying. The samples were then crushed using a mortar and pestle and sieved through a number #325 sieve ($45 \mu\text{m}$) to ensure uniformity. The sieved samples were stored under vacuum in a desiccator until testing on a Mettler Thermogravimetric Analyzer, Model TGA/DSC 1. During the test, the chamber gas used was nitrogen and the samples were contained in alumina crucibles with lids. The weight losses of the samples were recorded as they were heated from 40°C to 1000°C , at a rate of $20^\circ\text{C}/\text{min}$. The measured weight loss was used to plot the TGA curve. The heat flow during this interval was recorded as well and was used to plot the DSC curves. The DSC curve was used to pinpoint the exact temperatures between which the calcium hydroxide in the paste decomposed. Using those temperatures, the weight loss due to calcium hydroxide decomposition was calculated from the TGA curve. Finally, using molecular weights and the recorded weight change from water loss in the desiccator, the weight loss from calcium hydroxide decomposition was converted to the calcium hydroxide content per gram of cement in the initial paste.

3.1.5 Drying Shrinkage

Strains caused by drying shrinkage can lead to cracking in concrete. Although these cracks rarely propagate through the entire cross section, these cracks can increase the permeability of the concrete and allow the ingress of deleterious materials like sulfate and chloride ions. Therefore, in addition to more common durability problems like ASR, it is also important to assess whether the addition of SCMs to a cementitious mixture can increase the potential of drying shrinkage.

ASTM C 596 [143], which measures the length change of 1 in. x 1 in. x 11 ¼ in. mortar bars kept at 50% RH, was used to evaluate the drying shrinkage of the SCM mortar mixtures. As described in the standard, the mortars contained two parts standard graded sand to one part cement and a water content such that the mortar flow measured by ASTM C 1437 [134] was between 105% and 115%; therefore, these samples did not use a constant w/cm. The SCM mortars had 20% of the cement by mass replaced with SCM. After mixing and molding, the filled molds were placed in moist storage at 23 °C and 100% RH. After 24 hours in moist storage, the mortar bars were removed from the molds and placed in saturated lime water for 48 hours. After this initial 3-day cure, the mortar bars were weighed and their length was measured using a comparator. They were then left to air dry in a 23 °C, 50% RH environmental chamber. Measurements of the weight and the length change of the mortar bars were taken after 4, 7, 11, 18, 25, 56, 112, 224, and 448 days in the environmental chamber.

3.1.6 Resistance to Alkali-Silica Reaction

Degradation of concrete from ASR is a very common durability problem in Texas due to the wide availability of reactive aggregates that form expansive silica gel in the highly alkaline environment of concrete. As such, TxDOT requires that pozzolans be proven effective for controlling expansions from ASR before they can be used in a mixture design.

The accelerated mortar bar test method, from ASTM C 1567 [137], was used to evaluate the ability of the SCMs to control expansion from ASR. As described in the standard, the mortar mixtures contained 2.25 parts of the reactive fine aggregate to 1 part of cementitious material (cement + SCM) by weight. The dimensions of the mortar bars were 1 in. x 1 in. x 11 ¼ in. The steel gage studs at each end of the mortar bar made the gage length 10 in. The standard requires the mortar mixes to have a constant w/cm of 0.47 and a measured flow that is $\pm 7.5\%$ of the control mortar, with no SCMs. To meet the required flow, a polycarboxylate-based ASTM C 494 [144] Type F WRA distributed by Sika Corporation under the trade name Sika ViscoCrete 2100 was used in the mortar mixtures. The admixture dosages for these mortar mixtures are shown in Appendix B. Some of the SCM mortar mixtures required more than the recommended dose of this polycarboxylate WRA. For this reason, a different WRA was used for the sulfate mortar mixtures, described in Section 3.1.6 and 3.2.6 and the concrete mixtures, described in Chapter 4.

After mixing and verifying that the consistency was acceptable, the mortar was placed and compacted into molds. After 24-hour curing at 23 °C and 100% RH, the mortar bars were removed from the molds and their lengths were measured using a comparator (initial reading). After this, the bars were submerged in room temperature water, and placed in a sealed container in an oven set to 80 °C. After 24 hours in the oven, the mortar bars were taken out of the water and measured again using the comparator (zero reading). They were then submerged in a 1 N sodium hydroxide (NaOH) solution (that had already been heated to 80 °C) and placed back in the oven. Additional length readings were taken at 3, 7, 11, and 14 days after submersion in the

NaOH solution. Expansion was calculated by determining the length change of the mortar bars expressed as a percentage of the gage length (10 in.).

Since SCMs mainly control ASR by reducing the availability of alkalis, the ASTM C 1567 [137] test, which provides an inexhaustible source of alkalis at high temperature, simulates harsher conditions than what would be found in the field [145]. However, it is a good test for screening purposes, especially since the length of the test is only 16 days compared to the 2-year testing period that is required by ASTM C 1293 [146], the concrete prism test for ASR. Therefore, in the current study, the results from the ASTM C 1567 [137] accelerated mortar bar test is only used to find the optimal replacement dosage for the long-term ASTM C 1293 [146] ASR test. The initial SCM replacement dosage for the mortar bars was 20% by mass. Depending upon the results, the percentage was increased or decreased, to find the minimum replacement dosage at which expansions were kept below the 0.1% limit of ASTM C 1567 [137].

3.1.7 Resistance to Sulfate Attack

Unlike the requirements for ASR, TxDOT does not require SCMs that are being used in a mixture design to provide sulfate resistance. However, for a comprehensive analysis, the ability of these SCMs to resist sulfate attack was tested using ASTM C 1012 [147], which measures the length change of mortar bars submerged in a 5% sodium sulfate (Na_2SO_4) solution. Two different sets of sulfate mixtures were prepared. For the first set, the w/cm of the control (with no SCMs) was 0.485. As specified by the standard, the water content for the SCM mortar mixtures was such that the mortar flow measured by ASTM C 1437 [134] was within $\pm 5\%$ of the control mortar. However, the zeolite mortar mixtures were requiring extremely high w/cm to meet the flow requirements. Therefore, a second set of mortar mixtures were prepared for the zeolites, where the w/cm was kept constant at 0.51. A naphthalene-based ASTM C 494 [144] Type F WRA distributed by Sika Corporation under the trade name Sikament N was used for the constant w/cm mortar mixes to achieve the required flow.

As specified by this method, the mortar mixture contained 2.75 parts standard graded sand to 1 part cementitious material (cement + SCM). Six 1 in. x 1 in. x 11 ¼ in. mortar bars and six 2 in. mortar cubes were made from each mortar mixture. After mixing, the filled mortar bar molds and cube molds were sealed and submerged in a water bath set to 38 °C to accelerate curing. After 24 hours, the molds were taken out of the water bath, and the specimens were removed from the molds. After removal from the molds, the compressive strength of two mortar cubes was tested. If the compressive strength was less than 2850 psi, the mortar bars were placed in saturated lime water with the remaining mortar cubes until the average compressive strength of two mortar cubes reached 2850 psi. When the average compressive strength of the cubes reached this value, the length of the mortar bars were measured using a comparator. They were then submerged in a 5% sodium sulfate solution at room temperature. Subsequent length measurements of the mortar bars were taken at 1, 2, 3, 4, 8, 13, 15, 16, 24, 36, 48, 60, and 72 weeks.

ASTM C 1012 (2013) lists a maximum permissible range that the length change data must not exceed depending upon the number of samples. Due to the variable nature of the test, the range of data for a few samples with high sulfate expansions was found to be higher than the tolerance listed under the “Report” section of ASTM C 1012 (2013). Although not explicitly stated (as is the case for ASTM C 109, 2011), the language of the standard implies that bars that have expansions outside the tolerance limit of the data should be treated as outliers. Therefore in this study, the bar that deviated the most from the average out of the six bars was discarded and

the value of the range was checked to see if it met the listed tolerance of ASTM C 1012. If the range was still higher, then the bar with the second highest deviation from the average was also discarded and the range was checked again to ensure it was within the ASTM C 1012 tolerance. It must be noted that no more than two bars were removed for any sulfate mixtures in this study. Therefore, each of the average expansions was always calculated from four or more bars. ASTM C 1012 (2013) requires a minimum of three bars for calculating the average expansion.

Since there are no well-defined concrete tests for measuring susceptibility to sulfate attack, the ASTM C 1012 [147] results with mortar samples were used to make the final recommendations on the use of these new SCMs in sulfate environments. As such, instead of using a replacement dosage of 20%, like the other mortar tests, the replacement dosages of the sulfate mortar mixes were the same as the concrete mixture dosages that will be discussed in detail in Chapter 4. Pumice-D, Perlite-I, Metakaolin-D, and Zeolite-Z were tested for sulfate resistance at replacement dosages of 15% and 25% by mass of cement, whereas Vitric Ash-S, Shale-T, and Zeolite-T were tested at a replacement dosage of 25%. Zeolite-A was tested at a replacement dosage of 35%.

3.2 Results

The following sub-sections provide detailed results of the mortar and paste studies. Other than the ASTM C 1012 [146] results for resistance to sulfate attack, described in Section 3.2.7, most of the results were used as a screening tool to optimize the SCM replacement levels for the concrete mixtures. The ASTM C 1567 [137] ASR results determined the minimum replacement levels, while the rheology and compressive strength results were used to provide an indication of what the maximum replacement levels could be in the concrete mixtures.

3.2.1 Compressive Strength

Figure 3.1 shows the average compressive strength of the SCM mortars made at a w/cm of 0.5. The error bars represent the range of the data. All the ranges are within the limits prescribed by ASTM C 109, except for the 3-day compression strength of the Pumice-D mortar and the 1-day compression strength of the Metakaolin-D mortar. The range for these two readings were slightly above 8% of the average, instead of being less than or equal to 7.6%, as suggested by ASTM C 109 [131].

As Figure 3.1 indicates, all the SCM mixtures have a lower strength than the control at 1 and 3 days. However, by 28 days, most of the SCM mortars have strengths that are similar to that of the control, if not higher. By 365 days, all the SCM mortars, except for Shale-T, had strengths higher than that of the control, with the Pumice-D and Perlite-I mortars having the highest strength. Between 1 and 28 days of hydration, the mixture with Metakaolin-D had the fastest rate of strength gain, surpassing the strength of control mixture by 22% at 28 days. Its compressive strength was also higher than that of the fly ash mortar at 28 days. Although initially the Pumice-D and Perlite-I mortars gained strength at a slower rate than the Metakaolin-D mortar, by 90 days both the Pumice-D and Perlite-I mixtures had higher compressive strengths than the Metakaolin-D mixture. This means that although Metakaolin-D is fast to react, the more siliceous pozzolans like Pumice-D and Perlite-I improve the long-term strength of concrete more than Metakaolin-D. The Pumice-D and Perlite-I mixtures also had a higher strength than the fly ash mixture at 365 days.

Although the strength difference between the Vitric Ash-S mortar and the other unaltered volcanic pozzolan mortars were not apparent at 28 days, by 365 days the difference in strength

was significant. Despite being an unaltered volcanic pozzolan like Pumice-D and Perlite-I, Vitric Ash-S did not improve the 1-year compressive strength of the mortar mixtures as much as the pumice and perlite. The reason for the lower strength of Vitric Ash-S mortar compared to the Pumice-D and Perlite-I mortars may be related to its greater content of crystalline impurities, as shown by the XRD data presented in Chapter 2 and Appendix A. The mortar made with Shale-T, despite being a sedimentary pozzolan like the fast reacting Metakaolin-D, had the slowest rate of strength gain. Even at 365 days, its strength was only slightly higher than that of the control.

Figure 3.2 presents the average compressive strength of the mortar mixtures made with a w/cm of 0.55. The error bars represent the range of the data, and are all within the limits allowed by ASTM C 109 [131]. As Figure 3.2 indicates, the Zeolite-Z mortar gained strength rapidly, surpassing the strength of the control by only 28 days. On the other hand, even at 365 days, Zeolite-T and Zeolite-A had strengths that were approximately 70–75% of the control. The Zeolite-T and Zeolite-A powders were much coarser than the Zeolite-Z powder. Furthermore, XRD data from the Zeolite-T and Zeolite-A powders showed them to contain more crystalline impurities than the Zeolite-Z powder, which primarily consisted of clinoptilolite. The purity and the fineness of the Zeolite-Z powder is most likely why it performed better than the two other zeolites. Like Metakaolin-D, Zeolite-Z also seemed to react earlier than the other pozzolans. However, by 90 days its reactivity tapered off, and the strength of its mortar mixture, which was higher than the fly ash mixture at 28 days, fell below the strength of the fly ash mixture at 90 days.

3.2.2 Rheological Properties

Figure 3.3 presents the rheological flow curves of the control and SCM pastes. These flow curves illustrate how the shear stress in the pastes changed as the shear rate was decreased from 50 s^{-1} to 10 s^{-1} . The Bingham model [138], which was used to analyze the flow curves, employs a linear trend line to find the viscosity and yield stress of mixtures [140]. Although some of the zeolite paste flow curves were not fully linear, the coefficient of determination (R^2) values for the linear trend lines fitted to the flow curves were found to be above 0.95. As such the use of the Bingham model was considered to be appropriate for the zeolite mixtures as well. The yield stresses and viscosities of the different paste mixtures that were derived from the flow curves are presented in Table 3.2, along with the range of the data from duplicate tests.

The flow curves for the Zeolite-Z and Zeolite-T pastes have very steep slopes and high y-axis intercepts compared to the other SCM paste mixtures, which indicates that the viscosity and yield stress of these two zeolites pastes are much greater than those of the other SCM mixtures. Although these results are similar to those from the water requirement test, the rheology results give a more thorough understanding of the effect of the zeolites on mixture workability. For example, Zeolite-T had a water requirement value that was 16% higher than Zeolite-Z, which indicated that mixtures containing Zeolite-T would have lower slump values than mixtures containing Zeolite-Z. However, as Table 3.2 attests, Zeolite-Z and Zeolite-T affected rheological behavior in different ways. The Zeolite-Z paste had the highest viscosity among the SCM pastes, which means that while flowing, the Zeolite-Z mixture exhibited the highest amount of resistance to flow. In other words, a mixture containing Zeolite-Z would likely flow at a slower rate than a mixture containing an SCM like fly ash, which has a viscosity value that is approximately one-sixth that of Zeolite-Z. On the other hand, the Zeolite-T paste had the highest yield stress, which means that out of all the SCM pastes, the Zeolite-T mixture would likely require the greatest amount of force to be applied to it before the mixture could flow.

Of the eight SCMs tested, the viscosity and yield stress of the Shale-T paste was closest to that of the fly ash mixture, indicating its suitability for use as a fly ash replacement in applications where a low viscosity or “easily flowable” concrete mixture is required. With a viscosity lower than that of the control paste with no SCMs, Vitric Ash-S could also be used to make concrete mixtures more fluid and workable. The Pumice-D, Perlite-I, and Metakaolin-D SCMs are not expected to have an adverse effect on mixture workability as the viscosity and yield stress of their respective pastes were only slightly higher than those of the control paste.

Unlike the other SCMs, the rheology results of Zeolite-A did not match with its water requirement results. Although the Zeolite-A mortar failed the water requirement test, the viscosity and yield strength of the Zeolite-A paste was similar to that of the control. More research needs to be conducted to understand why the workability of the Zeolite-A mixture is different depending on whether the tests are carried out in paste or mortar.

3.2.3 Heat of Hydration

Figure 3.4 shows the rate of heat evolution of the paste mixtures per gram of cementitious material (cement + SCM). Similar to Class F fly ash, all eight pozzolans lowered the amount of heat evolved during hydration, which makes them suitable for concrete applications where thermal cracking is a potential issue. Furthermore, the plots did not show an increase in the length of the induction period (i.e., the time to the acceleratory phase of cement hydration), which indicates that none of the SCMs have an adverse effect on cement hydration.

3.2.4 Calcium Hydroxide Content

Figure 3.5 presents the calcium hydroxide contents of the pastes at 7, 28, and 90 days of hydration. The calcium hydroxide contents of the pastes were measured to observe whether the pozzolanic reaction was occurring in the SCM pastes. From the graph, we can see that the calcium hydroxide contents of the SCM pastes are generally always lower than that of the control with no SCM, suggesting that the calcium hydroxide in the SCM pastes is being depleted through the pozzolanic reaction. At both 28 and 90 days, the lowest calcium hydroxide content is seen for the Metakaolin-D and Zeolite-Z pastes. This ties in well with the ASTM C 618 [18] SAI results that showed the highest reactivity for the Metakaolin-D and Zeolite-Z powders.

Surprisingly, the Pumice-D and Perlite-I pastes, which seemed to have a high reactivity from the SAI and compressive strength results, were observed to have higher calcium hydroxide contents than the other pozzolan pastes at 7 days. In fact, the 7-day calcium hydroxide contents of the Pumice-D and Perlite-I pastes are similar to that of the control paste with no SCMs. However, by 90 days, both pastes have a significant reduction in their calcium hydroxide content, indicating that pozzolanic reactions are taking place in the mixture. The initial high calcium hydroxide content of the Pumice-D and Perlite-I pastes could be an effect of the SCMs’ small particle size that could contribute to an enhanced nucleation and growth of cement hydration products like calcium hydroxide.

Due to factors like nucleation and growth, which can increase the initial calcium hydroxide content of a mixture, perhaps a better way to gauge the level of pozzolanic reaction is to examine the difference in calcium hydroxide content between 7 and 90 days, instead of using only the 90-day calcium hydroxide content value. For example, the Vitric Ash-S, Shale-T, Zeolite-T, and Zeolite-A pastes have calcium hydroxide contents similar to those of the Pumice-D and Perlite-I pastes, indicating that their pozzolanic potential is similar. However, looking at the calcium hydroxide content difference instead of the absolute values shows us that Pumice-D

and Perlite-I reduced the calcium hydroxide content of the paste by 20% or more between 7 and 90 days, while the reduction was 10% or less for the Vitric Ash-S, Shale-T, Zeolite-T, and Zeolite-A pastes. This correlates better with results from the ASTM C 618 [18] SAI testing and the mortar cube compression testing that have shown the Pumice-D and Perlite-I to be more reactive than the Vitric Ash-S, Shale-T, Zeolite-T, and Zeolite-A SCMs.

3.2.5 Drying Shrinkage

Figure 3.6 shows the percent shrinkage over time of the mortar mixtures kept in a 50% RH environmental chamber. In general, the SCM mortar mixtures had a higher shrinkage than the control mortar. It must be noted here that all the drying shrinkage mortars had a variable w/cm to meet the flow requirements. As such, the shrinkage results can be unfavorable to SCMs like the zeolites, which required a much larger water content to achieve the desired flow. Figure 3.7 shows the correlation between the percent shrinkage and the percent weight loss of the samples. Other than for the zeolites, the shrinkage vs. weight loss plots for the SCM mortar bars show a fairly linear trend, which indicates that differences in shrinkage between the control mortar and the SCM mortars are due to water loss, instead of a change in the microstructure of C-S-H from the SCM addition. The curve of the shrinkage vs. weight loss plot of the zeolite mortar bars suggests that the materials themselves maybe contributing to shrinkage. This is explored in detail in the concrete studies, where a constant w/cm is used, to avoid any biases due to differing water contents between mixtures.

Table 3.3 shows the difference in weight loss and shrinkage compared to the control mixture at 64 weeks (448 days). As an optional requirement for Class N pozzolans, ASTM C 618 [18] specifies that SCM mortar bars made for drying shrinkage according to ASTM C 311 [123] should not increase the shrinkage strain by more than 0.03% when compared to that of the control mortar. While the mortar proportions used in the current test followed the directions of ASTM C 596 [143], which are different than the proportions specified by ASTM C 311 [123], it is interesting to note that the shrinkage value of all the SCM mortar bars other than the zeolites are under the ASTM C 618 [18] limit.

3.2.6 Resistance to Alkali-Silica Reaction

Figure 3.8 shows the results of ASTM C 1567 [137] testing on mortar bars where a 20% SCM replacement dosage was used. The graph indicates that only the Pumice-D, Perlite-I, Metakaolin-D, and Zeolite-Z mortar bars had expansions below the 0.1% limit after 14 days of submersion in NaOH solution. The Vitric Ash-S and Shale-T mortar mixtures just barely missed the limit, exceeding the 0.1% expansion after 12 days of submersion in NaOH solution. Zeolite-T and Zeolite-A crossed the expansion limit at 7 days and 3 days, respectively. Table 3.4 lists the expansion of the 20% mortar bars after 14 days of NaOH submersion, along with the range of the data.

For the second round of testing, the replacement dosage of Pumice-D, Perlite-I, Metakaolin-D, and Zeolite-Z was lowered to 15%, since they passed the ASTM C 1567 [137] test at a dosage of 20%. For the SCMs that failed to keep expansions below the limit at 20% replacement, the dosage was increased until they passed the ASTM C 1567 [137] test. Figure 3.9 shows the minimum SCM replacement dosages that were required for each SCM mortar mixture to pass the ASTM C 1567 [137] test. As Figure 3.9 indicates, the Pumice-D, Perlite-I, Metakaolin-D, and Zeolite-Z mortar bars had expansions lower than the 0.1% limit, even at a replacement dosage of 15%. The Vitric Ash-S, Shale-T, and Zeolite-T pozzolans can keep the

expansions of their mortar bars below the limit when used at a replacement dosage of 25%. However, Zeolite-A required a much higher dosage of 35% to pass the ASTM C 1567 [137] testing. This is not surprising, since Zeolite-A had the worst expansion after the control mortar mixture, when tested for ASR resistance at a replacement dosage of 20%. Table 3.5 lists the expansion of these mortar bars after 14 days of NaOH submersion, along with the range of the expansion data.

3.2.7 Resistance to Sulfate Attack

Figures 3.10 and 3.11 show the expansion of the ASTM C 1012 [147] mortar bars. For clarity, the mortar mixtures with the lower SCM replacement dosage of 15% are presented in Figure 3.10, while the mortar mixtures with the higher SCM dosages of 25% and 35% are presented in Figure 3.11. The yellow dots in the graph represent the “ACI 201: Guide to Durability” [148] limits of Class 1, Class 2 and Class 3 sulfate exposure. An SCM qualifies for a Class 1 mild sulfate exposure if it can keep expansions below 0.1% for 6 months, when tested for sulfate attack using ASTM C 1012. Similarly, an SCM qualifies for a Class 2 moderate sulfate exposure if it can keep expansions from ASTM C 1012 testing below 0.1% for 12 months. Finally, a Class 3 severe sulfate exposure requires the SCM to keep expansions from ASTM C 1012 testing below 0.1% for 18 months [148].

Figure 3.10 indicates that at a 15% replacement dosage, the mortars of Pumice-D, Perlite-I, and Zeolite-Z performed better than the fly ash mortar. All three pozzolans qualify for use in a Class 3 severe sulfate exposure environment, while the fly ash qualifies only for a Class 2 moderate sulfate exposure. Surprisingly, the 15% Metakaolin-D mortar had an inadequate performance under sulfate attack, crossing the 0.1% limit after 18 weeks, and completely cracking after 6 months. As Figure 3.11 indicates, Metakaolin-D does have a better performance when used at a higher replacement dosage. However, even at a 25% replacement, Metakaolin-D only qualifies for a Class 2 sulfate exposure, unlike the Pumice-D, Perlite-I, and Zeolite-Z mortars, which qualify for a Class 3 exposure at both 15% and 25% replacement levels. The fly ash mortar also qualified for a Class 3 exposure when a 25% replacement dosage was used. The Shale-T mortar, at 25% replacement, qualified for a Class 1 mild sulfate exposure. The 25% Vitric Ash-S mortar barely missed the Class 1 exposure limit, with expansions crossing the 0.1% limit just before 6 months. The Zeolite-T and Zeolite A mortars, at replacement dosages of 25% and 35% respectively, had inadequate performances under sulfate attack, with expansions as high as 0.4% by 8 weeks. By 13 weeks, all of the Zeolite-A bars had cracked completely, while the Zeolite-T bars cracked at 15 weeks.

Although Zeolite-T and Zeolite-A have consistently shown poor reactivity and performance, the researchers felt that the high w/cm that was used to achieve constant flow for the zeolite mortar mixtures could have contributed to the poor performance. To eliminate the effect of w/cm on performance, a second set of zeolite mortar mixtures was made with a fixed w/cm. The expansion results of these mortar bars with a fixed w/cm are shown in Figure 3.12. Although the performance of the Zeolite-T and Zeolite-A mortars improved a little with the lower w/cm, the mortar mixtures still exceeded the 0.1% expansion limit before 4 months, and could not even qualify for a Class 1 mild sulfate exposure. It was interesting to see that w/cm did not affect the performance of the Zeolite-Z mortar, since it qualified for a Class 3 sulfate exposure regardless of the w/cm used. Unlike Zeolite-Z, the effect of w/cm was very apparent for the fly ash mortar mixtures. When made with a lower w/cm (0.45–0.46), both the 15% and 25% fly ash mortars had a Class 2 and Class 3 sulfate exposure, respectively. However, when

made at a higher w/cm (0.51), both fly ash mortars only qualified for a Class 1 exposure. Table 3.6 provides a summary of the sulfate expansion along with the range of the data. With the exception of the 6-month reading of the 15% fly ash mortar (made with a w/cm of 0.51), all ranges are within the limits stated by ASTM C 1012, at expansions below 0.1%. At higher expansions, where the bars are undergoing heavy cracking, the range of the data became wider, as expected.

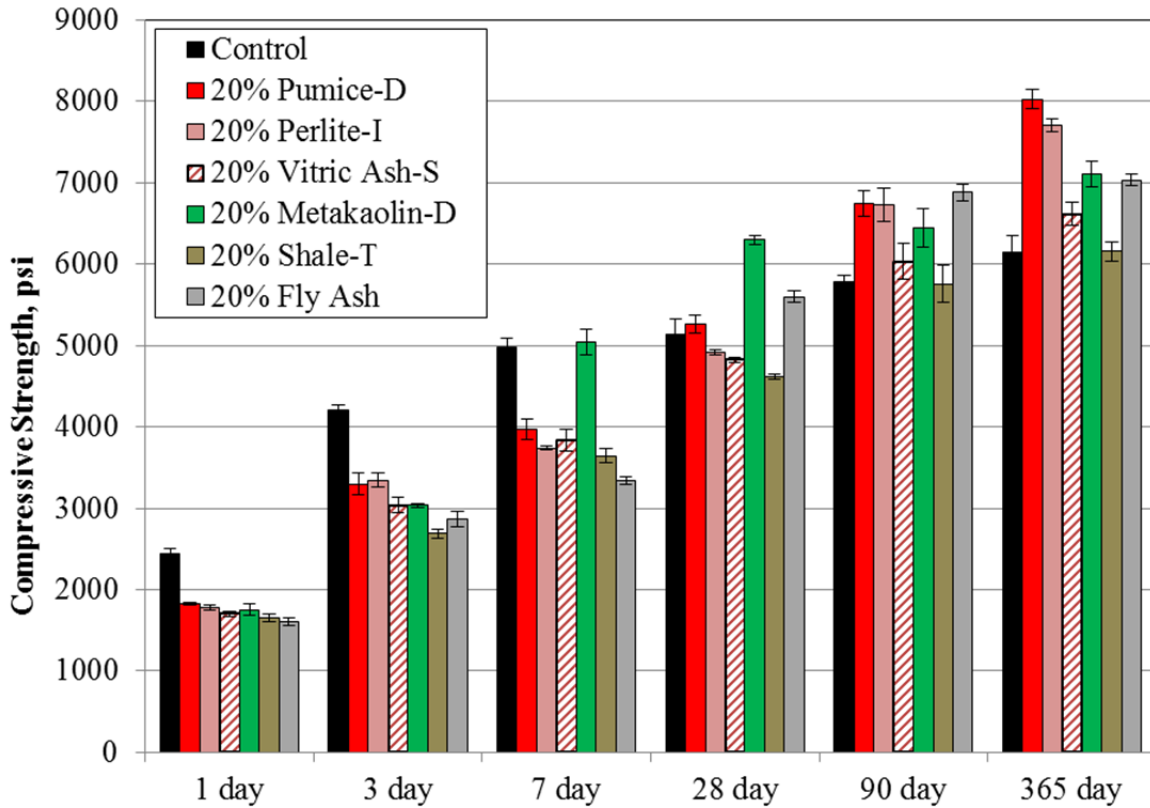


Figure 3.1: Compressive strength of mortar mixtures with a w/cm of 0.50

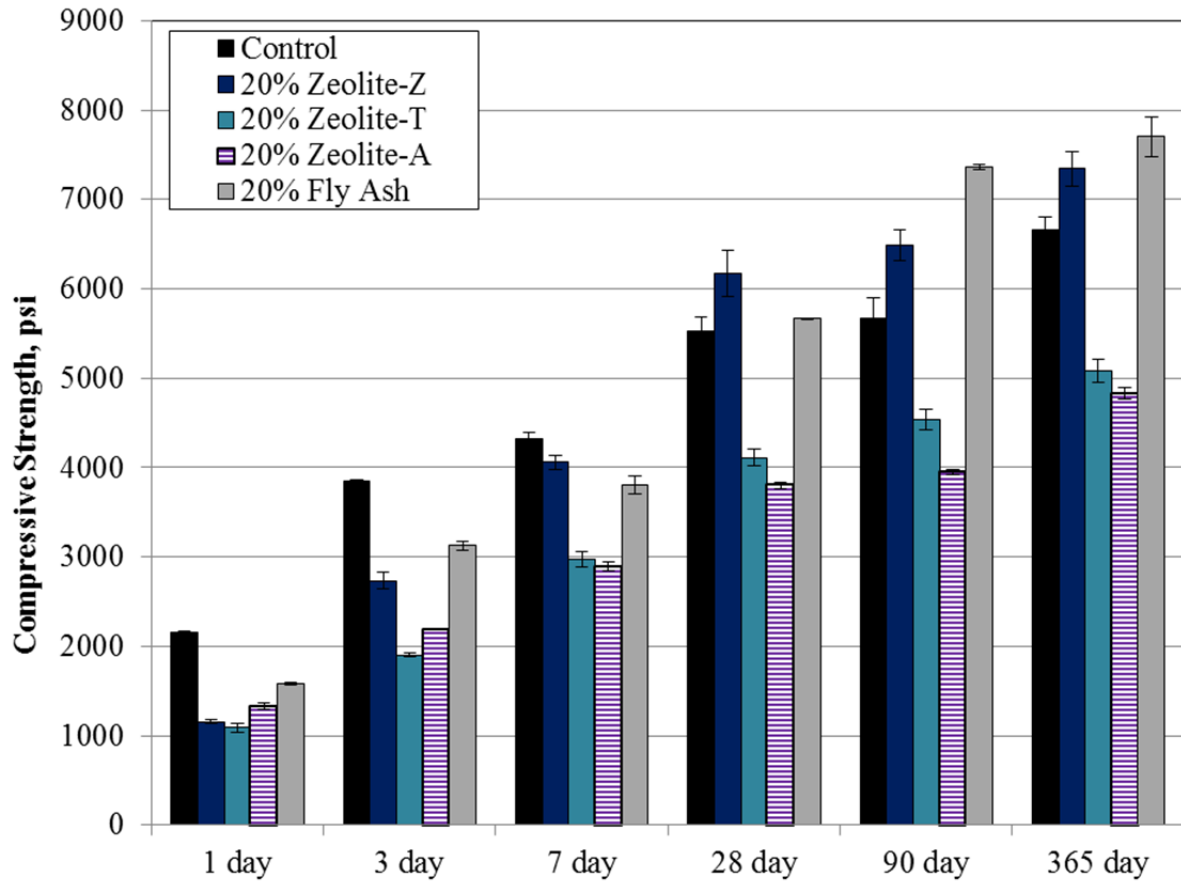


Figure 3.2: Compressive strength of mortar mixtures with a w/cm of 0.55

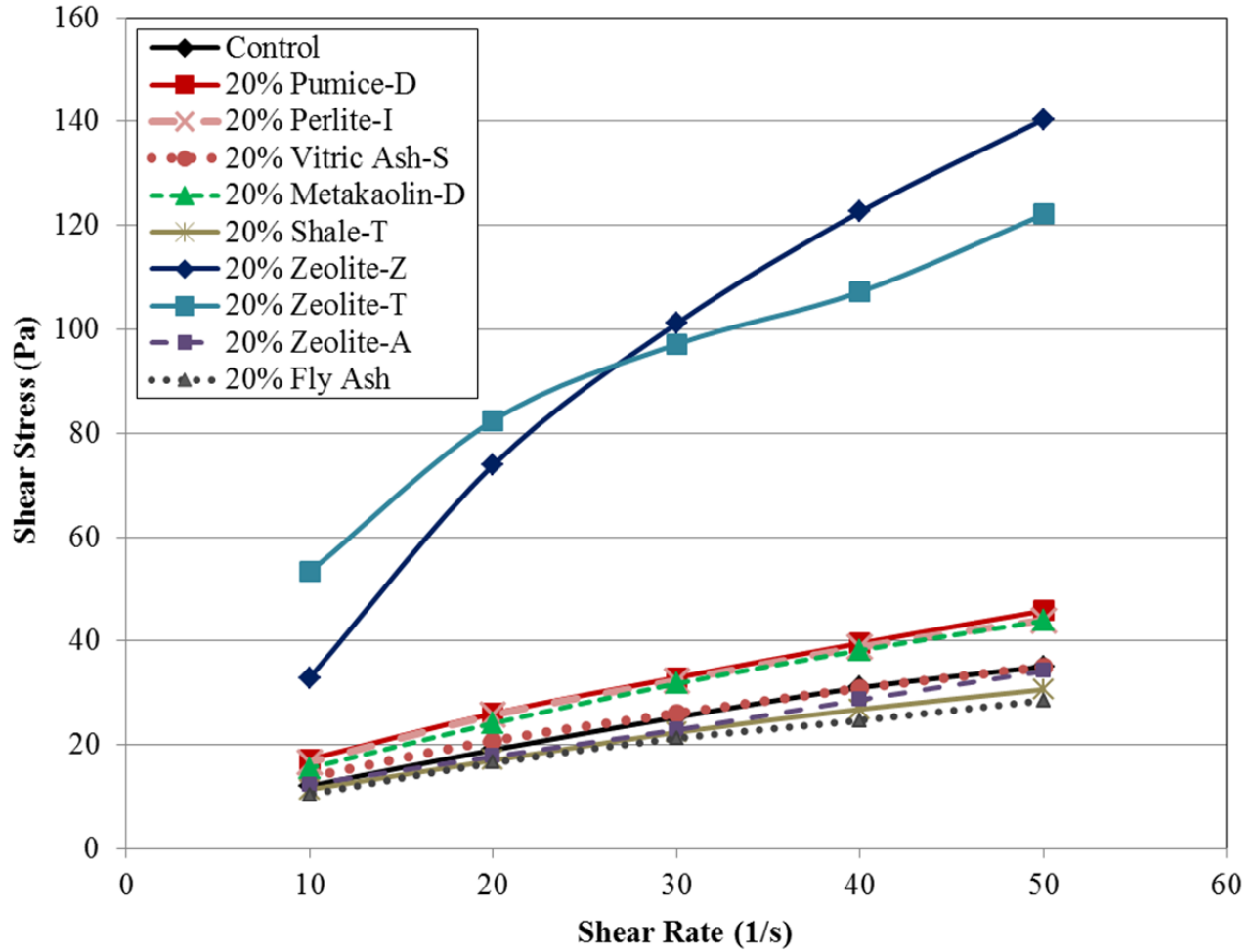


Figure 3.3: Representative rheology flow curves for control and SCM paste mixtures

Table 3.2: Yield Stress and Viscosity of Mixtures from Bingham Model

| Material | Replacement Dosage (%) | Yield Stress (Pa) | Viscosity (Pa.s) |
|--------------|------------------------|-------------------|------------------|
| Control | 0 | 7.78 ± 0.64 | 0.56 ± 0.01 |
| Pumice-D | 20 | 10.72 ± 0.39 | 0.73 ± 0.03 |
| Perlite-I | 20 | 11.77 ± 0.59 | 0.67 ± 0.01 |
| Vitric Ash-S | 20 | 9.91 ± 0.32 | 0.51 ± 0.01 |
| Metakaolin-D | 20 | 10.08 ± 0.60 | 0.70 ± 0.01 |
| Shale-T | 20 | 7.21 ± 0.01 | 0.48 ± 0.00 |
| Zeolite-Z | 20 | 15.41 ± 0.34 | 2.61 ± 0.03 |
| Zeolite-T | 20 | 45.61 ± 1.91 | 1.62 ± 0.00 |
| Zeolite-A | 20 | 8.53 ± 1.69 | 0.55 ± 0.00 |
| Fly Ash | 20 | 7.66 ± 0.64 | 0.44 ± 0.01 |

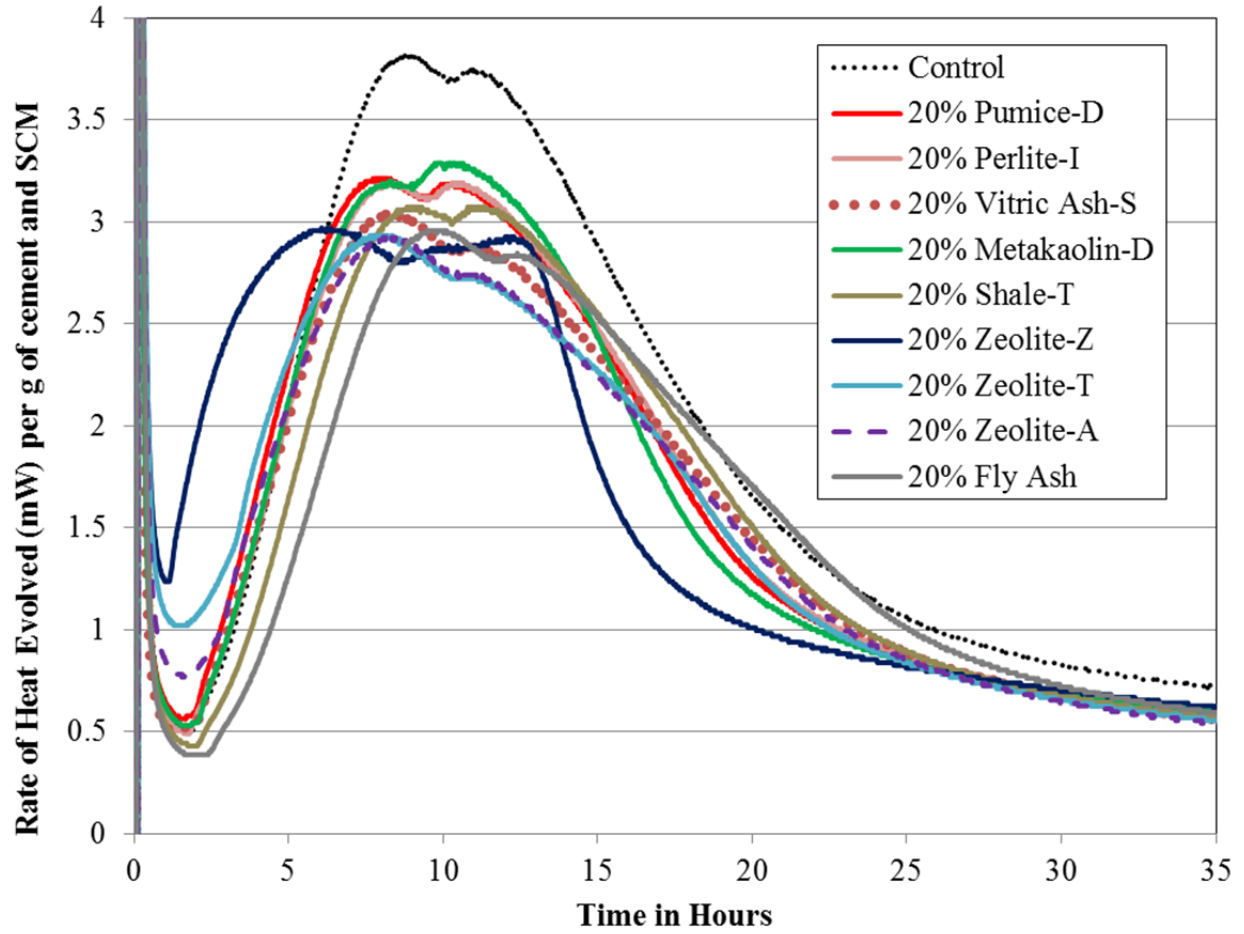


Figure 3.4: Rate of heat evolved during hydration per gram of cement and SCM

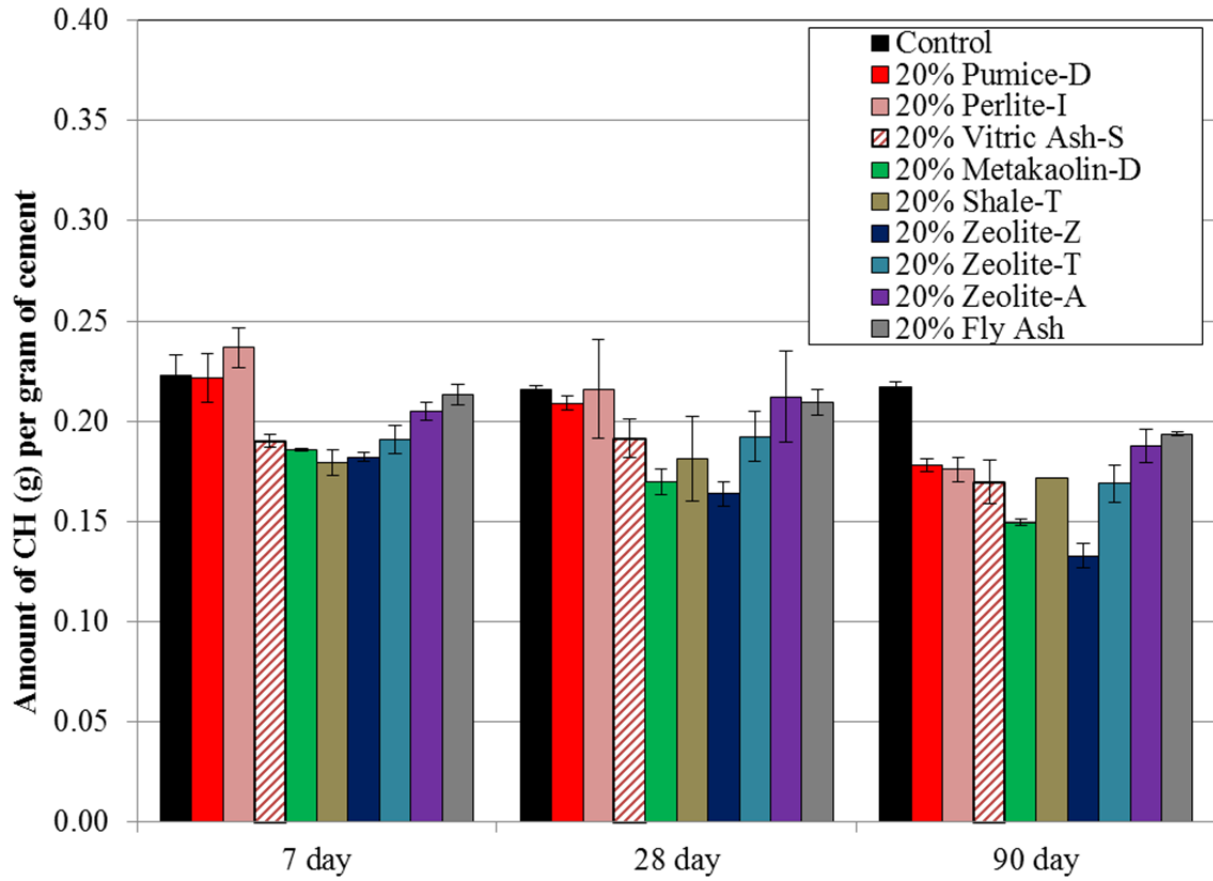


Figure 3.5: Calcium hydroxide content of pastes with 20% SCM

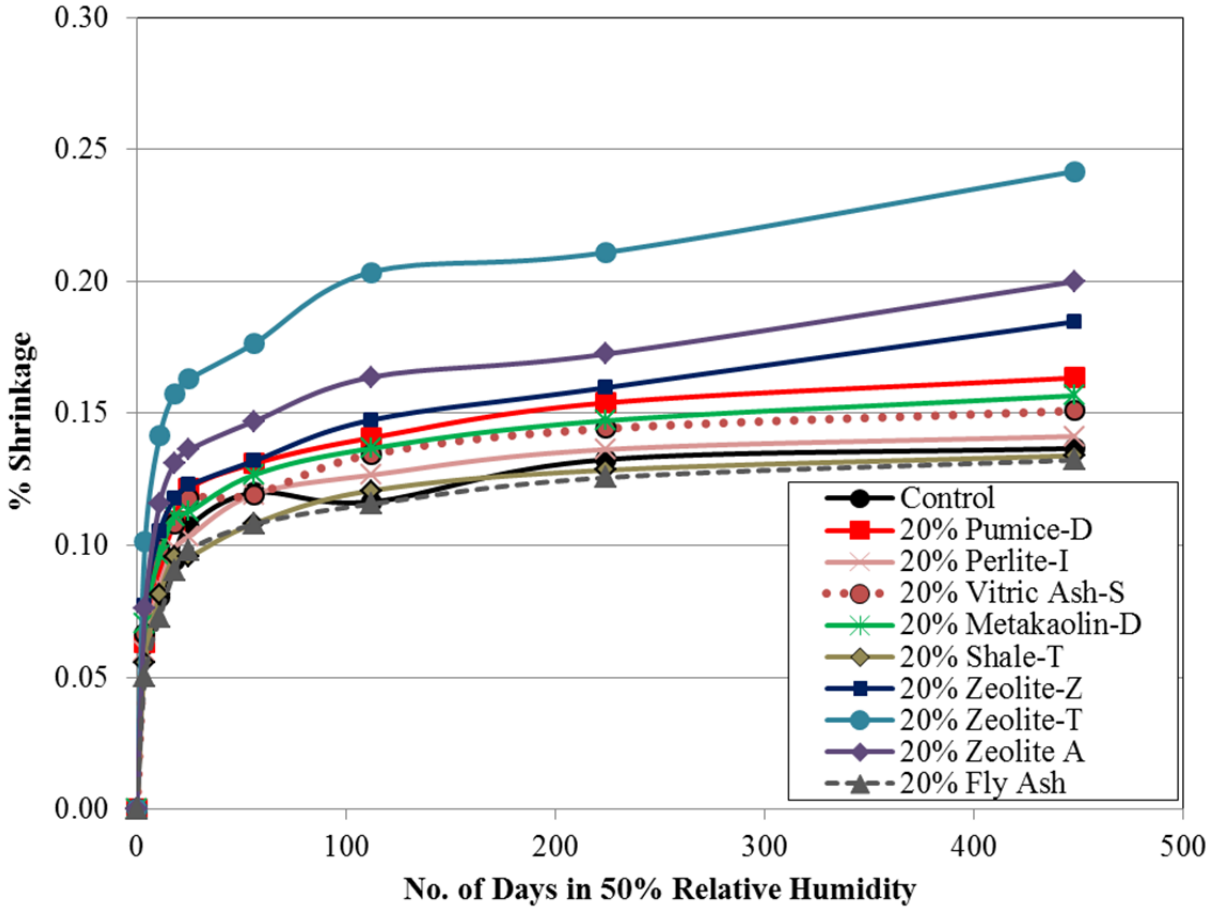


Figure 3.6: Percentage shrinkage of mortar mixtures in 50% RH

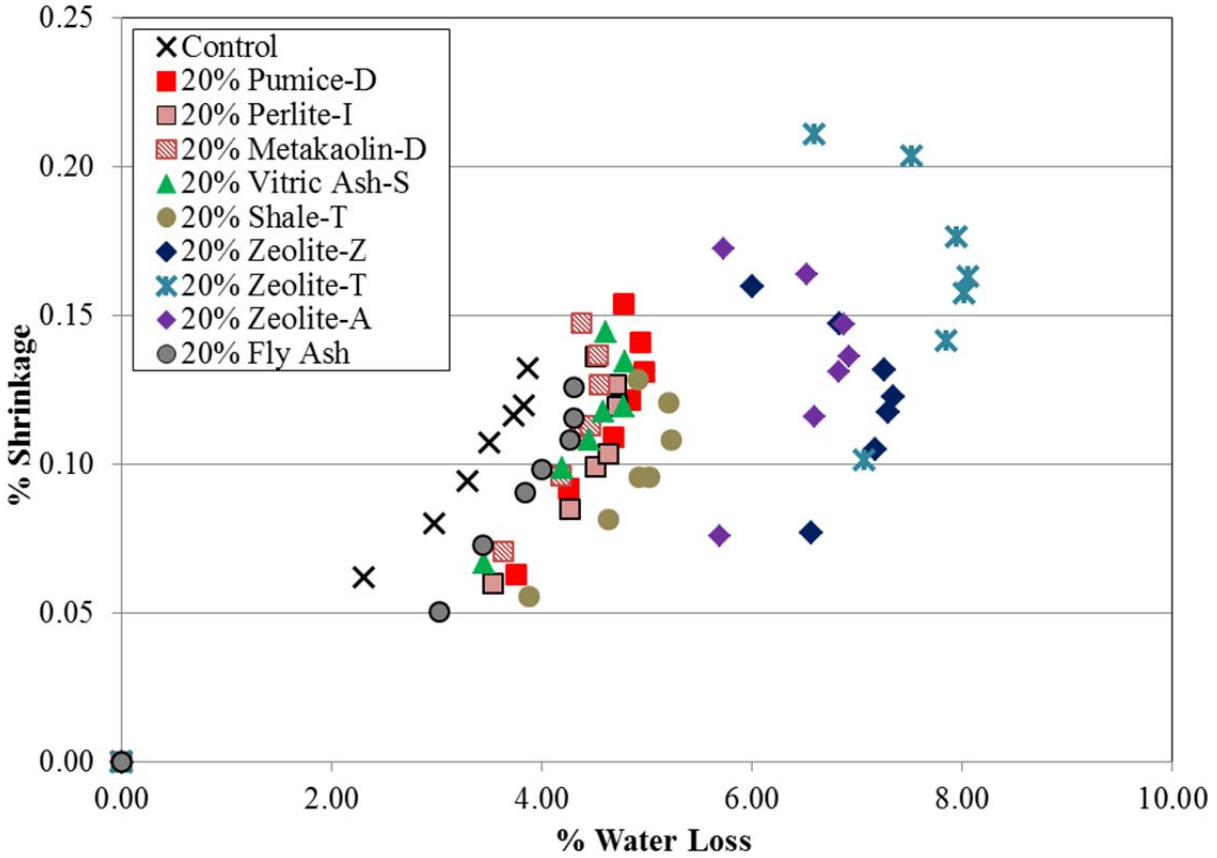


Figure 3.7: Shrinkage vs. weight loss of mortar mixtures in 50% RH

Table 3.3: Weight Loss and Shrinkage of SCM Mortar Bars Compared to Control

| Mortar Mixture Description | Weight Loss at 64 weeks (%) | Difference in weight loss compared to control (%) | Shrinkage at 64 weeks (%) | Difference in shrinkage compared to control (%) |
|----------------------------|-----------------------------|---|---------------------------|---|
| Control | 3.89 ± 0.04 | --- | 0.137 ± 0.002 | --- |
| 20% Pumice-D | 4.22 ± 0.03 | 0.33 | 0.164 ± 0.003 | 0.03 |
| 20% Perlite-I | 3.90 ± 0.09 | 0.02 | 0.141 ± 0.004 | 0.00 |
| 20% Vitric Ash -S | 3.91 ± 0.02 | 0.02 | 0.151 ± 0.002 | 0.01 |
| 20% Metakaolin-D | 3.84 ± 0.05 | -0.05 | 0.157 ± 0.007 | 0.02 |
| 20% Shale-T | 4.20 ± 0.11 | 0.31 | 0.134 ± 0.005 | 0.00 |
| 20% Zeolite-Z | 5.22 ± 0.07 | 1.33 | 0.185 ± 0.001 | 0.05 |
| 20% Zeolite-T | 5.81 ± 0.04 | 1.92 | 0.242 ± 0.004 | 0.11 |
| 20% Zeolite-A | 4.97 ± 0.04 | 1.08 | 0.200 ± 0.002 | 0.06 |
| 20% Fly ash | 3.92 ± 0.03 | 0.03 | 0.132 ± 0.002 | 0.00 |

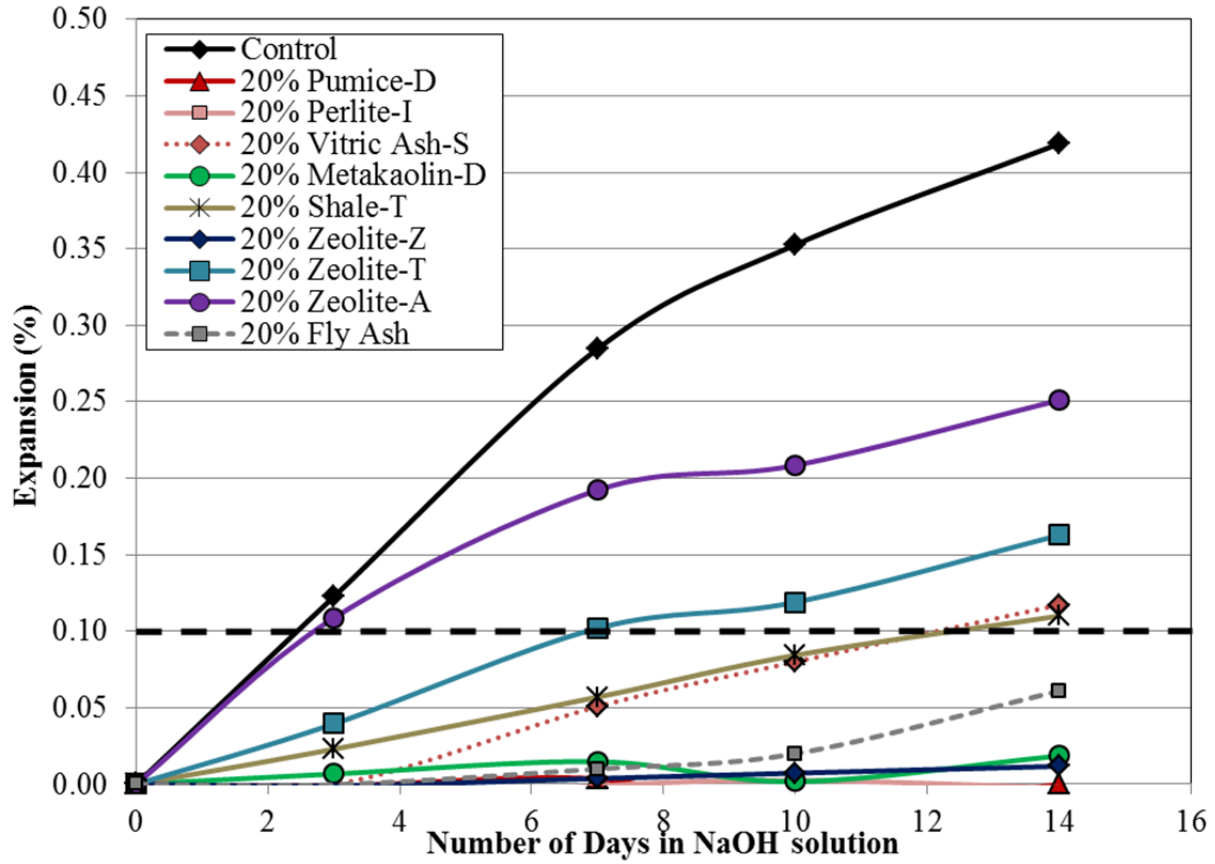


Figure 3.8: ASR expansion of mortar bars, with a 20% SCM replacement dosage

Table 3.4: Expansion of ASTM C 1567 Mortar Bars with 20% SCM

| Mortar mixture description | Expansion after 14 days of NaOH submersion |
|----------------------------|--|
| Control | 0.419 ± 0.007 |
| 20% Pumice-D | 0.000 ± 0.004 |
| 20% Perlite-I | -0.002 ± 0.003 |
| 20% Vitric Ash-S | 0.117 ± 0.012 |
| 20% Metakaolin-D | 0.019 ± 0.009 |
| 20% Shale-T | 0.110 ± 0.001 |
| 20% Zeolite-Z | 0.012 ± 0.007 |
| 20% Zeolite-T | 0.163 ± 0.016 |
| 20% Zeolite-A | 0.251 ± 0.018 |
| 20% Fly Ash | 0.061 ± 0.007 |

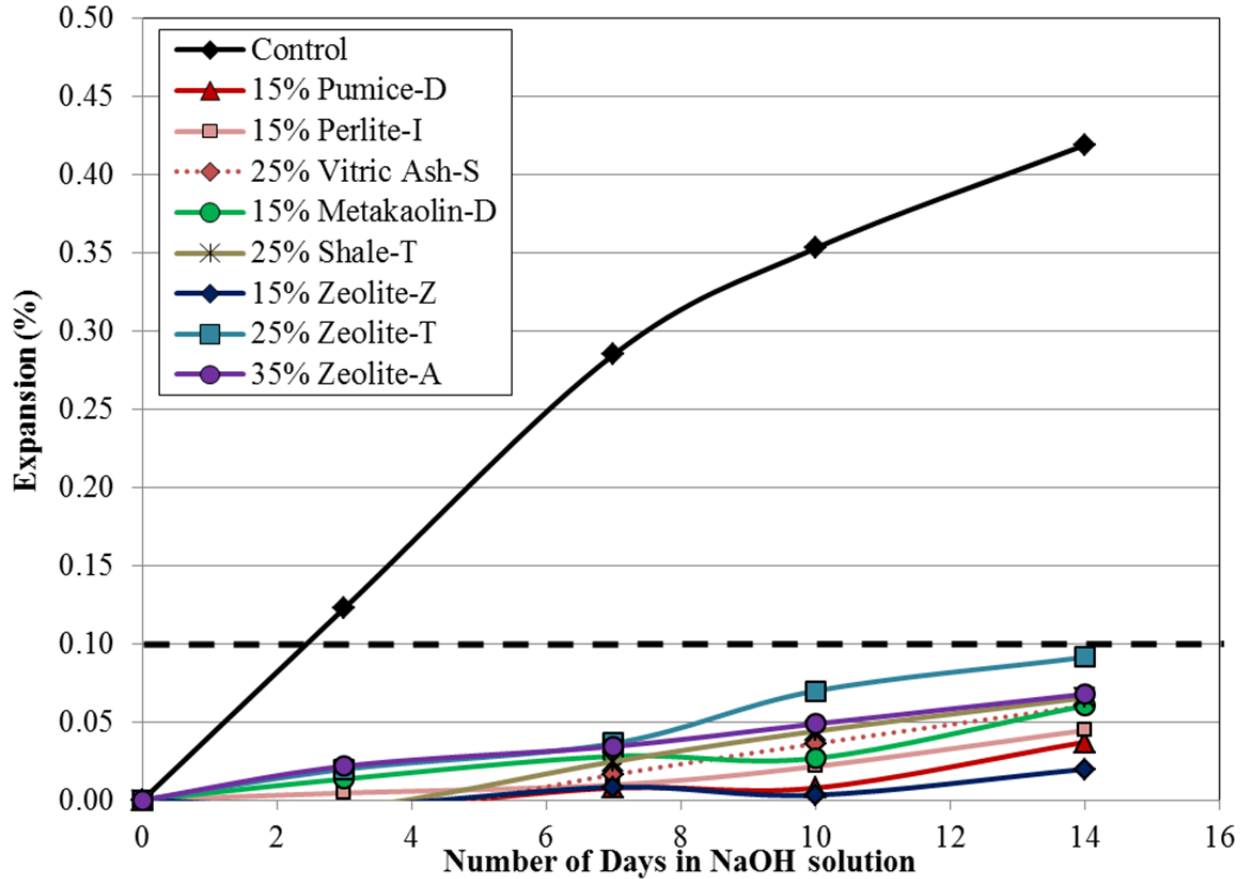


Figure 3.9: Minimum amount of SCM needed to pass ASTM C 1567ASR Testing

Table 3.5: Expansion of Mortar Bars with Adequate SCMs to Meet ASTM C 1567 Limit

| Mortar Mixture Name | Expansion after 14 days of NaOH submersion |
|---------------------|--|
| Control | 0.419 ± 0.007 |
| 15% Pumice-D | 0.037 ± 0.004 |
| 15% Perlite-I | 0.045 ± 0.005 |
| 25% Vitric Ash-S | 0.060 ± 0.003 |
| 15% Metakaolin-D | 0.060 ± 0.006 |
| 25% Shale-T | 0.065 ± 0.006 |
| 15% Zeolite-Z | 0.020 ± 0.003 |
| 25% Zeolite-T | 0.091 ± 0.008 |
| 35% Zeolite-A | 0.068 ± 0.002 |

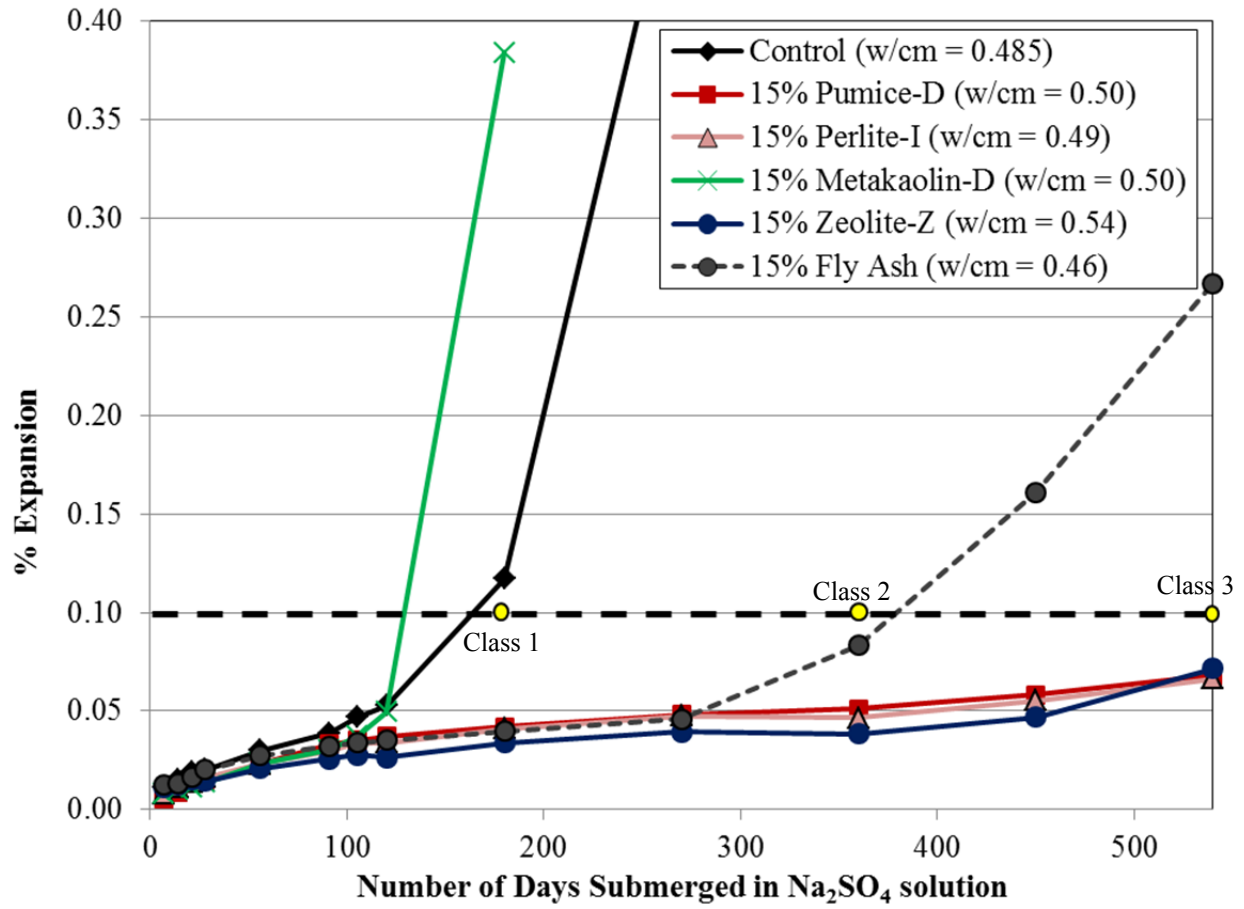


Figure 3.10: Expansions of ASTM C 1012 mortars bars, with 15% SCM replacement

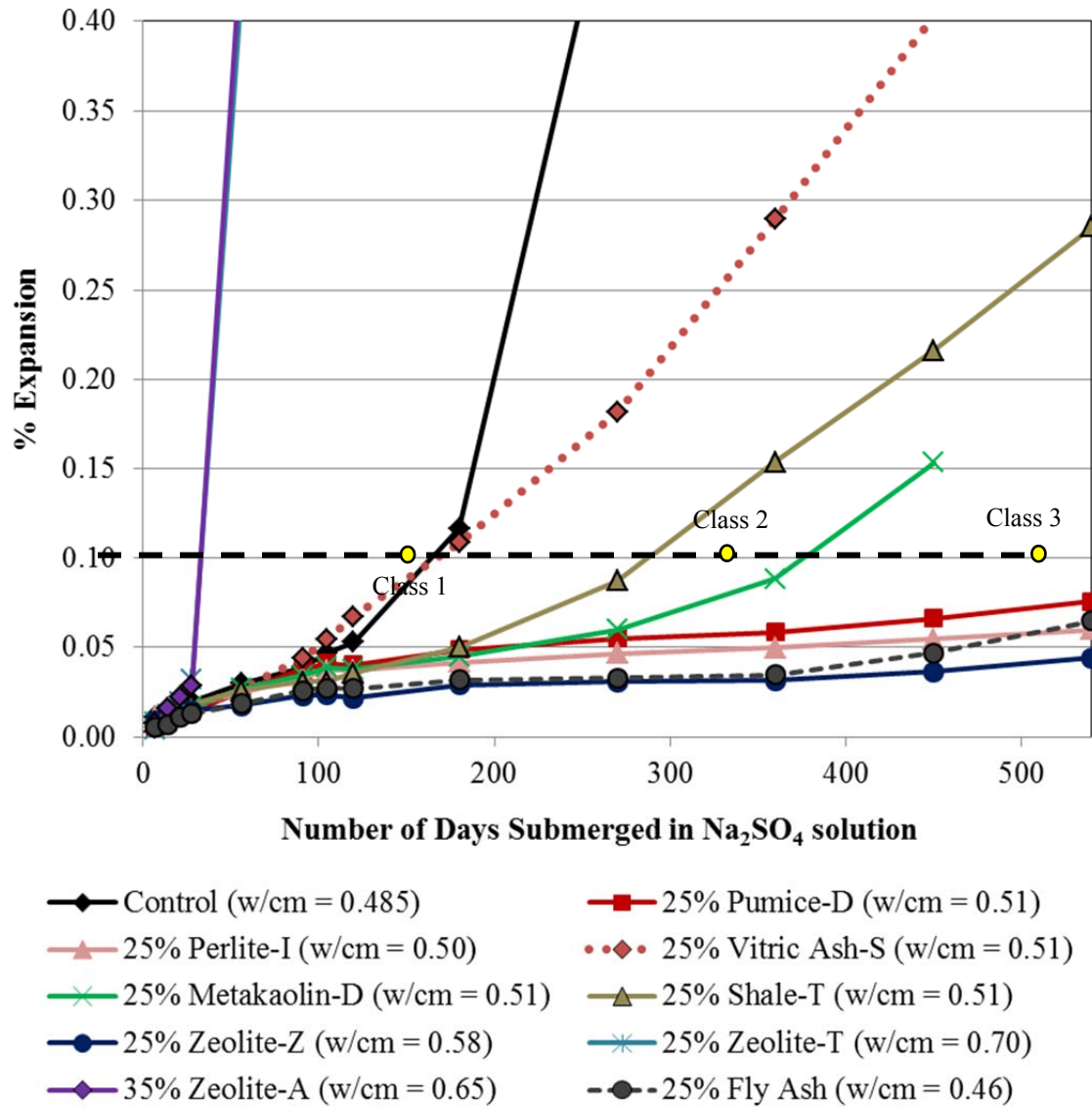


Figure 3.11: Expansion of ASTM C 1012 mortar bars with 25 or 35% SCM replacement

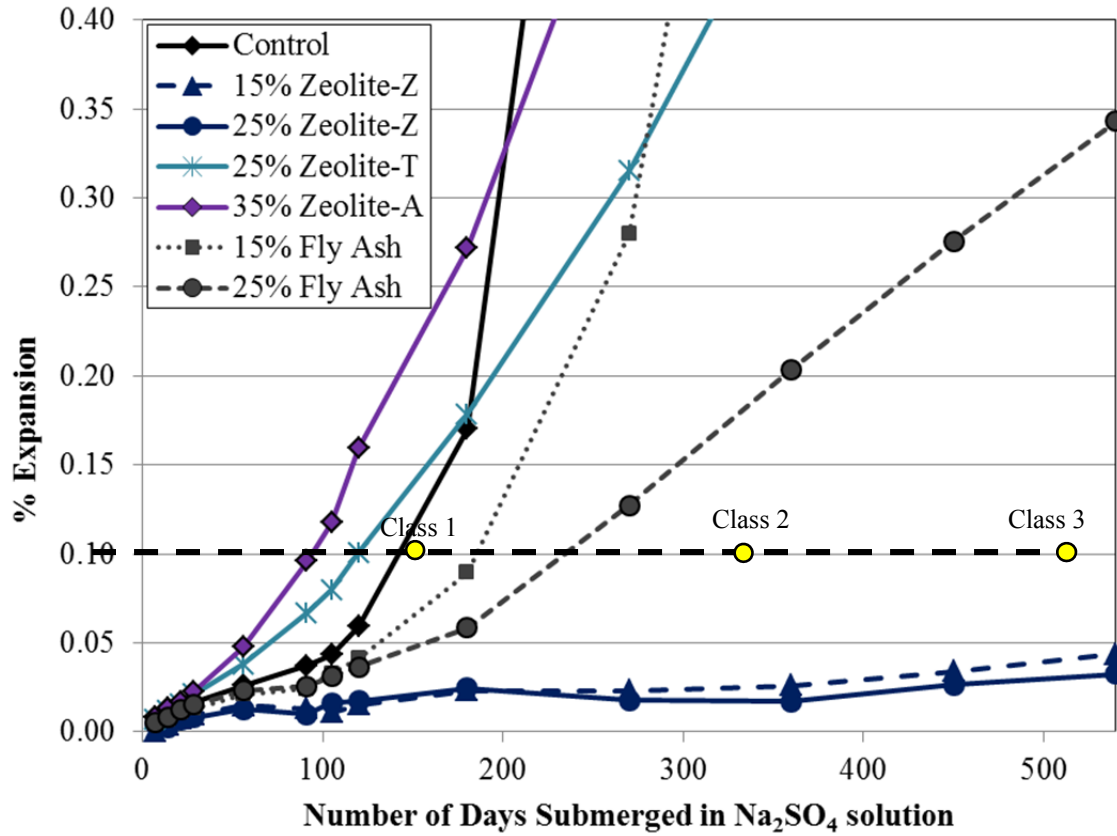


Figure 3.12: Expansion of ASTM C 1012 mortar bars made with a fixed w/cm

Table 3.6: Summary of Sulfate Exposure Qualification and Mortar Bar Expansion

| Mortar Mixture Description | w/cm | Sulfate Exposure | Expansion (%) of |
|-----------------------------------|-------------|-------------------------------|----------------------------|
| Control | 0.485 | Inadequate for sulfate attack | Exceeds 0.1 at 6 months |
| | 0.51 | Inadequate for sulfate attack | Exceeds 0.1 at 6 months |
| 15% Pumice-D | 0.50 | Qualifies for Class 3 | 0.068 ± 0.009 at 18 months |
| 25% Pumice-D | 0.51 | Qualifies for Class 3 | 0.076 ± 0.016 at 18 months |
| 15% Perlite-I | 0.49 | Qualifies for Class 3 | 0.066 ± 0.016 at 18 months |
| 25% Perlite-I | 0.50 | Qualifies for Class 3 | 0.060 ± 0.004 at 18 months |
| 25% Vitric Ash-S | 0.51 | Barely misses Class 1 limit | 0.109 ± 0.006 at 6 months |
| 15% Metakaolin-D | 0.50 | Inadequate for sulfate attack | Cracks at 6 months |
| 25% Metakaolin-D | 0.51 | Qualifies for Class 2 | 0.088 ± 0.017 at 12 months |
| 25% Shale-T | 0.51 | Qualifies for Class 1 | 0.050 ± 0.005 at 6 months |
| 15% Zeolite-Z | 0.54 | Qualifies for Class 3 | 0.072 ± 0.016 at 18 months |
| | 0.51 | Qualifies for Class 3 | 0.044 ± 0.009 at 18 months |
| 25% Zeolite-Z | 0.58 | Qualifies for Class 3 | 0.044 ± 0.008 at 18 months |
| | 0.51 | Qualifies for Class 3 | 0.033 ± 0.005 at 18 months |
| 25% Zeolite-T | 0.70 | Inadequate for sulfate attack | Cracks at 15 weeks |
| | 0.51 | Inadequate for sulfate attack | Exceeds 0.1 at 4 months |
| 35% Zeolite-A | 0.65 | Inadequate for sulfate attack | Cracks at 13 weeks |
| | 0.51 | Inadequate for sulfate attack | Exceeds 0.1 at 15 weeks |
| 15% Fly Ash | 0.46 | Qualifies for Class 2 | 0.083 ± 0.016 at 12 months |
| | 0.51 | Qualifies for Class 1 | 0.090 ± 0.033 at 6 months |
| 25% Fly Ash | 0.45 | Qualifies for Class 3 | 0.065 ± 0.009 at 18 months |
| | 0.51 | Qualifies for Class 1 | 0.059 ± 0.008 at 6 months |

3.3 Conclusions from Mortar and Paste Studies

The most important results from the mortar and paste studies were the ASTM C 1567 ASR expansion results, as they helped to determine the minimum dosages that would be used for the concrete mixtures. It was found that all pozzolans, except for Zeolite-A, could effectively keep expansions from ASR below the 0.1% limit at replacement dosages of 25% or less. The Zeolite-A mortar, however, needed a minimum replacement dosage of 35% to keep the ASR expansions below the limit. The rheology results were also important as they pinpointed how the zeolites would affect mixture workability. From the water requirement tests, it seemed that Zeolite-T would have the most adverse effect on concrete workability, but the rheology results showed that Zeolite-Z mixtures could also pose a potential problem due to high viscosity. Other results such as the calorimetry showed that the pozzolans did not negatively affect cement hydration. The decrease of calcium hydroxide content in the TGA results also suggested that pozzolans contributed to long-term strength by converting the calcium hydroxide in the paste to C-S-H. Results from the sulfate attack testing were also important, as they demonstrated that pozzolans that are good at preventing ASR expansions might not perform as well in a sulfate environment.

Chapter 4. Concrete Studies

The tests used in the concrete studies are shown in Table 4.1. Although some of the strength and durability experiments like drying shrinkage and resistance to ASR were performed on mortars, it is imperative to conduct the tests in concrete as well, since the mortar tests are accelerated in different ways and represent a more simplified system than actual concrete mixtures. In addition, some important durability tests, such as resistance to chloride ion penetration and measurement of the coefficient of thermal expansion (CoTE), do not have well-established mortar tests, so it was necessary to conduct concrete experiments to understand the performance of the pozzolans in those areas. In other words, while the mortar and paste results were helpful for an indication of pozzolan performance and optimal replacement dosages, the researchers used the concrete results to establish how well the SCMs would perform in real-world applications.

Although it varies from application to application, the minimum replacement limit for SCMs in concrete is usually dictated by its effect on concrete durability. In the case of this project, mitigating expansions from ASR was considered to be the most crucial and the results of the ASTM C 1567 [137] ASR testing on mortar bars was used to find the minimum SCM replacement dosages for the concrete mixtures. The mortar results indicated that most of the SCMs needed a replacement dosage of 25% or less, by weight of cement, to sufficiently keep expansions from ASR below the prescribed 0.1% limit of ASTM C 1567 [137]. The Pumice-D, Perlite-I, Metakaolin-D, and Zeolite-D mortars needed only a replacement dosage of 15%, while the Vitric Ash-S, Shale-T, and Zeolite-T mortars required a dosage of 25% to pass the standard. Zeolite-A was the exception, needing up to a 35% replacement dosage to meet the expansion criteria of the ASTM C 1567 [137] standard.

The maximum replacement dosage of a pozzolan in concrete is generally determined by the cost of the SCM and its effect on mixture workability. Strength is also an important factor to consider when determining maximum dosages, as the higher the replacement amount, the lower the early age strength of mixtures due to the dilution effect of replacing hydraulic cement with a slower reacting, pozzolanic material. In the current study, the maximum replacement dosages for the SCMs mixtures (except for the Zeolite-A mixture) were capped at 25%, since the prices per ton for most of the SCMs were higher than cement. Table 4.2 provides a list of the SCM replacement dosages in concrete mixtures.

Table 4.1: Tests Performed on Concrete Mixtures

| Strength and Durability Tests | Fresh State Tests |
|--|---------------------------|
| Compressive strength (ASTM C 39) | Slump (ASTM C 143) |
| Drying shrinkage (ASTM C 157) | Air content (ASTM C 231) |
| Resistance to ASR (ASTM C 1293) | Unit weight (ASTM C 29) |
| Resistance to chloride ion penetrability (ASTM C 1202) | Setting time (ASTM C 403) |
| CoTE (Tex-428-A) | --- |

Table 4.2: SCM Replacement Dosages (by Weight of Cement) in Concrete Mixtures

| SCM | Minimum (%) | Maximum (%) |
|--------------|-------------|-------------|
| Pumice-D | 15 | 25 |
| Perlite-I | 15 | 25 |
| Metakaolin-D | 15 | 25 |
| Vitric Ash-S | 25 | - |
| Shale-T | 25 | - |
| Zeolite-Z | 15 | 25 |
| Zeolite-T | 25 | - |
| Zeolite-A | 35 | - |

4.1 Procedures

This sub-section describes the procedures for the concrete experiments in detail. The criteria of success of the tests (if any) are also presented. With respect to the materials used, the cement for all the concrete mixtures was an ASTM C 150 [132] Type I portland cement. The coarse aggregate, a dolomitic limestone from TXI Bridgeport, was also kept the same across different concrete mixtures. The coarse aggregates were re-graded before mixing to ensure consistency between mixtures. The fine aggregate was the only component that varied depending upon the testing that was performed. A mixed quartz and chert sand from Texas, which was shown to be reactive in previous literature [136], was used in the concrete mixtures for ASTM C 1293 [146] to measure resistance to ASR. The concrete mixtures for testing fresh state properties, compression strength, drying shrinkage, chloride ion penetrability, and CoTE was made with non-reactive, Colorado River sand from TXI Webberville. Since the mortar results showed polycarboxylate admixtures to be ineffective for zeolite mixtures, a naphthalene-based ASTM C 494 [144] Type F WRA distributed by Sika Corporation under the trade name Sikament N was used in the concrete mixtures.

Along with the 8 different pozzolans, concrete mixtures with Class F fly ash from Rockdale, Texas, was also made so that the results of the new SCMs could be compared with the more commonly known performance results of Class F fly ash.

4.1.1 Mixture Design

Two different mixture designs were used in the current study. The concrete mixture design used for all concrete experiments, except the ASTM C 1293 [146] ASR testing, is shown in Table 4.3. Several factors were considered when designing this concrete mixture. First, the w/cm was set at 0.45, since it is commonly accepted as the maximum w/cm for load bearing structures. Next, the cement content was determined by estimating the cement paste necessary to ensure a workable mixture. The high water demand for the zeolite materials necessitated a relatively high cement content for the concrete mixtures, and as such a six-sack mix (564 lb of cement per yd³) was used. Finally, the aggregate gradation was determined by the type of testing planned for this research. Because the test for CoTE requires a specific coarse aggregate gradation, the gradation specified in Tex-428-A [149] was used for all concrete mixtures. Table 4.4 shows the mixture design used for ASTM C 1293 [146] tests. As specified by ASTM C 1293

[146], NaOH was added to the ASTM C 1293 concrete mixtures such that the alkali content of the concrete, expressed as Na_2O_e^1 , was 1.25% by mass of cement.

Both mixture designs used the same SCM replacement dosages. Since the SCMs have a lower specific gravity than cement, and the replacement dosages are in weight percent (instead of a volume percent), the volume of cementitious materials for all SCM mixtures was slightly greater compared to the control mixture.

Table 4.3: Mixture Design for All Concrete Experiments, except ASTM C 1293

| Component | Batch Weight, lb/yd ³ | Weight, % | Volume, % |
|-----------------------|----------------------------------|-----------|-----------|
| Coarse Aggregate | 1937 | 48.0 | 43.4 |
| Fine Aggregate | 1277 | 31.7 | 28.9 |
| Cementitious Material | 564 | 14.0 | 10.6 |
| Water | 254 | 6.3 | 15.1 |
| Air | -- | -- | 2.0 |

Table 4.4: Mixture Design for ASTM C 1293 ASR Testing

| Component | Batch Weight, lb/yd ³ | Weight % | Volume % |
|-----------------------|----------------------------------|----------|----------|
| Coarse Aggregate | 1937 | 48.3 | 43.4 |
| Fine Aggregate | 1257 | 31.3 | 28.9 |
| Cementitious Material | 564 | 14.1 | 10.6 |
| Water | 254 | 6.3 | 15.1 |
| Air | -- | -- | 2.0 |

4.1.2 Mixing, Casting, Consolidation, and Curing

A naphthalene-based superplasticizer was used to hit a target slump of 4 in. \pm 1 in. for each concrete mixture. An initial dose based on information obtained from characterization and mortar ASR testing was estimated and added to the mixing water prior to mixing (pre-dose). If the measured slump was not within the target range, more superplasticizer was added directly to the concrete in the mixer and mixed for an additional 60 seconds (post-dose). Pre- and post-dose values for each concrete mixture are shown in Appendix B. The concrete specimens used for compressive strength, drying shrinkage, rapid chloride ion penetration, and CoTE testing were mixed, cast, and consolidated according to the procedures described in ASTM C 192 [150]. Specimens were vibrated using a vibrating table for 30–45 seconds when the measured slump was less than 3 inches and rodded according to ASTM C 192 [150] if the measured slump was greater than 3 inches. After final finishing, the specimens were covered with wet burlap for 24 hours. After the specimens were removed from their molds at 24 hours, the cylinders were transferred to a moist room set to 23 °C and 100% RH and the prisms used for drying shrinkage were placed in saturated lime water at 23 °C. Please refer to Section 4.1.6 for more information on the curing of ASTM C 1293 [146] concrete prisms.

¹ $\text{Na}_2\text{O}_e = (\text{wt \% Na}_2\text{O}) + 0.658 * (\text{wt \% K}_2\text{O})$

4.1.3 Compressive Strength

Twelve 4-in. x 8-in. cylinders were cast for compressive strength testing at 7, 28, 56, and 90 days. At the appropriate ages, three cylinders were removed from moist storage and tested in a Forney FX-700 compression machine according to ASTM C 39 [151]. Neoprene pads with Shore A durometer hardness of 70 were used with metal retainers as end caps according to ASTM C 1231 [152]. The average compressive strength was calculated from three cylinders, except in cases where the range of the samples were higher than the 10.6% limit allowed in ASTM C 39 [151]. In such cases, the cylinder with the greatest strength differential from the average was discarded, and the compressive strength average was recalculated with two cylinders. The final range of the two samples was checked to see if it was less than or equal to 9.0% of the average, as instructed in ASTM C 39 [151].

4.1.4 Fresh State Properties

Concrete slump was measured according to ASTM C 143 [153]. As specified by this method, concrete was placed in the slump mold in three approximately equal layers and consolidated by rodding each layer 25 times with a smooth, straight steel tamping rod. After the top layer was compacted, the excess concrete was struck off and the mold was removed slowly. Slump was determined by measuring the change in height of the center of the cone of concrete to the nearest $\frac{1}{4}$ in. The air content of the fresh concrete mixtures was measured according to the pressure method described in ASTM C 231 [154]. The unit weight of the mixture was found using the procedures described in ASTM C 29 [155].

The setting time of concrete mixtures was found using the procedures of ASTM C 403 [156], which measures the resistance of the mixtures to penetration by standard needles at regular time intervals. The initial and final time of set corresponds to penetration resistance values of 500 psi and 4000 psi, respectively and is determined from a plot of penetration resistance versus elapsed time. The samples for measuring the time of set were prepared by wet-sieving fresh concrete through a 4.75-mm sieve.

In addition to the penetration resistance tests specified by ASTM C 403 [156], ultrasonic tests were investigated to continuously monitor the setting process on concrete samples and sieved mortar samples. This study aims to develop a field applicable nondestructive testing method for in-situ monitoring of the setting and hardening process of concrete. The details of test setup and data analysis are described in Appendix C

4.1.5 Drying Shrinkage

The drying shrinkage of the concrete bars was measured according to the procedures of ASTM C 157 [41], using 3 in. x 3 in. x 11 $\frac{1}{4}$ in. concrete prisms cast with gage studs at either end. After curing for 24 hours under wet burlap, the prisms were removed from the molds and placed in saturated lime water until an age of 28 days. After 28 days, the prisms were removed from the lime water, gently dried to remove any free water, and initial weight and length comparator readings were taken before the prisms were left to air dry in an environmental chamber at 50% RH and 23 °C. Subsequent length change and weight measurements were taken after 4, 7, 14, 28, 56, 112, 224, and 448 days in air storage. The average shrinkage for each mixture was calculated from three or more concrete bars, and the range of the data was checked to be within the limits stated in ASTM C 157 [41].

4.1.6 Resistance from Alkali-Silica Reaction

Resistance to ASR was measured according to the procedures of ASTM C 1293 [146], except for the concrete mixture design used, which was described in Table 4.4 in Section 4.1.1. In this test, 3 in. x 3 in. x 11 ¼ in. concrete prisms with gage studs at each end were cast into molds and cured for 24 hours under wet burlap. At an age of 24 hours, the prisms were demolded, measured using a comparator, and placed vertically on elevated stands in felt-lined 5-gallon buckets filled with water to a depth of approximately 1 in. These containers were then placed in an environmental chamber set to 38 °C. At ages of 7, 28, 56, 90, 180, 360, 540, and 720 days the length change of prisms were measured. After the measurements, the position of the bars within their respective containers was inverted so that the prisms were not stored with the same end up for two consecutive storage periods.

The average expansion for each mixture was calculated from three or more bars, and the range was checked to see whether it was within the limits stated in ASTM C 1293 [146]. In certain cases, the length change of one bar deviated significantly from the rest of the bars in the mixture. If the range of the expansion for these bars exceeded the limits of ASTM C 1293 [146], then a statistical test known as the Grubb's test or the maximum normed residual test was performed on the data to detect significant outliers with 95% confidence. Bars with expansion values that were statistically significant outliers were discarded and not used in the calculation for average expansion. Since ASTM C 1293 [146] requires that at least three bars be present for a valid expansion reading, after the outliers were discarded it was ensured that each concrete mixture had three or more concrete bars remaining, from which the average expansion was calculated.

4.1.7 Resistance to Chloride Ion Penetration

The research team did not measure the chloride ion penetration (one of the durability tests) during the initial phases of the project, since there are no well-established paste and mortar tests for this measurement. However, measuring this durability property is very important, as the ingress of chloride ions can depassivate the steel in concrete and cause corrosion, without needing a drop in the pH content [157].

The chloride penetrability of concrete cylinders that were cured for 32 weeks was measured according to ASTM C 1202 [158]. As this method specifies, 4 in. x 8 in. cylinders were cut into 2 in. thick slices and conditioned in a vacuum desiccator. After conditioning, the 2 in. slices were sealed in the test setup using rubber gaskets on either end of the slice to achieve a good seal. Once assembled, one side of the test cell was filled with a 3% NaCl solution and the other side was filled with a 0.3 N NaOH solution. The test cell was then connected to a 60 V power supply. Once the power supply was turned on, an initial current reading was taken. Additional readings were then taken every 30 minutes for 6 hours. The total charge passed through the test specimen was determined by finding the area under the current-time curve and adjusting the value for a 4 in. diameter cylinder.

Although the standard does not require repeat testing, three or more cylinders per concrete mixture were tested for rapid chloride penetrability. The range of the data was checked to see whether it was within the limits prescribed by ASTM C 1202 [158]. In the rare cases where the range exceeded the limits, then a statistical test known as the Grubb's test or the maximum normed residual test was performed on the data to detect significant outliers. Outliers were rejected with 95% confidence.

4.1.8 Coefficient of Thermal Expansion

CoTE measurement is another test that was not performed during the paste and mortar phase of the project. However, it is an important durability property to know, especially when considering the performance of concrete pavements, as concrete with a high CoTE can cause early age cracking and joint spalling [159]. In continuously reinforced concrete pavements, a high CoTE value of the concrete may increase the crack spacing and width, affecting the crack load transfer efficiency [160]. Although CoTE is primarily dominated by the aggregate type and source, the SCM type and content could also have smaller effects on the value [161]. As such, these experiments were conducted to ensure that these pozzolans did not have any detrimental effects on the CoTE value of concrete.

The CoTE value was measured according to the TxDOT procedures of Tex-428-A [149]. Two 4 in. x 8 in. concrete cylinders were cut to a length of 7 in. \pm 0.1 in. and submerged in water for 48 hours. The cut cylinders were then measured to the nearest 0.001 in. using a caliper and submerged in temperature-controlled water baths programmed to cycle between 10 °C and 50 °C. Inside the water baths the cylinders were placed in testing frames equipped with a differential variable reluctance transformer, which was used to measure the change in length of the specimen. After completing three cycles the specimens were removed and the data were analyzed using an Excel spreadsheet provided by TxDOT².

4.2 Results

4.2.1 Compressive Strength

Figure 4.1 and 4.2 show the compressive strengths of the control and the SCM concrete mixtures. The error bars represent the range of the data. Most of the SCMs performed well in terms of compressive strength. Similar to the results from the mortar studies, both the Metakaolin-D and Zeolite-Z concrete mixtures show a trend for earlier reactivity and have strengths that are either higher than or equal to the control concrete as early as 28 days. It is interesting to note that a higher SCM replacement dosage of 25% yielded a higher strength for the Metakaolin-D concrete mixture than what was seen with a replacement dosage of 15%. Previous research has suggested that the high alumina content of Metakaolin-D could be the reason behind its early reactivity. Perhaps a higher replacement dosage, which would result in the presence of more alumina particles, could accelerate cement hydration and enable the dilution effect to be overcome more rapidly, resulting in a higher strength than what was seen for a lower replacement dosage. The strength gain of the Shale-T concrete mixture was marginally faster than what was seen during the mortar studies. At a replacement dosage of 25%, the strength of the Shale-T concrete mixture was similar to the control by 56 days. Although, the Pumice-D concrete mixture gained strength slowly at first, it reached 95% of the control strength at 90 days with a 15% replacement and 99% of the control strength with 25% replacement. This is similar to the trend seen during the mortar studies.

In terms of strength, the mixtures with Perlite-I and Vitric Ash-S did not show as good results in the concrete experiments as was seen in the mortar studies. By 90 days, the mortar compressive strengths for both SCM mixtures were the same or higher than the control. However, at the same age, the strength of the Perlite-I and Vitric Ash-S concrete mixtures were only 85–90% of the control. The Zeolite-T mixture showed a major improvement in strength

² The Excel spreadsheet used for analysis was created by Jerry Peterson at TxDOT

when tested in concrete vs. in mortar, achieving about 84% of the control strength by 90 days. The improvement in strength of the Zeolite-T mixture could be due to the addition of superplasticizer in the concrete mixture, which allowed the use of a lower w/c and better consolidation.

The concrete mixture with Zeolite-A performed the worst out of the eight materials, achieving only 72% of the control strength at 90 days. However, it must be noted that concrete made with Zeolite-A had 35% of its cement replaced, while the maximum replacement dosage on the other SCM samples had been capped at 25%. This could account for the unusually low strength of the Zeolite-A concrete sample at 90 days. Also, it should be noted that although some of the SCM-concrete specimens gained strength slower than others, at 28 days all the samples had strengths that were greater than 4500 psi.

4.2.2 Fresh State Properties

Table 4.5 summarizes the fresh state properties of the concrete mixtures. Most of the concrete mixtures were able to achieve the target slump with the help of a superplasticizer, except for Zeolite-Z and Zeolite-T at a replacement dosage of 25%. These two SCMs were investigated further, to identify techniques that could help mitigate their water. The results are presented in Chapter 5 of this report. The ASTM C403 setting time measurements showed that adding the SCMs to the concrete mixtures did not dramatically increase the final set. Most of the SCM-concrete had a final set between 4.5 and 6 hours, compared to the final set of the control at 4.5 hours. Concrete mixtures made with Zeolite-T and Shale-T at a dosage of 25% and Zeolite-A at a dosage of 35% had the slowest rates of hardening with final sets between 5.5–6 hours.

4.2.3 Drying Shrinkage

The results of the concrete drying shrinkage experiments are presented in Figures 4.3–4.6. Figures 4.3 and 4.4 show the average shrinkage of the concrete mixtures at different replacement dosages while Figures 4.5 and 4.6 show the correlation between percent shrinkage and percent weight loss of the samples. The average weight loss and shrinkage of each mixture after being in a 50% RH for 64 weeks are presented in Table 4.6, along with the ranges of the data, which were all within acceptable limits of ASTM C 157 [41]. The difference in weight loss and shrinkage compared to the control at 64 weeks is also presented in Table 4.6. Metakaolin-D, Shale-T and Zeolite-Z had a negligible difference in shrinkage compared to the control, regardless of the replacement dosage used. Pumice-D and Perlite-I had negligible differences in shrinkage compared to the control when used at a replacement dosage of 15%. However, the amount of shrinkage increased to more than 0.010% of the control as the replacement dosage was increased to 25%. The 25% Vitric Ash-S concrete mixture had a similar shrinkage to the Pumice-D concrete. Similar to the mortar studies, Zeolite-T and Zeolite-A had the highest amount of shrinkage, about 0.02% different from that of the control. However, the linear trend of the shrinkage vs. weight loss plots, presented in Figures 4.5 and 4.6, indicates that differences in shrinkage between the control mortar and the SCM mortars are due to water loss, instead of a change in the microstructure of C-S-H from the SCM addition.

The mortar and concrete drying shrinkage results of the zeolites are contradictory, in that the mortar results suggest that zeolites increase drying shrinkage, whereas the concrete results indicate that the higher shrinkage is due to water loss instead of a change in the C-S-H microstructure. The deviation of the zeolite mortar shrinkage data was most likely due to the higher w/cm used for the zeolite mortar mixtures, compared to the other SCM mixtures.

4.2.4 Resistance to Alkali-Silica Reaction

Figures 4.7 and 4.8 show the expansion of the concrete prisms in the ASTM C 1293 test for ASR. All the SCMs performed very well, and kept expansions below the 0.04% limit of ASTM C 1293, validating the results found from the ASTM C 1567 [137] Accelerated Mortar Bar Test for ASR. Table 4.7 lists the average expansion of the concrete prisms at 24 months, along with the range of the data.

In some cases, the range of the expansion data was found to be larger than the limit specified in ASTM C 1293 [146]. In such cases, a statistical test known as the Grubb's test or the maximum normed residual test was performed on the data to reject significant outliers with 95% confidence. Since 4 bars were cast for each SCM concrete mixture, 3 bars still remained for calculation of average expansion in cases where one bar had to be discarded due to its outlier expansion values. In most cases, these outliers were found to be bars with a very low or negative expansion. Due to the nature of the test, some alkalis could have leached out contributing to the low expansion of these outliers. Only in the case of the 25% Zeolite-T mixture, the outlier was found to have a very high expansion (above the ASTM C 1293 limit of 0.04%). Although the 3 other bars remaining for the Zeolite-T mixture has expansions well below the 0.04% limit of ASTM C 1293 [146], the researchers feel that it would be prudent to do a retest of this particular concrete mixture before using Zeolite-T in field applications for ASR.

4.2.5 Resistance to Chloride Ion Penetration

Figure 4.9 presents the results of the ASTM C 1202 [158] Rapid Chloride Ion Penetration Test (RCPT). The error bars in the graph represent the range of the data. Four of the 17 concrete mixtures had ranges that exceeded the limit specified in ASTM C 1202 [158]. In such cases, a statistical test known as the Grubb's test or the maximum normed residual test was performed on the data to reject significant outliers with 95% confidence. The 15% Metakaolin-D mixture was the only one with a significant outlier. As such, the average RCPT of that mixture was computed from two cylinders. The averages for all the other mixtures were calculated from three or more concrete cylinders. ASTM C 1202 [158] does not state a minimum number of cylinders needed for each RCPT test.

At 32 weeks, all the SCM-concrete samples had less than 1000 coulombs of total charge passing through them when tested, which indicates very low chloride ion penetrability, according to ASTM C 1202 [158]. Other than the Perlite-I concrete mixture (which had a high range of measured values), the overall results indicated that increasing the SCM content also increased the specimen's resistance to chloride ion penetrability.

4.2.6 Coefficient of Thermal Expansion

Table 4.8 shows the results of the CoTE testing. All specimens tested for CoTE showed compliance with Tex-428-A [149]. The difference in CoTE values between the control specimen and the SCM-concrete specimens were small, indicating that the use of SCMs would not cause any detrimental effects to the CoTE value of concrete. The highest CoTE difference of 0.60 μ -strains/ $^{\circ}$ F came from the concrete mixture with Zeolite-Z at a replacement dosage of 25%.

4.2.7 Ultrasonic Tests for Setting Time Monitoring

The ultrasonic wave tests show strong correlation between shear wave velocities and penetration resistance measurements using ASTM C 403 [156] on mortar samples and mortar

sieved from concrete. These relationships are not affected by w/c, but they are affected by coarse aggregate contents. Figure 4.10 shows the correlation curve between ultrasonic shear wave velocity and penetration resistance measured on mortar sieved from concrete mixtures. The shear wave velocities at initial setting time are 392 ± 10 m/s in mortar, and 508 ± 16 m/s in mortar sieved from concrete, respectively. Refer to Appendix C for more detailed results and discussions.

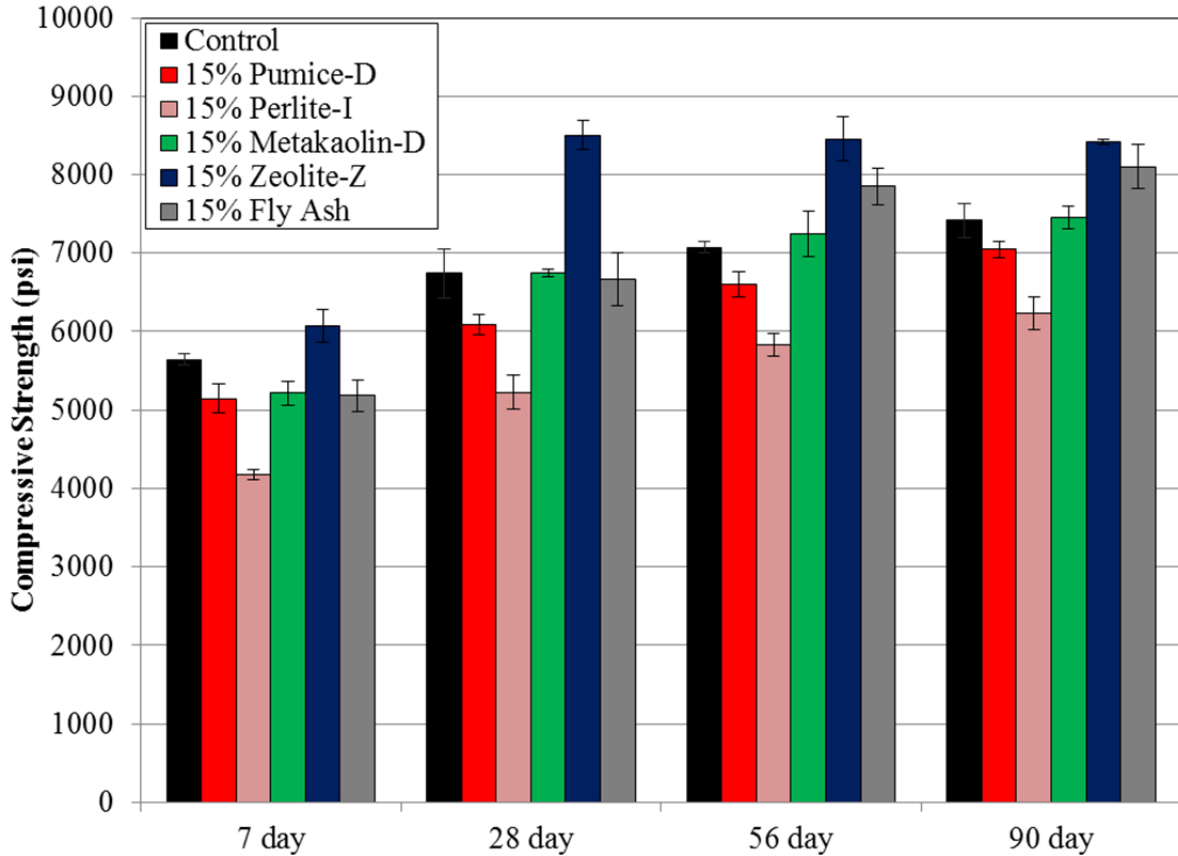


Figure 4.1: Compressive strength of concrete mixtures with 15% SCM

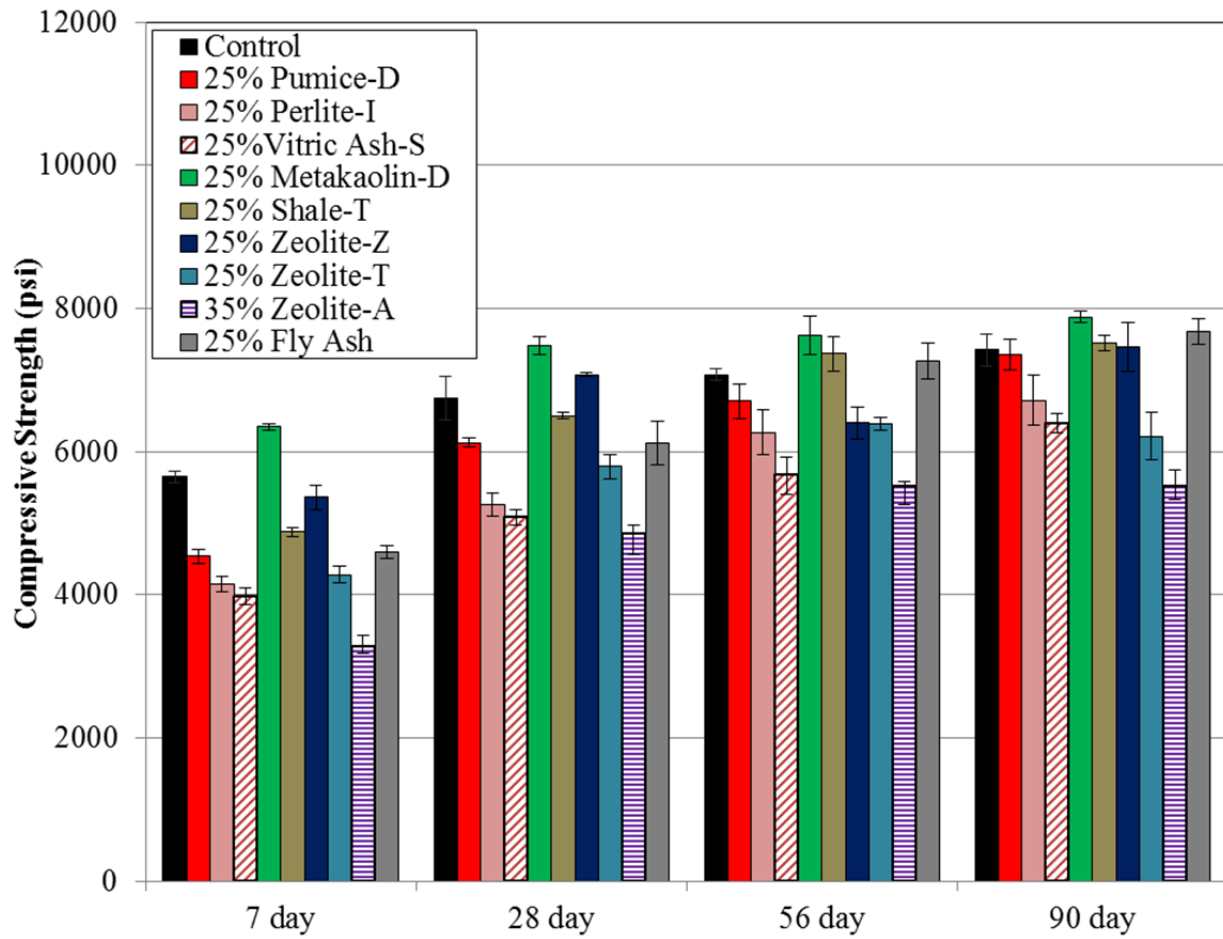


Figure 4.2: Compressive strength of concrete mixtures with 25% or 35% SCM

Table 4.5: Fresh State Properties of Concrete Mixtures

| Concrete Mixture Description | Admixture Dosage, % of max dosage | Slump, in | Air, % | Unit Weight, lb/ft ³ | Initial Set (hrs) | Final Set (hrs) |
|------------------------------|-----------------------------------|-----------|--------|---------------------------------|-------------------|-----------------|
| Control | 12.70 | 3.25 | 1.6 | 150.0 | 3.4 | 4.5 |
| 15% Pumice-D | 15.48 | 2.50 | 1.8 | 149.6 | 3.6 | 5.0 |
| 15% Perlite-I | 9.70 | 3.00 | 2.2 | 148.8 | 3.7 | 5.2 |
| 15% Metakaolin-D | 16.13 | 3.50 | 1.8 | 149.6 | 3.6 | 5.1 |
| 15% Zeolite-Z | 74.77 | 3.00 | 2.4 | 147.6 | 3.2 | 4.7 |
| 15% Fly Ash | 2.24 | 3.75 | 2.0 | 148.8 | 3.5 | 4.9 |
| 25% Pumice-D | 43.73 | 5.25 | 2.0 | 148.8 | 3.8 | 5.3 |
| 25% Perlite-I | 30.38 | 4.00 | 2.0 | 150.0 | 3.8 | 5.3 |
| 25% Vitric Ash-S | 21.65 | 4.50 | 2.0 | 150.8 | 3.5 | 5.1 |
| 25% Metakaolin-D | 34.13 | 3.50 | 1.8 | 150.0 | 3.7 | 5.5 |
| 25% Shale-T | 38.51 | 4.75 | 1.8 | 147.2 | 4.2 | 5.9 |
| 25% Zeolite-Z | 106.21 | 1.50 | 2.0 | 148.0 | 3.3 | 4.9 |
| 25% Zeolite-T | 86.68 | 1.00 | --* | 146.8 | 3.6 | 5.8 |
| 35% Zeolite-A | 74.71 | 3.50 | 2.1 | 147.2 | 3.8 | 6.0 |
| 25% Fly Ash | 0.00 | 5.50 | 1.6 | 148.8 | 3.9 | 5.3 |

* Air content reading was invalid.

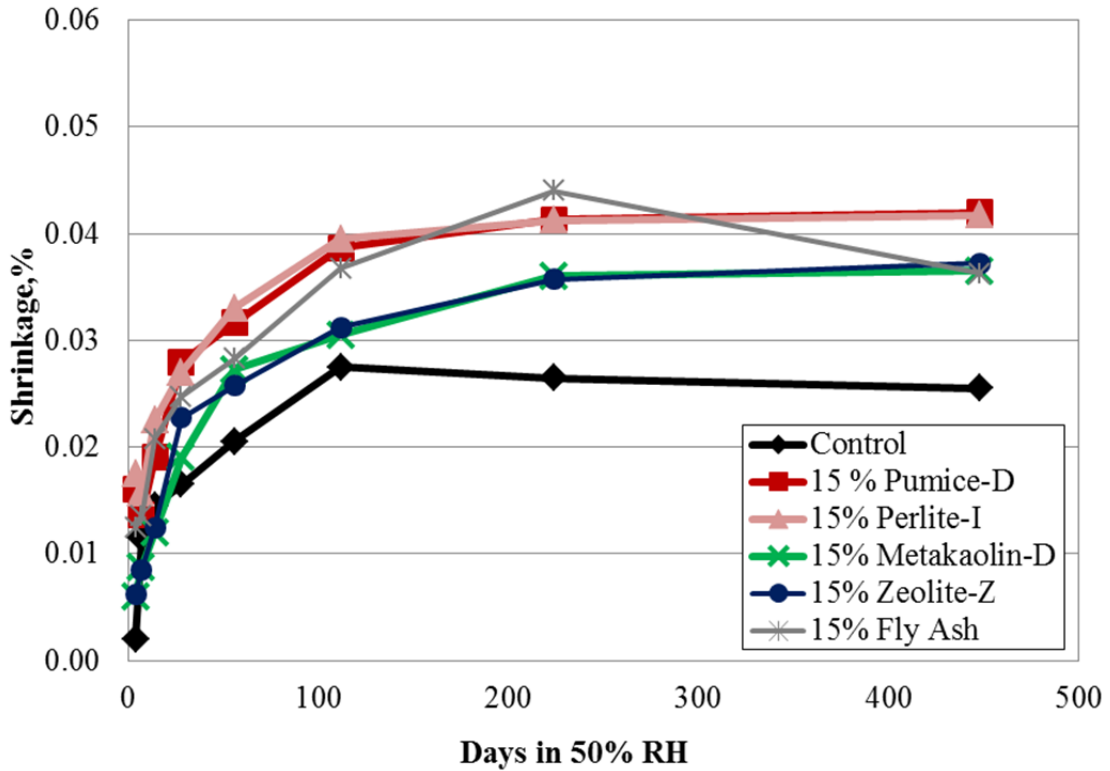


Figure 4.3: Percent shrinkage of concrete mixtures with 15% SCM

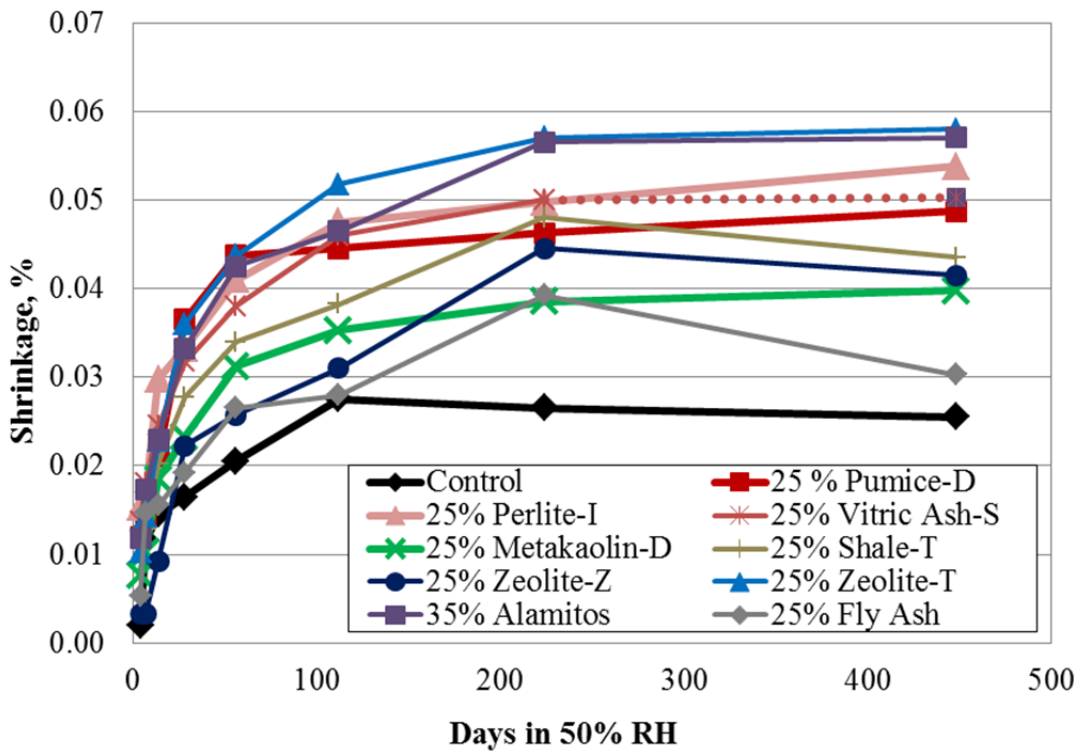


Figure 4.4: Percent shrinkage of concrete mixtures with 25% or 35% SCM

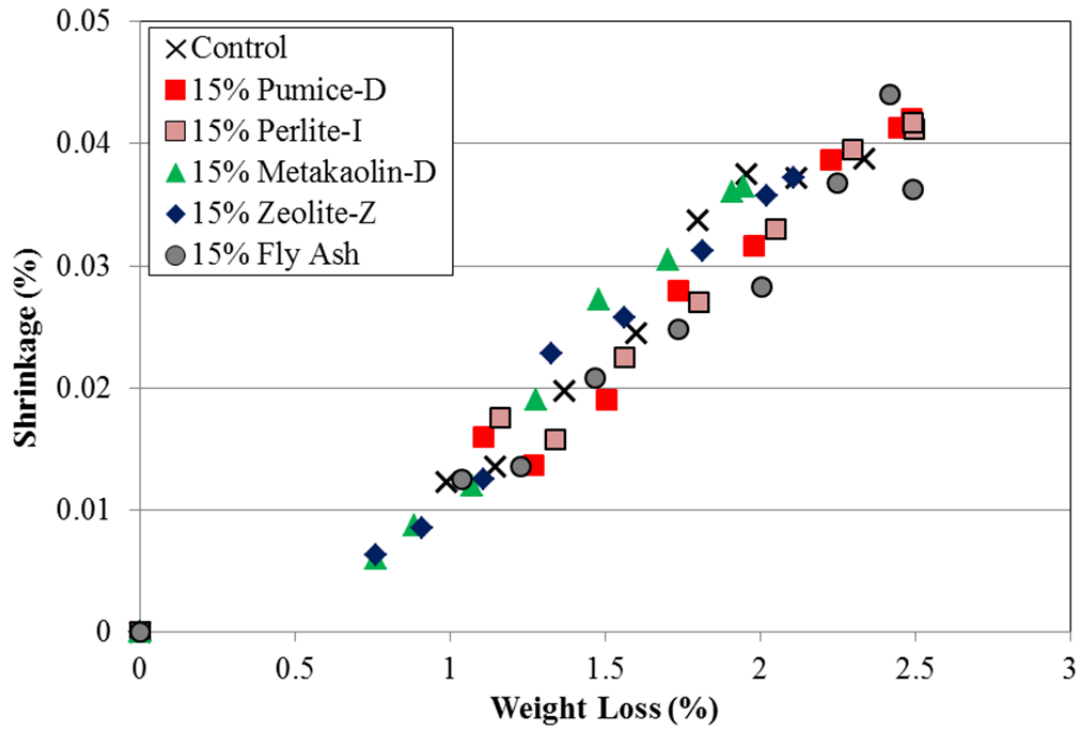


Figure 4.5: Drying shrinkage vs. weight loss of concrete mixtures with 15% SCM

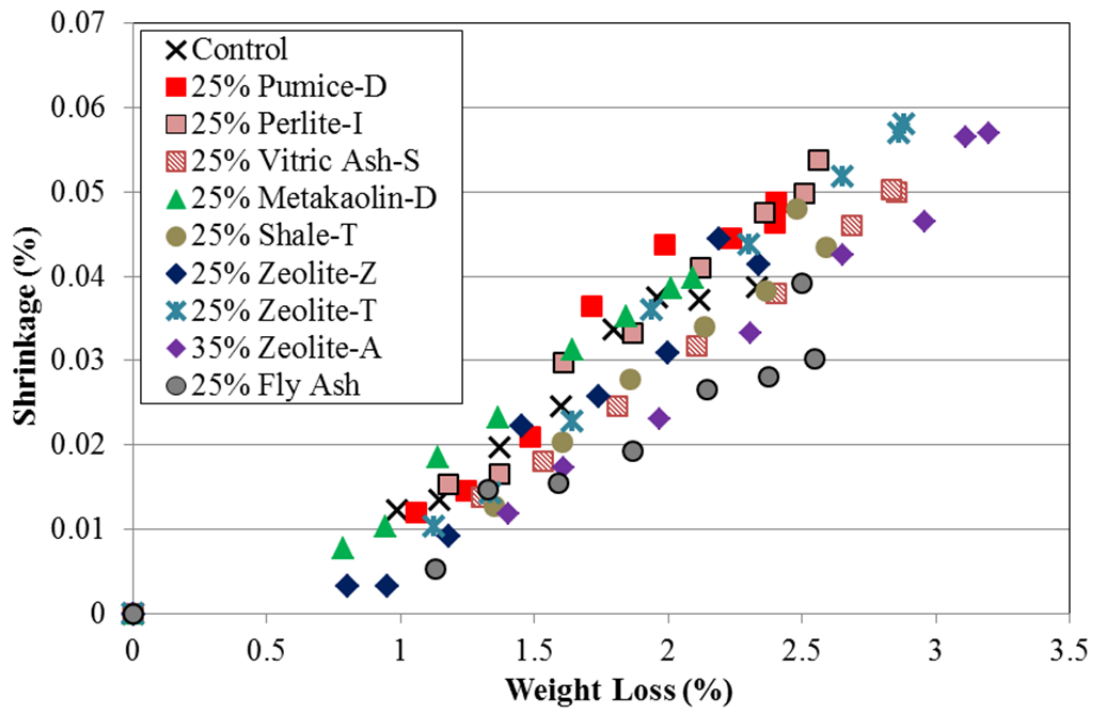


Figure 4.6: Drying shrinkage vs. weight loss of concrete mixtures with 25% or 35% SCM

Table 4.6: Weight Loss and Drying Shrinkage of SCM Mixtures at 64 Weeks

| Concrete Mixture Description | After 64 weeks in 50% RH | | | |
|------------------------------|--------------------------|-------------------------|---------------|-------------------------|
| | Weight Loss | | Shrinkage | |
| | Weight Loss (%) | Difference with Control | Shrinkage (%) | Difference with Control |
| Control | 2.332 ± 0.067 | --- | 0.039 ± 0.003 | --- |
| 15% Pumice-D | 2.487 ± 0.049 | 0.155 | 0.042 ± 0.006 | 0.003 |
| 15% Perlite-I | 2.493 ± 0.060 | 0.161 | 0.042 ± 0.005 | 0.003 |
| 15% Metakaolin-D | 1.945 ± 0.033 | -0.387 | 0.037 ± 0.003 | -0.002 |
| 15% Zeolite-Z | 2.106 ± 0.064 | -0.226 | 0.037 ± 0.001 | -0.002 |
| 15% Fly Ash | 2.492 ± 0.075 | 0.16 | 0.036 ± 0.002 | -0.003 |
| 25% Pumice-D | 2.403 ± 0.053 | 0.071 | 0.049 ± 0.002 | 0.010 |
| 25% Perlite-I | 2.560 ± 0.104 | 0.228 | 0.054 ± 0.003 | 0.015 |
| 25% Vitric Ash-S | 2.834 ± 0.046 | 0.502 | 0.050 ± 0.002 | 0.011 |
| 25% Metakaolin-D | 2.093 ± 0.056 | -0.239 | 0.040 ± 0.002 | 0.001 |
| 25% Shale-T | 2.587 ± 0.052 | 0.255 | 0.044 ± 0.003 | 0.005 |
| 25% Zeolite-Z | 2.337 ± 0.046 | 0.005 | 0.042 ± 0.004 | 0.003 |
| 25% Zeolite-T | 2.882 ± 0.012 | 0.55 | 0.058 ± 0.005 | 0.019 |
| 35% Zeolite-A | 3.199 ± 0.030 | 0.867 | 0.057 ± 0.005 | 0.018 |
| 25% Fly Ash | 2.546 ± 0.073 | 0.214 | 0.030 ± 0.002 | -0.009 |

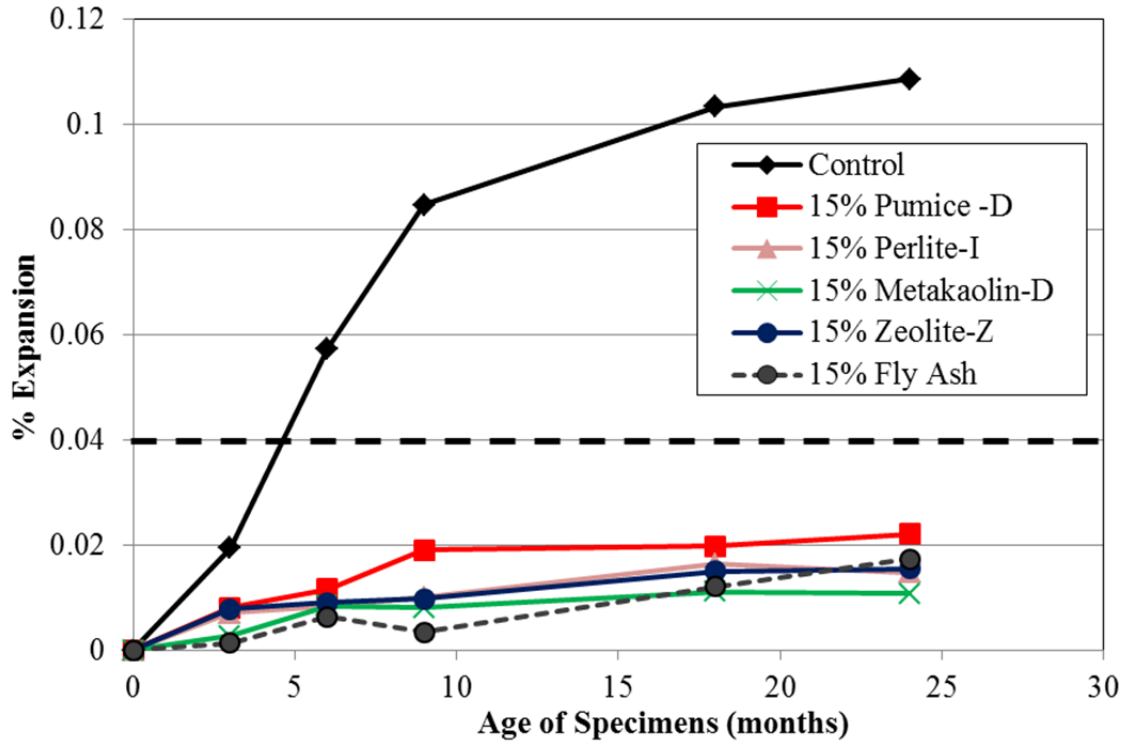


Figure 4.7: Average ASR expansion of concrete mixtures with 15% SCM

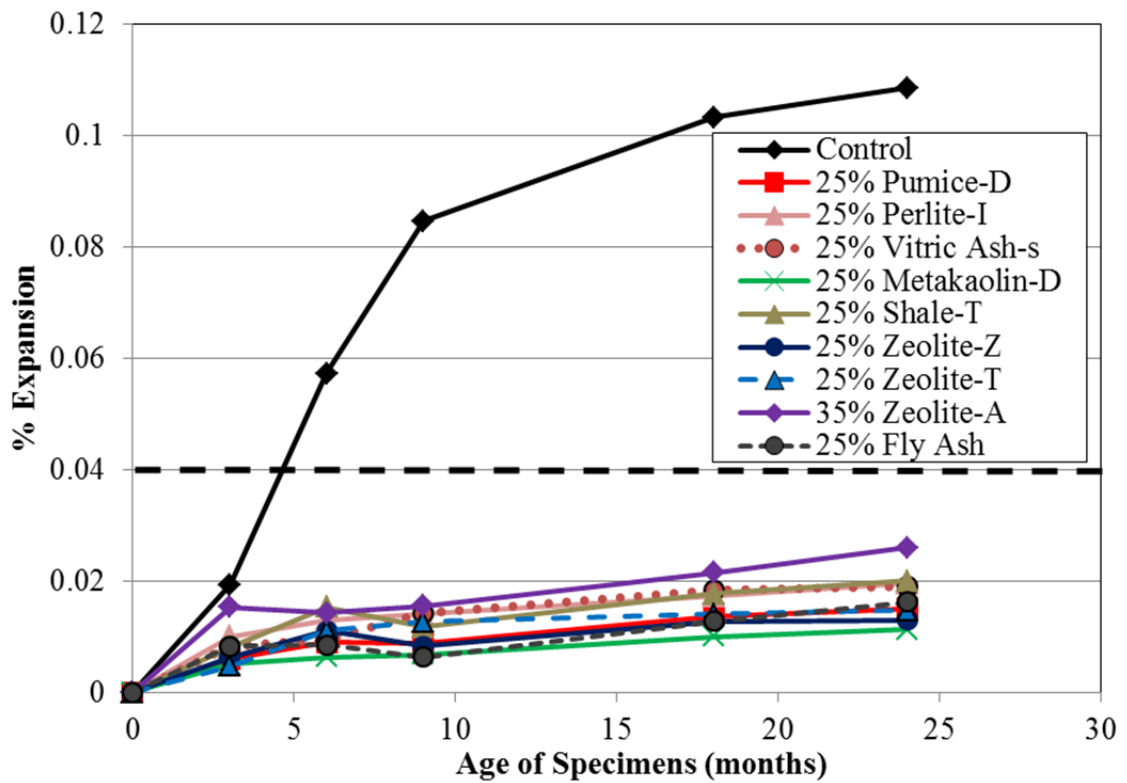


Figure 4.8: Average ASR expansion of concrete mixtures with 25% or 35% SCM

Table 4.7: Average ASR Expansion of Concrete Mixtures at 24 Months

| Concrete Mixture Name | Average ASR Expansion at 24 months (%) |
|------------------------------|---|
| Control | 0.109 ± 0.020 |
| 15% Pumice-D | 0.022 ± 0.007 |
| 15% Perlite-I | 0.015 ± 0.001 |
| 15% Metakaolin-D | 0.011 ± 0.002 |
| 15% Zeolite-Z | 0.016 ± 0.003 |
| 15% Fly Ash | 0.016 ± 0.017 |
| 25% Pumice-D | 0.015 ± 0.001 |
| 25% Perlite-I | 0.020 ± 0.013 |
| 25% Vitric Ash-S | 0.019 ± 0.004 |
| 25% Metakaolin-D | 0.011 ± 0.010 |
| 25% Shale-T | 0.020 ± 0.001 |
| 25% Zeolite-Z | 0.013 ± 0.005 |
| 25% Zeolite-T | 0.015 ± 0.009 |
| 35% Zeolite-A | 0.026 ± 0.004 |
| 25% Fly Ash | 0.016 ± 0.005 |

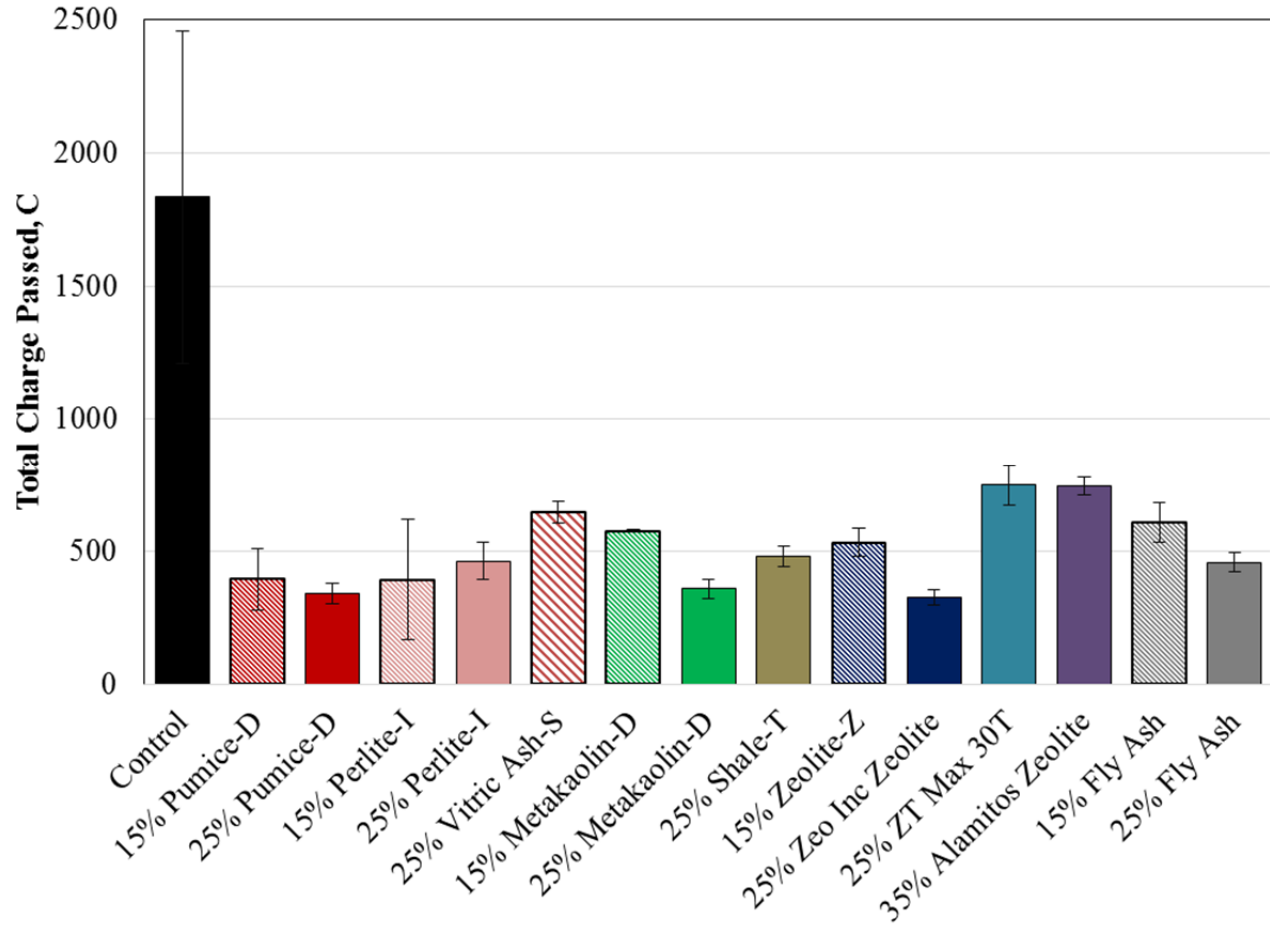


Figure 4.9: ASTM C 1202 rapid chloride testing results at 32 weeks

Table 4.8: CoTE Results of Concrete Cylinders

| Concrete Description | Cylinder 1 μ -strain/ $^{\circ}$ F | Cylinder 2 μ -strain/ $^{\circ}$ F | Average μ -strain/ $^{\circ}$ F | Difference from Control μ -strain/ $^{\circ}$ F |
|----------------------|--|--|-------------------------------------|---|
| Control | 3.61 | 3.56 | 3.59 | -- |
| 25% Pumice | 4.16 | 4.15 | 4.16 | 0.57 |
| 25% Ash | 4.19 | 3.94 | 4.07 | 0.48 |
| 25% Metakaolin | 4.22 | 3.99 | 4.11 | 0.52 |
| 25% Shale | 4.22 | 4.01 | 4.12 | 0.53 |
| 25% Zeolite-Z | 4.36 | 4.00 | 4.18 | 0.60 |
| 25% Fly Ash | 4.06 | 3.56 | 3.81 | 0.23 |

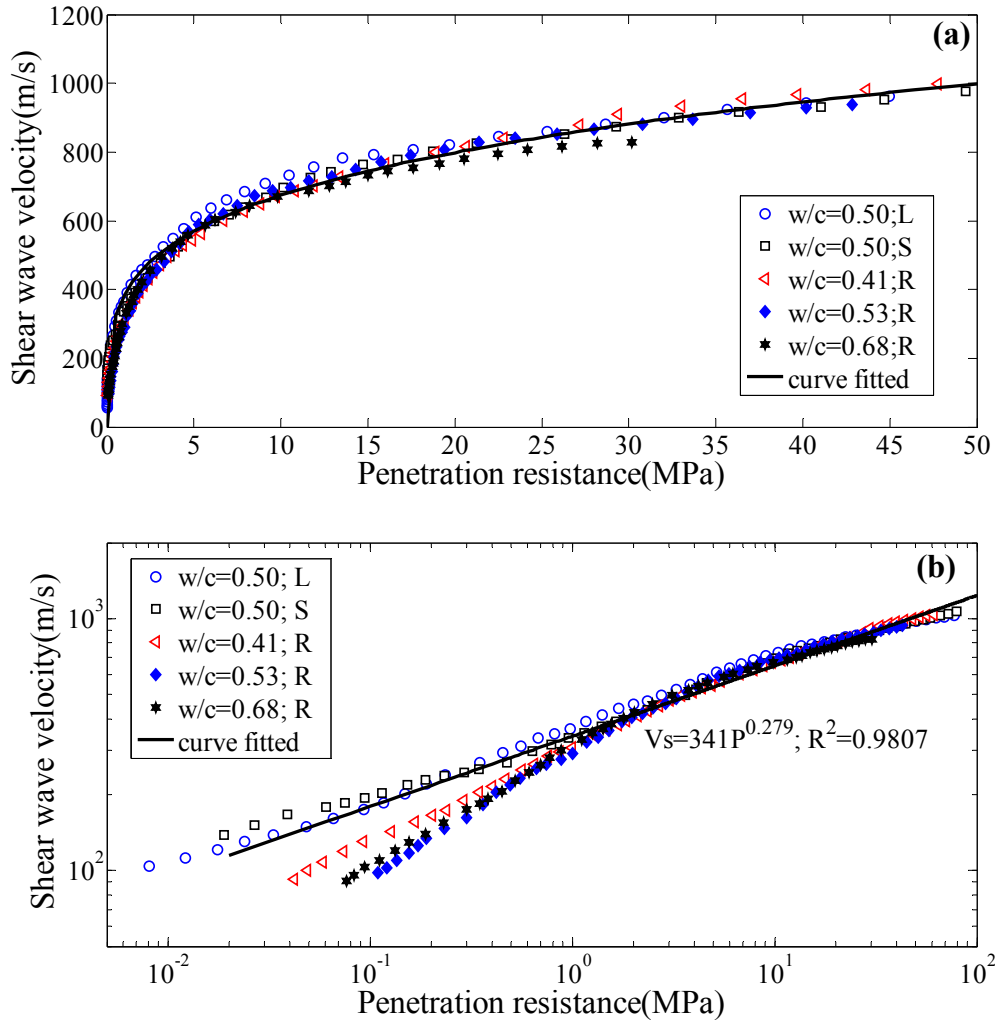


Figure 4.10: Correlation between shear wave velocity and penetration resistance on mortar sieved from concrete mixtures in (a) linear scale and (b) logarithm scale

4.3 Conclusions from Concrete Studies

Results from the concrete mixture were crucial in understanding how the pozzolans might perform in field applications of concrete. One of the most important concrete results was the validation of the accelerated mortar bar test (ASTM C 1567) for ASR using the longer term, more reliable ASTM C 1293 concrete prism test for ASR. Other than Zeolite-A, it was found that all the pozzolans could keep ASR expansions at 2 years below the 0.04% limit of ASTM C 1293 using replacements dosages of 25% or less. Zeolite-A needed a higher expansion of 35% to meet the ASTM C 1293 limits. Other important durability results showed that the use of these pozzolans increased the resistance of the concrete mixtures to chloride ion penetration. Additionally, the concrete results also showed that drying shrinkage and CoTE would not be a problem if these pozzolans were used in concrete mixtures. In terms of strength, the Pumice-D, Metakaolin-D, Shale-T, and Zeolite-Z mixtures performed very well with strengths similar to or higher than the control at 90 days. Other than the poor workability of the three zeolites, measurement of the fresh state properties of the concrete mixtures did not reveal any other problems.

Chapter 5. Treatments and Modification of SCMs

It was anticipated that some of the SCMs would have high water demand or low reactivity. Characterization testing along with paste and mortar studies identified the zeolites to have high water demand. This chapter describes some of the modification techniques that were used on the zeolites to try and mitigate their water absorption. The effects of the modification on mixture workability were assessed using rheometer testing, following the procedures listed in Section 3.1.2. In the initial mortar studies, a replacement dosage of 20% was used in the rheological tests. In this section, along with the 20% replacement, a higher replacement dosage of 30% was also tested, since some of the later testing showed that the zeolites need a higher replacement percentage to be effective in mitigating durability problems like ASR.

5.1 Modification Methods

Table 5.1 gives a list of the modification techniques used. Some of the techniques include calcination and soaking the zeolite powders in solutions to mitigate its water absorption. The coarser zeolites were also ground to see whether increasing fineness to improve reactivity would be feasible from a workability standpoint. It was expected that grinding the zeolites would worsen the workability of the mixture. As such, these ground zeolites were calcined as well to see if the workability of its mixture could be improved. The rest of this subsection will explain the modification processes in detail.

Table 5.1: Modification Techniques Used on Zeolite SCMs

| Modification Techniques | Performed on | Replacement Dosages Used |
|--------------------------------|---------------------------------|---------------------------------|
| Calcination | Zeolite-Z, Zeolite-T, Zeolite-A | 20%, 30% |
| Grinding | Zeolite-T, Zeolite-A | 20%, 30% |
| Grinding and Calcination | Zeolite-T, Zeolite-A | 20%, 30% |
| Soaking in Hydrated Lime | Zeolite-Z, Zeolite-T, Zeolite-A | 20% |
| Soaking in Polyethylene Glycol | Zeolite-Z, Zeolite-T, Zeolite-A | 20% |

5.1.1 Calcination

The high water absorption of the zeolites could either be due to its porous structure or due to clay impurities. In both cases, previous literature indicates that calcination of the zeolites would improve workability of mixtures containing zeolites. Earlier studies have suggested that calcination causes destabilization of the zeolite crystal latticework and increases the ability of the zeolites to participate in pozzolanic reactions [57, 74–76]. Although the effect of calcination on zeolite mixture workability has not been investigated in these previous studies, we hypothesized that the collapse of the zeolite structure would also decrease its water absorption ability. If the poor workability of the zeolite mixtures is caused instead by clay impurities, calcination should also mitigate the problem, since previous research has shown the workability of calcined clay mixtures to be better than that of untreated clays [85, 87].

To calcine the zeolites, 50g of the material was placed in the oven and the temperature was steadily increased from room temperature to 800 °C for 160 minutes (approximate rate of 5 °C/min). Once the oven temperature reached 800 °C, the temperature was kept constant for 5

hours. After five hours, the temperature was steadily reduced back down to room temperature over 160 minutes.

5.1.2 Crushing and Calcination

The mixtures with the coarser zeolites not only showed poor workability, but had poor performance in terms of strength and durability. Previous literature on zeolites has shown particle size to have a marked effect on compressive strength, with decreasing zeolite particle size leading to increasing compressive strengths in mortars [68]. However, since the zeolites also have a high water demand, increasing the fineness would most likely cause problems with mixture workability. As such, before testing the crushed zeolite powders for improved reactivity, the researchers wanted to test the workability of mixtures made with the ground zeolites.

The coarser zeolites were crushed using Bico Inc. UA V-Belt Drive Pulverizer and passed through a No. 200 sieve (with 75 μm opening). Some of the sieved zeolites were also calcined following the procedures listed under in Section 5.1.1, to see if calcination could reduce the water demand of the finer zeolite particles.

5.1.3 Pre-soaking in Hydrated Lime and Polyethylene Glycol

The zeolites were soaked in different solutions before use to see whether absorption of the solutions before mixing could improve their water demand. One of the pre-soak solutions used in this project was a hydrated lime (HL) solution. Hydrated lime is a common additive in asphalt mixtures that have aggregates with clay impurities. Previous research suggests that the calcium ions from the lime displace sodium ions in the clay layers, making them less prone to swelling [162]. The researchers wanted to test if the same concept of cation exchange could be applied to the zeolites to improve their mixture workability. For the HL solution, 0.952 grams of powdered CaO were mixed into 800 grams of water to form a saturated solution. Then, 50 grams of SCM was added to the solution and mixed for 72 hours. Finally, the HL solution was poured out and the SCM was oven dried for approximately 48 hours.

The second solution used was a 0.1% polyethylene glycol (PEG) solution. Previous research has shown PEG to counteract absorption problems when clay-containing aggregates are used in concrete mixtures [163]. The PEG solution is believed to be sacrificially adsorbed onto the clay layers, disabling its ability to swell and absorb water and WRAs [163]. The PEG solution for our project was made by adding 1 gram of powdered PEG to 1000 grams of water to make the solution. The zeolite powders were soaked in the PEG solution for 3 minutes before mixing.

5.2 Results

5.2.1 Zeolite-A

Plots of shear stress versus shear rate for the different materials tested are shown in Figures 5.1–5.3. The y-intercept represents the yield stress and the slope represents the plastic viscosity; higher values of these indicate poor workability. The results for the Zeolite-A mixtures are presented in Figure 5.1. In Chapter 3, we noted how the 20% Zeolite-A paste had a low viscosity and yield stress, despite showing poor workability in the water requirement mortar tests. However, an increase in the replacement dosage from 20% to 30% increased the yield stress and viscosity significantly. Calcination made the Zeolite-A pastes more workable, decreasing the yield stress and viscosity of mixtures at both the 20% and 30% replacement

dosage. Although grinding Zeolite-A reduced the mixture workability, as expected, grinding combined with calcination brought the rheological properties back to the original state (balancing positive and negative effects). Mixtures using the ground Zeolite-A or the ground and calcined Zeolite-A were only run at a 20% replacement rate, as increasing the replacement dosage made the mixtures too viscous to be able to run using a rheometer.

Soaking Zeolite-A in different solutions did not help to mitigate their absorption. Soaking Zeolite-A in PEG actually reduced workability of the 20% Zeolite-A mixtures while soaking in HL did not have a significant impact. Since these methods were ineffective using a 20% replacement, the higher replacement dosage mixtures were not tested. The yield stress and viscosity of the different Zeolite-A mixtures are presented in Table 5.2.

5.2.2 Zeolite-T

The rheology results for the Zeolite-T mixtures are shown in Figure 5.2. The rheology curves indicate that the yield stress and viscosity of the Zeolite-T mixture increased significantly when the replacement dosage was changed from 20% to 30%. However, calcination of the Zeolite-T powder worked well to mitigate its water absorption capacity. The yield stress and viscosity of both the 20% and 30% calcined Zeolite-T mixtures were similar to that of the control paste with no SCMs.

Grinding the Zeolite-T powder reduced the mixture workability to a point where the rheometer test could not be properly conducted for either the 20% or the 30% Zeolite-T mixtures. However, grinding combined with calcination lowered the yield stress and viscosity of the 20% Zeolite-T paste to values below the original unground and uncalcined state. Soaking the Zeolite-T powder in HL and PEG solution was not effective in improving mixture workability at a 20% replacement dosage. As such, experiments using the pre-soak method for higher replacement rates of 30% were not conducted. The yield stress and viscosity of the different Zeolite-T mixtures are presented in Table 5.3.

5.2.3 Zeolite-Z

The rheology results for the Zeolite-Z mixtures are shown in Figure 5.3. Zeolite-Z differs from the other zeolites in that its particle size is already small, so grinding was not attempted. Additionally, we were unable to do any rheometer testing for paste that had 30% Zeolite-Z since the mixture was too viscous to be placed and measured properly using the rheometer. At a replacement dosage of 20%, calcination of the Zeolite-Z powder improved its mixture workability. However, the improvement was not as significant as seen with the other two zeolites, where calcination reduced the yield stress and viscosity of the mixtures to values similar to the control paste. Finally, soaking the Zeolite-Z powder in the HL or PEG solution did not have a significant effect in mitigating the zeolite's water absorption. The yield stress and viscosity of the different Zeolite-Z mixtures are presented in Table 5.4.

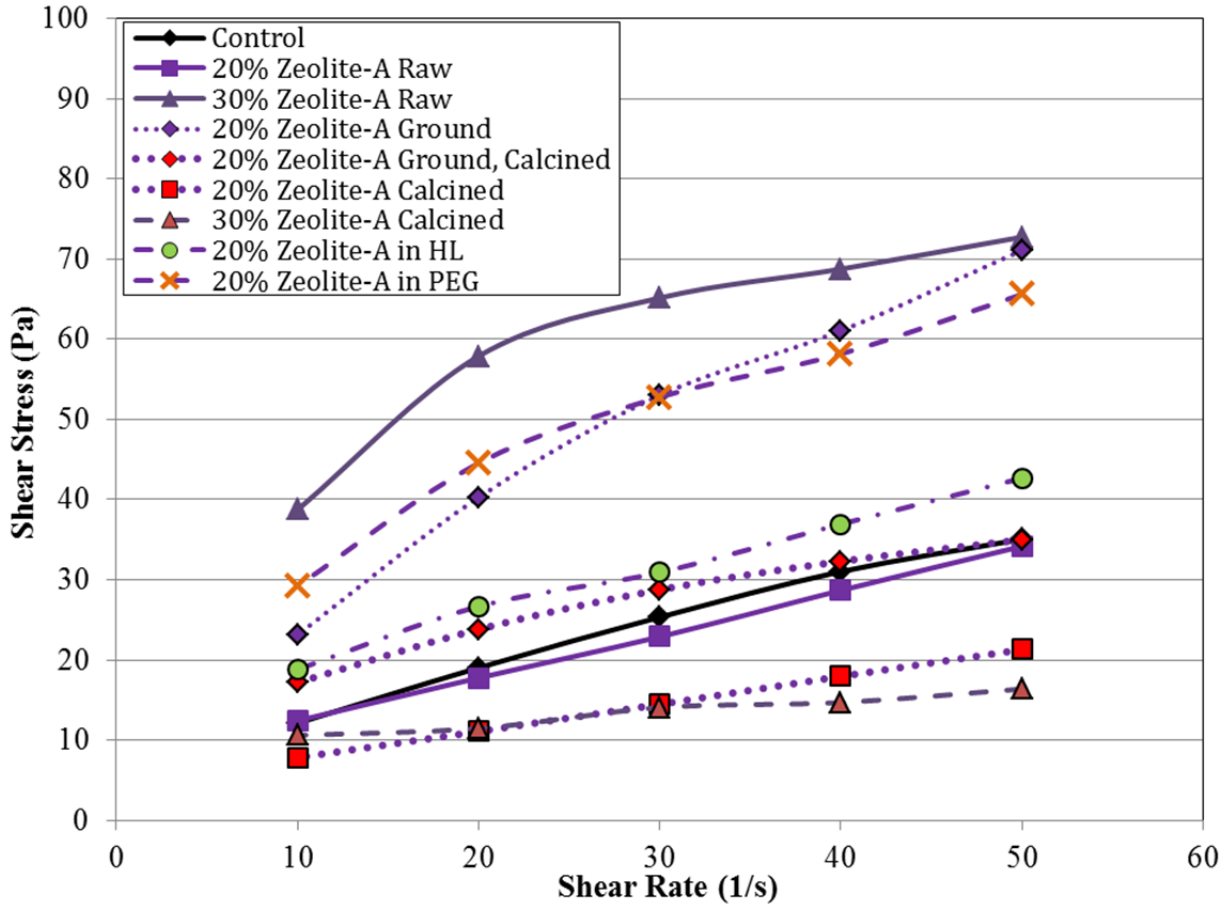


Figure 5.1: Effect of modification on the rheological properties of Zeolite-A mixtures

Table 5.2: Yield Stress and Viscosity of Zeolite-A Mixtures

| Paste Mixture Description | Yield Stress (Pa) | Viscosity (Pa.s) |
|-------------------------------|-------------------|-------------------|
| 20% Zeolite-A Raw | 8.53 ± 1.69 | 0.547 ± 0.003 |
| 30% Zeolite-A Raw | 35.10 ± 1.87 | 0.949 ± 0.159 |
| 20% Zeolite-A Ground | 13.61 ± 1.06 | 1.210 ± 0.042 |
| 20% Zeolite-A Ground Calcined | 14.54 ± 0.36 | 0.436 ± 0.006 |
| 20% Zeolite-A Calcined | 4.10 ± 0.26 | 0.333 ± 0.005 |
| 30% Zeolite-A Calcined | 9.21 ± 0.21 | 0.128 ± 0.020 |
| 20% Zeolite-A in HL | 11.94 ± 1.85 | 0.600 ± 0.019 |
| 20% Zeolite-A in PEG | 22.56 ± 1.58 | 0.894 ± 0.029 |

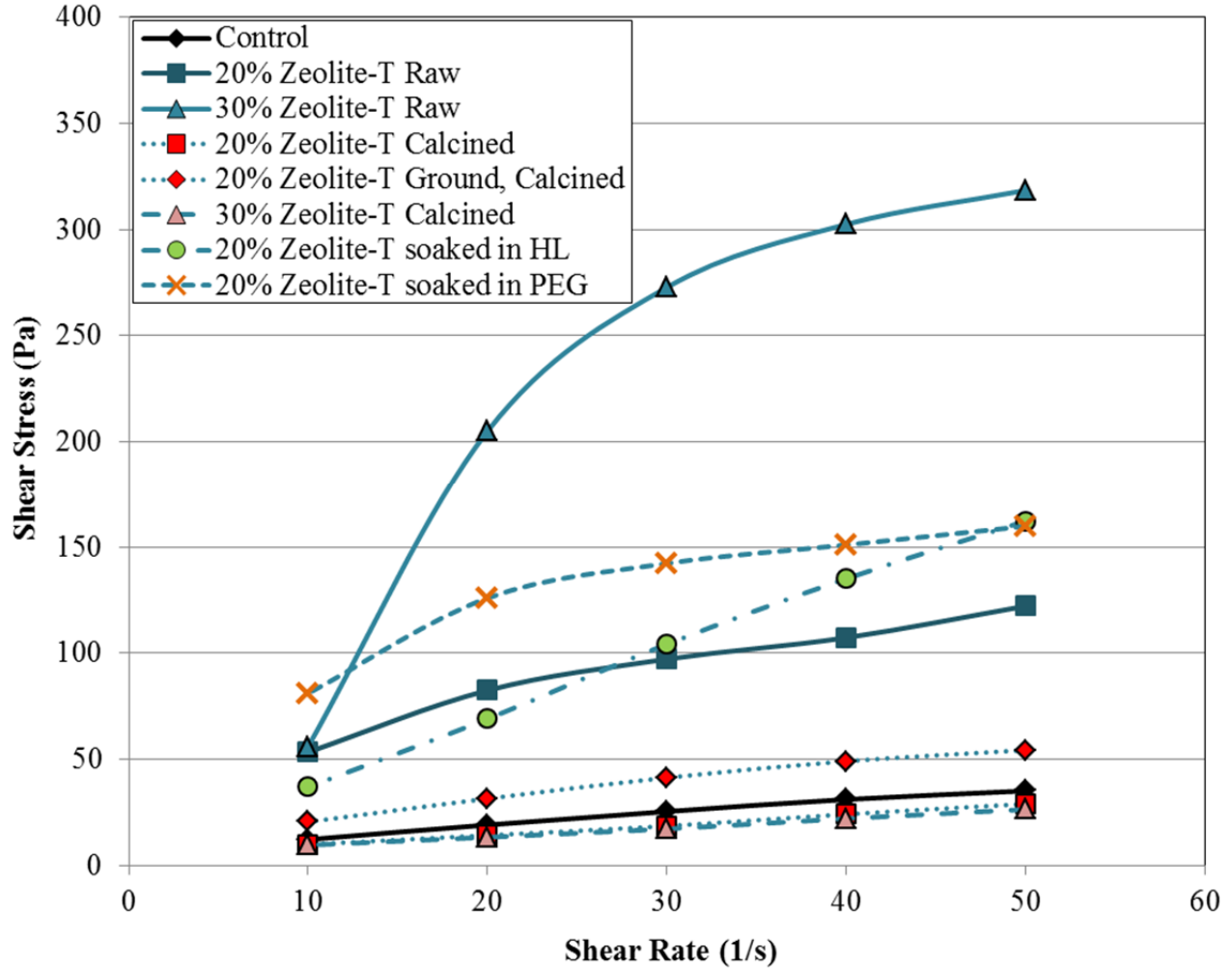


Figure 5.2: Effect of modification on the rheological properties of Zeolite-T Mixtures

Table 5.3: Yield Stress and Viscosity of Zeolite-T Mixtures

| Paste Mixture Description | Yield Stress (Pa) | Viscosity (Pa.s) |
|--------------------------------|-------------------|-------------------|
| 20% Zeolite-T Raw | 45.61 ± 1.91 | 1.619 ± 0.005 |
| 30% Zeolite-T Raw | 38.65 ± 5.62 | 5.674 ± 0.548 |
| 20% Zeolite-T Calcined | 4.89 ± 0.22 | 0.469 ± 0.011 |
| 30% Zeolite-T Calcined | 4.50 ± 0.40 | 0.435 ± 0.010 |
| 20% Zeolite-T Ground, Calcined | 14.06 ± 0.30 | 0.892 ± 0.040 |
| 20% Zeolite-T soaked in HL | 7.95 ± 1.53 | 3.612 ± 0.444 |
| 20% Zeolite-T soaked PEG | 60.58 ± 16.64 | 1.798 ± 0.026 |

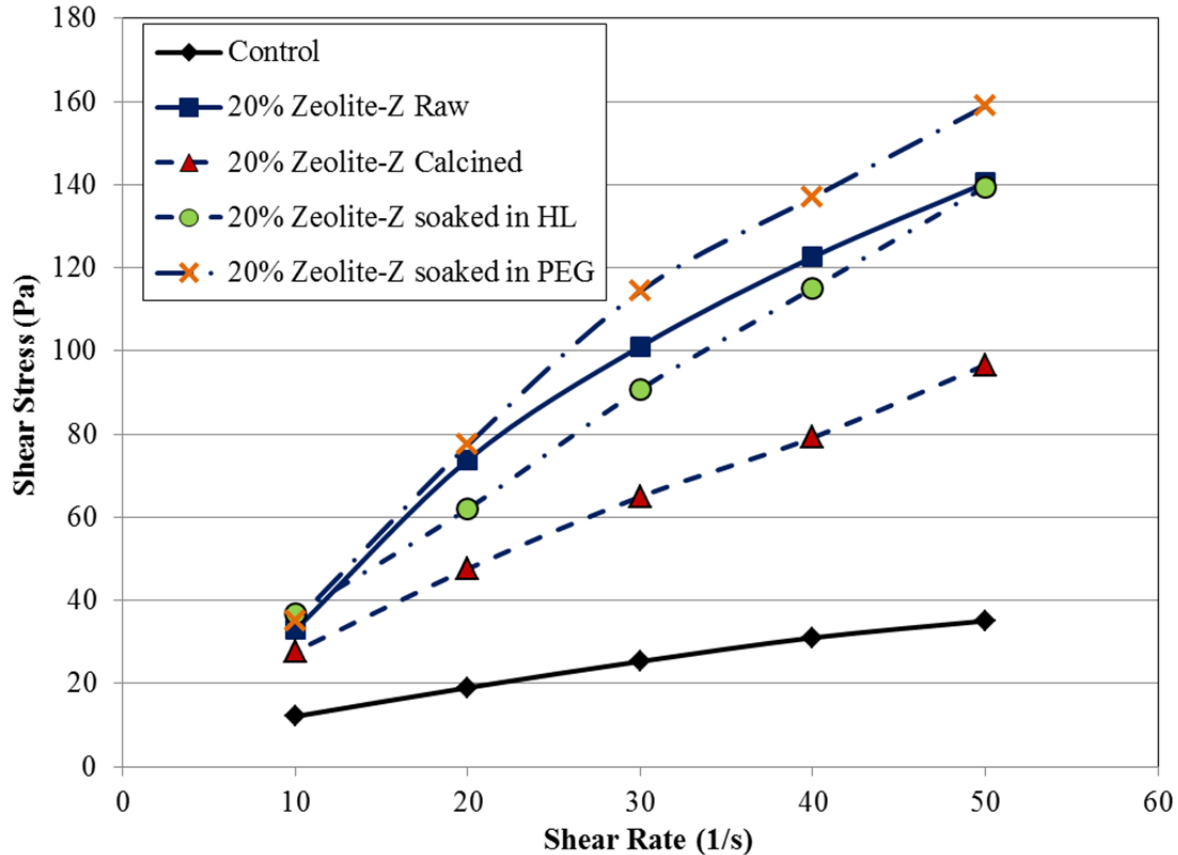


Figure 5.3: Effect of modification on the rheological properties of Zeolite-Z mixtures

Table 5.4: Yield Stress and Viscosity of Zeolite-Z mixtures

| Paste Mixture Description | Yield Stress (Pa) | Viscosity (Pa.s) |
|-----------------------------|-------------------|-------------------|
| 20% Zeolite-Z Raw | 15.41 ± 0.34 | 2.610 ± 0.027 |
| 20% Zeolite-Z Calcined | 11.55 ± 0.88 | 1.735 ± 0.042 |
| 20% Zeolite-Z soaked in HL | 15.50 ± 4.17 | 2.500 ± 0.084 |
| 20% Zeolite-Z soaked in PEG | 10.30 ± 2.03 | 3.205 ± 0.131 |

5.3 Conclusions from Material Treatment and Modification

Out of all the different modifications tried in this phase of the project, calcination of the zeolites was seen to be the only effective way to improve the workability of zeolite mixtures. Calcining the coarser zeolites, Zeolite-T and Zeolite-A, had higher impact on reducing the viscosity and yield stress of the paste mixtures than what was observed after calcining Zeolite-Z. Grinding the zeolites for improved reactivity was also shown to be impractical, as the workability of the zeolite particles decreased with decreasing particle size. Calcination of the ground zeolites did improve the workability for the 20% SCM paste mixtures, but not the 30% mixtures, which were still too viscous to be analyzed using the rheometer. This suggests that even with calcination, grinding zeolites to increase reactivity may not be a feasible idea, especially when a high dosage needs to be used.

Chapter 6. Conclusions and Recommendations

This chapter summarizes the results of this project and presents the guidelines that were created using performance data to help determine SCM replacement dosages for concrete mixtures in the field. This chapter also presents an evaluation of current testing practices for SCMs to assess whether they are sufficient for characterization of the material.

6.1 Optimum SCM Replacement Dosage

In this project we used a range of replacement dosages to evaluate optimum replacement levels for the SCMs in concrete mixtures. The minimum replacement limit for a given SCM was dictated by its effect on concrete durability—specifically, mitigating expansions from ASR, since ASR is a common source of durability problems in Texas. The minimum replacement level for SCMs in this project was determined through the accelerated mortar bar test for ASR (ASTM C 1567). Long-term measurements of concrete specimens using ASTM C 1293 confirmed these minimum replacement dosages to be effective in mitigating ASR. The maximum dosage was determined by the cost of the SCM and its effect on mixture workability. Strength was also an important factor in determining maximum dosage, as the higher the replacement amount, the lower the early age strength of mixtures, due to the dilution effect of replacing hydraulic cement with a slower reacting, pozzolanic material. Figure 6.1 shows a visual representation of how the optimum replacement dosages were determined.

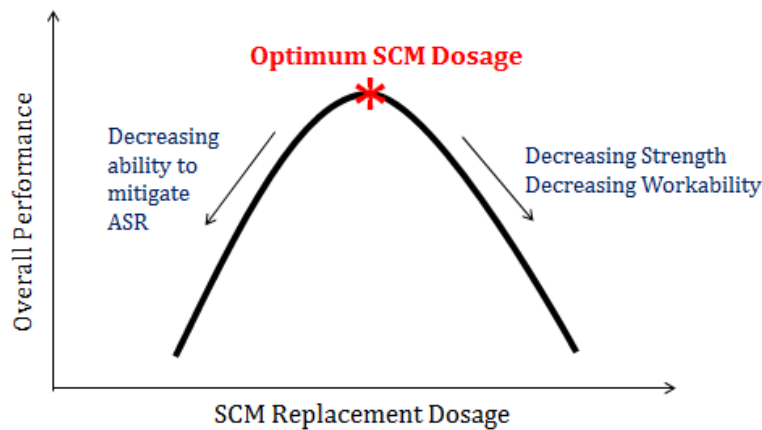


Figure 6.1: Finding the optimum replacement dosage

Other than Zeolite-A, all the SCMs needed a replacement dosage of 25% or less, by weight of cement, to sufficiently keep ASR-related expansions below the prescribed 0.1% limit of ASTM C 1567. Table 6.1 lists these minimum replacement dosages for ASR, along with a summary of the SCM performance in strength and durability tests. The maximum replacement dosages for the SCMs were generally capped at 25%, since the prices per ton for most of the SCMs were higher than cement. Table 6.1 also provides a list of the SCM prices.

Table 6.1 indicates that Pumice-D, Perlite-I, Metakaolin-D, and Zeolite-Z were able to keep ASR expansions below the limit at a replacement dosage of only 15%. In addition, these SCMs also performed well under sulfate attack, which was measured according to ASTM C 1012. At a replacement dosage of 15%, Pumice-D, Perlite-I, and Zeolite-Z were found to be

suitable for a Class 3 severe sulfate exposure level, based on “ACI 201: Guide to Durability” [148]. Although Metakaolin-D was not adequate for sulfate attack at a 15% replacement level, using a higher replacement dosage of 25% qualified it for a Class 2 moderate sulfate exposure. Among the SCMs that required a replacement level of 25% or higher to keep ASR expansions below the prescribed limit of ASTM C 1567, only Shale-T was suitable for use in a sulfate environment, qualifying for a Class 1 mild sulfate exposure level at a replacement dosage of 25%. The Vitric Ash-S barely missed the Class 1 limit, while the two coarse zeolites were found to be ineffective against sulfate attack.

In terms of compressive strength, mixtures made with Metakaolin-D, Zeolite-Z, and Shale-T had strengths that were similar to or higher than the control at 28 days. Given that these mixtures had an adequate strength even at a replacement of 25%, the maximum replacement level could have been pushed higher for these SCMs. However, the dosage for Metakaolin-D was capped at 25%, since its price is much higher than cement. Although the price of Zeolite-Z is reasonable, its maximum replacement dosage was also capped at 25%, since at high dosages this SCM tends to make mixtures highly viscous and cause workability problems. Shale-T, with its low cost and a 28-day strength comparable to that of the control, was the only SCM whose replacement dosage could have been pushed to higher values. More research needs to be conducted to evaluate how much cement can be replaced by Shale-T before the decrease in compressive strength starts to become an issue.

6.1.1 Specific Recommendations

Using the data summarized in Table 6.1, we have created some recommendations for the use of these SCMs in the field. In applications where both strength and durability are essential, the best SCMs to use would be Metakaolin-D and Zeolite-Z. If a severe sulfate exposure is expected, then the use of Zeolite-Z is recommended over Metakaolin-D. Pumice-D and Perlite-I will also perform well to increase the durability of concrete and are recommended in applications where high early strength is not a requirement. Shale-T is a low-cost SCM that performs well in terms of strength and ASR resistance and can be used in applications that do not require a high resistance to sulfate attack.

Table 6.1: Summary of SCM Performance at Different Replacement Dosages

| | Min. SCM Replacement for ASR, % | Sulfate Exposure Level | | Strength Relative to OPC Control at 28 Days | | Approx. Price per Ton | Workability Problems at High Dosages? |
|--------------|---------------------------------|------------------------|------------|---|------|-----------------------|---------------------------------------|
| | | 15% | 25% | 15% | 25% | | |
| Pumice-D | 15% | Class 3 | Class 3 | 90% | 91% | \$116 | NO |
| Perlite-I | 15% | Class 3 | Class 3 | 77% | 78% | \$124 | NO |
| Metakaolin-D | 15% | Unsuitable | Class 2 | 100% | 111% | \$325 (w/o shipping) | NO |
| Zeolite-Z | 15% | Class 3 | Class 3 | 126% | 105% | \$100 | YES |
| Shale-T | 25% | - | Class 1 | - | 96% | \$49–51 | NO |
| Vitric Ash-S | 25% | - | Unsuitable | - | 75% | \$100–\$160 | NO |
| Zeolite-T | 25% | - | Unsuitable | - | 86% | \$200 (w/o shipping) | YES |
| Zeolite-A | 35% | - | Unsuitable | - | 72% | \$150 | NO |

6.2 Evaluation of Current Testing Practices for SCMs

In addition to finding optimum replacement dosages, the research team also evaluated ASTM C 618, the standard specification for raw and calcined natural pozzolans, to assess whether the tests recommended therein are sufficient for a complete characterization of an alternative SCM. Based on the results of this project, we have determined that although ASTM C 618 does not thoroughly characterize the SCM, it serves as a good indicator for potential problems that could arise when using the SCM in concrete. For example, Zeolite-T and Zeolite-A, which failed more ASTM C 618 requirements than the other SCMs, turned out to be the poorest performers.

However, passing ASTM C 618 does not guarantee success of an SCM in concrete mixtures. Despite passing all the ASTM C 618 requirements, Vitric Ash-S did not perform quite as well as the other SCMs, especially in terms of strength and sulfate attack. Similarly, failing some of the requirements of the ASTM C 618 does not necessarily indicate that the SCM is unfit for use in concrete mixtures. Zeolite-Z, which failed the moisture content and water requirement test of ASTM C 618, turned out to be one of the best performers in this project in terms of strength and durability. While failing the ASTM C 618 water requirement test correctly predicted that Zeolite-Z would have workability issues, the use of WRAs enabled successful use of this SCM.

Many tests in ASTM standards, like the SAI in ASTM C 618, compare mortar mixtures on the basis of a constant flow, instead of a constant w/c. As a result, tests like the SAI tend to be unfavorable to SCMs that require a high w/c to meet the flow requirements. Instead of using the SAI test, our recommendation to TxDOT would be to use a fixed w/c to get a fair comparison of compressive strength between SCMs. Flow measurements, obtained via ASTM C 1437, can then be performed in conjunction with the compression strength tests to predict workability problems that may occur when the SCM is used in concrete.

Other recommendations include performing a laser particle size analysis on SCMs, if the equipment is available. Unlike the fineness test prescribed by ASTM C 618, which gives only a basic indication of material fineness, a laser particle size analysis can be used to determine the entire particle size distribution, which can be useful in predicting some early age properties, such as stimulation of cement hydration (the “filler effect”), increased reactivity, or decreased workability due to the presence of finer particles.

We also recommend conducting ASTM C 1567, in conjunction with ASTM C 618, to see how effective the SCMs are at mitigating expansion from ASR. However, we caution against extrapolating the ASR-related results to estimate resistance to sulfate attack, as our findings indicate that SCMs that perform well in ASR tests might not be as effective under sulfate attack. This outcome is not surprising, as the underlying mechanisms of ASR and sulfate attack are very different. If the SCMs are being considered for use in an environment with sulfate ions, we recommend conducting ASTM C 1012 testing. As with SAI, we also recommend the use of a fixed w/c for the ASTM C 1012 test, as it tends to be highly unfavorable to SCMs that require a high w/c to meet the flow requirements.

6.2.1 Specific Recommendations

In summary, we have determined that the ASTM C 618 tests provide a good initial characterization method for SCMs, as the tests have been able to filter out the poor performers in our project. However, we recommend the use of a fixed w/c for tests like SAI, which tend to be biased against SCMs with a high water demand. Along with ASTM C 618, we also recommend

conducting ASR testing using ASTM C 1567 and laser particle size analysis for a more complete characterization of the SCM. We caution against extrapolating the results from ASR testing to predict the SCM's sulfate resistance, since these two durability distresses have different underlying mechanisms. If the SCMs are being considered for use in an environment with sulfate ions, we recommend conducting ASTM C 1012 testing with a fixed w/c. Table 6.2 summarizes these evaluations and recommendations.

Table 6.2: Summary of Evaluations and Modifications Needed in Current Concrete Tests

| Tests | Evaluation | Recommendations |
|---------------------|--|---|
| ASTM C 618 | Good for basic characterization. Tests are able to filter out the bad performers, but tend to be biased against SCMs with a high water demand. | SAI should be run with a fixed w/c. The flow test of ASTM C 1437 can be used to detect workability problems. |
| ASTM C 1567 | A quick test for predicting optimum dosages for ASR mitigation in the field. | This test should be run with ASTM C 618, to understand the ASR mitigation potential of SCMs. |
| ASTM C 1012 | Good test for measuring sulfate resistance, but tends to be biased against SCMs with a high water demand. | We recommend running the test with a fixed w/c. We caution against extrapolating ASR results to predict the sulfate resistance of SCMs. |
| Laser Particle Size | Good for understanding entire particle size distribution, but requires special machine. | We recommend using this test instead of the fineness test in ASTM C 618. |

Appendix A. X-ray Diffractograms & TGA/DSC Plots of Pozzolans

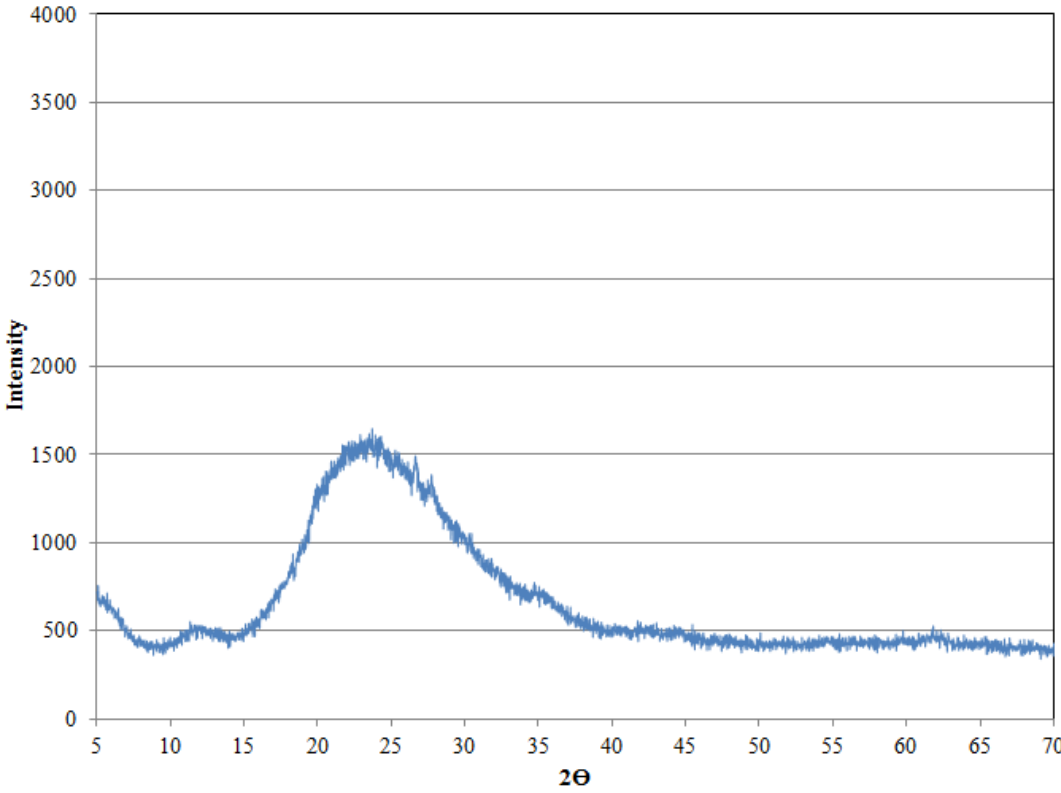


Figure A1: XRD plot of amorphous Pumice-D

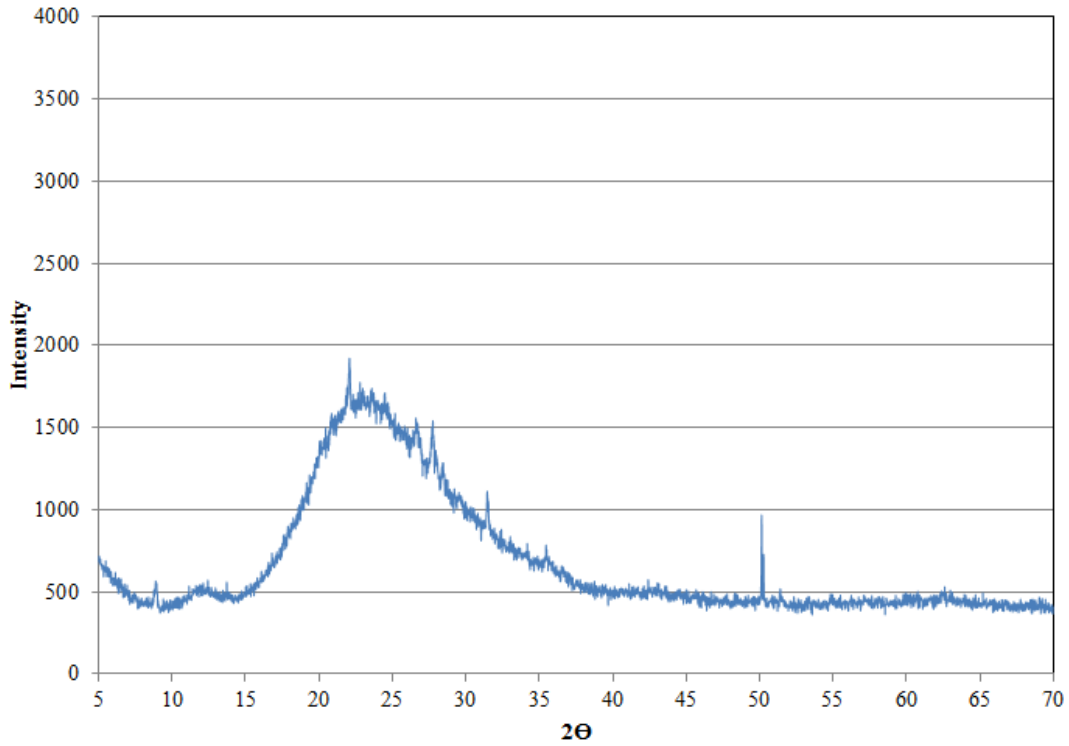


Figure A2: XRD plot of amorphous Perlite-I

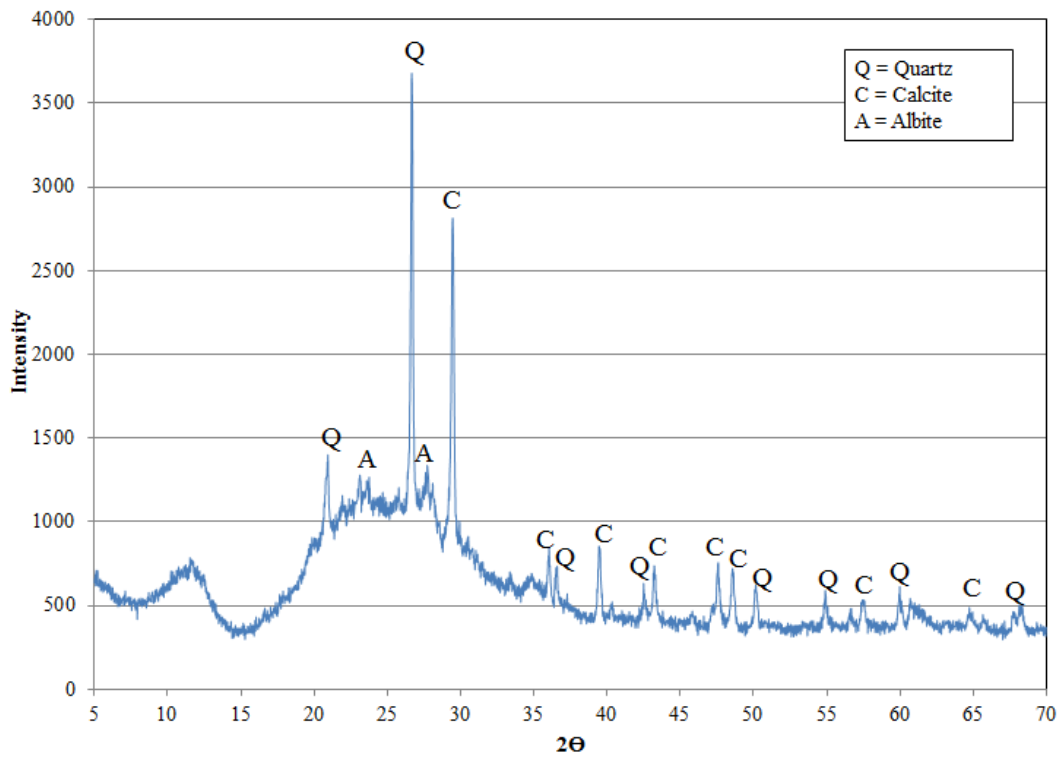


Figure A3: XRD plot of Vitric Ash-S with its crystalline impurities

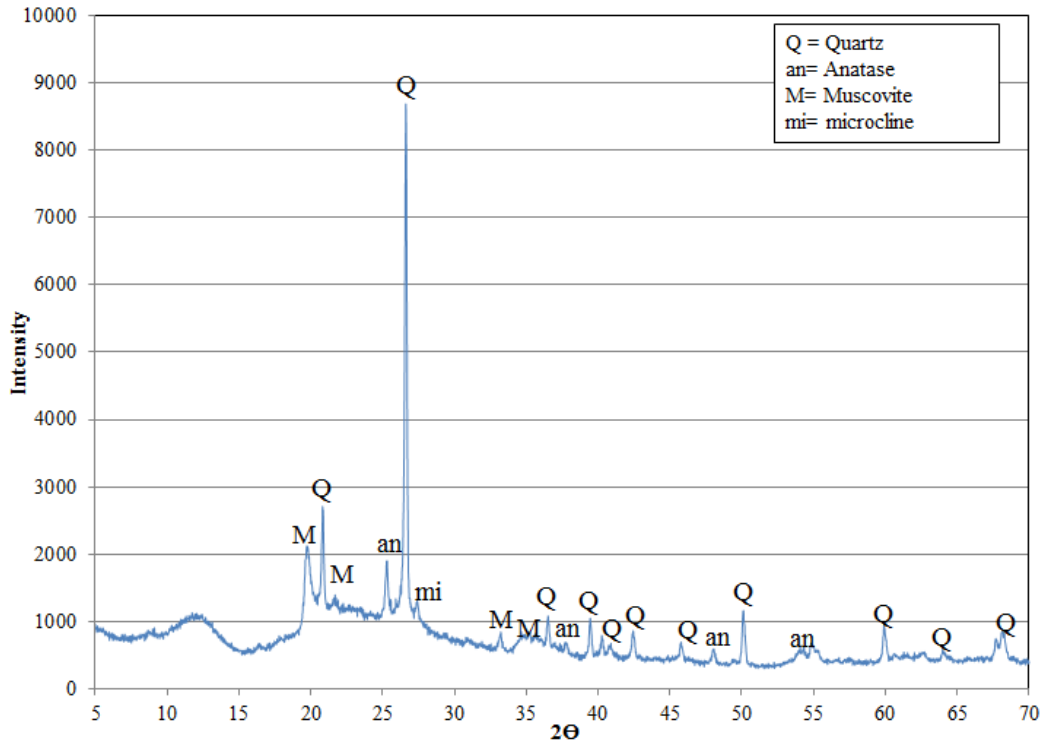


Figure A4: XRD plot of Metakaolin-D with its crystalline impurities

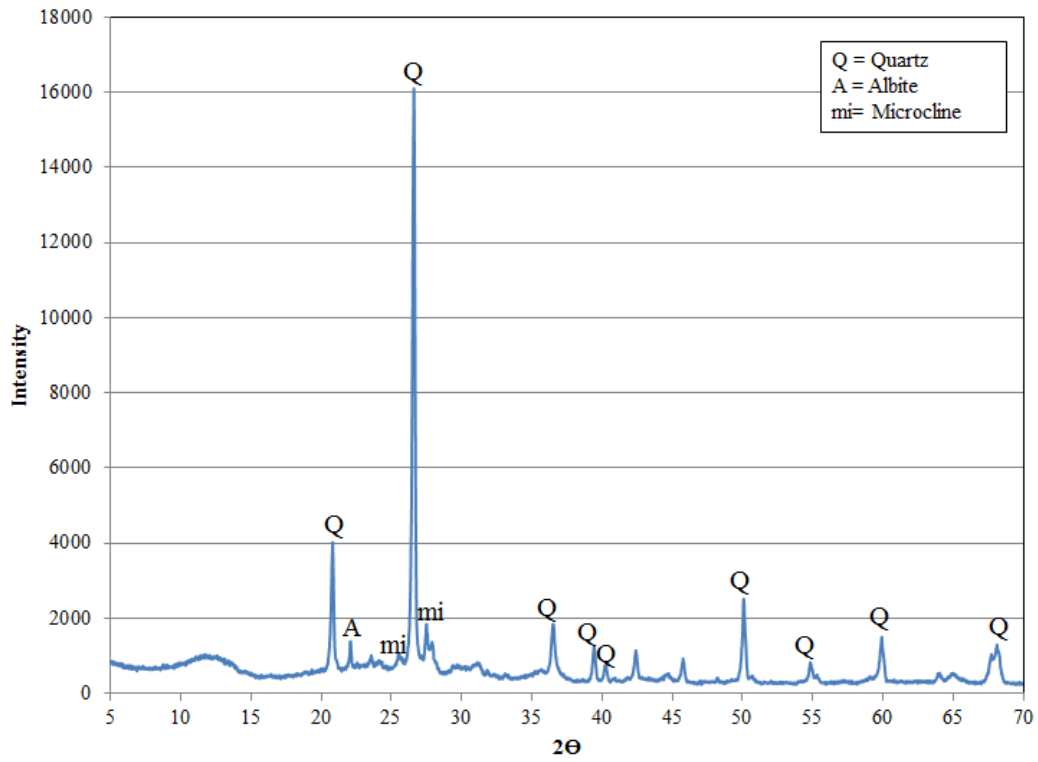


Figure A5: XRD plot of Shale-T with its crystalline impurities

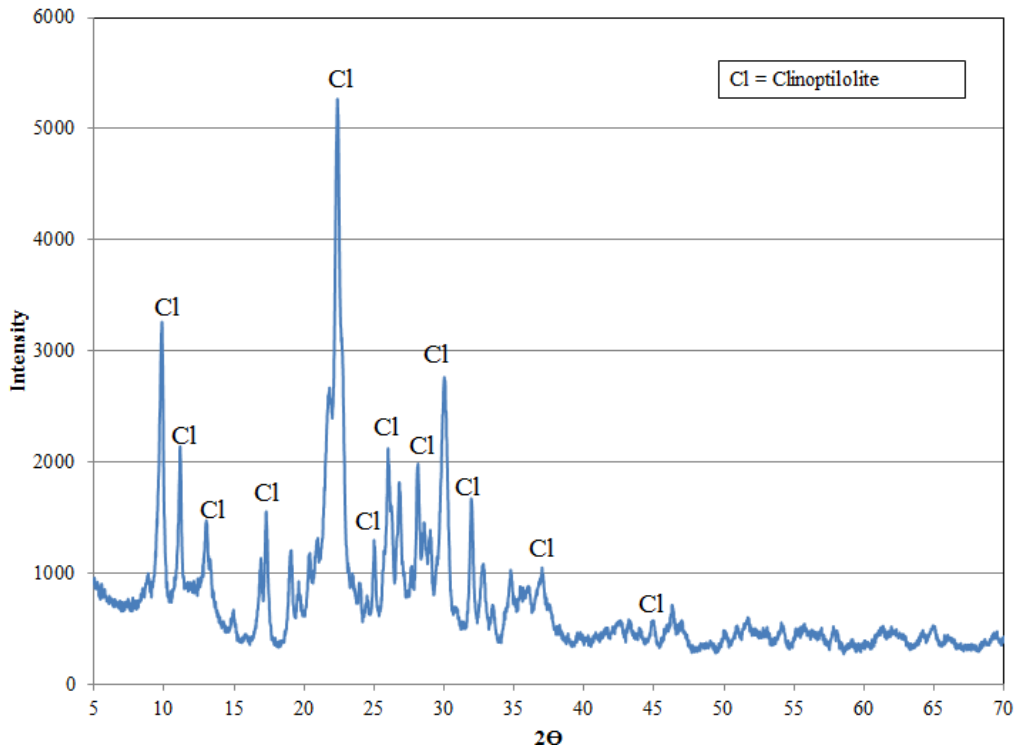


Figure A6: XRD plot of crystalline Zeolite-Z

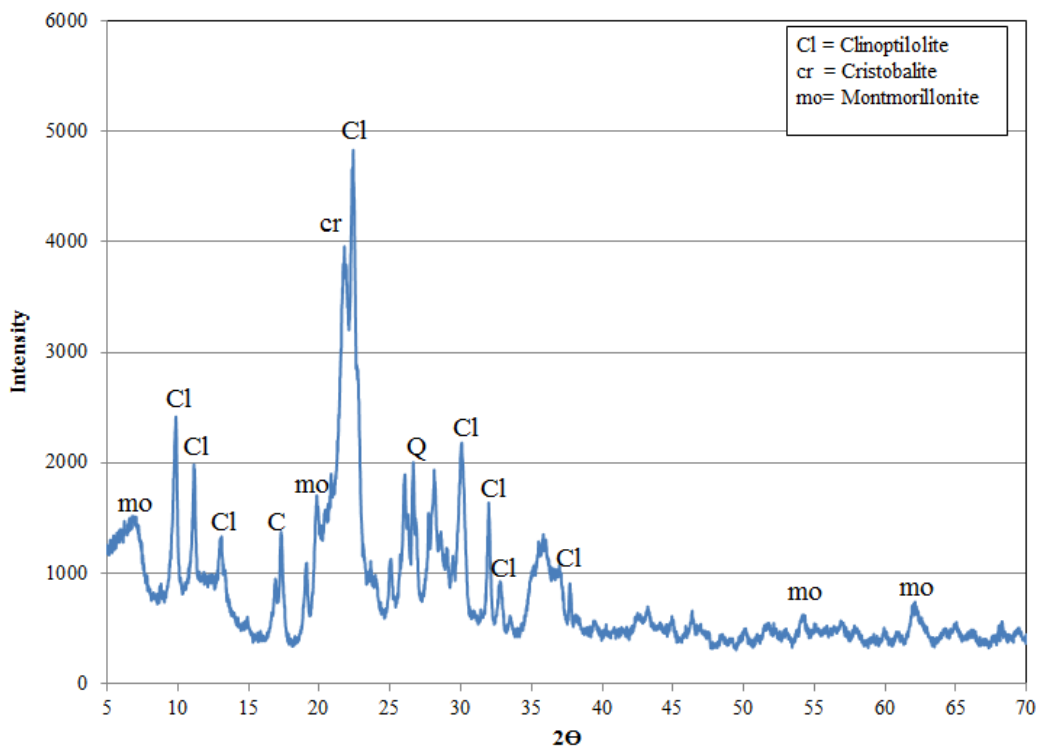


Figure A7: XRD plot of crystalline Zeolite-T

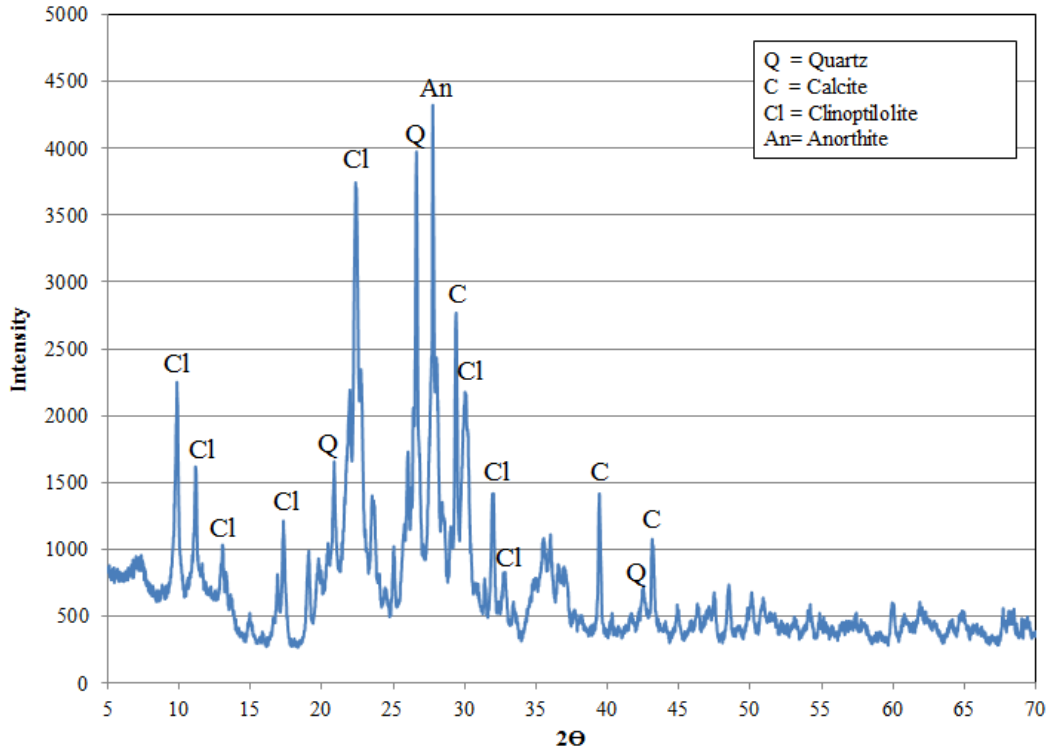


Figure A8: XRD plot of crystalline Zeolite-A

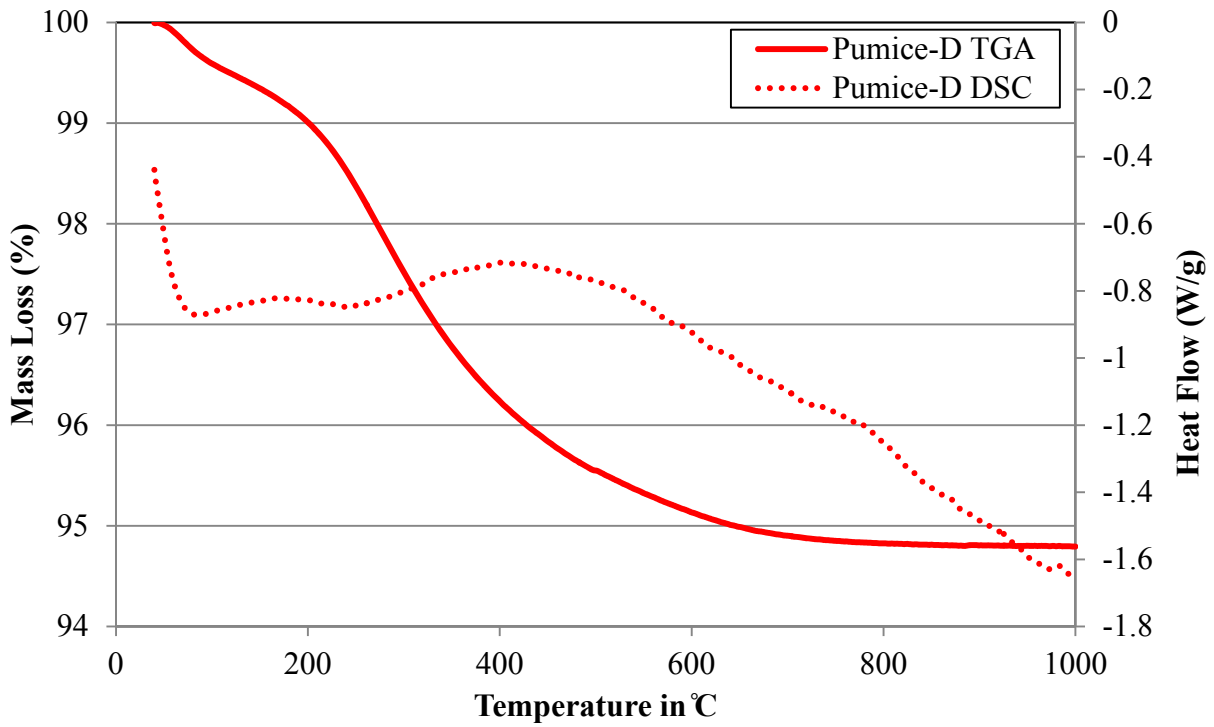


Figure A10: TGA/DSC plot of Pumice-D

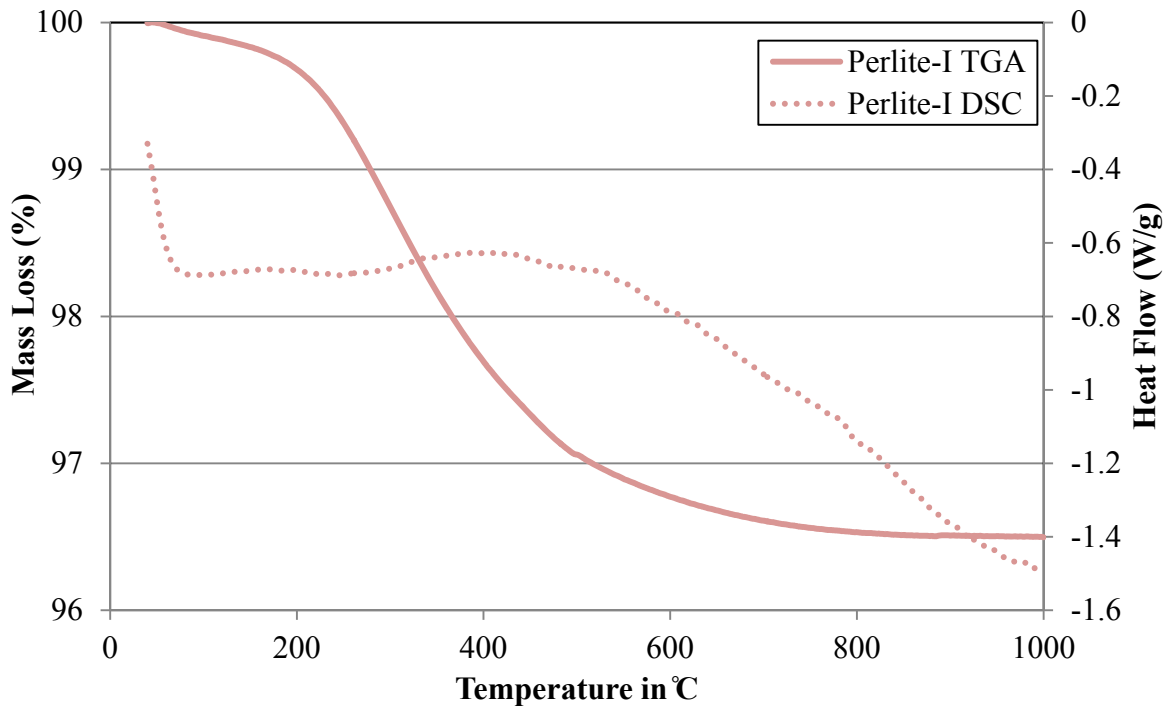


Figure A11: TGA/DSC plot of Perlite-I

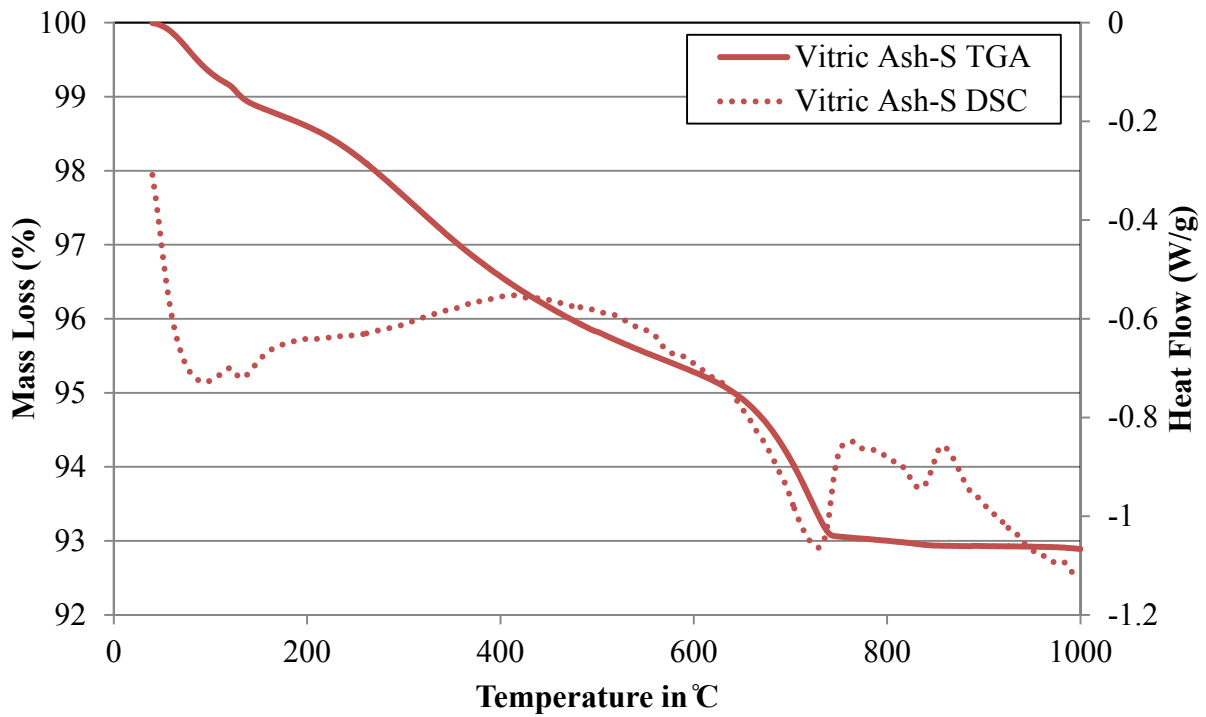


Figure A12: TGA/DSC plot of Vitric Ash-S

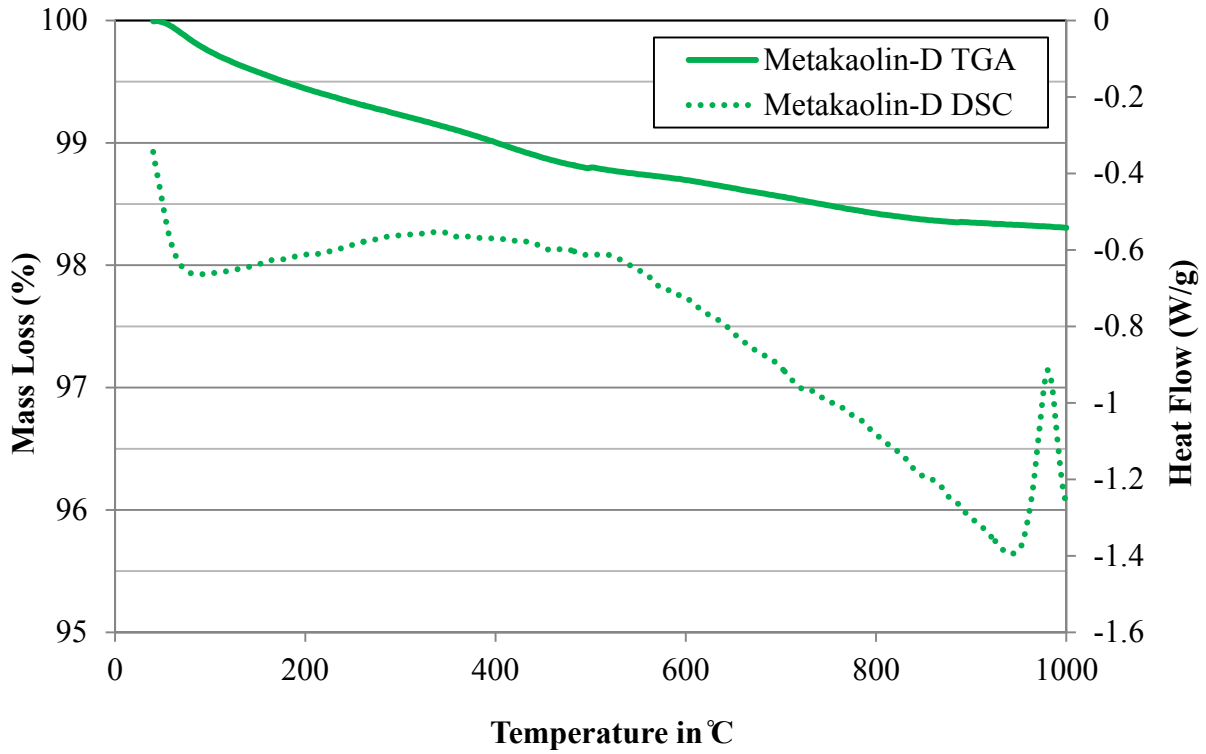


Figure A13: TGA/DSC plot of Metakaolin-D

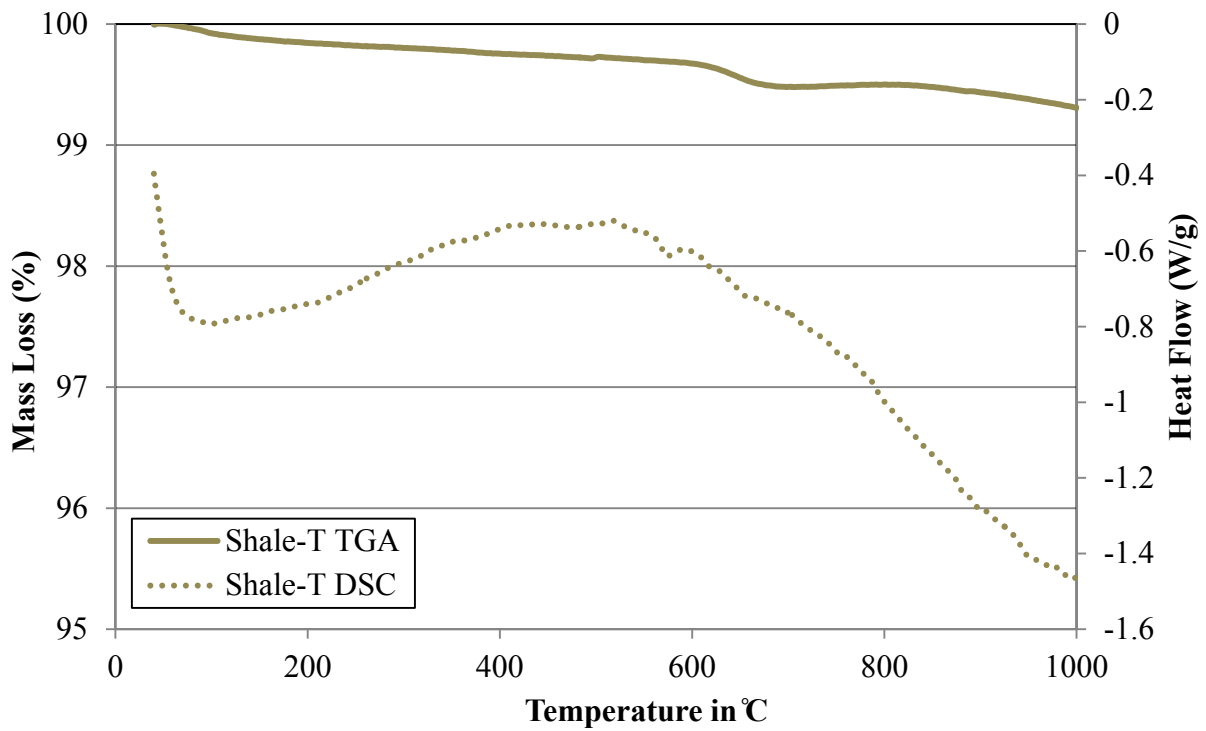


Figure A14: TGA/DSC plot of Shale-T

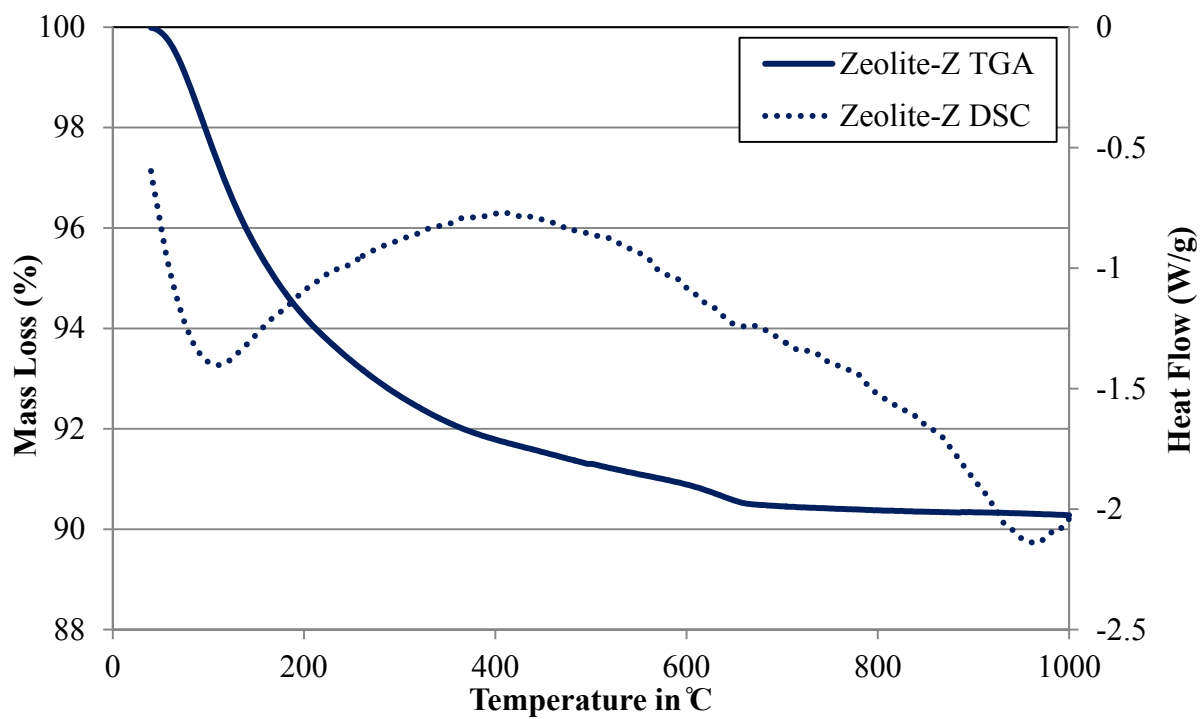


Figure A15: TGA/DSC plot of Zeolite-Z

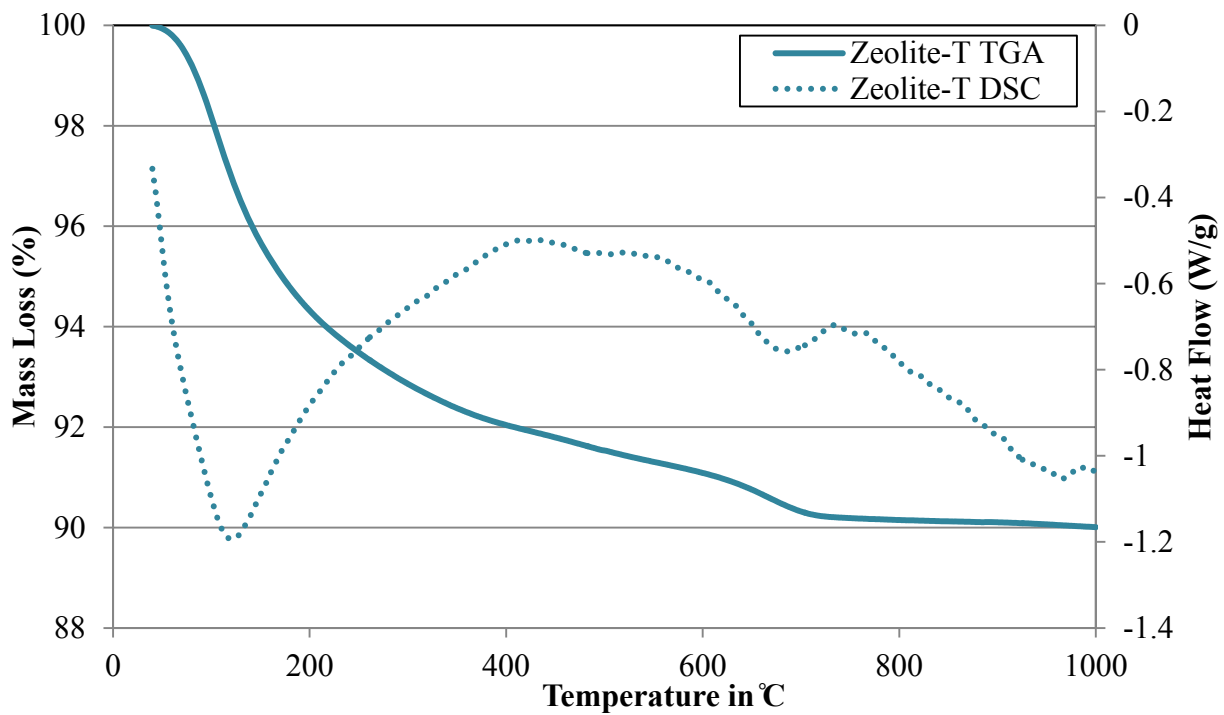


Figure A16: TGA/DSC plot of Zeolite-T

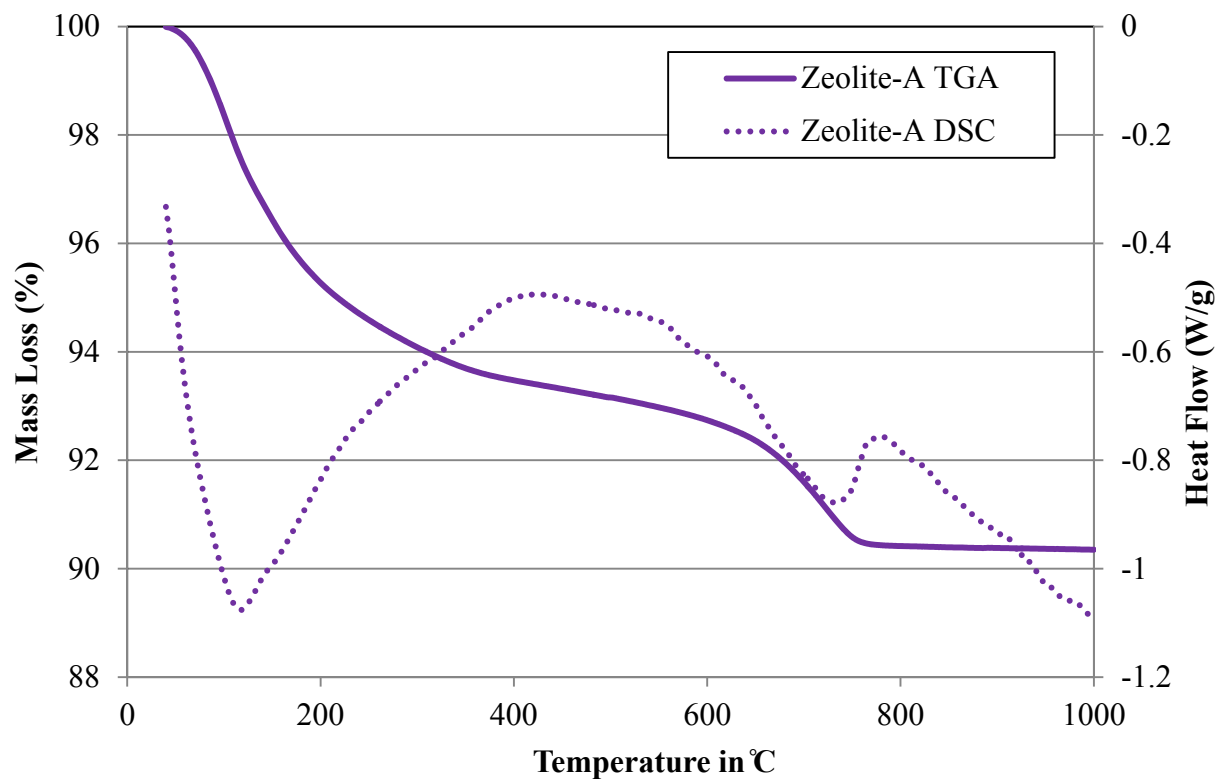


Figure A17: TGA/DSC plot of Zeolite-A

Appendix B. Admixture Dosages

Table B1: Admixture Dosage for ASTM C 1567 Mortar Mixtures

| Material | Admixture Dosage (mL/100 kg cement) | | | |
|--------------|-------------------------------------|---------|---------|---------|
| | 15% SCM | 20% SCM | 25% SCM | 35% SCM |
| Pumice-D | 155 | 127 | --- | --- |
| Perlite-I | 155 | 127 | --- | --- |
| Vitric Ash-S | --- | 127 | 139 | --- |
| Metakaolin-D | 155 | 183 | --- | --- |
| Shale-T | --- | 124 | 155 | --- |
| Zeolite-Z | 511 | 651 | --- | --- |
| Zeolite-T | --- | 1116 | 1426 | --- |
| Zeolite-A | --- | 356 | 806 | 1348 |
| Fly Ash | --- | 0 | --- | --- |

*Values in red represent dosages that are above the manufacturer recommended dosage

Table B2: Admixture Dosage for Concrete Used to Measure Fresh State Properties

| Description | Admixture | | |
|-----------------------|-------------|--------------|----------|
| | Pre-dose, g | Post-dose, g | Total, g |
| Control | 12.0 | 46.9 | 58.9 |
| 15% Pumice | 12.0 | 59.8 | 71.8 |
| 25% Pumice | 102.1 | 100.7 | 202.8 |
| 15% Perlite | 22.5 | 22.5 | 45.0 |
| 25% Perlite | 81.4 | 59.5 | 140.9 |
| 25% Ash | 100.4 | 0.0 | 100.4 |
| 15% Metakaolin | 20.0 | 54.8 | 74.8 |
| 25% Metakaolin | 80.2 | 78.1 | 158.3 |
| 25% Shale | 99.2 | 79.4 | 178.6 |
| 15% Zeolite-Z | 251.8 | 95.0 | 346.8 |
| 25% Zeolite-Z | 492.6 | 0.0 | 492.6 |
| 35% Zeolite-A | 190.8 | 155.7 | 346.5 |
| 25% Zeolite-T | 151.0 | 251.0 | 402.0 |
| 15% Fly Ash | 0.0 | 10.4 | 10.4 |
| 25% Fly Ash | 0.0 | 0.0 | 0.0 |

Appendix C. Ultrasonic Tests for Concrete Setting Time Measurement

C.1 Introduction

The penetration resistance test according to ASTM C403 [1] is the standard method to determine setting times by measuring penetration resistance of mortar mixtures or mortar sieved from concrete. However, this method is time consuming and not suitable for in-situ field testing. Researchers of this project developed an ultrasonic shear wave method to monitor the setting process of mortar and concrete.

During the past two decades, extensive effort has been focused on finding the correlation between the ultrasonic compression wave (P wave) velocity and the time of setting of cementitious materials [156]. Various criteria have been proposed for setting time determination based on features of the P wave velocity versus time curve. However, these criteria do not give consistent conclusions. Recent studies have indicated that the shear wave velocity is closely related to the stiffness (shear modulus) of the solid skeleton formed by cement hydration product, and it is a more reliable parameter for setting time measurements than the P wave velocity [164–167]. A challenge with shear wave velocity measurement is the high attenuation of shear waves in fresh concrete.

In this study, we proposed a new ultrasonic test setup using embedded piezoelectric bender elements. Compared to commercial ultrasonic transducers, the bender elements experience relatively large transverse deformation of fresh mortar and concrete, and effectively generate shear waves of low frequencies. This allows the shear waves to propagate through fresh concrete with less attenuation than typical ultrasonic transducers generate. The results from bender elements and ultrasonic transducers are compared and show good agreements. With the bender element setup, correlation between shear wave velocity and penetration resistance (ASTM C 403) was obtained for mortar mixtures and mortar sieved from fresh concrete. By using different mixture designs, we evaluated the effects of different water-to-cement ratios (w/c) and aggregate sizes and types on these ultrasonic measurements.

C.2 Materials and Experimental Setup

C.2.1 Materials

To investigate the effects of w/c and aggregate types on ultrasonic measurements of setting times, three mortar and five concrete mixtures with different w/c and coarse aggregates were tested. The setting time of each mixture was measured with a penetrometer, according to ASTM C 403. The ultrasonic test setups monitored the ultrasonic P wave and shear wave velocity simultaneously.

Table C.1 shows details of all eight mixtures investigated in this study. Three mortar mixtures were used to investigate the effect of w/c on setting time. Out of the five concrete mixtures, three were used to investigate the effects of w/c on setting time. The coarse aggregate volume fraction was kept the same for these mixtures, while the w/c was varied from 0.41 to 0.68. The coarse aggregate used for these mixtures was river gravel from Capitol Aggregates (Texas), with a relative density of 2.60, and a maximum size of 25.4 mm. The other two concrete mixtures had the same w/c of 0.5 and were used to investigate the effect of coarse aggregate size on setting time and wave velocities. The coarse aggregate used for these two mixtures was

dolomitic limestone from Bridgeport, Texas, with a relative density of 2.65. For the “large aggregate” concrete mix, the maximum aggregate size was larger than 19.1 mm, while the “small aggregate” mix used a maximum aggregate size of 12.7 mm.

Type I Portland cement was used in all eight mixtures. The fine aggregate used for both the mortar and concrete mixtures was Colorado River sand from Webberville, Texas, with a relative density of 2.62. The standard procedure described in ASTM C 192 [150] was followed to make these mixtures.

Table C1: Concrete and Mortar Mixture Designs, Setting Times, and Ultrasonic Test Setups

| w/c | Mixture type | Test setups | Coarse aggregate type | Coarse aggregate volume (%) | Sand volume (%) | Initial setting (min) | Final setting (min) |
|------|--------------|---|-----------------------------|-----------------------------|-----------------|-----------------------|---------------------|
| 0.40 | Mortar | | - | - | 62.3 | 171 | 257 |
| 0.45 | Mortar | B, P, S | - | - | 61.6 | 189 | 272 |
| 0.50 | Mortar | | - | - | 60.8 | 236 | 327 |
| 0.50 | Concrete | B, P, S (mortar sieved from concrete mixtures) | “Large” dolomitic limestone | 43.4 | 28.9 | 239 | 315 |
| 0.50 | Concrete | | “Small” dolomitic limestone | 43.4 | 28.9 | 226 | 309 |
| 0.41 | Concrete | | River gravel | 40.1 | 26.9 | 287 | 391 |
| 0.53 | Concrete | | River gravel | 40.1 | 29.9 | 314 | 413 |
| 0.68 | Concrete | | River gravel | 40.1 | 32.3 | 323 | 442 |

B: bender elements; P: P wave transducers; S: shear wave transducers.

C.2.2 Ultrasonic Test Setups

A pair of bender elements was used to generate and measure shear waves in both mortar and concrete mixtures, as shown in Figure C1. The terminal end of each bender was clamped onto an aluminum frame, which was placed in a wooden box with dimensions of 300 mm × 150 mm × 100 mm. The mixed mortar or concrete was poured into the wooden box to 90 mm height to cover the bender elements. The bender elements were about 75 mm below the mortar/concrete surface, which was covered by a layer of plastic film to reduce moisture evaporation.

During the test, one bender element was used as the actuator while the one served as the receiver. The actuating bender element was driven by a 100 kHz, 200 V square wave pulse generated from a pulser-receiver (Panametrics 5077PR), and the receiving bender element was connected to the pulser-receiver with a gain of 40 dB. The amplified receiving signals were then digitized by an NI-PXI5133 digitizer at a sampling rate of 10 MHz and transferred to a computer. Since ultrasonic waves have high attenuation in fresh mortar and concrete, 200 signals were averaged in each measurement to improve the signal-to-noise ratio. All mixtures were monitored until the time of final set as determined by the procedures of ASTM C 403.

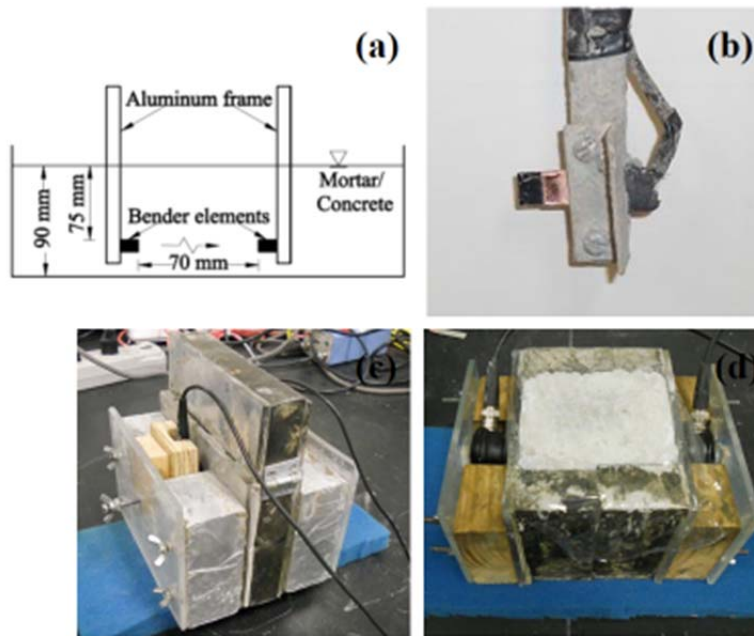


Figure C1: Ultrasonic test setups: (a) setup using bender elements, (b) picture of bender element, (c) setup using shear wave transducers, and (d) setup using P wave transducers

For comparison purposes, mortar and concrete mixtures from the same batch were also monitored using two types of commercial ultrasonic transducers: shear wave transducers and P wave transducers. Figure C1(c) and 1(d) illustrate the test setups. The larger container, with a sample holder of 109 mm thick, was used to test mortar and concrete mixtures using a pair of 500 kHz P wave transducers (Panametrics V101). The container with a specimen holder thickness of 27 mm was used for mortar and the mortar sieved from concrete mixtures using a pair of 500 kHz shear wave transducers (Panametrics V151). A smaller specimen thickness was used with the shear wave transducers because shear waves have very high attenuation in fresh mortar. The actual thicknesses of mixtures were measured after the ultrasonic testing.

C.3 Results and Discussion

C.3.1 Mortar Mixtures

The P and shear wave velocities measured in mortar mixtures using the bender elements setup are shown in Figure C2, with initial setting times measured from the ASTM C403 penetration tests marked on the velocity curves. The values of setting times are shown in Table C1. The P wave velocity curves are well above the shear wave velocity curves due to the high velocity of the P waves. As seen in Figure C2, although the mixtures have different w/c and setting times, the shear wave velocities at initial setting times for all mixtures are similar, with an average of 388 m/s. The good agreement between shear wave velocity and penetration resistance results at setting times indicates that both the shear wave velocity and penetration resistance tests measure the shear property of the solid framework in mortar. On the contrary, the P wave velocities at initial setting times show greater variability, which is consistent with previous studies.

Figure C3 shows the penetration resistance measurements vs. age for mortar mixtures with different w/c. The initial and final setting times correspond to the penetration resistance values of 500 psi and 4000 psi, separately. The initial and final setting times (detailed in Table C1) clearly increase significantly as the w/c increases.

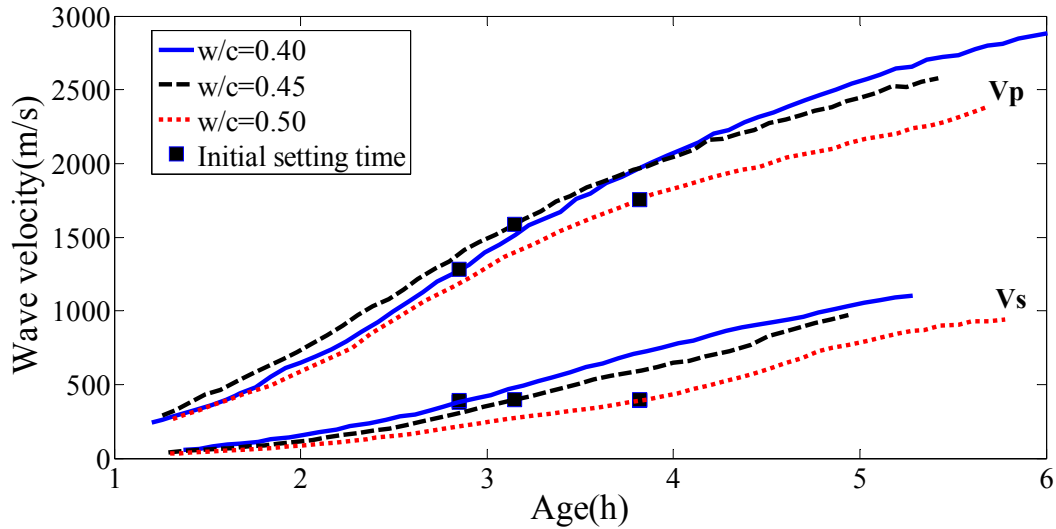


Figure C2: Ultrasonic P wave and shear wave velocities measured in mortar mixtures

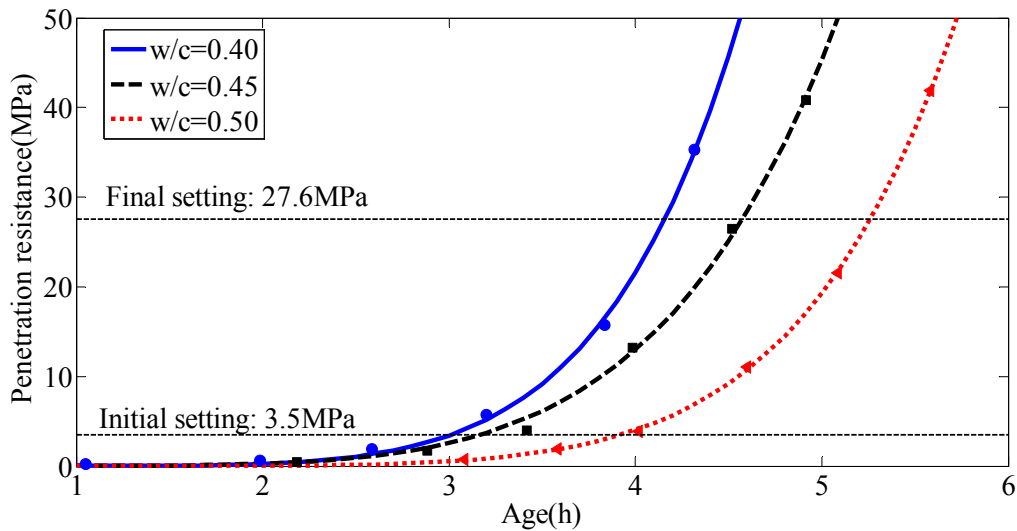


Figure C3: Penetration resistance of mortar mixtures with different w/c

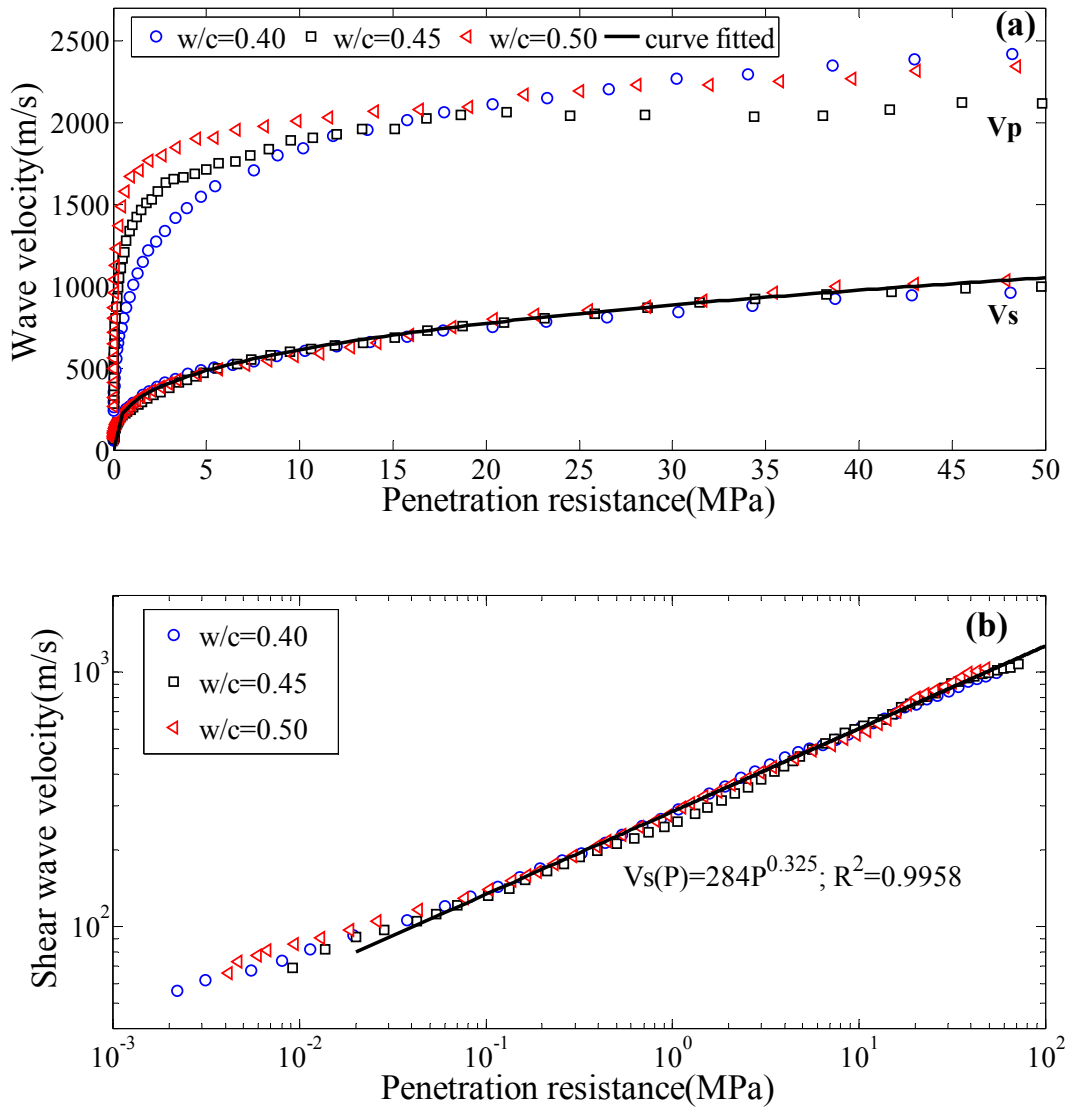


Figure C4: Correlation between P and shear wave velocities and penetration resistance on mortar mixtures with different w/c in (a) linear scale and (b) logarithm scale (shear wave velocity only)

Figure C4 plots the shear wave velocity vs. penetration resistance. The penetration resistance data points in Figure C4 were calculated by interpolating the equations in Figure C3 at ages when shear wave velocities were measured. The figure evinces a clear correlation between the shear wave velocity and the penetration resistance, even though the mortar mixtures have different w/c . Figure C4(b) shows the shear wave vs. penetration resistance data in logarithm scale. This correlation can be well represented by a power function with a correlation coefficient $R^2 > 0.99$. For comparison, the P wave velocity vs. penetration resistance is also shown in Figure C4 (a). Although the data for each mixture shows a power function trend, the data from different mixtures do not show a unique correlation with the penetration results. The strong correlation between shear wave velocity and penetration resistance measurements is attributed to the fact that both measurements are directly related to the shear properties (modulus and resistance) of

the solid frame in fresh mortar, while P wave velocity is also affected by the property and air voids in the fluid phase of mortar. Since setting times are determined by the penetration resistance test, the shear wave velocity is a more reliable parameter for setting time monitoring than the P wave velocity.

C.3.2 Mortar Sieved from Concrete Mixtures

Figure C5 shows development of P wave and shear wave velocities vs. age measured on five sieved concrete (mortar) mixtures. These concrete mixtures have different w/c and aggregate types. However, the similar shear wave velocities are similar at the initial setting times for all mixtures, with an average of 508 m/s. The P wave velocities at initial setting times show large variance among different mixtures. This finding agrees with what was observed in the mortar tests discussed in the previous section.

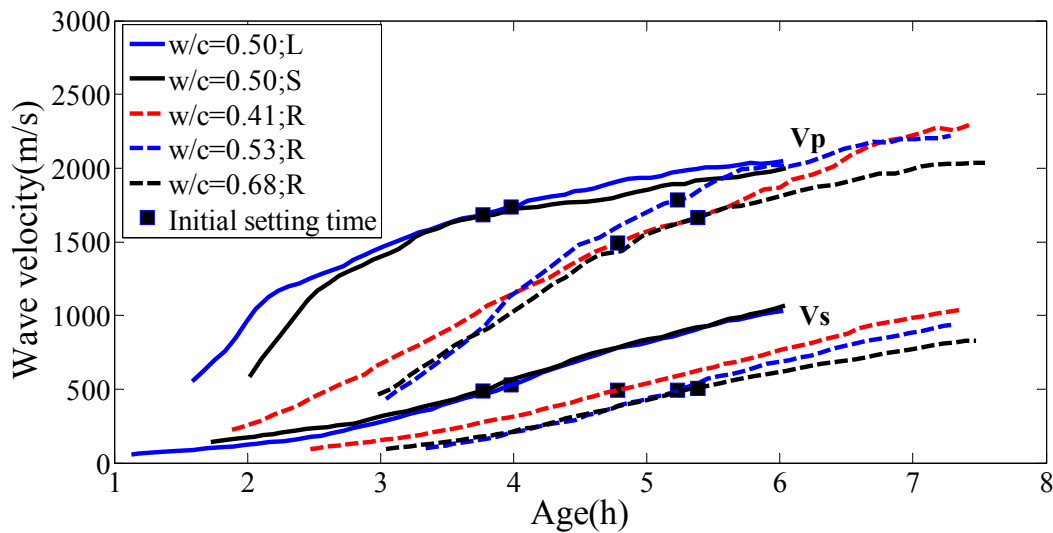


Figure C5: Ultrasonic P and shear wave velocities in sieved concrete mixtures

The measured shear wave velocities were correlated to the penetration resistance of the mortar sieved from concrete mixtures, and are presented in Figure C6 in linear and logarithm scales. The data at very early age ($V_s < 100$ m/s) show large scattering, especially between the concrete using dolomitic limestone and river gravel aggregates. For $V_s > 100$ m/s, a clear correlation is obtained between the shear wave velocity and penetration resistance for all mortar mixtures sieved from concrete, with R^2 of 0.9807.

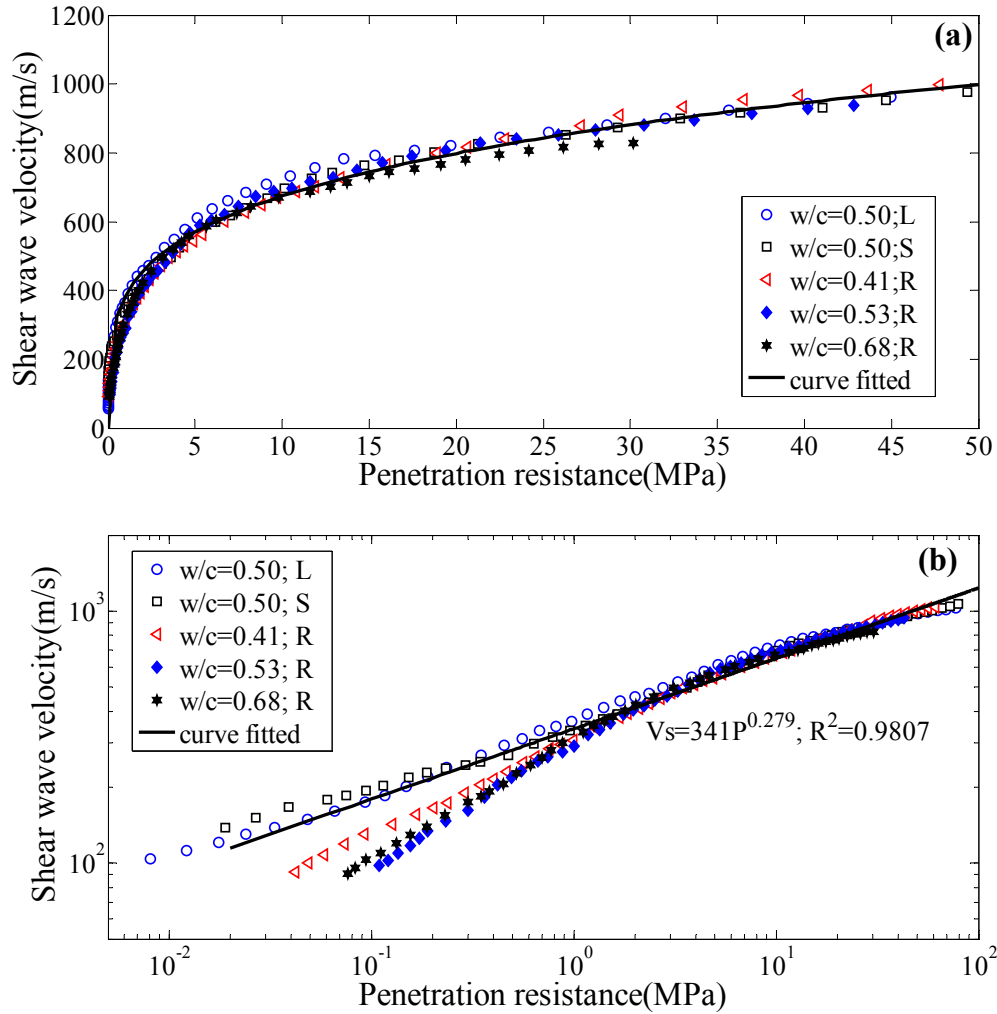


Figure C6: Correlation between shear wave velocity and penetration resistance on mortar sieved from concrete mixtures in (a) linear scale and (b) logarithm scale

C.3.3 Concrete Mixtures

Figure C7 shows the correlation between P-wave and shear wave velocities measured on concrete mixtures vs. penetration resistance on the sieved mortar mixtures. Unlike the mortar tests, there is no unique relationship between shear wave velocity and penetration resistance measurements, although the data from each mixture still show similar power function trends. The presence of coarse aggregates in concrete strongly affects both P wave and shear wave velocities, while the penetration resistance measured on sieved mortar is not affected. This study demonstrates the challenges for in-situ monitoring of fresh concrete using ultrasonic wave velocity methods.

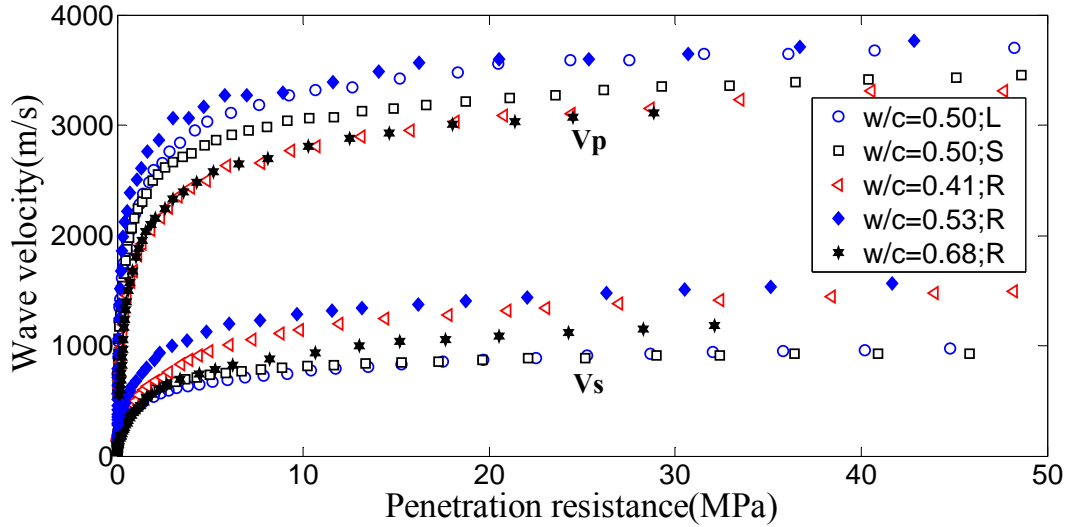


Figure C7: Correlation between P and shear wave velocities and penetration resistance of different concrete mixtures

The wave velocities at setting times and standard deviation are summarized in Table C2. It is reasonable to conclude that the large variance in measured data is caused by the heterogeneous nature of concrete. Coarse aggregates typically have much higher velocities than cement paste and mortar, and the velocity also varies significantly for different types of coarse aggregates. In addition, the actual coarse aggregate content in each concrete mixture might be different due to the small volume of concrete used in ultrasonic tests. Therefore, ultrasonic velocities measured on concrete mixtures are higher than those measured on the mortar sieved from the same batch of concrete, and the test results also show larger variance.

Table C2: Ultrasonic Wave Velocities Measured at Initial and Final Setting Times

| Mixtures | P wave velocity (m/s) | | Shear wave velocity (m/s) | |
|-----------------|-----------------------|---------------|---------------------------|---------------|
| | Initial setting | Final setting | Initial setting | Final setting |
| Mortar | 1563±164 | 2131±120 | 392±10 | 847±12 |
| Sieved concrete | 1672±98 | 2033±102 | 508±16 | 855±19 |
| Concrete | 2674± 268 | 3355± 217 | 678± 76 | 1020± 186 |

C.4 Conclusions

Ultrasonic tests were used to monitor the setting process in fresh mortar and concrete mixtures. A clear correlation exists between the shear wave velocity and penetration resistance for mortar mixtures and sieved concrete samples. This relationship is not affected by the w/c of the mixture, but is affected by aggregate contents. The researchers found that the shear wave velocities at initial setting time are 392 ± 10 m/s in mortar, and 508 ± 16 m/s in mortar sieved from concrete, respectively. There is a clear correlation between the shear wave velocity and the penetration resistance measured in early age mortar mixtures through the entire process.

Unlike in mortar tests, there is no unique correlation between P wave or shear wave velocity in concrete and penetration resistance measurements, as wave velocities are strongly

affected by coarse aggregates, while the penetration test is performed on sieved mortar samples, which is not affected by coarse aggregates. Further study is needed to reduce the effects of coarse aggregate on ultrasonic wave measurements.

References

1. K. Humphreys, M. Mahasanen, Towards a sustainable cement industry, Sub-study 8: Climate Change (2002), Accessed on April 24th, 2014 from: <http://www.groundwork.org.za/Cement/Climate%20change%20&%20the%20cement%20industry.pdf>
2. Texas Department of Transportation, Technical Advisory: Fly Ash Supply, Construction and Bridge Division (2010). Accessed on July 24th, 2014 from http://ftp.dot.state.tx.us/pub/txdot-info/cst/tips/fly_ash.pdf
3. M. Thomas, The effect of supplementary cementing materials on alkali-silica reaction: A review, *Cement and Concrete Research* 41 (2011) 1224–1231
4. M.H. Shehata, M.D.A Thomas, The effect of fly ash composition on the expansion of concrete due to alkali-silica reaction, *Cement and Concrete Research* 30 (2000) 1063 – 1072
5. R. Dhole, M.D.A Thomas, K.J. Folliard, T. Drimalas, Characterization of Fly Ashes for Sulfate Resistance, *ACI Materials Journal* 110–2 (2013) 159–168
6. W. Nocun-Wczelik, Heat Evolution in Hydrated Cementitious Systems Admixture with Fly Ash, *Journal of Thermal Analysis and Calorimetry* 65 (2001) 613–619
7. ARTBA Transportation Development Foundation, The Economic Impacts of Prohibiting Coal Fly Ash Use in Transportation Infrastructure Construction (2011), Accessed on April 24th, 2014 from: http://db78bc60e308ad8dc7c2-6f6534a35fc09b927eb00e4333a7f4cf.r47.cf2.rackcdn.com/uploaded/s/0e927411_study2011flyash.pdf
8. American Coal Ash Association, ACAA 2012 Fly Ash Production by Year (1966–2012). Accessed on July 24th, 2014 from http://www.aaa-usa.org/Portals/9/Files/PDFs/1966-2012_FlyAsh_Prod_and_Use_Charts.pdf
9. NRMCA Advocacy and Government Affairs, Fly Ash (2014). Accessed on July 24th, 2014 from <http://nrmcavoice.com/issues/environment>
10. US EPA, Coal Combustion Residuals—Proposed Rule (2013). Accessed on July 24th, 2014 from <http://www.epa.gov/epawaste/nonhaz/industrial/special/fossil/ccr-rule/index.htm>
11. US EPA, Clean Air Interstate Rule (CAIR) (2014). Accessed on July 24th, 2014 from <http://www.epa.gov/cair/index.html>
12. US EPA, Cross-State Air Pollution Rule (CSAPR) (2014), Accessed on July 24th, 2014 from <http://www.epa.gov/crossstaterule/index.html>

13. R. Hill, S. Sarkar, R. Rathbone, J. Hower, An Examination of Fly Ash Carbon and Its Interactions with Air Entraining Agent. *Cement and Concrete Research* 27-2(1997) 193–204
14. J. Tishmack, J. Olek, S. Diamond, Characterization of High-Calcium Fly Ashes and Their Potential Influence on Ettringite Formation in Cementitious Systems. *Cement, Concrete, and Aggregates* (1999) 82–92
15. M.R. Jones, L.K.A. Sear, M.J. McCarthy, R.K. Dhir, Changes in Coal Fired Power Station Fly Ash: Recent Experiences and Use in Concrete, Proceedings of Ash Technology Conference, UK Quality Ash Association, 2006. Accessed on April 24, 2014 from: <http://www.ukqaa.org.uk/wp-content/uploads/2014/02/AshTech-2006-Jones-et-al.pdf>
16. Texas Department of Transportation, Standard Specifications for Construction and Maintenance of Highways, Streets, and Bridges. Adopted June 1, 2004
17. ASTM C 125-12, Standard Terminology Relating to Concrete and Concrete Aggregates, ASTM International (2012) West Conshohocken, PA
18. ASTM C 618-08a, Standard Specification for Coal Fly Ash and Raw or Calcined Natural Pozzolan for Use in Concrete, ASTM International (2008) West Conshohocken, PA
19. F. Bektas, L. Turanli, P.J.M. Monteiro, Use of Perlite Powder to suppress alkali-silica reaction, *Cement & Concrete Research* 35 (2005) 2014–2017
20. M. Rotella, G. Simandl, Marilla Perlite—Volcanic Glass Occurrence, British Columbia, Canada, Geological Fieldwork 2002, Paper 2003-1
21. T.K. Erdem, C. Meral, M. Tokyay, T.Y. Erdog˘an, Use of perlite as a pozzolanic addition in producing blended cements, *Cement & Concrete Composites* 29 (2007) 13–21
22. A. Ray, R. Sriravindrarajah, J.P. Guerbois, P. S. Thomas, S. Border, H. N. Ray, J. Haggman and P. Joyce, Evaluation of Waste Perlite Fines in the Production of Construction Material, *Journal of Thermal Analysis and Calorimetry* 88 (2007) 1, 279–283
23. L.H. Yu, H. Ou, L.L Lee, Investigation on pozzolanic effect of perlite powder in concrete, *Cement and Concrete Research* 33 (2003) 73–76
24. J.S. Denton, H. Tuffen, J.S. Gilbert, N. Odling, The hydration and alteration of perlite and rhyolite, *Journal of the Geological Society, London* 166 (2009) 895–904
25. B. Uzal, L. Turanli, P.K. Mehta, High Volume Natural Pozzolan Concrete for Structural Applications, *ACI Materials Journal* 104 (2007) 5, 535–538

26. H.S. Gokce, O. Simsek, S. Korkmaz, Reduction of alkali-silica reaction expansion of mortars by utilization of pozzolans, *Magazine of Concrete Research* 65-7 (2013) 441–447
27. USGS, Perlite, Mineral Commodity Summaries, (2012). Accessed on August 4th, 2014 from: <http://minerals.usgs.gov/minerals/pubs/commodity/perlite/mcs-2012-perli.pdf>
28. USGS, 2011 Mineral Yearbook Perlite (Advance Release). Accessed on August 4th, 2014 from: <http://minerals.usgs.gov/minerals/pubs/commodity/perlite/myb1-2011-perli.pdf>
29. G. C. Presley, Pumice, pumicite, and volcanic cinder, in J.E. Kogel, N.C. Trivedi, J.M. Barker, S.T. Krukowski, *Industrial Minerals and Rocks*, 7 edition: Littleton, CO, Society for Mining, Metallurgy, and Exploration, Inc. (2006) 743–754.
30. R. Snellings, G. Mertens, J. Elsen, Supplementary Cementitious Materials, *Reviews in Mineralogy & Geochemistry* 74 (2012) 211–278.
31. U. Ramasamy, P. Tikalsky, Evaluation Report of Hess Pumice, Concrete and Materials Research and Evaluation Laboratory, Department of Civil and Environmental Engineering, The University of Utah, June 11, 2012. Accessed on August 4th, 2014 through: <http://www.hesspozz.com/PDFs/HessPozz-StudyResults.pdf>
32. ACI Committee 232, Report on the Use of Raw or Processed natural Pozzolans in Concrete (ACI 232.1R-12). Farmington Hills, MI: American Concrete Institute (2012)
33. R.J. Elfert, Bureau of Reclamation Experiences with Fly Ash and Other Pozzolans in Concrete, Information Circular No. 8640, U.S. Bureau of Mines, Washington DC, (1974) 80–93
34. H.S. Meissner, Pozzolans used in Mass Concrete, Symposium on Use of Pozzolanic Materials in Mortars and Concretes, STP-99, ASTM, Philadelphia, (1950)16–30.
35. K.M.A. Hossain, Blended cement using volcanic ash and pumice, *Cement and Concrete Research* 33 (2003) 1601–1605.
36. K.M.A. Hossain, Potential Use of Volcanic Pumice as a Construction Material, *ASCE Journal of Materials in Civil Engineering* 16 (2004) 573–577.
37. K.M.A. Hossain, Chloride induced corrosion of reinforcement in volcanic ash and pumice based blended concrete, *Cement and Concrete Composites* 27 (2005) 381–390.
38. K.M.A. Hossain, S. Ahmed, M. Lachemi, Lightweight concrete incorporating pumice based blended cement and aggregate: Mechanical and durability characteristics, *Construction and Building Materials* 25 (2011) 1186–1195.

39. R.C. Mielenz, L.P. Witte, and O.J. Glantz, Effect of Calcination on Natural Pozzolana, Symposium on Use of Pozzolanic Materials in Mortars and Concretes, STP-99, ASTM (1950) 43–91
40. K.M.A. Hossain, M. Lachemi, Performance of volcanic ash and pumice based blended cement concrete in mixed sulfate environment, *Cement and Concrete Research* 36 (2006) 1123–1133.
41. ASTM C 157-08, Standard Test Methods for Length Change of Hardened Hydraulic-Cement Mortar and Concrete, ASTM International (2008) West Conshohocken, PA
42. G.G. Litvan, Further Study of Particulate Admixture for Enhanced Freeze-Thaw Resistance of Concrete, *ACI Journal* September/October (1985) 724–730
43. ASTM C 666-08, Standard Test Method for Resistance of Concrete to Rapid Freezing and Thawing, ASTM International (2008) West Conshohocken, PA
44. USGS, Pumice and Pumicite, Mineral Commodity Summaries (2012). Accessed on August 4th, 2014 from <http://minerals.usgs.gov/minerals/pubs/mcs/2012/mcs2012.pdf>
45. USGS, 2011 Minerals Yearbook Pumice and Pumicite (Advanced Release). Accessed on August 4th, 2014 from: <http://minerals.usgs.gov/minerals/pubs/commodity/pumice/myb1-2011-pumic.pdf>
46. D.H. Campbell, C.H. Weise, H. Love, Mount St. Helens Volcanic Ash in Concrete, *Concrete International* July (1982) 24–31
47. K.M.A. Hossain, Volcanic ash and pumice as cement additives: pozzolanic, alkali-silica reaction and autoclave expansion characteristics, *Cement and Concrete Research* 35 (2005) 1141–1144
48. K.M.A. Hossain, M. Lachemi, Development of Volcanic Ash Concrete: Strength, Durability, and Microstructural Investigations, *ACI Materials Journal* 103 (2006) 11–17
49. K.M.A. Hossain, M. Lachemi, Strength, Durability and Micro-Structural Aspects of High Performance Volcanic Ash Concrete, *Cement and Concrete Research* 37 (2007) 759–766
50. K.M.A. Hossain, S. Ahmed, Lightweight Concrete Incorporating Volcanic Ash-Based Blended Cement and Pumice Aggregate, *Journal of Materials in Civil Engineering* 23 (2011) 493–498
51. J.J. Escalante-Garcia, J.H. Sharp, The effect of temperature on the early hydration of Portland cement and blended cements, *Advances in Cement Research* 12 (2000) 121–130
52. ASTM C 191-08, Standard Test Methods for Time of Setting of Hydraulic Cement by Vicat Needle, ASTM International (2008) West Conshohocken, PA

53. W.S. Moen, G.B. McLucas, Report of Investigations 24: Mount St. Helens Ash – Properties and Possible Uses, Washington Department of Natural Resources, Division of Geology and Earth Resources (1981) 23–27
54. R. Pabalan, P. Bertetti, Cation-exchange properties of natural zeolites, *Reviews in Mineralogy and Geochemistry* 45 (2001) 1 453–518
55. C. Colella, M. Gennaro, R. Aiello, Use of zeolitic tuff in the building industry, *Reviews in Mineralogy and Geochemistry*, 45 (2001) 1 551–587
56. M. Sprynskyy, B. Buszewski, A.P. Terzyk, J. Namiesnik, Study of the selection mechanism of heavy metal adsorption on clinoptilolite, *Journal of Colloid and Interface Science*, 304 (2006) 21–28
57. T. Perraki, G. Kakali, E. Kontori, Characterization and pozzolanic activity of thermally treated zeolite. *Journal of Thermal Analysis and Calorimetry*, 82 (2005) 1 109–113
58. B. Ahmadi, M. Shekarchi, Use of natural zeolite as a supplementary cementitious material, *Cement and Concrete Composites*, 32 (2010) 134–141
59. C. Bilim, Properties of cement mortars containing clinoptilolite as a supplementary cementitious material, *Construction and Building Materials* 25 (2011) 3175–3180
60. L.E. Gordon, N.B. Milstone, M.J. Angus, The Immobilisation of Clinoptilolite Within Cementitious Systems, *Materials Research Society Symposium Proceedings* (2008) V. 1107
61. V. Lilkov, I. Rostovsky, O. Petrov, Physical and mechanical characteristics of cement mortars and concretes with addition of clinoptilolite from Beli Plast deposit (Bulgaria), silica fume and fly ash, *Clay Minerals* 46 (2011) 213–223
62. V. Lilkov, O. Petrov, V. Petkova, N. Petrova, Y. Tzvetanova, Study of the pozzolanic activity and hydration products of cement pastes with addition of natural zeolites, *Clay Minerals*, 46 (2011) 241–250
63. G. Mertens, R. Snelling, K.V. Balen, B. Bicer-Simsir, P. Verlooy, J. Elsen, Pozzolanic reactions of common natural zeolites with lime and parameters affecting their reactivity, *Cement and Concrete Research* 39 (2009) 233–240
64. F. Naiqian, J. Hongwei, C. Enyi, Study on the suppression effect of natural zeolite on expansion of concrete due to alkali-aggregate reaction, *Magazine of Concrete Research* 50 (1998) 1 17–24
65. T. Perraki, E. Kontori, S. Tsivilis, G. Kakali, The effect of zeolite on the properties and hydration of blended cements, *Cement and Concrete Composites* 32 (2010) 129–133

66. E.A. Ortega, C. Cheeseman, J. Knight, M. Loizidou, Properties of alkali-activated clinoptilolite, *Cement and Concrete Research* 30 (2000) 1641–1646
67. D. Caputo, B. Liguori, C. Colella, Some advances in understanding the pozzolanic activity of zeolites: The effect of zeolite structure, *Cement and Concrete Composites* 30 (2008) 455–462
68. M. Rosell-Lam, E. Villar-Cocina, M. Frias, Study on the pozzolanic properties of a natural Cuban zeolitic rock by conductometric method: Kinetic parameters, *Construction and Building Materials* 25 (2011) 644–650
69. W. Mozgawa, M. Krol, W. Pichor, W. Nocun-Wczelik, Immobilization of selected ions in natural clinoptilolite incorporated in cement pastes, *International Conference on the Chemistry of Cement*, July 8–10, 2011
70. R. Snellings, G. Mertens, O. Cizer, J. Elsen, Early age hydration and pozzolanic reaction in natural zeolite blended cements: Reaction kinetics and products by in situ synchrotron X-ray powder diffraction, *Cement and Concrete Research* 40 (2010) 1704–1713
71. C. Karakurt, I.B. Topcu, Effect of blended cements produced with natural zeolite and industrial by-products on alkali-silica reaction and sulfate resistance of concrete, *Construction and Building Materials* 25 (2011) 1789–1795
72. I. Janotka, M. Osacky, M. Krizma, L. Bagel, Performance Study of Slovak Natural Zeolite – Containing Cement Compositions, *International Conference on the Chemistry of Cement*, July 8–10, 2011
73. ASTM C 1157-11, Standard Performance Specification for Hydraulic Cement, ASTM International, (2011) West Conshohocken, PA
74. R. Fernandez, R. Vigil de la Villa, R. Garcia, O. Rodriguez, M. Frias, E. Villar-Cocina, Characterization and pozzolanic activity of a calcined natural zeolite, *International Conference on the Chemistry of Cement*, July 8–10, 2011
75. E. Liebig, E. Althaus, Pozzolanic Activity of Volcanic Tuff and Suevite: Effects of Calcination, *Cement and Concrete Research* 28 (1998) 4 567–575
76. G. Habert, N. Choupay, J.M. Montel, D. Guillaume, G. Escadeillas, Effects of the Secondary Minerals of the Natural Pozzolans on their Pozzolanic Activity, *Cement and Concrete Research* 38 (2008) 963–975
77. V.J. Inglezakis, M.M. Loizidou, H.P. Grigoropoulou, Ion exchange studies on natural and modified zeolites and the concept of exchange site accessibility, *Journal of Colloid and Interface Science* 275 (2004) 570–576

78. R.P. Townsend, P. Fletcher, M. Loizidou, Studies on the prediction of multicomponent, ion-exchange equilibria in natural and synthetic zeolites, Proceedings of the 6th International Zeolite Conference, Butterworths, United Kingdom (1984) 110–121
79. R. Snellings, G. Mertens, J. Elsen, Calorimetric evolution of the early pozzolanic reaction of natural zeolites, Journal of Thermal Analysis and Calorimetry, 101 (2010) 97–105
80. USGS, 2011 Mineral Yearbook Zeolites (Advance Release). Accessed on August 4th, 2014 from <http://minerals.usgs.gov/minerals/pubs/commodity/zeolites/myb1-2011-zeoli.pdf>
81. USGS, Zeolites, Mineral Commodity Summaries (2012). Accessed on August 4th, 2014 from <http://minerals.usgs.gov/minerals/pubs/commodity/zeolites/mcs-2012-zeoli.pdf>
82. USDA, Soil Mechanics Level 1, Module 3 – USDA Textural Soil Classification, Study Guide (1987). Accessed on August 4th, 2014 from <ftp://ftp.wcc.nrcs.usda.gov/wntsc/H&H/training/soilsOther/soil-USDA-textural-class.pdf>
83. ASTM D 2487-11, Standard Practice for Classification of Soils for Engineering Purposes (Unified Soil Classification System), ASTM International (2011) West Conshohocken, PA
84. ASTM D 4318-10, Standard Test Methods for Liquid Limit, Plastic Limit, and Plasticity Index of Soils, ASTM International (2010) West Conshohocken, PA
85. R. Fernandez, F. Martirena, K.L. Scrivener, The origin of the pozzolanic activity of calcined clay minerals: A comparison between kaolinite, illite and montmorillonite, Cement and Concrete Research 41 (2011) 113 – 122
86. M.D. Foster, The Relation between Composition and Swelling in Clays, Clays and Clay Minerals 3 (1954) 205–220. Accessed on August 4th, 2014 from: <http://www.clays.org/journal/archive/volume%203/3-1-205.pdf>
87. C. He, E. Makovicky, B. Osbaeck, Thermal stability and pozzolanic activity of raw and calcined mixed-layer mica/smectite, Applied Clay Science 17 (2000) 141–161
88. B.B. Sabir, S. Wild, J. Bai, Metakaolin and calcined clays as pozzolans for concrete: a review, Cement and Concrete Composites 23 (2001) 441–454
89. G. Habert, N. Choupay, G. Escadeillas, D. Guillaume, J.M. Montel, Clay content of argillites: Influence on cement based mortars, Applied Clay Science 43 (2009) 322–330
90. J. Ambroise, M. Murat, J. Pera, Hydration Reaction and Hardening of Calcined Clays and Related Minerals. V. Extension of the Research and General Conclusions, Cement and Concrete Research 15 (1985) 261–268

91. T. Ramlochan, M. Thomas, K.A. Gruber, The effect of metakaolin on alkali-silica reaction in concrete, *Cement and Concrete Research* 30 (2000) 339–344
92. M.H Zhang, V.M. Malhotra, Characteristics of a Thermally Activated Alumino-Silicate Pozzolanic Material and its Use in Concrete, *Cement and Concrete Research* 25 (1995) 1713–1725
93. E. Guneyisi, M. Gesoglu, K. Mermerdas, Improving strength, drying shrinkage, and pore structure of concrete using metakaolin, *Materials and Structures* 41 (2008) 937–949
94. E. Badogiannis, V.G. Papadakis, E. Chaniotakis, S. Tsivilis, Exploitation of poor Greek kaolins: Strength development of metakaolin concrete and evaluation by means of k -value, *Cement and Concrete Research* 34 (2004) 1035–1041
95. J. Mirza, M. Riaz, A. Naseer, F. Rehman, A.N. Khan, Q. Ali, Pakistani bentonite in mortars and concrete as low cost construction material, *Applied Clay Science* 45 (2009) 220–226
96. S. Ahmad, S.A. Barbhuiya, A. Elahi, J. Iqbal, Effect of Pakistani bentonite on properties of mortar and concrete, *Clay Minerals* (2011) 46, 85–92
97. S.A. Memon, R. Arsalan, S. Khan, T.Y. Lo, Utilization of Pakistani bentonite as partial replacement of cement in concrete, *Construction and Building Materials* 30 (2012) 237–242
98. N.M. Al-Akhras, Durability of metakaolin concrete to sulfate attack, *Cement and Concrete Research* 36 (2006) 1727–1734
99. J.M. Khatib, S. Wild, Sulphate Resistance of Metakaolin Mortar, *Cement and Concrete Research* 28 (1998) 83–92
100. USGS, Clay and Shale, Mineral Commodity Summaries (2012). Accessed on August 4th, 2014 from: <http://minerals.usgs.gov/minerals/pubs/commodity/clays/mcs-2012-clays.pdf>
101. USGS, 2010 Mineral Yearbook, Clay and Shale (Advance Release). Accessed on August 4th, 2014 from <http://minerals.usgs.gov/minerals/pubs/commodity/clays/myb1-2010-clays.pdf>
102. D.J. Cook, Calcined Clay, Shale and other soils, *Cement Replacement Materials* (1986), 40–72
103. P. Ramsburg, R.E. Neal, The Use of a Natural Pozzolan to Enhance the Properties of Self – Consolidating Concrete,” *Conference Proceedings of the First North American Conference on the Design and Use of Self-Consolidating Concrete*, (2002) 401–405

104. R.L. Khanna, M.L. Puri, The Use of Calcined Shale as Pozzuolana in Mass Concrete, *Indian Concrete Journal*, August (1957) 257–263
105. L. Pepper, B. Mather, Effectiveness of Mineral Admixtures in Preventing Excessive Expansion of Concrete due to Alkali-Aggregate Reaction, *ASTM Proceedings* (1959) V. 59, 1178–1203
106. T.E. Stanton, Studies of Use of Pozzolans for Counteracting Excessive Concrete Expansion resulting from Reaction between Aggregates and the Alkalies in Cement, *STP-99*, ASTM, Philadelphia (1950) 178–203
107. G. Davies, R.E. Oberholster, Use of the NBRI Accelerated Test to Evaluate the Effectiveness of Mineral Admixtures in Preventing the Alkali-Silica Reaction, *Cement and Concrete Research* (1987) Vol 17, 97–107
108. G.L. Kalousek, L.C. Porter, E.J. Benton, Concrete for long-time service in Sulfate Environment, *Cement and Concrete Research* (1972) Vol. 2, 79–89
109. U.S Energy Information Administration, Review of Emerging Resources: U.S. Shale Gas and Shale Oil Plays, July 2011
110. Colorado Oil and Gas Association, The Basics: Oil Shale vs. Shale Oil (2013). Accessed on August 4th, 2014 from http://www.coga.org/pdf_Basics/Basics_OilShale.pdf
111. U.S Energy Information Administration, Review of Emerging Resources: U.S. Shale Gas and Shale Oil Plays, July 2011
112. M.G. Stamatakis, D. Fragoulis, G. Csirik, I. Bedeleian, S. Pedersen, The influence of biogenic micro-silica-rich rocks on the properties of blended cements, *Cement & Concrete Composites* 25 (2003) 177–184
113. USGS, 2011 Minerals Yearbook, Diatomite (Advanced Release). Accessed on August 4th, 2014 from <http://minerals.usgs.gov/minerals/pubs/commodity/diatomite/myb1-2011-diato.pdf>
114. B. Yilmaz, Effects of Molecular and Electrokinetic Properties of Pozzolans on Hydration, *ACI Materials Journal* 106 (2009) 128–137
115. B. Yilmaz, A study on the effects of diatomite blend in natural pozzolan-blended cements, *Advances in Cement Research* 20 (2008) 13–21
116. D. Kastis, G. Kakali, S. Tsivilis, M.G. Stamatakis, Properties and hydration of blended cements with calcareous diatomite, *Cement and Concrete Research* 36 (2006) 1821–1826
117. V.G. Papadakis, S. Tsimas, Supplementary cementing materials in concrete Part I: efficiency and design, *Cement and Concrete Research* 32 (2002) 1525–1532

118. A. Tagnit-Hamou, N. Petrov, K. Luke, Properties of Concrete Containing Diatomaceous Earth, *ACI Materials Journal* 100 (2003) 73–78
119. R.E. Davis, A. Klein, The Effect of the Use of Diatomite treated with Air Entraining Agents upon the Properties of Concrete, *Symposium on Use of Pozzolanic Materials in Mortars and Concrete*, STP No. 99, ASTM, Philadelphia (1950) 178–203
120. N. Degirmenci, A. Yilmaz, Use of diatomite as partial replacement for Portland cement in cement mortars, *Construction and Building Materials* 23(2009) 284–288
121. E. J. Sierra, S.A. Miller, A.R. Sakulich, K. Mackenzie, M. Barsoum, Pozzolanic Activity of Diatomaceous Earth, *Journal of the American Ceramic Society* 93(2010) 3406–3410
122. M.I. Sanchez de Rojas, M.P. Luxan, M. Frias, N. Garcia, The Influence of Different Additions on Portland Cement Hydration Heat, *Cement and Concrete Research* 23 (1993) 46–54
123. ASTM C 311-11b, Standard Test Methods for Sampling and Testing Fly Ash or Natural Pozzolan for Use in Portland-Cement Concrete, ASTM International (2011) West Conshohocken, PA
124. TxDOT, Tex-317-D, Test Procedure for Preparation of Cement Samples for Chemical Analysis (2012)
125. ASTM D 4326, Standard Test Method for Major and Minor Elements in Coal and Coke Ash By X-Ray Fluorescence, ASTM International (2011) West Conshohocken, PA
126. ASTM C 114-11b, Standard Test Methods for Chemical Analysis of Hydraulic Cement, ASTM International (2011) West Conshohocken, PA
127. ASTM C 430, Standard Test Method for Fineness of Hydraulic Cement by the 45- μ m (No. 325) Sieve, ASTM International (2008) West Conshohocken, PA
128. ASTM C 604, Standard Test Method for True Specific Gravity of Refractory Materials by Gas-Comparison Pycnometer, ASTM International (2007) West Conshohocken, PA
129. ASTM C 151, Standard Test Method for Autoclave Expansion of Hydraulic Cement, ASTM International (2009) West Conshohocken, PA
130. ASTM C 187, Standard Test Method for Amount of Water Required for Normal Consistency of Hydraulic Cement Paste, ASTM International (2011) West Conshohocken, PA.
131. ASTM C 109, Standard Test Method for Compressive Strength of Hydraulic Cement Mortars (Using 2-in. or [50-mm] Cube Specimens), ASTM International (2011) West Conshohocken, PA

132. ASTM C 150, Standard Specification for Portland Cement, ASTM International (2011) West Conshohocken, PA
133. ASTM C 778, Standard Specification for Standard Sand, ASTM International (2012) West Conshohocken, PA
134. ASTM C 1437 Standard Test Method for Flow of Hydraulic Cement Mortar, ASTM International (2007) West Conshohocken, PA
135. R.V. Villa, R. Fernandez, O. Rodriguez, R. Garcia, E. Villar-Cocina, M. Frias, Evolution of the pozzolanic activity of a thermally treated zeolite, *Journal of Material Science* (2013) 48 3213–3224
136. J.H. Ideker, A.F. Bentivegna, K.J. Folliard, M.C.G. Juenger, Do Current Laboratory Test Methods Accurately Predict Alkali-Silica Reactivity, *ACI Materials Journal* 109 – 4 (2012) 395–402
137. ASTM C 1567, Standard Test Method for Determining the Potential Alkali-Silica Reactivity of Combinations of Cementitious Materials and Aggregate (Accelerated Mortar-Bar Method), ASTM International (2013) West Conshohocken, PA
138. V. Mechtcherine, A. Gram, K. Krenzer, J.H. Schwabe, S. Shyshko, N. Roussel, Simulation of fresh concrete flow using Discrete Element Method (DEM): theory and applications, *Materials and Structures* 47 (2014) 615–630
139. N. Roussel, M.R. Geiker, F. Dufour, L.N. Thrane, P. Szabo, Computational modeling of concrete flow: General overview, *Cement and Concrete Research* 37 (2007) 1298–1307
140. S. Mindess, J.F. Young, D. Darwin, *Concrete* 2nd Edition, New Jersey: Pearson Education (2002)
141. ASTM C 1679, Standard Practice for Measuring Hydration Kinetics of Hydraulic Cementitious Mixtures Using Isothermal Calorimetry, ASTM International (2013), West Conshohocken, PA
142. ASTM C 1702, Standard Test Method for Measurement of Heat of Hydration of Hydraulic Cementitious Materials Using Isothermal Conduction Calorimetry, ASTM International (2013), West Conshohocken, PA
143. ASTM C 596 Standard Test Method for Drying Shrinkage of Mortar Containing Hydraulic Cement, ASTM International (2009) West Conshohocken, PA
144. ASTM C 494, Standard Specification for Chemical Admixtures for Concrete, ASTM International (2013) West Conshohocken, PA

145. M. Thomas, The effect of supplementary cementing materials on alkali-silica reaction: A review, *Cement and Concrete Research* 41 (2011) 1224–1231
146. ASTM C 1293-08b, Standard Test Method for Determination of Length Change of Concrete Due to Alkali-Silica Reaction, ASTM International (2008) West Conshohocken, PA
147. ASTM C 1012, Standard Test Method for Length Change of Hydraulic-Cement Mortars Exposed to a Sulfate Solution, ASTM International (2013) West Conshohocken, PA
148. ACI 201.2R-08, Guide to Durable Concrete, American Concrete Institute (2008) Farmington Hills, Michigan
149. TxDOT, Tex-428-A, Test Procedure for Determining the Coefficient of Thermal Expansion (2011)
150. ASTM C 192-12a, Standard Practice for Making and Curing Concrete Test Specimens in the Laboratory, ASTM International (2012) West Conshohocken, PA
151. ASTM C39-12a, Standard Test Method for Compressive Strength of Cylindrical Concrete Specimens, ASTM International (2012) West Conshohocken, PA
152. ASTM C 1231, Standard Practice for Use of Unbonded Caps in Determination of Compressive Strength of Hardened Concrete Cylinders, ASTM International (2012) West Conshohocken, PA
153. ASTM C 143, Standard Test Method for Slump of Hydraulic-Cement Concrete, ASTM International (2012) West Conshohocken, PA
154. ASTM C 231, Standard Test Method for Air Content of Freshly Mixed Concrete by the Pressure Method, ASTM International (2014) West Conshohocken, PA
155. ASTM C 29, Standard Test Method for Bulk Density (“Unit Weight”) and Voids in Aggregate, ASTM International (2009) West Conshohocken, PA
156. ASTM C 403, Standard Test Method for Time of Setting of Concrete Mixtures by Penetration Resistance, ASTM International (2008) West Conshohocken, PA
157. K.Y. Ann, H.W. Song, Chloride threshold level for corrosion of steel in concrete, *Corrosion Science* 49 (2007) 4113–4133
158. ASTM C 1202, Standard Test Method for Electrical Indication of Concrete's Ability to Resist Chloride Ion Penetration, ASTM International (2012) West Conshohocken, PA

159. G.L. Crawford, J.M. Gudimettla, J. Tanesi, J., Interlaboratory Study on Measuring Coefficient of Thermal Expansion of Concrete, *Transportation Research Record*, 2164-1 (2010) 58–65
160. J. Mallela, A. Abbas, T. Harman, C. Rao, R. Liu, M.I. Darter, Measurement and Significance of the Coefficient of Thermal Expansion of Concrete in Rigid Pavement Design. *Transportation Research Record*, 1919-1 (2005) 38–46
161. T.R. Naik, R.N. Kraus, R. Kumar, Influence of Types of Coarse Aggregates on the Coefficient of Thermal Expansion of Concrete. *Journal of Materials in Civil Engineering*, 23-4 (2011) 467-472
162. D.N. Little, J.C. Petersen, Unique Effects of Hydrated Lime on the Performance Related Properties of Asphalt Cements: Physical and Chemical Interactions Revisited, *Journal of Materials in Civil Engineering* 17-2 (2005) 207–218
163. A.A Jeknavorian, L. Jardine, C.C. Ou, H. Koyata, K. Folliard, Interaction of Superplasticizers with Clay-Bearing Aggregates, Seventh CANMET/ACI International Conference on Superplasticizers and other Chemical Admixtures in Concrete Special Publication 217 (2003) Farmington Hills, Michigan
164. G. Trtnik, M. Gams, Recent advances of ultrasonic testing of cement based materials at early ages, *Ultrasonics* 54 (2014) 66–75
165. R. D'Angelo, T.J. Plona, L.M. Schwartz, P. Coveney, Ultrasonic measurements on hydrating cement slurries: Onset of shear wave propagation, *Advanced Cement Based Materials* 2 (1995) 8–14
166. J. Zhu, S.H. Kee, D. Han, Y.T. Tsai, Effects of air voids on ultrasonic wave propagation in early age cement pastes. *Cement and Concrete Research* 41 (2011) 872–881
167. J. Zhu J, Y.T. Tsai, S.H. Kee, Monitoring early age property of cement and concrete using piezoceramic bender elements. *Smart Materials and Structures* 20 (2011) 1–7